UNIVERSITY OF LONDON THESIS

Degree PHD Year 2008 Name of Author WANG, CHIUHUI, MARY

COPYRIGHT

This is a thesis accepted for a Higher Degree of the University of London. It is an unpublished typescript and the copyright is held by the author. All persons consulting the thesis must read and abide by the Copyright Declaration below.

COPYRIGHT DECLARATION

I recognise that the copyright of the above-described thesis rests with the author and that no quotation from it or information derived from it may be published without the prior written consent of the author.

LOAN

Theses may not be lent to individuals, but the University Library may lend a copy to approved libraries within the United Kingdom, for consultation solely on the premises of those libraries. Application should be made to: The Theses Section, University of London Library, Senate House, Malet Street, London WC1E 7HU.

REPRODUCTION

University of London theses may not be reproduced without explicit written permission from the University of London Library. Enquiries should be addressed to the Theses Section of the Library. Regulations concerning reproduction vary according to the date of acceptance of the thesis and are listed below as guidelines.

A. Before 1962. Permission granted only upon the prior written consent of the author. (The University Library will provide addresses where possible).

B. 1962 - 1974. In many cases the author has agreed to permit copying upon completion of a Copyright Declaration.

C. 1975 - 1988. Most theses may be copied upon completion of a Copyright Declaration.

D. 1989 onwards. Most theses may be copied.

This thesis comes within category D.

☐ This copy has been deposited in the Library of UCL

☐ This copy has been deposited in the University of London Library, Senate House, Malet Street, London WC1E 7HU.

THE ROLE OF GAP JUNCTIONS IN DIABETIC WOUND HEALING

A thesis submitted to University College London
for the degree of Doctor of Philosophy

by

Chiuhui Mary Wang

April 2008

Department of Anatomy and Developmental Biology
UCL
Gower Street, London, WC1E 6BT

I, Chiuhui Mary Wang, confirm that the work presented in this thesis is my own. Where information has been derived from other sources, I confirm that this has been indicated in the thesis.

ProQuest LLC
789 East Eisenhower Parkway
P.O. Box 1346
Ann Arbor, MI 48106-1346

ABSTRACT

The process of wound healing is slow in diabetes, often resulting in infection or chronic wounds that can lead to amputation. Cell-cell communication through the gap junction protein connexin 43 (Cx43) and the dynamic regulation of Cx43 expression play pivotal roles in the wound healing process. Acute streptozotocin-induced diabetes in rats altered connexin expression in uninjured back skin, decreasing Cx26, Cx30 and Cx43 protein and gap junctional communication in the epidermis and increasing Cx43 protein and communication in the dermis. Diabetes was also found to alter the dynamic changes of connexins associated with the wound healing response. Within 24 hours, Cx43 was upregulated in a thickened bulb of keratinocytes at the wound edge (rather than downregulated, as in controls which formed a thin process of migratory cells). Cx43 protein reduction was delayed until 48 hours when re-epithelialisation then began. Although Cx26 protein was upregulated as usual in diabetes, its distribution at the wound edge was abnormal, being more widespread. Preventing the abnormal upregulation of Cx43 expression in wound edge keratinocytes with Cx43 specific antisense oligodeoxynucleotides doubled the rate of re-epithelialisation to control levels and above. Other subsequent events of wound healing including the inflammatory response and granulation tissue maturation were also greatly improved. These results imply that diabetes-induced changes in connexin expression dynamics contribute to delayed wound healing and that targeting Cx43 expression is of potential therapeutic value in diabetic wound healing. A pilot study showed that Cx43 plays a role in the early activation of endothelial cells during inflammation. The data in this thesis provide further evidence for the central roles of connexins in the homeostasis of skin and response to injury. In particular, its role in the coordination of inflammatory response can have a pivotal impact on the quality of cutaneous wound repair.

ACKNOWLEDGEMENT

No PhD project will ever be completed without the generous support from the supervisors. I would like to thank Dr David Becker for always keeping his door open for my questions. I am grateful of his constant guidance and critical comments throughout the years. And to my second supervisor Dr Jill Lincoln, who always had constructive comments at times of trouble. I also appreciate the Biotechnology and Biological Sciences Research Council for providing my studentship.

To all the present and past members of Becker lab, I thank them for sharing the moments, both the good and the bad. To Kieran Power, for his enthusiasm for the project. To Dr Ariadna Mendoza, for sharing the late nights and the stimulating chats. To Dr Kevin Webb who was always there to help and problem-solve. To Chih-Chi Lin, who understood the pain of writing. I thank Jane Pendjiky, Daniel Ciantar and Dr Chris Thrasivoulou of the Confocal/Image Analysis team who gave up their valuable time and patiently helped with the technical issues and answered my endless questions. To Dr Sachie Yamaji and Dr Marta Varela who were generous in sharing their resources. Also a big note to those who made a great effort to read the drafts of my thesis: Dr Jeremy Cook, Dr Greg Campbell and Professor Tim Cowen.

To our collaborators Dr Ryoichi Mori and Professor Paul Martin, University of Bristol for their expertise in wound healing and the opportunity to complete an exciting project together. A special thanks to Dr Susanna Colli and Dr Sonia Eligini in University of Milan, Italy, for offering me a Marie Curie Early Stage Training fellowship and allowing me to elaborate on my ideas. To Edlira and Veronica I thank them for introducing me to the great Italian espresso.

A debt of gratitude to my dear friends and family for bearing with me, especially during the last few months of thesis preparation. To Maurizio who understood it all. To my incomparable flatmate and sister Tracy for enduring my absent mindedness and her unconditional support throughout my project. The last but not the least I thank my parents for always believing in me and encourage me in their own endearing ways.

TABLE OF CONTENTS

LIST OF FIGURES

LIST OF TABLES

LIST OF ABBREVIATIONS

AD	Adjacent region
ANOVA	Analysis of variance
AP-1	Activator Protein - 1
asODN	Antisense oligodeoxynucleotide
ATP	Adenosine triphosphate
BSA	Bovine serum albumin
Ca^{2+}	Calcium ion
CCL-2	Chemokine CC ligand – 2
COX-1	Cyclooxygenase 1
COX-2	Cyclooxygenase 2
Cx	Connexin
Cy3	Cyanine3
DTT	DL-dithiothreitol
dpw	Days post wounding
EGF	Epidermal growth factor
EIA	Enzyme Immunoassay
ELISA	Enzyme-linked immunosorbent assay
FCS	Fetal calf serum
FFA	Flufenamic acid
FGF	Fibroblast growth factor
FITC	Fluorescein isothiocyanate
GJIC	Gap junctional intercellular communication
HCAECs	Human coronary artery endothelial cells
HUTECs	Human tonsil endothelial cells
HUVECs	Human umbilical vein endothelial cells
ICAM	Intercellular adhesion molecules
IP_3	Inositol 1,4,5,-trisphosphate
IL-1	Interleukin - 1
IL-8	Interleukin – 8
iNOS	inducible nitric oxide synase
KGF	Keratinocyte growth factor

LE	Leading edge
LiCl	Lithium Chloride
LY	Lucifer Yellow
MCP-1α	Monocyte chemotactic protein – 1 alpha
MIP-1α	Macrophage inflammatory protein – 1 alpha
MMP	Matrix metalloproteinases
NO	Nitric oxide
NOS3	Nitric oxide synthase 3
ODN	Oligodeoxynucleotide
PBS	Phosphate buffered saline
PDGF	Platelet derived growth factor
PGE_2	Prostaglandin E_2
PKC	Protein kinase C
PLGF	Placenta growth factor
SDS	sodium dodecyl sulfate
SMA	Smooth muscle actin
sODN	sense oligodeoxynucleotide
STZ	Streptozotocin
TGF-α	Transforming growth factor - alpha
TGF-β	Transforming growth factor - beta
TNF-α	Tumour necrosis factor - alpha
VCAM-1	Vascular cell adhesion molecule - 1
VEGF	Vascular endothelial growth factor
WE	Wound edge

1 GENERAL INTRODUCTION

1.1 The skin

Skin is one of the largest organs of the human body, accounting for approximately 15% of the body weight of an average individual. The skin provides our body with a tough, yet flexible protective barrier to the external environment. In addition, it plays important roles in regulating water balance, blood pressure and body temperature. The field of cutaneous biology is an active one involving all aspects of skin and its formation and repair. An introduction to the anatomy of skin is presented here before an overview of cutaneous wound healing and the important role gap junctions play in skin homeostasis and repair.

The skin is characterised by two layers of specialised tissues; the thinner outer epidermis and the underlying thicker dermis, separated by a basement membrane. Extensive networks of nerves, blood vasculature and skin appendages are embedded in the dermis, where they partake in temperature, water regulation and other processes (Montagna and Parakkal, 1974).

1.1.1 The epidermis

The epidermis is a stratified squamous epithelium that is formed by thin layers of keratinocytes. Its key functions are to waterproof the body and offer resistance to friction from the outer world. To maintain this outer barrier for friction, keratinocytes require a constant turnover to sustain the stratified epithelium. The basal layer of keratinocytes contains stem cells that continuously divide to provide a pool of cells

that differentiate and accumulate keratin as they mature (Wood and Bladon, 1985). The differentiating keratinocytes migrate towards the outer surface until they become cornified and eventually shed. In man, a keratinocyte typically matures, depending on the region of skin, in 14-30 days from terminal cell division in the basal layer, until it is shed (Wood and Bladon, 1985). As the cells progress with differentiation they become flattened and this morphologic change can be recognised in the epidermal layers, which are named according to their appearance (Montagna and Parakkal, 1974). From the basal lamina (basement membrane), moving towards the outer surface, the epidermal layers are as follows: *stratum basale* (basal layer), *stratum spinosum* (spinous layer), *stratum granulosum* (granular layer), *stratum lucidum* (transitional layer) and *stratum corneum* (cornified layer). Basal keratinocytes are anchored to the basement membrane by hemidesmosomes and to each other by desmosomes. To establish the waterproof epidermis, keratinocytes express different types of keratin filaments as they undergo terminal differentiation. In the stratum spinosum and stratum granulosum the keratinocytes express keratin filaments associated with differentiation. At the stratum corneum, the keratinocytes are dead after undergoing terminal differentiation. These dead cells are full of keratin proteins that are the foundation of the tough barrier to the outer environment (Wood and Bladon, 1985). The keratin intermediate filament cytoskeleton is formed by pairs of type I (acidic K9-K20) and type II (basic K1-K8) filaments, and is attached to the hemidesmosomes and desmosomes for anchorage. Different pairs of keratin filaments are associated with keratinocyte morphogenesis, for example Keratin 1 and Keratin 10 are found in the spinous layer and Keratin 5 and 14 pairs are expressed in the basal layer (Moll et al., 1982). Keratins are also the main constituent of hair and nails (Wood and Bladon, 1985).

Other minority cell types found in the epidermis are melanocytes, Langerhan's cells and Merkel cells (Wood and Bladon, 1985). Melanocytes are usually found near the basal layer and produce melanin with specialised, pigment-containing organelles, melanosomes, giving skin its colour. Langerhan's cells are antigen-presenting dendritic cells, found in the basal and spinous layers and functioning as a part of the immune system. Merkel cells are associated with sensory nerve terminals and function as touch sensors.

1.1.2 The dermis

Dermis is a tough, elastic layer of tissue that cushions the underlying organs against mechanical injuries. It is composed mainly of fibroblastic connective tissues with thick collagen bundles that also act as a scaffold for extensive nervous and vascular networks (Montagna and Parakkal, 1974). The elastic nature of dermis is important to allow body movement and provide further resilience against pressure. This is achieved by the network of elastin fibres in the extracellular matrix alongside the dense collagen (mainly type I) fibres that provide great tensile strength (Wood and Bladon, 1985). Ground substance in the extracellular matrix is made up of glycosaminoglycans (hyaluronic acid, chrondroitin sulphate, heparin, dermatan sulphate). The papillary dermis found right beneath the epidermis is formed of loose connective tissue, consisting of thin collagen and elastin fibres. Here, dermal papillae interdigitate with epidermal rete ridges to sustain the better attachment of the epidermis to the dermis. Nerve endings and blood capillaries that support the avascular epidermis are also located within these papillae to facilitate nutrient exchange. The

reticular dermis is found below the papillary layer and comprises fibroblastic connective tissue with coarse elastin and collagen bundles, providing the main mechanical strength to skin. Hypodermis is found beneath the dermal layers where loose connective tissue and large numbers of adipocytes are found, providing body insulation and further shock absorption.

The well vascularised and innervated dermis is important for the inner regulation of the body. Larger vessels are buried in the deep dermis and finer branches of capillaries and plexuses extend towards the dermal papillae near the epidermis. In addition to bringing nutrients to the tissue, the vasculature has an important role in regulating body temperature. Through vasodilation and vasoconstriction, respectively, blood flow increases to assist heat dispersion, and decreases to conserve body temperature. Sensory neurons constantly supply important information such as change in temperature in the environment to the brain so that water balance and temperature can be monitored. Specialised sensory structures (e. g. Merkel cells, Meissners corpuscles), receptive to information from the external environment are present in the dermis. Due to the range of sensory receptor types, there is a clear distinction transmitted to the brain of the different mechanical stimuli such as touch, texture, pressure or pain.

1.1.3 The skin appendages

Skin appendages also play a part in regulating body temperature and water balance. Hair follicles, sebaceous glands and sweat glands each have a separate role in preserving or dispersing heat and moisture. Hair follicles are tubular invaginations of the epidermis into the dermis where a bulbous root sheath structure is formed at the

end for hair growth. The hair shaft grows from the root towards the epidermis and is supported by the surrounding hair follicle. Connected to the hair follicle is an arrector pili muscle, involved in body temperature control by pulling the hair straight to trap air and thus conserve heat by insulating the body in cold temperatures. Hair is generally found in every region of skin in mammals except palms of the hands and soles of the feet where a thick epidermis is found. Sebaceous glands are associated with the hair follicles but also are found in areas where hair is absent. Sebaceous glands are holocrine glands, secreting an oily sebum into the lumen by membrane rupture. The sebum is thought to waterproof skin and hair to prevent water loss. The importance of sweat and sweat glands for body temperature regulation is well known. Sweat glands are tubular merocrine glands with an excretory duct leading sweat to the outer surface of the epidermis. As sweat evaporates from the skin surface excess heat is dissipated and the body cools down.

1.2 Wound healing

A rupture in the skin needs to be sealed and restored as soon as possible to reduce the chance of infection to ensure survival. Cutaneous wound healing is a complex cascade of events that kick-start immediately after injury to ensure recovery of dermal and epidermal integrity. Wound healing is a highly conserved ability through evolution and consequently model organisms such as Drosophila, zebrafish and rodents have been used to understand the healing events (Grose and Werner, 2003; Redd et al., 2006). The wound healing cascade can be divided into four overlapping stages: initiation,

inflammation, tissue proliferation/migration and tissue maturation (Martin, 1997; Singer and Clark, 1999).

1.2.1 Initiation

When skin is broken, blood from disrupted blood vessels quickly forms a clot to stop the bleeding and act as a temporary plug in the open wound to prevent infection. The blood clot is formed by a meshwork containing degranulated platelets, extracellular matrix proteins: fibronectin, vitronectin, thrombospondin and fibrin fibres. There are two pathways of blood coagulation, the intrinsic (contact activation) and extrinsic (Tissue factor) pathways that lead to fibrin clot formation. Briefly, the contact pathway is initiated with the exposure of platelets to collagen and the extrinsic pathway is prompted by the release of Tissue factor from endothelial cells. Both of these pathways trigger a series of coagulating factors whose activity releases thrombin from prothrombin. At the end of these pathways thrombin converts fibrinogen into fibrin to form the cross-linked fibrin clot. In addition to acting as a seal, the clot is also a reservoir of cytokines and growth factors that initiate the subsequent steps of the healing process. Activated platelets release cytokines such as platelet-derived growth factor (PDGF), transforming growth factor β1 (TGF-β1) and fibroblast growth factors (FGF) in the clots, that are chemotactic for neutrophils (Assoian et al., 1983; Grainger et al., 1995). Inflammatory cells are attracted by the high concentration of cytokines to infiltrate the wound site for the next steps of the wound healing process.

Immediately after injury the blood vessels at the site of injury initially vasoconstrict to reduce the extent of haemorrhage but soon after coagulation they vasodilate under the

influence of prostaglandins and nitric oxide released by endothelial cells. Vessel permeability also increases which facilitates inflammatory cells transmigration into the wound tissue. Macroscopically at this early time, the wound shows rubor (redness), tumor (swelling) and calor (heat), corresponding to the increased blood flow to the region.

1.2.2 Inflammation

The inflammatory stage begins minutes after injury and typically lasts about 4 days. Mast cells are one of the earliest cell types to arrive at the wound site and once activated, release histamine and serotonin locally to control vascular permeability, and tumour necrosis factor α (TNF-α) to recruit neutrophils. The role of mast cells in wound healing was confirmed by the impaired healing of mast cell knockout mice (Weller et al., 2006). These mast cell deficient mice showed impaired healing and decreased extravasation and neutrophil recruitment. Interestingly, in normal mice where histamine H-1 receptor was blocked by an antagonist, wound healing was impaired but no changes were observed when TNF-α was absent (Weller et al., 2006).

Inflammatory cells that migrate into the wound play an important role in the wound healing process. In the early inflammatory phase, polymorphonuclear leukocytes including neutrophils are attracted to the wound area and act as the primary line of defence against bacterial infection (Witte and Barbul, 1997). High concentrations of TNF-α in the wound induce an elevation in surface adhesion molecule expression in the endothelial cells for leukocyte transmigration. The general concept of leukocyte extravasation involving tethering, rolling adhesion and tight adhesion for

transmigration is widely accepted as the pathway for leukocyte transmigration (Weber et al., 2007). In the initial adhesion, leukocytes first adhere to endothelial cells via surface P- and E- selectins. As they slow down from the "rolling", integrins on leukocytes bind to adhesion molecules such as VCAM, platelet-endothelial cell adhesion molecule – 1 (PECAM-1), and intercellular adhesion molecules (ICAM) on the endothelial cells. Firm attachments of the integrins to the adhesion molecules are required prior to transmigration. Diapedesis, the transmigration process through endothelial cells, of leukocytes is tightly controlled via junctional adhesion molecule - 1 (JAM-1), PECAM-1 and CD99 as they migrate between endothelial cells through adherens and tight junctions to extravasate into the surrounding tissue (Aurrand-Lions et al., 2002).

Neutrophils are the first to arrive at the wound site and remain for several days to clear and debride the wound. Once transmigrated into the tissue, neutrophils migrate towards the chemoattractants in the wound. At the wound site, neutrophils begin the phagocytic debridement process via release of reactive oxygen species (ROS) and proteases during phagocytosis. At the same time neutrophils release further TNF-α, interleukin-8 (IL-8) and chemokines that amplify the inflammatory response, leading to macrophage and lymphocyte infiltration which forms the next step in the repair process. These cytokines (see later section) also stimulate keratinocytes and fibroblasts to dedifferentiate and proliferate to continue the healing process. Neutrophils are cleared away by the infiltrating macrophages or excluded via eschar with the formation of scabs as they become spent in the wounds,

Subsequently, the late inflammatory stage of wound healing is marked by the presence of macrophages removing the remaining debris and secreting cytokines to amplify the signal for the repair process after neutrophil accumulation. Circulating monocytes transmigrate through the endothelial cells with similar adherin, integrin binding processes as neutrophil extravasation, in addition to regulation by vascular cell adhesion molecule-1 (VCAM-1) (Issekutz et al., 1995). Once in the tissue and in contact with extracellular matrix the monocytes differentiate into macrophages and become activated to clear away debris at the wound site and the release further cytokines (Dipietro et al., 2001). Chemokines such as TNF-α, CCL-2 and important cytokines such as epidermal growth factor (EGF), vascular endothelial growth factor (VEGF), FGF, TGFβ, IL-1 and IL-6 that mediate fibroblasts, keratinocytes and endothelial cells in the wound healing process are secreted by macrophages (Leibovich and Ross, 1975). The production of nitric oxide (NO) by inducible nitric oxide synthase (iNOS) in macrophages is also angiogenic and at the same time anti-bactierial. Macrophages disappear around 5 days after injury. T lymphocytes are the last cells to infiltrate the wound region after the main waves of neutrophils and macrophages (Fishel et al., 1987). T lymphocytes are thought to be involved in increasing wound tensile strength and collagen content (Efron et al., 1990; Peterson et al., 1987).

However, the role of the inflammatory response in wound healing is controversial and has been under debate in the past decade. The examples of embryonic wounds healing perfectly without any scarring in the absence of inflammatory responses, first raised the question of the necessity for the inflammatory response in tissue repair (Nodder and Martin, 1997; Redd et al., 2004). In contrast, late stage embryonic wounds (near gestation point) and adult wounds exhibit a robust inflammatory response and

subsequently permanent tissue scarring after the healing process. Early fetal cutaneous wounds treated with exogenous TGFβ caused scarring similar to adult wounds and give further credence to the view that pro-inflammatory cytokines may have adverse effects on healing (Lanning et al., 1999). TGFβ mediator Smad3 knockout mice also demonstrate reduced monocyte infiltration and general inflammatory responses with accelerated wound re-epithelialisation (Ashcroft et al., 1999). TNF-α p55 receptor deficient mice show accelerated re-epithelialisation with reduced macrophage recruitment (Mori et al., 2002). Similarly, neutropenic wounds (wounds that lack neutrophils) do not alter wound debridement, macrophage infiltration or wound repair (Simpson and Ross, 1972). More recent research shows that neutrophil-depleted mice demonstrate an accelerated wound re-epithelialisation rate (Dovi et al., 2003). PU.1 null mice lacking several lineages of inflammatory cells (macrophages, neutrophils, mast cells) can heal perfectly without scarring suggesting they may be dispensable in the wound healing process (Martin et al., 2003). Recently it has been suggested that neutrophils may do more damage to the surrounding tissue by the release of ROS and proteases than previously thought (Dovi et al., 2004). The robust inflammation may be disadvantageous in terms of the additional tissue damage it causes while providing its purpose of protection and debridement. Nevertheless, the positive effect of cytokine signalling in different aspects of wound healing cannot be disputed. Numerous cytokines are positively involved in processes like keratinocyte migration, fibroblast contraction and endothelial cell proliferation, and remain a central component in understanding the wound healing cascade (Werner and Grose, 2003).

1.2.3 Tissue proliferation & migration

A period of massive tissue proliferation and migration takes place soon after the initial inflammatory events in order to restore skin integrity. Cytokines produced by macrophages stimulate fibroplasias and angiogenesis at the wound site, forming the granulation tissue. At the same time keratinocytes migrate into the wound to re-epithelialise the raw tissue. The proliferation and migration processes are tightly controlled by an array of cytokines including PDGF, TGF-α, TGF-β, KGF, EGF and VEGF (Grose and Werner, 2003; Werner and Grose, 2003).

Activated basal keratinocytes and hair follicles behind the wound edge start to proliferate and migrate forward into the wound between the dry scab and viable tissue to re-epithelialise skin (Garlick and Taichman, 1994). A whole array of growth factors act as potent mitogens and motogens to the keratinocytes, especially EGF and KGF (Beer et al., 1997; Bhora et al., 1995; Marchese et al., 1995; Werner et al., 1993). Several matrix metalloproteinases (MMPs) actively facilitate the migration by first detaching keratinocytes from their tight anchorage to the basal lamina (MMP-9) and then dissolving the ECM (MMP-1/collagenase) to make pathway for migration (Saarialho-Kere et al., 1992). The re-epithelialisation is assisted by the underlying granulation tissue contraction that brings the wound edges closer together. Re-epithelialisation is complete when the migrating keratinocytes from the wound edges meet and cover the wound surface. At this point migration ceases and epidermal differentiation resumes to establish the stratified epidermis with a basal lamina.

Fibroblasts have an important task to provide the basic dermal framework for tissue reconstruction in the wound. Growth factors PDGF, FGF and TGFβ1 are known to promote fibroplasias in the wound (Greiling and Clark, 1997). Within 3-5 days the fibroblasts in the dermal fascia layer proliferate and migrate into the wound space synthesising collagen, fibronectin and hyaluronic acid as bases for ECM (Spyrou et al., 1998). The ECM acts as a temporary scaffold for angiogenesis and innervations of the granulation tissue.

Massive angiogenesis also occurs during granulation tissue formation. Pericytes and endothelial cells from the subdermal and adjacent tissue sprout into the new matrix forming blood vessels to provide nutrients to the metabolically active cells (Risau, 1997; Tonnesen et al., 2000). The direction of angiogenesis appears to be controlled by the low oxygen concentration in the wound (Risau, 1997). Angiogenesis is mediated by VEGF and FGFs secreted by activated keratinocytes and macrophages (Brown et al., 1992; Frank et al., 1995; Nissen et al., 1998; Peters et al., 1993; Werner et al., 1992). Angiogenesis and wound repair was significantly delayed in VEGF-A knockout mouse (Rossiter et al., 2004).

1.2.4 Tissue maturation

Wound matrix synthesis and remodelling continue gradually over a long period of time, for up to years after injury as the granulation tissue matures into a scar. As the matrix matures, the cross-linked collagen bundles increase in diameter and change orientation which are important to restore tissue tensile strength (Paul et al., 1997). In scars, type

III collagen is the predominant collagen, as opposed to type I in normal skin (Betz et al., 1993; Clore et al., 1979). Although the remodelling does gradually balance the scar ECM back to type I collagen as the tissue matures, the scar fibrous collagen bundles are never exactly like the basket weave organisation of collagen fibres in uninjured skin (Diegelmann et al., 1979) and the rebuilt scar can only be maximally 70% as strong as normal skin (Levenson et al., 1965).

Wound contraction is also a part of tissue remodelling that organises collagen orientation as well as reducing the size of granulation tissue (Grinnell, 1994). This is achieved by fibroblasts, differentiating into myofibroblasts, containing smooth muscle actin bundles and microfilaments, that pull the wound edges closer as they contract (Risau, 1997; Tomasek et al., 2002). After contraction myofibroblasts undergo apoptosis and disappear from the granulation area (Desmouliere et al., 1995). Newly formed blood vessels at this stage also undergo reconstruction and maturation, the density of blood vessels diminishes with the increase in tissue collagen content. Growth factors TGF-β1, TGF-β2, PDGF and FGF with a combination of MMPs and tissue inhibitors of metalloproteinases (TIMPs) mediate the delicate process of ECM remodelling and scar formation (Birkedal-Hansen, 1995; Grinnell, 1994; Montesano and Orci, 1988).

1.2.5 Inflammatory cytokines in wound healing

Inflammatory responses are essential for defending the body against invading microbes. The release of cytokines and chemokines by the local cells and recruited leukocytes orchestrate the inflammatory response against pathogens as well as

promoting the wound healing process. Cytokines are small protein and peptide signalling molecules that stimulate a change in the behaviour of other cells; they can be categorised into three subsets: 1) chemokines that stimulate chemotaxis, 2) pro-inflammatory cytokines that amplify the inflammatory response and 3) growth factors that act on cells. A vast number of cytokines are involved in the wound healing process and have been extensively reviewed by Werner and Grose (2003). Numerous different knockout mice studies in the past decade also add to our understanding of the function of these cytokines in wound repair (Grose and Werner, 2003). The key cytokines that are involved in the wound healing process were mentioned in the previous sections. Clearly cytokines are involved in multiple phases and processes of the wound cascade. A summarised list of key cytokines involved and their functions in the cutaneous healing process can be found in Appendix I.

1.2.6 Diabetic wound healing

Abnormal wound healing occurs when a normal step in the wound healing process becomes disrupted or unbalanced. Keloid and hypertrophic scars are examples of abnormal wound healing where excess levels of cytokines and inflammation in the wounds lead to an over accumulation of collagen and hyperproliferative fibroblasts during tissue maturation (Diegelmann et al., 1979). High levels of IL-6 and TGF-β1 in fibroblasts have been reported in keloid scars (Ghazizadeh et al., 2007) and PDGF overexpression in hypertrophic scars (Niessen et al., 2001). Chronic wounds are those wounds that fail to close, leaving an open lesion in the skin that is prone to bacterial infections. In particular, chronic wounds in diabetic patients can result from abnormalities in multiple factors including poor blood flow, neuropathy, venous inflammation and continuous friction trauma. The abnormal wound healing process can cause the progression of infection and ulceration, often leading to amputation.

The prevalence for diabetes is on the increase worldwide. In USA alone, diabetes affects 20.8 million individuals in 2005 (National Diabetes Information Clearinghouse, NIH), creating huge social and financial burdens on the health services. In the UK, 2.2 million people were diagnosed in 2006, and the disease prevalence of 3.54% of the population was predicted to increase every year (British Diabetes Association). Diabetes mellitus is a complex metabolic disorder characterised by insulin deficiency (Type I) or development of resistance in insulin receptors (Type II). Type I diabetes is characterised by the loss of insulin production by the beta cells of the islets of Langerhans in the pancreas. Patients with type I diabetes represent approximately 10%

of the disease population and require insulin injections to regulate blood glucose levels. Type II diabetes is characterised with the development of insulin resistance due to the lack of sensitivity to insulin by the receptors on cell surfaces. Type II patients are usually not insulin dependent but require a strict diet. The prolonged elevation in glucose level and the lack of appropriate feedback regulation for insulin secretion led to the many secondary complications in diabetes mellitus. Microvascular disease, retinopathy, neuropathy and nephropathy are some of the most common complications observed in both Type I and Type II diabetes patients. Peripheral neuropathy and angiopathy are the main causes of diabetic wound ulcerations. The lose of sensation in feet and limbs due to peripheral neuropathy often results in failure to detect lesions or ischemic conditions in skin, and allowing repeated trauma at pressure points. Normal wound healing process is impeded, resulting prolonged open wounds.

The tendency of diabetic wounds to heal much more slowly than normal wounds has been documented over the past decade (Brown et al., 1994; Falanga, 2005; Franzen and Roberg, 1995; Sullivan et al., 2004) . Several factors responsible for delayed diabetic healing have been reported over time. Prolonged inflammation and alterations in levels of growth factors, cytokines and proteases are reoccurring observations in many studies (Goren et al., 2006; Harris et al., 1995; Loots et al., 1998; Maruyama et al., 2007; Wetzler et al., 2000). Reduced PDGF, PDGF receptor, and FGF-1, -2, -7 expressions, and aberrant TGF-β expression pattern have all been demonstrated to contribute to delayed and abnormal healing in diabetes (Beer et al., 1997; Bitar and Labbad, 1996; Shukla et al., 1998; Werner et al., 1994). The infiltration of inflammatory cells after wounding is delayed (Greenhalgh et al., 1990) but the total number of leukocytes accumulating at the wound is elevated (Loots et al., 1998;

Wetzler et al., 2000). Although the number of macrophages in ulcer wounds is high, they appear to be inactivated (Moore et al., 1997). Nevertheless, the persisting presence of neutrophils and macrophages in wounds can sustain the presence of chemokines thus preventing the normal progression of the repair phases (Wetzler et al., 2000).

Other common phenotypes of abnormal diabetic wound healing include the delayed rate of wound re-epithelialisation and wound granulation tissue maturation (Franzen and Roberg, 1995). Other than external trauma, the intrinsic diabetic condition of the skin cells can also delay the wound repair response as hyperglycaemia is associated with changes in cell morphology, decreased proliferation and differentiation of keratinocytes (Spravchikov et al., 2001; Wertheimer et al., 2000). The changes in cell proliferation and morphology could impede keratinocyte migration to reseal the open skin. Reduced collagen deposition, delayed granulation tissue formation and apoptosis give a weak scar tissue that may be prone to tear again at pressure points (Bitar, 1998; Greenhalgh et al., 1990). Increased MMP levels was also found in the diabetic granulation tissue, possibly damaging surrounding healthy tissue and preventing proper tissue maturation, thus increasing the possibility of reoccurring wounds (Norgauer et al., 2002; Saarialho-Kere, 1998).

As many of the wound healing processes are orchestrated by cytokines, topical application of growth factors to diabetic wounds as apart of a wound management program was thought to be a good method to promote tissue repair. Some growth factors in trials do improve diabetic wound repair with varied degrees of success (Pierce and Mustoe, 1995). Topical application of human recombinant PDGF was

shown to improve the quality of wound healing in db/db mice, human diabetic ulcers and pressure wounds (Greenhalgh et al., 1990; Mandracchia et al., 2001; Nagai and Embil, 2002; Robson et al., 1992b; Wieman et al., 1998). Cell infiltration, re-epithelialisation, angiogenesis and apoptosis during granulation tissue maturation appeared to become more normal after such PDGF treatment in diabetic mice (Greenhalgh et al., 1990) and human diabetic wounds (Mandracchia et al., 2001; Robson et al., 1992b; Wieman et al., 1998). Recombinant PDGF has since then been approved by the Food and Drug Administration for wound treatment. The treatment is now licensed and prescribed for neuropathic diabetic wounds under the name Becaplermin or Regranex Gel. Other growth factors including FGF (Greenhalgh et al., 1990; Robson et al., 1992a) and TGF-α (Brown et al., 1994) applications to diabetic lesions have all improved wound closure and granulation tissue formation. EGF application improved diabetic foot ulcers (Tsang et al., 2003) but not in venous ulcers (Richard et al., 1995). Different growth factors are being devised for different wound problems: PDGF and FGF stimulate ECM synthesis and angiogenesis that is more suited in pressure ulcers (Wieman et al., 1998), while in venous ulcers where re-epithelialisation is abnormal KGF or EGF treatment is more appropriate (Falanga, 2000).

1.3 Gap Junctions

Communication between different cell types is important during wound healing to co-ordinate the cells to ensure a swift restoration of skin integrity. Direct cell-to-cell communication via gap junctions has been shown to play important roles in the wound healing processes to synchronise and coordinate cells for migration (Goliger and Paul, 1995; Kretz et al., 2003; Qiu et al., 2003). A thorough review on gap junctions is included in the following sections.

1.3.1 Gap junctions, connexons and connexins

1.3.1.1 DISCOVERY AND IDENTIFICATION

Gap junction proteins have been identified in all vertebrates including mammals, birds, amphibians and fish but not in invertebrates. Through genetic screening of *C. elegans* and *Drosophila,* analogous genes that are functional in electrical and dye coupling were discovered in invertebrates (Phelan et al., 1996; Starich et al., 1996). Though topologically and functionally similar, the invertebrate analogs, termed innexins, lack sequence homology to connexins (Phelan et al., 1998). No innexins were found in mammals but in recent years a second family of gap junction proteins called pannexins was identified in the vertebrates. Pannexins show homology to innexins and appear to have some properties of connexins. Only connexins are considered for the purpose of this thesis.

The importance of gap junctional intercellular communication was first noted in the electrical synapses between neurons of crayfish, where induction of current in the pre-synaptic lateral giant fibre produced a voltage change in the post-synaptic motor fibre (Furshpan and Potter, 1959; Watanabe and Grundfest, 1961). However, the structure of a gap junction plaque could not be directly resolved by light microscopy, and only when electron microscopy had progressed and become the primary technique were gap junctions defined and recognised (Dewey and Barr, 1962; Karrer, 1960; Severs, 1995). Since the first observation of gap junctions in the heart by Sjostrand and Andersson (1954), gap junctions were identified in many tissue types including nervous tissue of several fishes (Furshpan, 1964), smooth and cardiac muscles (Dewey and Barr, 1962; Dewey and Barr, 1964), and between epithelia and glands (Kanno and Loewenstein, 1966).

The structure of the gap junction plaque was not proposed until Revel and Karnovsky (1967) demonstrated the penetration of extracellular tracer lanthanum between the closely apposed segments of neighbouring plasma membranes and distinguished gap junctions from the tight junctions which did not allow lanthanum penetration. The observation of a 2-3 nm gap between the neighbouring plasma membranes gave rise to the name "gap" junctions. Early freeze-fracture electron micrographs of plasma membrane showed gap junction plaques of 8-9 nm width, containing tens to hundreds of closely packed particles (Goodenough and Revel, 1970; Kreutziger, 1976; McNutt and Weinstein, 1973). Later X-ray diffraction and negative staining techniques revealed similar model to those observed in EM micrographs (Caspar et al., 1977; Makowski et al., 1977; Sosinsky, 1996). Particles of the gap junction plaque from freeze-fracture EM were identified as individual gap junction channels and depicted as

a hexagonal tube with a central lumen penetrating the two layers of plasma membrane (Bruzzone et al., 1996; Sosinsky, 1996; White and Bruzzone, 1996; Wolburg and Rohlmann, 1995).

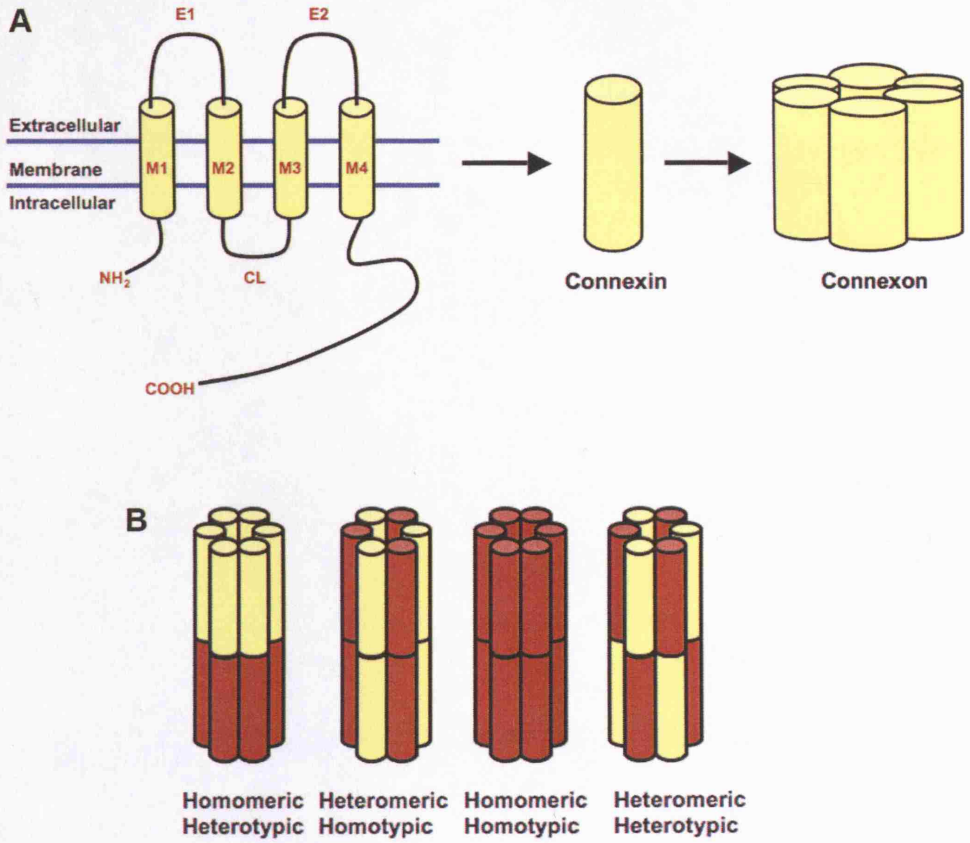

Figure 1.1 Connexin protein topology and types of gap junctions. (A) Connexin protein topology showing transmembrane domains (M1-M4), cytoplasmic (CL) and extracellular (E1-E2) loops. Six connexin proteins then oligomerise into a connexon. (B) A gap junction can be formed by different combinations of connexins and connexons.

1.3.1.2 CONNEXIN TOPOLOGY

Gap junction channels are formed by the docking of two separate connexons, or hemichannels, from the two neighbouring cell membranes allowing continuum of cytoplasm between cells. Each connexon is made up of six connexin (Cx) protein subunits, where the connexins align laterally to form the wall of a connexon (Makowski et al., 1977; Unwin and Ennis, 1984). The first connexin (Cx32) was cloned from rat hepatic cells (Paul, 1986). The homologous Cx32 in the human and mice genomes was subsequently identified (Heynkes et al., 1986; Kumar and Gilula, 1986). To date, a family of 20 connexins has been identified in human and mouse genomes (Willecke et al., 2002). Connexons formed with six identical connexins (homomeric) or of different types of connexins (heteromeric) have been observed. A gap junction can also be homotypic with two identical homomeric connexons, or heterotypic with two different connexons (Figure 1.1). Different connexins give different properties to a gap junction channel (Cao et al., 1998; Elfgang et al., 1995).

Most connexin genes share basic features showing two coding exons separated by one intron in the genomic sequences (Willecke et al., 1991). The amino acid topology is also highly conserved in the connexin family (Milks et al., 1988; White and Bruzzone, 1996; Zimmer et al., 1987). Connexins are a family of transmembrane proteins that contain four hydrophobic transmembrane domains (M1–M4), two extracellular loops (E1–E2), one intracellular loop and the Amino (N–) and Carboxyl (C–) termini facing the cytoplasm. The four α-helical domains M1-M4 anchor the polypeptide to the cell membrane. The extracellular loops determine connexin–connexin compatibility for docking and junction formation (White et al., 1994b; Yeager et al., 1998). Both loops

contain conserved cysteine residues linked by intramolecular disulphide bonds (Dupont et al., 1989; John and Revel, 1991; Rahman and Evans, 1991), allowing successful docking to form heterotypic channels as observed in *in vitro* expression systems (Dahl et al., 1992; Elfgang et al., 1995; White and Bruzzone, 1996; White et al., 1995). However, not all the connexins will dock with one another (Harris, 2001). In addition, extracellular loop E1 has a voltage-sensing mechanism that establishes charge selectivity (White et al., 1995). The intracellular loop varies in length in different connexins and is suggested to be involved in chemical gating. The amino N–terminus is conserved between connexins while the C–terminus varies greatly between the members of the connexin family. The C–terminus is involved in chemical gating, pH sensitivity and post–translational modifications through phosphorylation and glycolysis (White et al., 1995).

1.3.1.3 NOMENCLATURE

Connexin isoforms are identified using two alternative nomenclature systems. The most commonly used is based on the molecular mass of the isoform in kilodaltons (kDa), for example Connexin-43 is a 43kDa protein (Beyer et al., 1987). An additional prefix can included to indicate the species of origin when required (e. g. h for human, m for mouse). The alternative nomenclature method is based on phylogenetic sequence and topology similarities, subcategorising connexins using Greek letters (α, β, γ and δ classes) (Bennett et al., 1991; Sohl and Willecke, 2003; Willecke et al., 2002). However, neither nomenclature system is satisfactory and was subject to great debate in the recent years with discoveries of homologous proteins in different organisms. Complications for the molecular mass system arose while distinguishing the different isoforms with similar molecular masses, or functional orthologues with different

molecular mass (e. g. rat Cx46, bovine Cx44 and chick Cx56). Problems with the Greek letter system arose when it failed to define and group many of the more recently cloned connexins. A unified nomenclature system for gap junction gene family that does not depend on sequence similarity or molecular mass is being debated in the field (Gap Junction Conference 2005, 2007; 46th ASCB Gap junction special interest subgroup meeting, 2006). For the remainder of this thesis the molecular mass system is used (Table 1.1).

Table 1.1 List of connexin genes with corresponding nomenclature in human and mouse.

Gene (Human)	Protein (Greek)	Human protein (MW)	Mouse protein (MW)
GJB7	β7	Cx25	Cx25
GJB2	β2	Cx26	Cx26
GJB6	β6	Cx30	Cx30
GJE1	γ1	Cx30.2	Cx29
GJB5	β5	Cx30.3	Cx30.3
GJB3	β3	Cx31	Cx31
GJB4	β4	Cx31.1	Cx31.1
GJB1	β1	Cx32	Cx32
GJA4	α4	Cx37	Cx37
GJA2	α2	Cx38	Cx38
GJA5	α5	Cx40	Cx40
GJA1	α1	Cx43	Cx43
GJA7	α7	Cx45	Cx45
GJA3	α3	Cx46	Cx46
GJA12	α12	Cx47	Cx47
GJA8	α8	Cx50	Cx50
GJA10	α10	Cx59	-
-	-	Cx62	Cx57
Gjb6	α6	-	Cx33

1.3.1.4 GAP JUNCTION ASSEMBLY AND DEGRADATION

The assembly, turnover and degradation of gap junctions are very dynamic and the half-life of the gap junctions can be very short, between 1 and 4 hours depending on tissue type (Beardslee et al., 1998; Laird, 1996). The synthesis and assembly of

connexons were demonstrated *in vitro* where they assembled in microsomal membrane and reconstituted in the synthetic lipid bilayers (Falk et al., 1997). The formation of gap junctions starts from the transcription of the connexin gene and the translation of mRNA in the endoplasmic reticulum. Intramolecular disulphide bonds are formed between the cysteine residues in the extracellular loop when the connexins are in the RER (Evans, 1994; Rahman et al., 1993). The connexin proteins oligomerise into connexons and are transported to the plasma membrane via the trans-golgi network (Martin et al., 2001; Musil and Goodenough, 1993). However, alternative pathways may exist as evidence suggests that Cx26 can reach the cell surface independent of the trans-golgi network pathway, as demonstrated after disruption of this pathway using brefeldin A (Evans et al., 1999; George et al., 1999). Alternative trafficking involves a microtubule-dependent pathway (George et al., 1999). Vesicles containing connexons are transported to the membrane where they aggregate to form a gap junction plaque at sites of cell contact, involving microfilaments and regulation by cAMP (Wang and Rose, 1995). The docking of connexons from the two neighbouring extracelluar loops completes the formation of the gap junction (Evans, 1994; Laird, 1996; Rahman et al., 1993) and this can be influenced by adhesion molecules such as N- and E-cadherin (Fujimoto et al., 1997; Jongen et al., 1991; Wei et al., 2005), or ZO-1/β-catenin (Wu et al., 2003). The docking of two connexons is inhibited by the binding of gap junction mimetic peptides to the extracellular loops (Dahl et al., 1992; Warner et al., 1995) or antibodies (Meyer et al., 1992).

In a gap junction plaque, new connexons are added at the edge of the plaque and the older junctions removed for degradation from the plaque centre (Gaietta et al., 2002). The removal involves internalization of gap junctions and degradation of Cx (Guan

and Ruch, 1996; Laing and Beyer, 1995; Laird, 1996; Larsen et al., 1979). The removal of gap junction plaques from the membrane requires endocytosis of gap junctions with two layers of plasma membranes from both cells (annular gap junctions) into one of the two neighbouring cells (Jordan et al., 2001; Larsen et al., 1979). Internalised gap junctions undergo either lysosomal degradation (Guan et al., 1996; Laing et al., 1997) or ubiquitin–mediated proteasomal proteolysis (Laing and Beyer, 1995), depending on cell type and experimental conditions. Regulation of gap junction assembly and degradation is important in modulating intercellular communication.

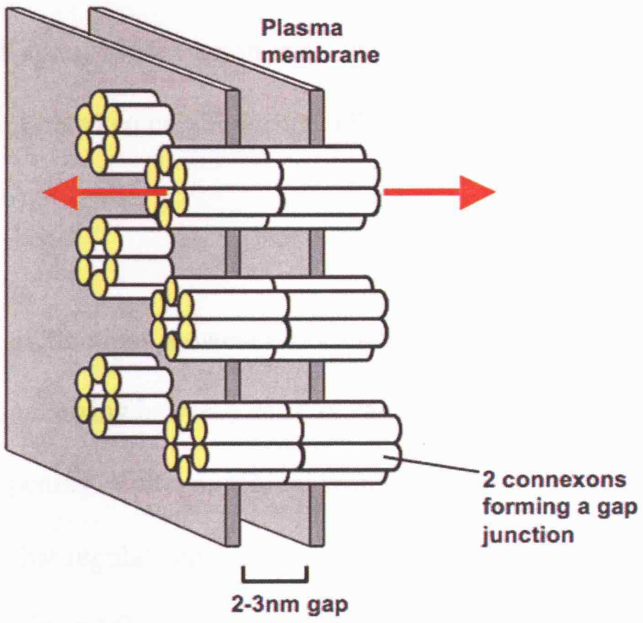

Figure 1.2 Gap junction plaque. Formation of gap junction channels facilitates the direct movement of small ions and secondary metabolites between cells.

1.3.1.5 CHANNEL GATING AND REGULATION

The formation of gap junctions between cells facilitates direct cell-to-cell communication by allowing the direct movement of small ions, metabolites and secondary messengers (Ca^{2+}, IP_3, cAMP, ATP) up to 1 kDa (Carter et al., 1996; Kumar and Gilula, 1996; Saez et al., 1989; Willecke et al., 2002). Except for some terminally differentiated cells such as skeletal muscle, erythrocytes, platelets and mature spermatozoa, most cells do generally express one or more types of connexin, indicating the importance of gap junctional intercellular communication (GJIC) in cell and tissue homeostasis (Kumar and Gilula, 1996). Two classical techniques are used for gap junction functional studies: intercellular dye transfer to monitor the movement of tracers between neighbouring cells (Elfgang et al., 1995; Flagg-Newton et al., 1979; Loewenstein and Kanno, 1964; Payton et al., 1969), and electrophysiological recording of current between neighbouring cells (Chanson et al., 1994; Kanno and Loewenstein, 1966).

The presence of gap junctions, however, does not automatically mean that communication is occurring between cells as various gating mechanisms exist to regulate channel opening. Voltage, pH, calcium and post–translational modifications are among factors that regulate channel opening (Bennett et al., 1978; Turin and Warner, 1977; Unwin and Ennis; Zimmer et al., 1987). Gap junctions composed of different connexins can also exert selectivity on the passing particle, depending mainly on size, charge and hydration state of the particle (Goldberg et al., 2004). For example the dye Lucifer Yellow (molecular weight 453 Da, charge -2) is permeable through Cx32 and Cx43 but not through Cx30 or Cx45 (Manthey et al., 2001; Valiunas et al.,

2002). However, there is no selectivity on monovalent cations such as K^+, Na^+ and Li^+. The regulation of GJIC is highly important as demonstrated in its roles in processes such as neural crest development (Becker et al., 1998; Laird et al., 1992), the synchronisation of heart contraction (Simon et al., 1998), diapedesis (Oviedo-Orta et al., 2002), folliculogenesis (Ackert et al., 2001), electrical coupling between neurons (Nelles et al., 1996) and cell growth and neoplasia (Kanczuga-Koda et al., 2005; King and Bertram, 2005).

Voltage

Voltage gating in gap junctions was first discovered between the blastomeres of *Xenopus* and *Fundulus* (Bennett et al., 1978). Channel conductance can be sensitive to both transjunctional and transmembrane voltage, where increased voltage causes channel closure (Dahl, 1996). Transjunctional voltage can cause rectification, where transjunctional passage of currents in one direction is preferred, as observed at crayfish synapses (Furshpan and Potter, 1959). Heterotypic channels usually have different voltage sensitivity to their homotypic channels counterparts (Barrio et al., 1991; Bruzzone et al., 1994). Multiple regions of the connexin protein have been implicated in voltage gating including both intracellular N- and C-terminae (Moreno et al., 2002; Verselis et al., 1994).

pH gating

Uncoupling of gap junctions due to elevated cytoplasmic acidity was first observed in the *Xenopus* embryo (Turin and Warner, 1977). Most connexins exhibit a variable degree of sensitivity to low pH (Ek et al., 1994; Liu et al., 1993; White et al., 1994a). Intracellular acidification can reversibly inhibit GJIC, possibly a protective response in

pathological situations, in which the damaged cells become isolated from the healthy neighbouring cells. The regulatory sites for pH sensitivity have been shown to locate at the C-terminus of the connexin protein (Ek et al., 1994; Liu et al., 1993; Morley et al., 1996).

Post-translational modification

Other than by physiological gating mechanisms, gap junction regulation can take place at transcription, translation and post-translational stages (Zimmer et al., 1987). Connexin post-translational phosphorylation was first reported in hepatocyte Cx32 (Traub et al., 1987). Connexin phosphorylation at serine and tyrosine residues in the C-tail is thought to be relevant in regulating both connexin life cycle (Musil et al., 1990; Musil and Goodenough, 1991; Wagner et al., 2002) and channel gating (Darrow et al., 1995; Lampe et al., 2000; Lau et al., 1996). Many classes of protein kinases including PKC (Saez et al., 1997), PKA (Kwak and Jongsma, 1996), MAPK (Warn-Cramer et al., 1998) and tyrosine kinases (Filson et al., 1990) are involved in connexin post-translational modification (Figure 1.2). Some tissue specificity in phosphorylation state was observed in Cx43 (Kadle et al., 1991). Most connexins are subject to post-translational modification except Cx26, because its short C-tail contains no sites for modification (Saez et al., 1990).

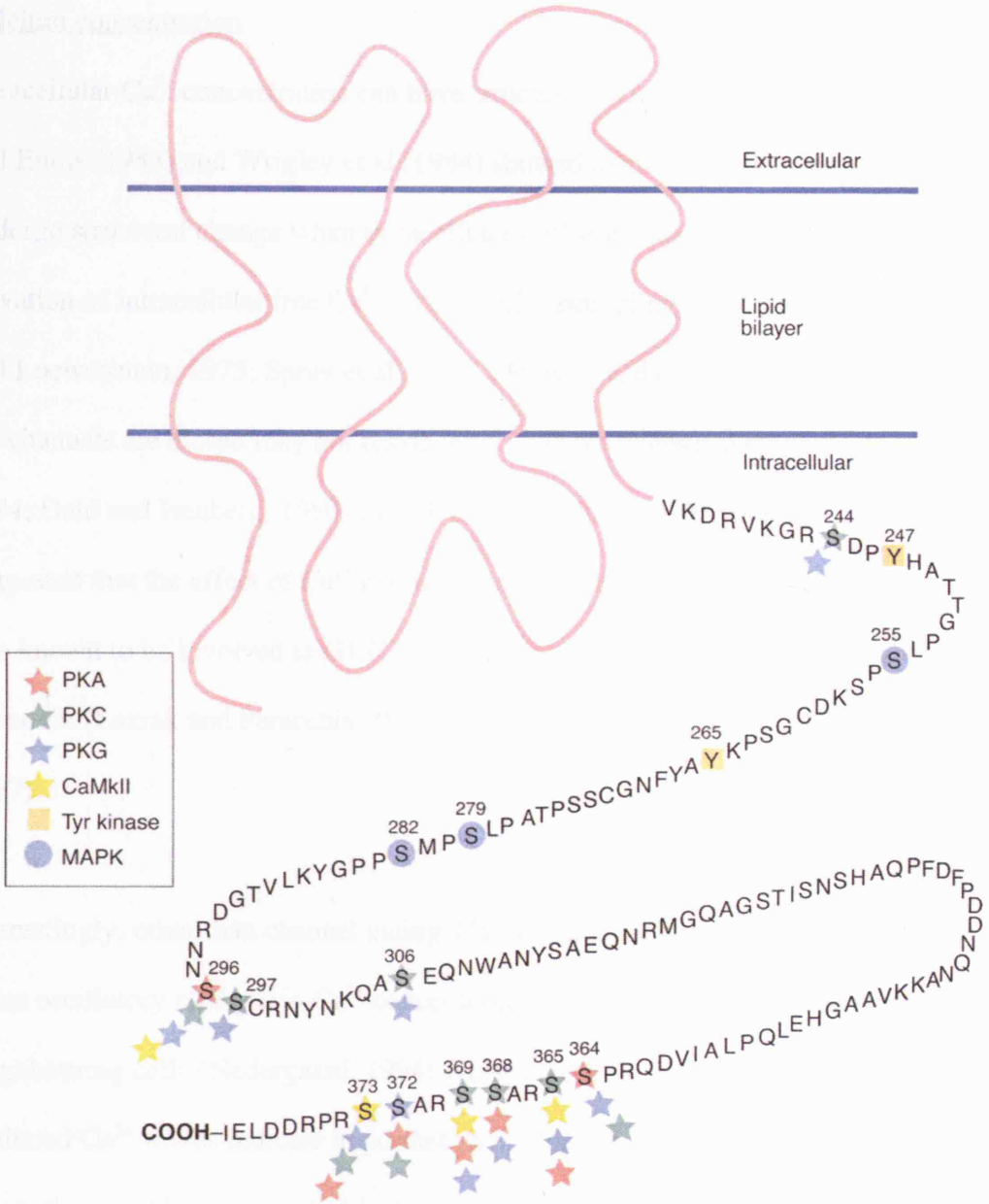

Figure 1.3 Schematic diagram of Cx43 showing post–translational modification sites in the C-tail. The cytoplasmic COOH-tail contains many serine phosphorylation sites for protein kinases. Image taken from Hossain and Boynton (2000).

Calcium concentration

Intracellular Ca^{2+} concentration can have structural and gating effects on GJIC. Unwin and Ennis (1983) and Wrigley et al (1984) showed that mammalian gap junctions undergo structural change when intracellular Ca^{2+} is decreased. On the other hand, the elevation of intracellular free Ca^{2+} induces cell uncoupling and decreases GJIC (Rose and Loewenstein, 1975; Spray et al., 1985). However, the Ca^{2+} concentration at which the channels are closed may not reside within the physiological range (Chanson et al., 1994; Dahl and Isenberg, 1980; Lazrak and Peracchia, 1993; Spray et al., 1985). It was suggested that the effect of Ca^{2+} gating is modulated via calmodulin and PKC, which was known to be involved in GJIC and a binding site in the cytoplasmic side of the connexin (Lazrak and Peracchia, 1993; Peracchia and Bernardini, 1984; Zimmer et al., 1987).

Interestingly, other than channel gating, Ca^{2+} can diffuse through gap junctions that cause oscillatory changes in Ca^{2+} concentrations (Ca^{2+} wave propagation) in the neighbouring cells (Nedergaard, 1994; Weissman et al., 2004). The gap junction mediated Ca^{2+} waves indicate important physiological roles in neuron-astrocyte interactions and hearing control in the cochlea of the inner ear (Sun et al., 2005; Zhang et al., 2005).

1.3.2 Hemichannels

Prior to docking and formation of gap junctions, pools of connexons or hemichannels are found in the plasma membrane. The classic view was that hemichannels were generally closed to avoid cell content leakage. This proposal was challenged recently

in experiments which demonstrated the existence of hemichannels with functional openings (Dermietzel et al., 2003; Saez et al., 2003). The positive uptake of tracer dyes such as LY, calcein, fura-2 and propidium iodide from the culture media indicated hemichannel opening in different cell types such as astrocytes and cardiac myocytes (Contreras et al., 2003; John et al., 1999; Valiunas et al., 2002). The opening of hemichannels appears be regulated by calcium and has multiple functions in intercellular signalling by the release of ATP and the propagation of calcium waves in different cell types (Braet et al., 2003; De Vuyst et al., 2006; Gomes et al., 2005; Stout et al., 2002; Weissman et al., 2004).

The gating mechanism of hemichannels remains unclear but hemichannel signalling has been implicated in many physiological conditions (Cherian et al., 2005; Stout et al., 2002; Ye et al., 2003). Mechanical stimulation was shown to induce hemichannel opening in astrocytes (Stout et al., 2002) and osteoblasts (Romanello et al., 2003). The release of glutamate via hemichannels has a great influence in the extent of ischemia in the central nervous system (Ye et al., 2003). In addition, the discovery that shear stress induced release of prostaglandin E_2 by osteocytes further raised the dimensions of hemichannel functionality (Cherian et al., 2005).

1.3.3 Connexins in diseases

Point mutations in different connexins can result in the development of disease with a wide spectrum of clinical manifestations (Richard, 2000) including erythrokeratoderma variabilis (mutation in Cx31), syndromic and non–syndromic deafness caused by mutation in Cx26 (Kelsell et al., 1997; Maestrini et al., 1999;

Richard et al., 1998b), congenital cataracts (Mackay et al., 1999), sex-linked Charcot-Marie-Tooth disease with Cx32 mutations (Bergoffen et al., 1993) and congenital heart malformations or oculodentodigital dysplasia with Cx43 mutation (Britz-Cunningham et al., 1995; Paznekas et al., 2003). The link between connexin gene mutations and inherited defects was extended by the study with Cx43 knockout mouse which die at birth owing to the right ventricular outflow tract obstruction by abnormal formation of myocardial septae (Reaume et al., 1995). In the adult heterozygote ($Cx43^{+/-}$), the ventricular epicardial conduction was reduced (Guerrero et al., 1997). The wide range of disease phenotypes from connexin mutations indicates the importance of GJIC in the normal functioning of tissues (Table 1.2).

Table 1.2 Mutation in connexins result in a large spectrum of diseases. (Adapted from (Bruzzone et al., 1996; De Maio et al., 2002; Willecke et al., 2002)

Connexin	Human diseases	References
Cx26 (*GJB2*)	Dominant and recessive nonsyndromic deafness, Palmoplantar keratoderma, Vohwinkel syndrome, KID	(Kelsell et al., 1997)
Cx30 (*GJB6*)	Dominant hearing loss, Palmoplantar keratoderma	(Kelsell et al., 2001)
Cx30.3 (*GJB4*)	Dominant erythrokeratoderma variabilis (EKV), non–syndromic hearing loss	(Macari et al., 2003; Richard et al., 2003)
Cx31 (*GJB3*)	Recessive non–syndromic hearing loss, EKV, peripheral neuropathy	(Kelsell et al., 1997; Richard et al., 1998a)
Cx32 (*GJB1*)	X-linked Charcot-Marie-Tooth (myelin disruption and axonal degeneration)	(Bergoffen et al., 1993)
Cx43 (*GJA1*)	Visceroatrial heterotaxia, autosomal dominant oculodentodigital dysplasia	(Britz-Cunningham et al., 1995)
Cx46 (*GJA3*)	Autosomal dominant congenital cataracts	(Mackay et al., 1999)
Cx50 (*GJA8*)	Autosomal dominant congenital cataracts	(Kelsell et al., 1997)

1.4 Connexins in the skin

Nine different connexins are differentially expressed in the skin (Butterweck et al., 1994; Di et al., 2001; Richard, 2000; Risek et al., 1994). In rodent epidermis, Cx40, Cx43 and Cx45 are found in the suprabasal layer keratinocytes, whereas Cx26, Cx30, Cx30.3, Cx31 and Cx37 are found at low levels in the differentiating spinous to granular layer keratinocytes. Cx31.1 is associated with terminal differentiation and therefore found in the upper granular layer of the epidermis (Brissette et al., 1994). Skin appendages including hair follicles and sebaceous glands express Cx31, Cx40 and Cx43, while Cx37, Cx40 and Cx43 are found in the microvascular and smooth muscle system (Richard, 2000). Cx43 is also expressed in dermal fibroblasts, making it the predominant connexin in the skin and found in high levels in the epidermal basal layer, in the dermal fibroblasts and the skin appendages including hair follicles, sweat glands and blood vessels (Salomon et al., 1994; Tada and Hashimoto, 1997). Connexins are involved in skin and hair development (Kamibayashi et al., 1993; Risek et al., 1992) but the significance of the complex distribution and expression pattern of connexins in skin requires further investigation. Nevertheless, genetic disorders of skin resulting from point mutations in connexins has emphasised the importance of connexins in skin homeostasis.

One such role of connexins is demonstrated in the protective function of skin. Epidermal keratinocyte differentiation depends greatly upon the calcium gradient that exists in the epidermal layers, which is at low Ca^{2+} levels in the basal layer and high levels in the granular layer (Elias et al., 1998). The presence of Ca^{2+} induces keratinocyte differentiation and stratification that is fundamental in the formation of

the protective stratified squamous epithelium in response to friction. The change in Ca^{2+} concentration coincides with the switch of connexin expression in the epidermal layers that is thought to allow the gradient formation (Brissette et al., 1994; Risek et al., 1994; Wiszniewski et al., 2000). For instance, expression of Cx26 has been associated with hyperproliferative keratinocytes as well as epidermal differentiation (Labarthe et al., 1998; Lucke et al., 1999). Studies using transgenic mice also revealed valuable information about Cx in skin homeostasis; for instance mice with Cx43 protein C-terminus truncation revealed a defective epidermal water barrier (Maass et al., 2004).

The roles of connexins in signalling and cellular processes are slowly emerging in skin. Furthermore, the dynamic expression of connexins after skin injury indicates multiple roles in the overlapping processes involved in restoring skin integrity (Coutinho et al., 2003; Goliger and Paul, 1995; Kretz et al., 2003; Qiu et al., 2003). This will be reviewed in detail in the following sections.

1.5 Connexins and wound repair in the skin

Connexins have been shown to have a regulatory role in several aspects of wound repair including initiation and synchronisation of cell migration (Cao et al., 2002; Coutinho et al., 2003; Ehrlich and Diez, 2003; Kretz et al., 2003; Moyer et al., 2002). After injury, the activated keratinocytes, dermal fibroblasts and recruited leukocytes must work together to ensure a swift and accurate tissue repair to reseal the skin. The expression of connexins Cx26, Cx30, Cx31.1 and Cx43 in the leading edge epidermis changes dynamically after skin injury and the changes have been associated with the different phases of wound healing process (Coutinho et al., 2003; Goliger and Paul, 1995).

Connexins (Cx26, Cx30, Cx31.1 and Cx43) are differentially regulated in the epidermal wound edge after injury and they gradually revert to normal levels after the completion of re-epithelialisation (Coutinho et al., 2003; Mori et al., 2006). After wounding, Cx26 and Cx30 protein expression upregulates at the wound edge epidermis, reaching the maximum expression during epithelial migration after injury and thereafter returning back to normal levels as the wound heals (Coutinho et al., 2003; Kretz et al., 2003). Cx43 protein expression is initially downregulated between 1-2 days, and gradually increased behind the wound edge of the epidermis around 2-4 days, reaching maximum at day 4 before returning to normal levels in the nascent epidermis. Cx31.1 protein expression in the upper granular epidermis increases 4 days after wounding and remains high during nascent epidermal stratification stage (Coutinho et al., 2003; Goliger and Paul, 1995). High levels of Cx43 protein expression was found in proliferating keratinocytes behind the wound edge epidermis

4 days after injury (Coutinho et al., 2003). Cx26 was shown to associate with hyperproliferative epidermis, in particular those in the nascent epidermis (Goliger and Paul, 1995; Labarthe et al., 1998). Normally Cx26/Cx30 expression is restricted to the spinous layer and Cx43 expressed at the basal layer of the epidermis, to allow the formation of calcium gradient required for epidermal differentiation. The high Cx26/Cx30 expression throughout the nascent epidermis after injury has been proposed to prevent the formation of calcium gradient associated with epidermal differentiation before epidermal migration has completely closed the wound (Kretz et al., 2004).

The regulation of connexin expression during wound healing must be dynamic to respond to the changes and the progression of wound repair. The temporal regulation of Cx43 was attributed to post-translational phosphorylation of serine 368 (s368) residue in the C-terminus of the protein (Richards et al., 2004). The level of phosphorylation by Protein Kinase C (PKC) at s368 significantly increased in basal keratinocytes near the wound edge after a scratch wounding. The phosphorylation of Cx43 s368 residue created an epidermal compartment at the wound edge that transferred GJ permeant dye differently (Richards et al., 2004). The formation of the compartment was proposed to be important in the synchronisation of epidermal leading edge migration. Recently, transcription factor Activator Protein - 1 (AP-1) subunits were also shown to regulate the down and upregulation of Cx43 gene expression and inflammatory response during wound repair (Neub et al., 2007). However, different factors are likely be involved in regulation of different connexins in response to injury.

The knockdown of Cx43 protein expression with antisense oligodeoxynucleotides (Cx43-asODN) in excisional, incisional and burn wounds (Coutinho et al., 2005; Mori et al., 2006; Qiu et al., 2003), and mice deficient of Cx43 offered interesting information in the role of Cx43 in skin wound repair (Kretz et al., 2003). The rates of re-epithelialisation after wounding in skin wounds treated with Cx43-asODN (Mori et al., 2006; Qiu et al., 2003) and the wounds of transgenic mice with inducible Cx43 gene deletion (Kretz et al., 2003) were accelerated. However, no changes in the wound healing process were reported in Cx30 and Cx31 knockout mice (Kretz et al., 2003). This suggested the importance of Cx43 during the wound healing process, in particular the re-epithelialisation. Downregulation of Cx43 protein expression in the wound edge keratinocytes was observed in normal wounds and those treated with Cx43-asODN, both of which began re-epithelialisation once Cx43 protein expression was lowered. Interestingly, in human *ex vivo* venous ulcers where wound closure was delayed, Cx43 protein remained highly expressed in the wound edge epidermis (Brandner et al., 2004). The reduction or the absence of Cx43 protein in the wound edge epidermis immediately after injury appeared to be important to initiate the keratinocyte migratory processes (Kretz et al., 2003; Qiu et al., 2003).

Transient knockdown of Cx43 expression using asODN not only accelerated the natural downregulation of the connexin expression in the wound edge epidermis but also Cx43 expression in the surrounding tissue in the first 24 hours after injury. However, the effect of the knockdown could be observed in the downstream wound healing cascade, beyond 24 hours. The previously mentioned faster re-epithelialisation was observed many days after wounding when the effect of asODN had already worn off. Interestingly, knockdown of Cx43 expression also had a considerable effect on the

inflammatory response after injury. The recruitment of neutrophils and macrophages was reduced in the wound region, as well as lowered levels of chemokines TNF-α and CCL-2, and increased expression of TGF-β in the keratinocytes and fibroblasts (Mori et al., 2006; Qiu et al., 2003). The application of Cx43-asODN in the wound will have knocked down Cx43 expression in many cell types in the skin including keratinocytes, fibroblasts and endothelial cells which all play a part in the wound healing process. However, how the initial knockdown of Cx43 expression brought by the later changes in the healing cascade, even during granulation tissue maturation is not known (Mori et al., 2006; Qiu et al., 2003).

1.6 Hyperglycaemia and connexins

The expression of connexins in diabetic conditions has not been studied extensively. However, the available literature suggests that diabetes or hyperglycaemia does affect connexin expressions either *in vivo* or *in vitro* (Kuroki et al., 1998; Li et al., 2003; Oku et al., 2001; Pitre et al., 2001; Sato et al., 2002). These data suggest that hyperglycaemia can cause a differential regulation of connexins at transcriptional, posttranslational or degradation stages for the different cell types that were examined.

An early study of aortic smooth muscle cells cultured in hyperglycaemic conditions showed that they have reduced gap junctional intercellular communication via Cx43 gap junctions (Kuroki et al., 1998). However, Western blot analysis showed no change in the total Cx43 protein content but an increased ratio of phosphorylated P3 form corresponding to a reduction in non-phosphorylated P0 form Cx43 proteins. The

phosphorylation ratio was brought back to normal when the cell culture was incubated with a PKC inhibitor calphostin C, and the rate of GJIC was restored (Kuroki et al., 1998). It is generally known that hyperglycaemia induces a persistent activation of PKC (Xia et al., 1994). Kuroki et al (1998) suggested that excess PKC activity could cause the reduced GJIC in the cells in hyperglycaemic conditions via post-translational regulation. Another group of researchers observed that in rat microvascular endothelial cells that are commonly affected in diabetes, Cx43 was significantly reduced at the protein and mRNA level, suggesting hyperglycaemia can also reduce GJIC by inhibiting Cx43 gene expression (Sato et al., 2002). Interestingly Cx37 and Cx40, also expressed in the endothelial cells (Sato et al., 2002), did not show any expressional changes in hyperglycaemic conditions, implying a differential regulatory effect of hyperglycaemia on expressions of different connexins.

Many studies observed a downregulation of connexin protein expression in cells in different diabetes models (Chang et al., 2005; Li et al., 2003; Pitre et al., 2001; Sato et al., 2002). Cultured human and bovine retinal pericytes had reduced Cx43 mRNA and total Cx43 protein content, corresponding to reduced number of connexin plaques (Li et al., 2003). Similar reduction in Cx43 protein was found in cultured bovine retinal endothelial cells (Fernandes et al., 2004) and oocytes of diabetic mice (Chang et al., 2005). Decreased Cx32 and Cx26 expressions were observed in diabetic rat perineurium (Pitre et al., 2001). In addition to post-translational regulation via PKC, an abnormality in degradational control could also downregulate Cx43 expression. In the bovine retinal endothelial cells GJIC was rescued by a proteasome inhibitor MG132 and lactacystin, suggesting downregulation may also occur in a protease dependent manner (Fernandes et al., 2004).

The changes in connexin expression could be observed within days after the onset of diabetes (Oku et al., 2001; Pitre et al., 2001). The abnormal connexin expression in diabetes or hyperglycaemia has been proposed to have a detrimental effect on tissue homeostasis (Chang et al., 2005; Li et al., 2003; Pitre et al., 2001). Using whole retina freshly isolated from streptozotocin induced diabetic rats, Oku et al (2001) showed reduced GJIC in the retinal microvessels in the diabetic rats but not in those receiving insulin. Abnormal cellular organisation was observed in the diabetic microvessels with disrupted cell coupling. Authors suggested that the GJIC disruption may have led to the metabolic isolation of pericytes causing cell death and diabetic retinopathy. The hyperglycaemia-induced change in connexin expression could cause tissue dysfunction in diabetes disease complications.

Nevertheless, hyperglycaemia does not always reduce GJIC or connexin expression in tissue. As already mentioned, Cx37 and Cx40 expression was not affected in hyperglycaemic endothelial cells when Cx43 was (Sato et al., 2002). Indeed, Abdullah et al. (1999) have demonstrated greater GJIC and increased Cx43 protein expression in human diabetic skin fibroblasts grown *in vitro* compared to normal fibroblasts. At the same time, the authors noted a reduced cell doubling time in the diabetic fibroblast cultures, suggesting that an increase in cell coupling may correlate with a decrease in rate of proliferation. Evidently, diabetes and hyperglycaemia have a profound effect on connexin expression and GJIC via multiple regulatory mechanisms for different connexins and cell types. More research is required to fully understand the abnormal regulatory mechanisms that control connexin expressions. This may elucidate

therapeutic intervention to prevent the development of tissue dysfunctions related to diabetes.

1.7 Diabetic wounds and connexins

Different factors may account for the delayed wound healing in diabetes and the development of chronic wounds as described in Chapter 1.2.6. Clearly, connexin expressions and GJIC are affected by elevation in glucose concentration in the environment (Fernandes et al., 2004; Kuroki et al., 1998; Oku et al., 2001; Sato et al., 2002). The dynamic regulation of connexin expression during wound healing is important but very little is known about connexin expression in diabetic wounds. Two papers from the same group have identified abnormal connexin expressions in the wound edge epidermis (Brandner et al., 2004; Brandner et al., 2007). Brandner et al (2004) described an abnormal persistent expression of Cx26, Cx30 and Cx43 in the human *ex vivo* model of chronic venous/diabetic ulcers. Loss of dynamic regulation in connexin expression in wound can have a profound effect on the rate of wound closure. My PhD project aims to study the dynamics connexin expressions during diabetic wound repair in order to further understand the roles of connexins in wound healing.

1.8 Aims of the thesis

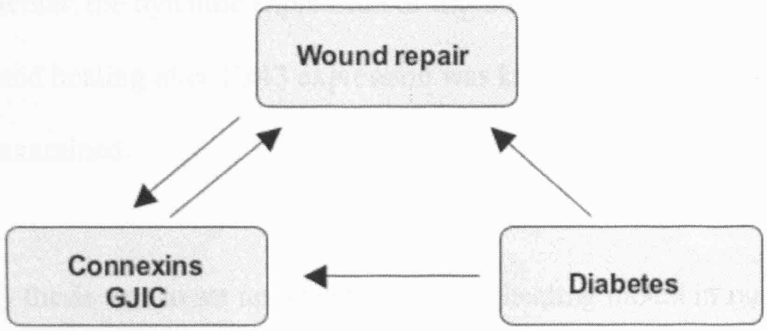

Figure 1.4 Interactive relationship between wound repair, connexins and diabetes. The direction of arrow indicates direct or indirect influence of a component on another. Diabetes was shown to affect the wound repair process and the normal connexin expressions in various tissue types. Connexins are important in wound repair processes and the microenvironment of cytokines can in turn regulate connexin functionality.

Wound healing is a complex process involving many cell types working together and communication is pivotal to ensure correct and swift tissue repair. However, diabetic wound repair is delayed and often becomes chronic which is detrimental to patient wellbeing. Gap junction intercellular communication and the dynamic expression of connexin proteins were shown to be important in the wound healing process and the homeostasis of skin. The dynamics of Cx43 expression during wound healing can have a significant consequence on the inflammatory response and the subsequent healing events. Conversely, cytokines in the wound microenvironment can also exert regulatory control on connexins (Hossain et al., 1998; Hossain et al., 1999). A fine

balance in communication via both cytokines and gap junctions are required for a rapid wound repair. Furthermore, diabetes evidently has a profound effect on both gap junctions and the progression of wound repair (Figure 1.4). The relationship between connexin expressions in diabetic skin and diabetic wound healing is explored in this thesis. In particular, the dynamic expression of Cx43 in diabetic wounds and the quality of wound healing after Cx43 expression was knocked down using Cx43-asODN were examined.

The aim of my thesis was to set up a diabetic wound healing model in rats to elucidate the effect of diabetes on connexin expression in the skin and wounds. I have examined the expression of Cx26, Cx30 and Cx43 protein in unwounded diabetic skin of the back and heel, following on to study the dynamic expression of Cx26 and Cx43 proteins the wound healing process. These results are presented in Chapters 3 and 4.

The knockdown of Cx43 expression using antisense oligodeoxynucleotide immediately after injury significantly improved the rate and the quality of wound healing in normal skin wounds (Coutinho et al., 2005; Mori et al., 2006; Qiu et al., 2003). In Chapter 5 I present the effect of Cx43-asODN treatment in diabetic wounds.

The endothelial cells, in the early inflammatory phase of the wound healing, play an important part in controlling vessel permeability and leukocyte transmigration processes. The involvement of Cx43 in blood vessel leakiness after injury was investigated and reported in Chapter 6. A critical analysis on the implications of my data is detailed in the final discussion Chapter 7.

2 MATERIALS AND METHODS

2.1 Animals

In order to assess the effect of diabetes on connexin expression in skin and wound healing, Wistar (Royal Free Hospital, UCL) or Sprague-Dawley (UCL breeding colony originally from Harlan, UK) rats were used in this thesis. Rats were used as they are an established model for diabetes and have a good success rate for diabetes induction using streptozotocin (Franzen and Roberg, 1995; Szkudelski, 2001; West et al., 1996). Adult male Wistar and Sprague-Dawley (SD) rats (350-400 g) were used to quantify Cx26, Cx30 and Cx43 expression in uninjured back and heel skin and dye transfer studies. For wound healing studies adult male SD rats of 350-400 g were used. Weight matched rats were used as controls. All the animals were kept according to the UK Home Office Animals (Scientific Procedures) Act 1986 Code of Practice. The animals were housed in 12 hours light and dark cycles in a climatically controlled room with free access to water and food.

Acute diabetes was induced in the rodents by one intraperitoneal injection of streptozotocin (65 mg/kg). Preparation of streptozotocin for injection was carried out according to the methods of Shotton et al. (2003). Streptozotocin (Sigma, Poole, UK) was made up in 20mM citrate buffer (pH 4.6) to reach the concentration of 100mg/ml. Citrate buffer was made up of 20 mM citric acid and 20 mM sodium citrate which was used to adjust the pH level. Each animal was weighed before the injection. As an example, a 350 g rat will receive 227 µl of streptozotocin (100 mg/ml), injected intraperitoneally using a 0.8x40 mm, number 21 gauge needle without any anesthetics. No obvious discomfort was observed in the rats immediately after injection. Rats were

housed, at maximum three rats per cage, for a further two or eight weeks before wound or intact skin studies respectively. Diabetes was confirmed 3 - 5 days after streptozotocin injection using urinary glucose strips (Clinistix, Bayer, Newbury, UK). The rats were weighed every other day to monitor weight loss due to diabetes induction. No more than 20% of weight loss was allowed or the animal would be terminated immediately. The cages were cleaned and water bottles refilled more frequently as diabetic rats drink and urinate more frequently than control rats. Precise blood glucose level was taken from diabetic and control animals at the time of killing using ACCU-CHEK Advantage test strip with ACCU-CHEK Advantage systems (Roche Diagnostics, Mannheim, Germany). Blood glucose levels typically range from 4.5-5.5 mmol/L in control and 27-32 mmol/L in diabetic animals. Diabetic animals with blood glucose less than 22 mmol/L were excluded from the experiments.

2.2 *In vivo* scrape loading dye transfer

Scrape loading dye transfer experiments were carried out in freshly excised Wistar normal and 8-week diabetic rat skin. Control experiments with different tracers and gap junction blocker were also carried out in 2-week diabetic rats. Small pieces of gel foam were soaked with 10 μl of dye solution and placed into a fresh wound. In initial experiments, 4% Lucifer Yellow (LY) CH dilithium salt (MW 453 Da, Sigma, Poole, UK) was allowed to transfer for 1, 2 and 5 minutes (min) and the skin was immediately fixed in 4% paraformaldehyde for 30 min in room temperature (Goliger and Paul, 1995). Tissues were then frozen in Tissue-Tek O. C. T. (Sakura, Zoeterwoude, Netherlands) for cryosectioning and imaging. The optimal time for dye

transfer was identified to be 5 min after a preliminary study, and in the subsequent experiments the dyes were allowed to diffuse for 5 min. To distinguish dye transfer via gap junctions from diffusion through extracellular space, 10 µl of gap junction blocker octanol was added to the excision for 2 min prior to LY (Harks et al., 2001; Mantz et al., 1993). To demonstrate that molecules smaller than 1kDa pass diffuse through the cells via gap junctions, a combination of water soluble cascade blue (8-methoxypyrene-1,3,6-trisulfonic acid, trisodium salt, Molecular Probes) and 10 kDa Dextran-FITC (4%, Sigma, Poole, UK) which is too large to travel through GJ was placed in the incision. To demonstrate that LY indeed did pass intercellularly through GJs, an unfixable form of LY, LY-methoxycarbonyl (Molecular Probes), was used as only the dye inside the cells will be retained and the dye in the extracellular space will be not be fixed in place and washed away during rinsing. This method would only indicate LY based the GJIC.

2.3 *In vivo* excisional wound model

SD rats two weeks after diabetes induction and weight matched normal healthy rats were used for the *in vivo* excisional wounds. Anaesthesia was induced by inhalation (halothane 5% mixed in 20% oxygen and 10% nitrogen) and was maintained at 1.5% halothane with constant monitoring. The back of the rat was shaved and wiped with a tissue soaked in 70% ethanol. Wound positions were measured and marked 3 cm from the neck and 5 mm away from the midline (Figure 2.1). Four 5x5 mm boxes were outlined, 1 cm apart from each other. Full thickness excisional wounds were made with a sterile number 15 scalpel blade (Swann-Morton, Sheffield, UK) then 50 µl of

cold control sense or antisense oligodeoxynucleotide pluronic gels were applied immediately into the wound. For details of oligodeoxynucleotide and pluronic gel preparations see chapter 2.9.1 and 2.9.2. Animals were allowed to recover in a heated chamber where they awaken normally within 10-15 min after operation.

Skin and wound samples were collected at 1, 2, 5, 10 and 15 days post wounding. At the time of tissue collection, animals were terminated by Schedule 1 method with an overdose of chloroform and cervical dislocation in accordance with UK Home Office Animals (Scientific Procedures) Act 1986 Code of Practice. A minimum of six animals was used in each control and diabetes groups for each time point.

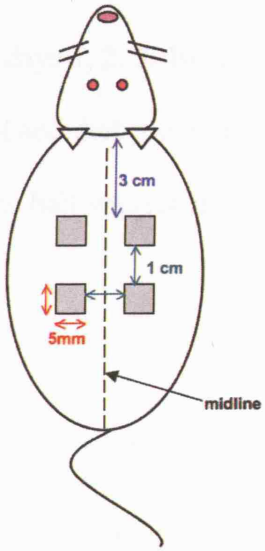

Figure 2.1 Schematic diagram of the in vivo excisional wound set up. Two pairs of full thickness 5x5 mm excisional wounds were made on the shaved back of SD rats as diagrammed (not to scale). The wounds were positioned 3 cm from the neck down the midline and 1 cm apart from each other.

2.4 Tissue collection and processing

2.4.1 Tissue collection

To isolate intact (uninjured) back skin, a fresh area of back was shaved and small pieces of skin approximately 5x3 mm excised and snap frozen in Tissue-Tek O. C. T. (OCT) using dry ice. Heel skin (Figure 2.2) was also excised and frozen in OCT immediately. Back skin and heel skin used in the first connexin quantification experiments was collected eight weeks after diabetes induction in male Wistar rats under the same procedures. These diabetic skin samples were collected by Dr Jill Lincoln. Six animals were used in each control and diabetic group.

Wound samples were excised carefully with at least 5 mm of skin around the wound edges. Tissues were collected on days 1, 2, 5, 10, 15 days post wounding (dpw). Six animals were used in each control and diabetic group for each time point. The wounds were bisected horizontally and one half was fixed in 4% paraformaldehyde and the other half frozen in OCT.

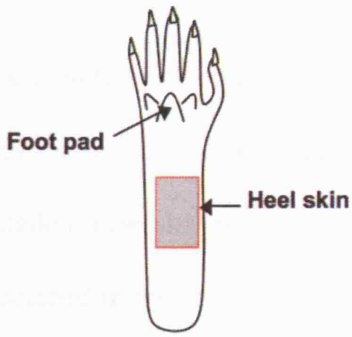

Figure 2.2 Diagram of a rat foot for heel skin collection. Heel skin identified as flat skin found below the footpads of the underside of the foot (marked with the red box).

2.4.2 Tissue cryosectioning

All tissue blocks (back, heel and wounds) were sectioned using Leica cryostat (JUNG CM3000) in chamber temperature –19°C. Each tissue section was cut at 10-12 μm and mounted onto gelatin subbed microscopic slides. The slides were dried briefly at room temperature before storing in –20°C until use.

2.4.3 Gelatin coated microscopic slides

Gelatin solution was made of 0.5% gelatin (Sigma, Poole, UK) and 0.05% of chromic potassium sulphate (BDH, Poole, UK) distilled water. Water was first heated to approximately 50°C to dissolve the gelatin and chromic potassium sulphate was only added after all the gelatin has dissolved. Slides were coated by dipping into the solution and allowed to air dry for 30 min. The slides were coated in a total of three times and allowed to dry in a hot oven.

2.5 *In vivo* blood vessel permeability assay

The leakiness of the blood vessels in the wound region in control, diabetic wounds and those treated with Cx43-asODN was examined. Four pairs of full thickness incisional wounds of 5mm length were made on the shaved backs on the rats in a similar pattern to excisional wound model described in the previous section. Pluronic gel containing sODN or asODN (10 μM) were applied to the wounds (N = 4 for each group). At 3 hours after wounding 300 μl of FITC-BSA (3% solution in PBS, Sigma) was injected

into the tail vein of the rat using a 27 gauge needle (modified from (Yamaki et al., 2002). The FITC-BSA was allowed to circulate in the rats for 1 hour and the animals were killed 4 hours after the wounding for tissue collection.

The wounds were cryosectioned and mounted with Citifluor (Citifluor, UK) and imaged using a confocal microscope. Five optical section images were taken adjacent to the wound and another taken approximately 300 μm away (Figure 5.4) for each animal. Subsequently the images were analysed using NIH ImageJ software. A standard threshold was set for the images to eliminate background and binary images were generated. All positive pixels were counted to show the amount of FITC-BSA present in the wound regions.

2.6 Human Umbilical Vein Endothelial Cells (HUVECs) culture

Both freshly isolated HUVEC cells from umbilical cords and commercially pooled HUVEC (TCS CellWorks) were used in the experiments. The unpooled primary cells were used at passage 2 whereas commercial cells were used between passages 4-6. When the cells reached confluence in a T25 flask they were detached using 0.025% trypsin. The cells were typically seeded to three gelatin coated 6-well plates or 24-well plates containing Thermanox plastic coverslips (Nunc, Thermo Fisher Scientific) and used once they reached 100% confluency in the wells. HUVECs do not grow on glass substrates, even those coated with gelatin. Plastic coverslips (Thermanox, Nunc) were used for immunofluorescent staining and microinjection studies.

2.6.1 Primary HUVECs isolation

All umbilical cords were acquired anonymously from healthy deliveries in Macedonio Melloni Hospital, Milan, Italy with informed consent provided according to the Declaration of Helsinki. HUVECs can be isolated from umbilical cords up to 4 days old that were kept at 4°C.

The isolation protocol was modified from Jaffe et al. (1973) and Tremoli et al. (1993). Briefly, the cord was trimmed from both ends and a large needle was inserted into the vein from one end and clamped into place. There are three blood vessels in an umbilical cord; umbilical vein is the largest blood vessel of three. The vein was first washed to remove blood clots and this was done by connecting a syringe to the inserted needle and perfusing 50 ml of PBS through. After rinsing, the vein was canalized by fixing another needle to the other end of the cord, and 10 ml of collagenase (0.2%, Sigma) was injected into the vein to dissociate the cells. To enhance dissociation, the whole cord was placed in 37°C water bath and incubated for 3min. The cord was massaged throughout to make sure the endothelial cells were completely detached, and the collagenase was squeezed out and collected in a 50 ml falcon tube containing 10 ml of HUVEC growth medium to inactivate the collagenase. A further 30 ml PBS was used to flush the vein to collect remaining cells for maximum yield. The endothelial cells were then collected by centrifugation at 12000 rpm for 10 min at 4°C. The supernatant was aspirated away and the cell pellet resuspended with HUVEC growth medium and plated on gelatin (0.2%) precoated flasks. Each 10 cm of umbilical cord can be seeded into one T25 flask. The cells were grown in 37°C incubator with 5% CO_2. The cells were washed the next day to remove red blood

cells and new medium was added. The cells were then allowed to grow to confluency, usually within 3-5 days.

2.6.2 Gelatin for substrate coating

A solution of 0.2% of gelatin was made in sterile distilled water. Six-well plates were coated with 1 ml of gelatin and 24-well plates received 500 µl each. Gelatin was left in the wells for 30 min for coating and then aspirated away. The cells were seeded directly and no washing or drying of the gelatin substrate was required.

2.6.3 HUVEC culture media

HUVECs growth medium was made of M199 (BioWhittaker BE12-117F, contain EBSS, L-glutamine, HEPES) containing 10% human serum (Maggiore Hospital, Milan, Italy or 20% fetal calf serum), 2 mM L-glutamine, 15 µg/ml Heparin (Sigma), crude endothelial cell growth factor (ECGF) extract from homogenized bovine brain 50 µg/ml (provided by the technician in Dept of Pharmacology in University of Milan), antibiotics (500 U/ml penicillin, 50 µg/ml streptomycin and 100 µg/ml neomycin). Growth medium was changed every other day and replaced with a medium without ECGF and Heparin one day before experiments. For experiments a "treatment" medium was used. Treatment medium was made with M199 containing 2 mM L-glutamine, antibiotics, 10% FCS and 0.75% BSA.

2.7 HUVECs injury model

Confluent HUVECs were incubated in a treatment medium containing histamine (100 nM or 1 μM) as an injury stimulus with or without a gap junction manipulator for 3, 6 and 24 hours (see Table 2.1).

When cells were treated with Cx43-asODNs the serum was omitted in the treatment medium to prevent ODN degradation by enzymes in the serum. At the end of the time point cells were washed twice with PBS and collected in lysis buffer for Western blot or those grown on plastic coverslips fixed in cold ethanol for 1 min. For ELISA, medium was collected and kept frozen in -20°C and the cells were collected using ELISA homogenizing buffer (see Chapter 2.15).

Table 2.1: List of gap junction manipulators used in the HUVEC injury model

Agent	Origin	Stock	Diluent	Working concentration
GAP27 mimetic peptide (sequence: SRPTEKTIFII)	Genescript (Custom made)	30mM	DMSO/ dH_2O	600 μM
NS398 (COX-2 inhibitor)	Cayman 70590	100mM	DMSO	10 μM
Cx43-asODN	Sigma-Genosys (Custom made)	1mM	DEPC dH_2O	25 μM + 25 μM

2.8 Endothelial cell in vitro permeability assay

HUVEC cells were seeded on culture inserts (Costar, 3 μm pore size) made for 24-well plates, in the upper chamber, and checked regularly using phase contrast microscopy to make certain that they were confluent before use (Figure 2.3). On the day of the experiment, the medium in the lower chamber was replaced with 500 μl of treatment medium. Media in the upper chamber was replaced with 200 μl of treatment medium containing FITC-BSA (100 ng/ml, Sigma, Poole, UK), stimulus and gap junction manipulator according to the experimental plan. FITC-BSA used as a tracer for endothelial cell permeability because albumin is a protein naturally found in the blood and does not normally leak out. The fluorescent tag allowed easy quantification of leakage using a microplate reader. FITC-BSA was allowed to diffuse from the upper chamber through to the lower chamber in the presence of histamine with or without manipulators (Table 2.1). Medium was collected from each upper (10 μl) and lower (50 μl) chamber at 3, 6 and 24 hours after incubation. To measure the amount of FITC-BSA in the chambers, samples were diluted 1:50 using distilled water, loaded in black walled 96-well plates in duplicates. The amount of fluorescence was read using a fluorescent microplate reader (Victor^2 1420 Multi label Counter, Perkin Elmer) with a Fluorescein protocol of excitation wavelength 485 nm (0.1 s) and emission 535 nm bandpass filter. Samples were loaded alongside a standard curve made of dilutions with stock FITC-BSA (2 ng/ml, 1 ng/ml, 0.5 ng/ml, 0.25 ng/ml, 0.125 ng/ml, 0.0625 ng/ml) for reading. Output data were viewed using Wallac 1420 Manager software and exported to spreadsheets for calculations.

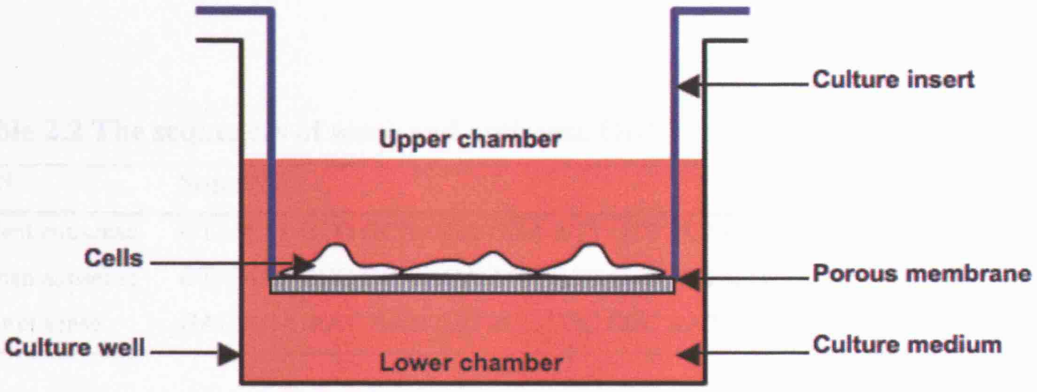

Figure 2.3 Diagram of in vitro permeability assay with HUVECs. Cells were seeded in the upper chamber on to the porous membrane of the culture insert and grew to confluency. Histamine or other stimulus and gap junction blockers were added in the upper chamber only. FITC-BSA was also added in the upper chamber and the amount of leakage across the cells into the lower chamber was measured.

2.9 Oligodeoxynucleotides and pluronic gel preparation

2.9.1 Oligodeoxynucleotides

Antisense oligodeoxynucleotides (asODN) targeting Cx43 and control sense oligodeoxynucleotides (sODN) were designed previously by Dr David Becker (Becker et al., 1999; Becker and Mobbs, 1999; Law et al., 2006). The oligodeoxynucleotides were ordered from Sigma-Genosys with desalted purification (Table 2.2). ODNs were diluted to 1 mM or 10 mM stocks using DEPC-treated water and kept in –20°C.

Table 2.2 The sequences of sense and antisense ODNs.

ODN	Sequence	Molecular weight
Rodent antisense	GTA ATT GCG GCA GGA GGA ATT GTT TCT GTC	9307.8
Human antisense	GTA ATT GCG GCA AGA AGA ATT GTT TCT GTC	9275.8
Control sense	GAC AGA AAC AAT TCC TCC TGC CGC AAT TAC	9103.8

2.9.2 30% Pluronic gel

Pluronic gel is a good vehicle for drug or ODN delivery *in vivo* by acting as a slow release reservoir for the agents (Becker et al., 1999; Cronin et al., 2006). Pluronic gel (30%) was made by mixing pluronic F-127 powder (Sigma) in DEPC-treated water and shaken constantly at 4°C until the powder dissolved into a clear liquid-gel. The pluronic gel remains in a liquid form at 4°C but would solidify in higher physiological temperatures. The gel was kept at 4°C until use. Once the gel solidified, the ODNs were slowly released into the wound with minimal ODN degradation inside the gel (Qiu et al., 2003).

For *in vivo* wounds, 50 µl of gel containing 10 µM ODN was used in each excisional wound. The ODN stock was diluted in the 30% pluronic gel directly to achieve the correct working concentration, vortexed three times and kept on ice. The pluronic gel solidified very quickly above 4°C therefore all pipette tips and tools were kept on ice until use.

2.10 Immunohistochemistry

2.10.1 Immunofluorescence staining

Fixation

Cryosectioned tissue slides were brought out from the –20°C freezer, thawed and allowed to air dry. Sections were fixed 7 min in 4°C acetone and allowed to dry again at room temperature. Coverslips from cell cultures were fixed immediately at the time of collection therefore did not require this step prior immunofluorescent staining.

Permeabilization

A wax ring was then drawn around the tissue sections with a pap pen (Dako, Cambridgeshire, UK) and tissue sections were incubated in blocking solution 0.1 M L-Lysine (Sigma) and 0.05% Triton X-100 (Sigma) in PBS for 1 hour. When necessary 5% normal sheep serum was added to prevent high background staining. For cell coverslips blocking for 25 min was sufficient.

Staining

Primary antibody was diluted in blocker solution and applied to the tissue/cells and incubated for usually 1 or 2 hours at room temperature (see Table 2.3 for a list of antibodies used). Slides were washed three times for 5 min with PBS prior to secondary antibody incubation with either Cy3 or FITC - conjugate for 1 hour. Secondary antibody was diluted in PBS only. For double-labelling of Cx26 and Cx30, Mouse monoclonal Cx26 and rabbit polyclonal Cx30 primary antibodies were used with the appropriate secondary antibodies respectively. Both primary antibodies were

diluted in the same blocking solution and secondary antibodies in the same PBS solution. Finally, the slides were washed again in PBS and HOECHST (1:25 000, Sigma) was applied as a nuclear counter stain. Slides were mounted using Citifluor mounting medium (Citifluor, UK) and then the coverslip was sealed with nail varnish. Tissue samples were viewed with fluorescent or confocal microscopy.

Table 2.3: A list of primary antibodies used in the thesis.

Antibody	Epitopes	Source	Species	Dilution	Reference
GAP1A (Cx43)	C-terminus residues 131-142	homemade	Mouse monoclonal	1:100	Wright et al., 2001
Anti-Cx43	C-termius residues 363-382	Sigma	Rabbit	1:5000	
GAP7M (hemichannel)	Extracellular loop residues 43-59	homemade	Rabbit	1:200	Becker et al., 1995
Des3 (Cx26)	Cytoplasmic loop residue 106-119	homemade	Rabbit	1:200	Monaghan et al., 1994
Anti-Cx26	N/A	Zymed	Mouse monoclonal	1:200	
Anti-Cx30	N/A	Zymed	Rabbit polyclonal	1:100	
Anti-Myeloperoxidase	Full length (human)	Dako UK	Rabbit	1:300	
Ki-67 (clone SP6)	C-terminus	NeoMarkers, Fremont, CA	Rabbit monoclonal	1:500	
Anti Type I collagen	N/A	Southern Biotech	Goat	1:100	
Anti Type III collagen S-17	N-terminus	Santa Cruz Biotechnology	Goat	1:100	
Rhodamin Phalloidin		Invitrogen		1:500	
Actin		Abcam	Mouse	1:2000	
COX-2	Residues 580-599	Cayman	Rabbit	1:500	
β-Tubulin		Abcam	Mouse	1:2000	

2.10.2 DAB-HRP staining

This staining technique using horseradish peroxidase (HRP) was used only to stain for neutrophils (myeloperoxidase) and proliferating cells (Ki-67) in the wound area. The antibodies used for these cell types stained the whole cell, for cell counting, using HRP staining technique allowed reliable image acquisition using a light microscope.
The tissue sections were fixed in acetone as for the fluorescent staining protocol. After fixation the sections were treated with 0.3% Hydrogen Peroxide diluted in PBS for 15 min to remove endogenous peroxide that may react with HRP. The sections were then washed three times 5 min with PBT (PBS containing 0.1% Tween 20) to remove traces of Hydrogen Peroxide. The slides were incubated in blocker solution (5% normal sheep serum, 0.1% Tween 20, 1 mg/ml BSA in PBS) for 1 hour before primary antibody incubation overnight in 4°C. The slides were washed in PBT three times for 5 min after primary antibody incubation and an anti- mouse or rabbit HRP conjugated secondary antibody was applied for 1-2 hours at room temperature (Table 2.4). Both primary and secondary antibodies were diluted in blocker solution. The slides were washed again with PBT and DAB solution (5 ml PBT + 50 µl DAB + 1 µl 30% Hydrogen Peroxide) was applied for a maximum of 30 min, as the DAB-HRP development will have ceased. At the end of reaction time slides were rinsed with PBT. Methyl green (Dako, Cambridgeshire, UK) was used as nuclear counter stain. At the end of staining the slides were rinsed briefly with PBT and dehydrated by dipping in alcohol series (70%, 100% and 100% for 1 min each) and cleared in 100% Xylene (BDH) twice for 10 min each. The slides were coversliped with DPX (BDH) and can be kept permanently in room temperature in the dark.

Table 2.4: List of secondary antibodies used in this thesis.

Antibody name	Source	Dilution
Polyclonal swine anti-rabbit IgG FITC	Dako, Cambridgeshire, UK	1:200
Goat anti-mouse IgG (H+L) FITC	Zymed, San Francisco, USA	1:200
Polyclonal rabbit anti-mouse Ig FITC	Dako, Cambridgeshire, UK	1:200
Goat anti-rabbit IgG (H+L) Cy3	Zymed, San Francisco, USA	1:200
Goat anti-mouse IgG (H+L) Cy3	Zymed, San Francisco, USA	1:300
Donkey anti-goat Alexa 568	Molecular Probes	1:500
Goat anti-moue IgG-HRP	Santa Cruz Biotechnology	1:2000
Goat anti-rabbit IgG-HRP	Santa Cruz Biotechnology	1:2000
Donkey anti-rabbit Ig, biotin	Amersham, Buckinghamshire, UK	1:200
Fluorolink Cy3 labelled streptavidin	Amersham, Buckinghamshire, UK	1:1000

2.10.3 Haematoxylin & Eosin staining on frozen skin sections

Haematoxylin & Eosin (H & E) is a common histological stain that is useful for viewing tissue structures and layout. Haematoxylin is blue and stains for nuclear DNA whereas eosin is red/pink staining for proteins and extracellular matrix.

Skin sections were fixed in acetic alcohol (3% acetic acid in 95% methanol) for 1 min and washed in tap water for 5 min. The slides were stained with Harris' Haematoxylin (Sigma) for 1 min followed by quick rinsing in distilled water and a 5 min wash in running tap water. Excess haematoxylin in the tissue was removed by dipping the slides in acid ethanol (1% HCl in 70% ethanol). The slides were washed in tap water for a further 5 min before the 1 min eosin (Sigma) stain. The stained sections were dehydrated by going through alcohol series of 70% ethanol for 3 min, 90% ethanol for 3 min and twice in 100% ethanol for 3 min each. The slides were cleared twice in

Xylene for 5 min and 10 min each. The slides were mounted using DPX (BDH) and viewed using a light microscope. Digital images were acquired using a Leica DC300F camera.

2.11 Confocal microscopy

For quantification of connexin proteins in intact and wounded skin, immunostained sections were imaged using Leica SP2 or SPUV confocal microscopes. Laser wavelength 543 nm was used to excite Cy3, 488 nm to excite FITC and 363 nm UV laser to excite HOECHST. Optimum gain and offset settings were adjusted to pick up positive staining while keeping the background minimal. For the intact skin study, six single optical section images were taken at random along the epidermis for each animal sample (six control and six diabetic animals). For studying Cx expression dynamics during wound healing days 1, 2, and 5 after wounding, three areas in the epidermis 'leading edge (LE)', 'wound edge (WE)' and 'adjacent zone (AD)' were imaged (see Figure 4.1) for connexin protein quantification. Similarly in the wound expression study, six images were taken at the wound zones (AD, WE and LE) for each of the animals. All parameters of laser power, pinhole, gain/offset and lens were kept constant for each pair of control and diabetic groups to allow later comparable quantification. All microscope parameters were kept constant throughout to allow later image analysis. HUVECs Cx43 protein expressions in knock down experiments using asODN were imaged the same way (six images per coverslip).

For *in vivo* FITC-BSA wound leakage quantification, Leica SP2 confocal microscope was used with 488 nm laser to excite FITC fluorophore. Six single optical sections were imaged in sites I and II for each animal (N=4). Optimum gain and offset settings were adjusted to pick up FITC signals in the blood vessels without saturating the image to avoid false positive signals.

2.12 Image analysis

ImageJ NIH version 1.35c software was used to quantify the connexin immunostaining images from intact skin and wound areas. Images have a intensity threshold from 0 (black) to 255 (saturation). For each of the connexins studied, a threshold was set to account for maximum number of gap junction plaques without picking up background noise and was kept constant for the paired control and diabetic groups. For the uninjured skin, epidermis and dermis were quantified separately using the marking tool to demarcate the area for quantification. For studies of Cx expression in the epidermis during wound healing the confocal images were analysed the same way. The length of the skin or the area of dermis was also measured accordingly in each of the images. Connexins in the epidermis were expressed per 100 μm of skin and in the dermis Cx43 was expressed as per 10,000 μm^2 to reflect the larger dermal area. The number and the size of connexin plaques and total positive staining area were recorded by ImageJ for each image and exported to an Excel worksheet for further statistical analysis. This method of quantification was favoured than Western blot analysis because it separated the epidermal and dermal comparisons. However, no information on the phosphorylation state of the connexins would be available.

ImageJ software was also used for in vivo FITC-BSA quantification. An optimal threshold was selected to elimilate background noise in the confocal images. All the signals below the threshold were subtracted and the images made binary (all FITC signals above the threshold were included irrespective of its intensity). Total area (pixels) occupied by FITC were quantified and recorded. Minimum of six images were analysed for each site (Figure 5.4) for each animal (N = 4).

Quantification Cx43 protein expression after Cx43-asODN application was carried out similarly to quantifying Cx in skin. An optimal threshold was selected to pick up positive staining while avoiding background noise. The number of Cx43 gap junction plaques and total staining area were recorded from individual images.

2.13 Western Blot

2.13.1 Western lysis buffer

A base buffer was made containing Tris-HCl (20 mM), SDS (4%) and glycerol (20%). Thereafter 10 ml was used as base to make lysis buffer with EDTA (1 mM), orthovanadate (1 mM), protease inhibitor (1 µl/ml, Sigma) and DTT (0.5 mM). To collect the HUVEC samples from culture plates for protein analysis, the cells were first washed twice with PBS and 150 µl of lysis buffer was added to each well of a 6-well plate to scrape off the cells. The lysis buffer containing cells was passed through an insulin syringe to assist lysis. The protein was collected and kept in -20°C.

Table 2.5 Recipes for the base and protein lysis buffers.

BASE buffer	**Working concentration**	**Stock concentration**	**50 ml**
Tris-HCl pH 6.8	20 mM	0.5 M	2 ml
SDS	4%	10%	20 ml
Glycerol	20%	100%	10 ml
dH_2O			18 ml
Lysis buffer			**Add to 10 ml of BASE**
EDTA	1 mM	100 mM	100 µl
Orthovanadate	1 mM	100 mM	100 µl
Protease Inhibitor cocktail (Sigma)	1000x		10 µl
DTT	0.5 mM	500 mM	100 µl

2.13.2 SDS-Polyacrylamide gel

Western blot was set up using Biorad Mini Protein II electrophoresis and transfer systems. Glass plates were cleaned with 70% ethanol prior use and the gel cast was assembled with either 0.75 mm or 1.5 mm strips. The casts were filled with distilled water to check for any leakages. SDS-Polyacrylamide gel (8% or 10%) was made according to Table 2.6 (adapted from Harlow and Lane, 1988). Optimal percentage for Cx43 is 8% where the different phosphorylated forms could be clearly distinguished. The ammonium persulfate (10%, Sigma) and TEMED (Sigma) were added at the very end because gel will start to polymerise soon afterwards. The gel solution was poured into the casts immediately after mixing and 500 µl of dH_2O was added to level the top of the gel. The gel normally took 20-30 min to set and the water was poured away. A stacking gel was made and poured with the comb inserted.

Table 2.6: Recipe for SDS-Polyacrylamide gel (lower and stack) for Western blot.

Gel percentage	8%	8%	10%	10%	STACK
dH_2O	4.6	9.3	4	7.9	2.1
30% Acrylamide mix	2.7	5.3	3.3	6.7	0.5
Tris base 1.5M (pH 8.8)	2.5	5	2.5	5	
Tris 1M (pH 6.8)					0.38
10% SDS	0.1	0.2	0.1	0.2	0.03
10% ammonium persulfate	0.1	0.2	0.1	0.2	0.03
TEMED	0.006	0.012	0.004	0.008	0.003
Total (ml)	10	20	10	20	3

2.13.3 Sample preparation for gel electrophoresis

For wells made with a 1.5 mm comb 40-50 µl of loading samples were required, and for 0.75 mm combs 20-30 µl of samples were required. The lysates were thawed from –20°C and made up with 10% DTT (0.25 M, Sigma) and 1 µl of Bromphenol blue (Sigma). Lysate samples were loaded into the wells using a Hamilton syringe. Samples were run with 5 µl of standard ladder Amersham protein mix 17044601 or Precision Plus Protein Standards (Bio-Rad).

2.13.4 Gel electrophoresis

After samples were loaded in the wells, the tank was filled with 1x electrophoresis buffer (diluted using distilled water, Table 2.7) and the gel electrophoresis was run at 90 V constantly for the stacking gel and 140 V for the lower gel until the front line reaches the bottom of the gel. It was important to use Tris Base and not Tris-HCl otherwise the protein will be denatured during gel electrophoresis.

Table 2.7 Electrophoresis and transfer buffer stocks for Western blot.

Electrophoresis buffer	**5x**	**10x**	**(in 1 L dH_2O)**
Tris BASE (Sigma)	15.15 g	30.3 g	
Glycine (Sigma)	72.05 g	144.1 g	
SDS (Biorad)	5 g	10 g	
Transfer buffer pH 8.3		**10x**	**(in 1 L dH_2O)**
Tris BASE		30.3 g	
Glycine		144.1 g	
HCl used to adjust the pH			

2.13.5 Transfer to membrane

After gel electrophoresis, gels were removed and transfer 'sandwiches' were set up to transfer protein onto the hybridization membranes Optitran 0.45 μm (Whatman 10439196) or Hybond C++ (Amersham). In the semi-dry system, gel-membrane sandwiches were soaked in transfer buffer made from a 10x stocks to working concentration (Tris Base 25 mM, glycine 192 mM, SDS 0.01% and 15% methanol in dH_2O) and transferred for 90 min at a constant 200 mA. In the wet system, the 0.75 mm gels were transferred in cold temperatures at constant 125 V for 50 min, or 80 V for 2 hours. The transfer buffer must be cold before use and it was usually chilled in a 4°C fridge. At the end of the transfer the membranes were stained with Ponceau Rouge (0.4%) to check the quality of transfer. Ponceau was then rinsed off using TBS-Tween (Tris Base 50mM, NaCl 250mM, Tween20 0.1%).

2.13.6 Membrane Hybridization

The membranes were blocked in TBS-Tween containing 5% of skimmed milk (Marvel) for 90 min at room temperature with constant shaking. Blocking milk was rinsed off with TBS-Tween for a few seconds and membranes were incubated in primary antibody for 90 min at room temperature or overnight at 4°C in a plastic pouch. Membranes were washed in TBS-T twice for 10 min and twice for 5 min before secondary antibody incubation. Secondary antibody (-HRP conjugated) was similarly incubated for 2 hours on a rotary shaker.

2.13.7 Protein band detection

ECL Western blotting detection reagent kit (Amersham) was used according to manufacturer's instruction by mixing solution 1 and solution 2 (1:1) and applied to the membranes. Homemade peroxidase detection reagents were also used. Similar to the commercial detection kit, two solutions (solutions A and B) were made from stocks and mixed with ratio 1:1 just prior to use (Table 2.8). After 1 min incubation with either commercial or homemade detection mix, the membranes were wrapped in Saran wrap (Fisher Scientific) for exposure. Hyperfilms (Amersham) were exposed in the dark room for protein bands and developed with an automated system (X-O Graph, Compact X2). Films were scanned and protein bands analysed using ImageJ.

Table 2.8 Homemade peroxidase detection stock solution and reagents.

Stock solutions	Concentration
Luminol (Sigma)	250 mM in DMSO (aliquots kept in the dark at –20°C)
Coumaric acid (Sigma)	90 mM in DMSO (aliquots kept in the dark at -20°C)
Tris-HCl (Sigma)	1 M pH8.5
Hydrogen peroxide (Sigma)	30% v/v
Solution A	0.5 ml Luminol (250 mM), 0.22 ml coumaric acid (90mM), 5 ml Tris-HCL (1 M pH8.5), made up to 50 ml with dH_2O.
Solution B	32 µl 30% Hydrogen peroxide, 5 ml Tris-HCL (1 M pH 8.5), made up to 50 ml with dH_2O

2.14 Lucifer Yellow dye transfer in HUVECs

A classic way to assess cell couping is by following the transfer of tracer dyes from one cell to another (Flagg-Newton et al., 1979; Loewenstein and Kanno, 1964). HUVECs were grown to confluency on the plastic coverslips and transferred into a medium-filled chamber for microinjection. Microelectrodes were pulled from Borosilicate glass capillaries (1.5 mm OD, 0.86 mm ID, Harvard Apparatus) using a micropipette puller (Model P-97, Sutter Instruments, CA, USA). The electrode tips were filled with 4% Lucifer Yellow CH dilithium salt (MW 453 Da, Sigma, Poole, UK) and backfilled with 1 M Lithium Chloride (Sigma). After forming a circuit with some medium, the electrode has a resistance of 3-5 MΩ. The cells were viewed using a fixed stage microscope (Leica DMLFS, epifluorescence and infrared) using a 40x (NA 0.8) ceramic dipping objective. A meniscus was created for the electrode to be inserted into place. The electrode was brought near the cells by manipulating the driving system

with constant monitoring through the objective. The LY dye was injected into a single cell by iontophoresis and allowed to transfer to neighbouring cells for 1 min. At least ten cells were injected on each coverslip for each experimental condition (see Chapter 2.7) and repeated for 4 coverslips. Images of dye spread were taken with a digital cameral (DC900FL) for analysis.

2.15 Prostaglandin E_2 ELISA

Culture media were collected from HUVECs stimulated with histamine and/or GJ blockers over for 3 and 6 hours for PGE_2 release assay (extracellular) using ELISA. HUVECs were also collected and lysed using ELISA homogenization buffer (0.1 phosphate buffer pH 7.4 containing 1mM EDTA and 10 μM indomethacin) for measuring intracellular PGE_2 content. A Prostaglandin E_2 Monoclonal EIA kit (Cayman) was used following the manufacturer's protocol and reagents shown in Table 2.9.

For the PGE_2 microplate assay, each medium or lysate sample was diluted to 1:50 and 1:150 using EIA buffer (Table 2.9). The 96-well PGE_2 plate was rinsed with 1x with ELISA wash buffer and 50 μl of each sample was added in the wells in duplicates. The PGE_2 EIA standard curve (stock supplied in the kit) was diluted and loaded also in duplicates (1 ng/ml, 500 pg/ml, 250 pg/ml, 125 pg/ml, 62.5 pg/ml, 31.3 pg/ml, 15.6pg/ml, 7.8 pg/ml). PGE_2 Monoclonal antibody (50 μl) was added to all the wells (sample and standard curve) except blank (B_0) and non-specific-binding (NSB) wells. PGE_2 EIA AchE Tracer (50 μl) was also added into all the wells except the blank well.

B_0 wells contain no samples (maximum binding). The plates were incubated overnight (at least 18 hours) at 4°C. The mixture in the wells was poured away and the plates washed 4 times with wash buffer. In each well 200 µl of Ellman's Reagent was added and the plate sealed to develop on an orbital shaker for 60-90 minutes or until B_0 absorbance reading is between 0.3-0.8. The plate was read at absorbance of 405-420 nm using a microplate reader (BioRad model 680).

Table 2.9 Reagents for ELISA.

Homemade EIA buffer
50 ml Phosphate buffer 1M, 50 mg Sodium Azide (Sigma), 11.7g NaCl, 185 mg EDTA.4Na+ (Sigma) or 190 mg of EDTA.2Na+ and 500 mg BSA (Sigma) made up to 500 ml with dH_2O
Homemade ELISA wash buffer (10 mM Phosphate buffer, 0.05% Tween 20)
Mix 10 ml of 1 M phosphate buffer and 500 µl Tween 20 (Santa Cruz Biotechnology), made up to 1 L with dH_2O.
Homemade Ellman's reagent (100x)
In 1 ml Phosphate buffer (1 M), dissolve 20 mg acetylcholine, 21.5 mg DTNB (Sigma). Divide the 1 ml to five 200 µl portions into 50 ml falcon tubes and keep in –80 °C freezer, dilute to 20 ml with dH_2O prior to use.

2.16 Statistical methods

A number of different statistical tests were used in this thesis to test the difference in the measurements between control and diabetic animals and/or treatments. Significant difference was taken when $P < 0.05$. In Chapter 3, the connexin expressions study in intact skin and scrape loading dye transfer experiments, a Mann-Whitney U Test was

used to compare control and diabetic skins. The samples from control and diabetic skin were assumed to be random, independent and non-parametric (not assuming normal distribution). For the connexin expression during wound healing in Chapter 4, two-way ANOVA statistics was used to test the effect of diabetes and injury on connexin expression in multiple time points. For multiple group comparisons, one-way ANOVA was used. When significant difference ($P < 0.05$) was found in the ANOVA to a post-hoc Newman-Keuls test was used identify the statistical differences between the sample groups. One-way ANOVA was the main test used in Chapter 5 to compare the control, diabetic, control with asODN, diabetic with asODN wounds and in Chapter 6 for experiments with endothelial cells.

The tests were run using Statview 5.0.1, Prism (GraphPad, USA) or SigmaPlot (Systat, UK) statistical packages.

3 CONNEXINS IN DIABETIC SKIN

3.1 Chapter introduction

Diabetes is a complex disorder affecting multiple tissues and organs in the human body. In particular, diabetic patients commonly suffer from skin wounds that heal poorly or develop into chronic wounds that do not heal (Falanga, 2005). Homeostasis of skin is important to sustain the integrity of the barrier to the outer environment. Neuropathy and microangiopathy are known factors that can cause delayed wound healing in diabetic patients. Connexins have been shown to have important roles in the homeostasis of skin and epidermis, where point mutations in connexins can result in development of different skin diseases. For example, autosomal dominant mutation in Cx30 causes palmoplantar keratoderma (Kelsell et al., 2001) and mutations in Cx26 lead to erythrokeratoderma variabilis (EKV) or Vohwinkel Syndrome, showing general or localised hyperkeratosis (Kelsell et al., 2000; Maestrini et al., 1999). Examining connexins in diabetic skin will provide further information on the role of connexins in skin as well as in diabetes disease.

Several *in vitro* studies have demonstrated that hyperglycaemic conditions can alter Cx expression in many cell types (Hills et al., 2006; Kuroki et al., 1998; Lin et al., 2003; Pitre et al., 2001; Sato et al., 2002). However, the effect of hyperglycaemia appears to be tissue and connexin specific. In microvascular endothelial cells, aortic smooth muscle cells (Inoguchi et al., 2001; Kuroki et al., 1998; Sato et al., 2002) and oocytes (Chang et al., 2005), Cx43 expression and gap junctional intercellular communication (GJIC) are decreased in hyperglycaemic cultures. Conversely, Cx43 expression and coupling increased dramatically in renal cells (Hills et al., 2006), and Cx37 and Cx40 expression was not affected by hyperglycaemia (Sato et al., 2002). Changes in connexin expression can lead to functional changes as shown in the heart intercalated

disc of diabetic animals which exhibit beat abnormalities (Howarth et al., 2007; Okruhlicova et al., 2002). Although hyperglycaemia has been shown to alter connexin expression in other cell systems, whether connexin expressions and function in skin are affected had not been studied extensively. An *in vitro* study showed cultured primary human diabetic fibroblasts have elevated Cx43 expression (Abdullah et al., 1999), but *in vivo* data is generally absent in the literature. In this chapter, I set out to examine Cx26, Cx30 and Cx43 protein expressions and gap junctional communication in intact diabetic skin.

3.2 Brief methodology

A single intraperitoneal injection of streptozotocin (65mg/kg) induced diabetes in adult Wistar or Sprague-Dawley (SD) rats (350-400g) used in the experiments. Back and heel skin of streptozotocin-induced diabetic rat were collected at 2 or 8 weeks after diabetes induction for Cx expression studies. The isolated skin samples were fresh frozen in OCT and cryosectioned (10-12 μm thick) for immunostaining and H & E histological staining. Control and diabetic skins were stained for Cx26 (Des3, dilution of 1:200, (Monaghan et al., 1994), Cx30 (dilution 1:200, Zymed) and Cx43 (GAP1A, dilution 1:100, Wright et al., 2001) and images were acquired using confocal microscopy. For each connexin, skin sections from 6 control and 6 diabetic rats were used and stained in a single staining run. For quantification, immunofluorescent staining was imaged using confocal microscopy using an optimal setting that was kept constant for all the images acquired. For each animal, 6 random images were taken and were used to calculate a mean value for the animal. In each image, areas of epidermis or dermis were demarcated manually using NIH ImageJ software and connexin

expression automatically quantified using an optimal threshold that was kept constant for control and diabetic skins for each connexin.

To assess gap junctional intercellular communication in the epidermis and the dermis, a scrape-loading method using Lucifer Yellow tracer dye was employed. Gel foam loaded with dye was inserted into full thickness incisions in freshly excised control and diabetic skin (N = 4 each) and dye allowed to diffuse across the epidermis and dermis for 1, 2 and 5 min. Additional control experiments using gap junctional blocker octanol, Dextran-FITC (10kDa, Sigma), cascade blue (water soluble 8-methoxypyrene-1, 3, 6-trisulfonic acid, trisodium salt, Molecular Probes), unfixable LY methoxycarbonyl were included (N = 7 each). At the end of the diffusion time the gel foam was removed and skin was fixed in 4% paraformaldehyde for 30 min. Skin samples were embedded in OCT and cryosectioned (10-12 μm) prior to confocal microscope imaging. The slides were rehydrated and counterstained with propidium iodide (1 μg/ml in PBS). Six single-optical images were captured for each animal using the same microscope settings. Using ImageJ, a 1500 pixel x 50 pixel box was demarcated in the centre of the dermis to plot a histogram of dye intensity across the dermis. The cut off point for positive dye transfer was taken at threshold intensity of 50 (the distance of dye transfer is where the intensity drops below 50). For the epidermis a line was drawn along the suprabasal layer to plot the histogram. Three lines were drawn for each image to improve the accuracy of the histogram.

Mann-Whitney U test was used for of all the results in this chapter. Numbers are expressed as mean ± standard error of the mean.

3.3 Streptozotocin-induced diabetic rats

Streptozotocin (STZ) induces diabetes by specifically destroying the insulin producing β-cells in the pancreas and abolishing insulin production, resulting in acute type I diabetes in the animals (Szkudelski, 2001; West et al., 1996). Extra monitoring on the animals was necessary as diabetic rats lose weight dramatically soon after diabetic induction. Animals were weighed every other day as weight loss more than 20% was not allowed in accordance to UK Home Office Animals (Scientific Procedures) Act 1986. Extra water bottles were refilled and bedding was changed every other day as diabetic rats wet the cages more. Diabetes was confirmed with urine glucose test 3-5 days after intraperitoneal injection of STZ and blood glucose measurement were taken when the animal was killed (N = 50 for the entire thesis, 27.07 ± 1.09 mmol/L or 487.26 mg/dl, equivalent of 4.87 g/L).

Initially, diabetes was allowed to develop for 8 weeks in Wistar rats before back and heel skin tissue collection (these were carried out by Dr. Jill Lincoln). Later, SD rats diabetic for 2 weeks were also used for Cx43 expression analysis. SD rats that have been diabetic for 2 weeks were also used for diabetic wound healing studies in Chapters 4 and 5.

3.4 Connexins 26, 30 and 43 in diabetic back skin

Examining the H & E staining of control and diabetic skin, although the epidermis in diabetic skin appeared thinner at places where stratum basale is less distinct, no great

difference in the histology was observed. In the rat back skin, typical punctate Cx43 immunostaining was found in the basal and suprabasal layers of the epidermis and dermal fibroblasts (Figure 3.1). Cx26 expression was detected in the stratum spinosum and straum granulosum, and Cx30 was detected in the stratum granulosum of the epidermis as expected from literature (Brissette et al., 1994; Butterweck et al., 1994). Interestingly, double-staining of Cx26 and Cx30 revealed some co-localisng gap junction plaques in the differentiating epidermis. However, whether the co-localised plaques resulted from heterometric gap junction could not be confirmed at this resolution using immunofluorescent staining.

Quantification of Cx43 expression in the epidermis using the confocal images revealed that in 8-week diabetic skin, expression was significantly reduced in the epidermal basal layers (Figure 3. 2, 3. 3), in terms of both the number of gap junction plaques ($P = 0.0039$) and total staining area ($P = 0.0065$; Table 3.1). Cx43 expression was reduced to only 37% of control levels. No differences in plaque size distribution were found. A lack of change in plaque size and reduced total staining indicated that the number of connexin plaques was reduced.

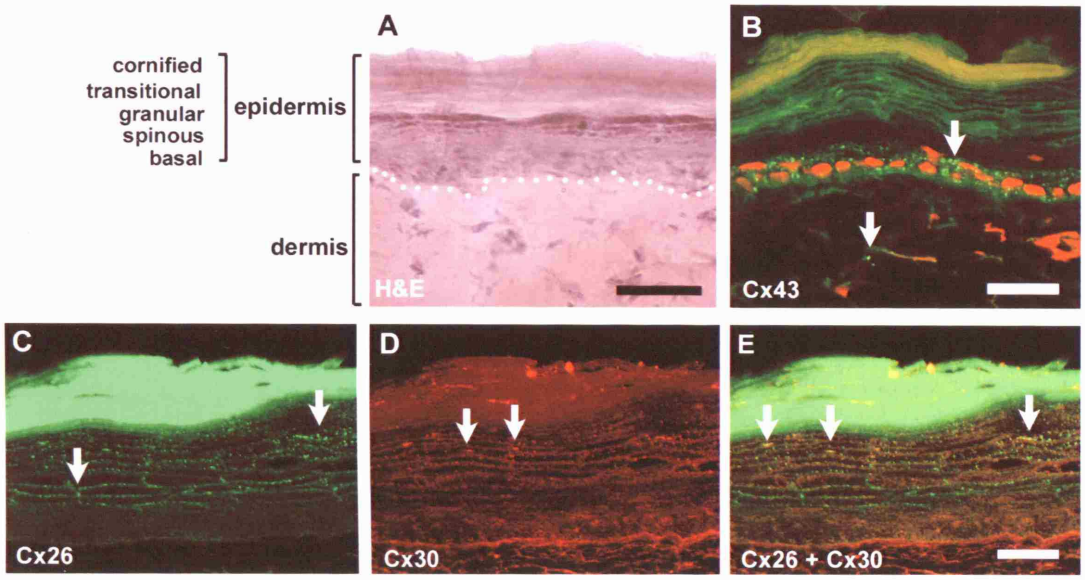

Figure 3. 1 Histology and Cx26, Cx30 and Cx43 expression in the normal Wistar rat epidermis. H & E histological staining of interfollicular skin, where the white dotted line marks the border of epidermis (above) and dermis (below). Different layers of epidermis are clearly presented with this stain. (B) Typical punctate Cx43 staining can be seen in the basal epidermis and dermis (arrows). Cx43 is shown in green and red is nuclei counterstaining. (C) Cx26 staining (green puncta, arrows) and (D) Cx30 (red puncta, arrows) are expressed in the spinous and granular layers of epidermis. (E) Overlay of Cx26 and Cx30 double staining revealed a few co-localising gap junction plaques in the granular epidermis (yellow plaques pointed by arrows). Scale bars (A-B) 50 μm and (C-E) 25 μm.

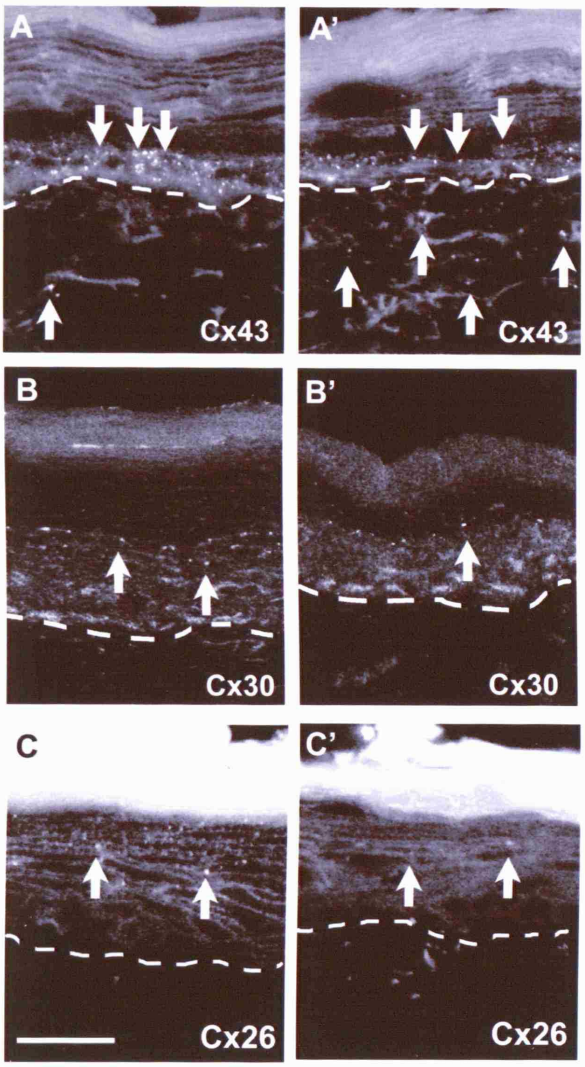

Figure 3. 2 Cx26, Cx30 and Cx43 expression in control and 8-week diabetic rat skin. Cx43 (A, A'), Cx30 (B, B') and Cx26 (C, C') staining (arrows) in normal (A, B, C) and STZ diabetic (A', B', C') interfollicular rat skin, 8 weeks after induction of diabetes. The dashed line marks the boundary between the epidermis (above) and dermis. The protein expression of all three connexins was significantly reduced in the diabetic epidermis. However, Cx43 expression in the diabetic dermis was increased. Scale bar 25 μm.

Table 3.1 Changes in connexin expressions in Wistar 8-week diabetic back skin compared to control (mean ± SEM).

	Cx		No. of plaques /100 μm	Total staining /10,000 μm^2	Plaque size (μm^2)
Epidermis	Cx43	Control	26.80 ± 2.44	122.35 ± 23.03	0.95 ± 0.11
		Diabetes	10.17 ± 1.44	32. 06 ± 4.67	0.75 ± 0.46
	Cx26	Control	17.46 ± 2.48	25.80 ± 3.82	0.32 ± 0.01
		Diabetes	1.97 ± 0.25	2.75 ± 0.39	0.31 ± 0.02
	Cx30	Control	15.18 ± 2.50	3.47 ± 0.74	0.23 ± 0.01
		Diabetes	2.30 ± 0.39	0.55 ± 0.11	0.21 ± 0.01
			No. of plaques / 10,000 μm^2	Total staining /10,000 μm^2	Plaque size (μm^2)
Dermis	Cx43	Control	10.32 ± 1.46	43.80 ± 7.30	0.89 ± 0.04
		Diabetes	15.46 ± 2.29	69.25 ± 10.64	1.02 ± 0.05

Cx26 and Cx30 expression was also dramatically downregulated in the diabetic epidermis compared to control (Figure 3.2). The number of plaques and total staining area were significantly reduced for both connexins ($P < 0.01$; Table 3.1; Figure 3. 3). Cx26 expression is reduced to 11% and Cx30 to 15% of normal level.

However, this was not a global downregulation of connexins in response to diabetes as a contrasting effect was observed in dermal fibroblasts; in these, a distinct increase in the size and number of Cx43-positive plaques was observed (Table 3.1; Figure 3. 2 and 3.3). There was approximately a 50% increase in the number of Cx43 plaques in diabetic dermis.

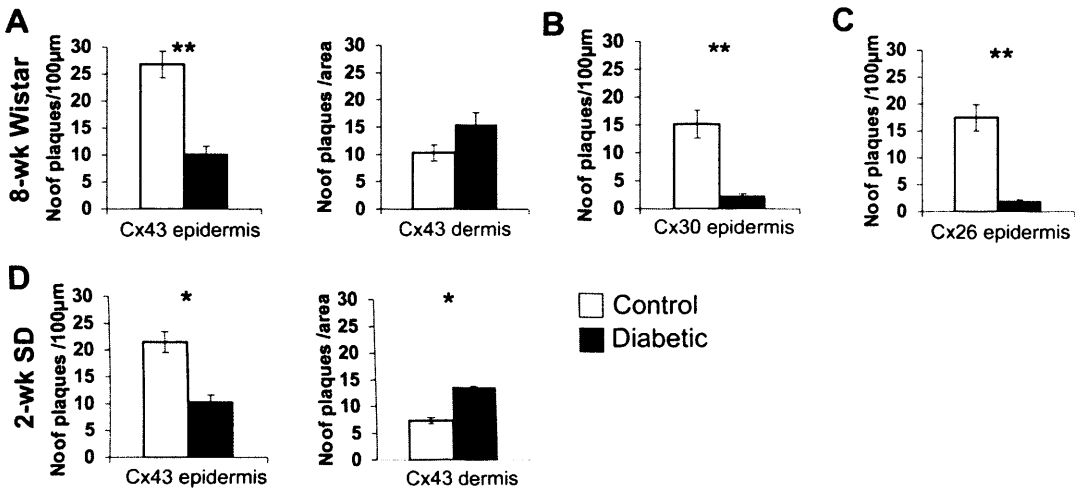

Figure 3. 3 Quantification of Cx26, Cx30 and Cx43 expression in control and diabetic back skin. In skin, 8 weeks after induction of diabetes in Wistar rats, the number of Cx43 (A), Cx30 (B) and Cx26 (C) plaques was significantly decreased in the epidermis. However, Cx43 was found to be increased in the diabetic dermis (A). This change in expression was also observed as early as 2-week (D) after induction of diabetes in SD rats (*$P < 0.05$, **$P < 0.01$). White bars represent control and black bars for diabetic skin.

Table 3.2 Changes in Cx43 expression in back skin 2 weeks after diabetes induction in SD rats. Significant differences in the number of Cx43 plaques were found in control and diabetic skin (*P < 0.05).

	Cx		Nr of plaques /100μm	Total staining /10,000μm^2
Epidermis	Cx43	Control	21.53 ± 3.98	68.55 ± 15.97
		Diabetes	9.24 ± 3.44	15.47 ± 5.50
			Nr of plaques / 10,000μm^2	Total staining /10,000μm^2
Dermis	Cx43	Control	9.64 ± 1.24	4.89 ± 2.03
		Diabetes	21.37 ± 5.22	16.99 ± 3.74

The first set of experiments was carried out of 8-week diabetic Wistar rats that belonged to Dr Jill Lincoln at the UCL Royal Free Campus for neuropathy studies. However, Wistar rats became unavailable and therefore subsequent experiments were carried out on Sprague-Dawley rats at the main UCL campus. As 2-week diabetic rats, before the development of neuropathic complications, were to be used for the later wound healing studies, Cx43 protein expression was also examined in their uninjured skin.

Similar changes in Cx43 expression were seen in skin two weeks after STZ induction of diabetes in the SD rats (Table 3.2; epidermis P = 0.037, dermis P = 0.025). Cx43 expression was reduced in the epidermis and increased in the dermis in diabetic skin both 2 and 8 weeks after diabetes induction. When comparing the Cx43 expression in the epidermis of 8-week diabetic Wistar rat skin with 2-week diabetic SD rat, it appeared that the magnitude of change was larger in the 8-week diabetic skin (Table

3.3). There appeared to be minor differences in the level of control Cx43 protein expression in the epidermis between the two rat strains although this did not reach statistical significance. Interestingly, greater reduction in Cx43 protein expression was observed in the 8-week than 2-week diabetic epidermis (Control Wistar versus Diabetic Wistar, and Control SD versus Diabetic SD). This observation might be caused by the longer period of diabetic development and further skin complications such as angiopathy or neuropathy.

Table 3.3 Comparison of Cx43 expression between Wistar and SD diabetic rats. Similar proportional changes in the number of plaques were observed in the epidermis of 8-week diabetic Wistar and the 2-week diabetic SD rats.

Rat	Cx		Nr of plaques /100μm	Total staining /10 000μm^2
Wistar (8wk)	Cx43	Control	31.94 ± 4.86	97. 46 ± 15.35
		Diabetes	8.02 ± 1.72	22.47 ± 5.22
SD (2wk)	Cx43	Control	42.68 ± 6.35	98.03 ± 22.41
		Diabetes	19.98 ± 5.77	40.77 ± 12.89

3.5 Connexins 26, 30 and 43 in diabetic heel skin

In diabetic patients, feet are a common area where chronic wounds develop owing to high pressure and friction. Therefore, I have also examined the expression of connexins in the heel skin of diabetic rats. Although heel skin comprises of epidermis – dermis structures, it differs significantly to back or interfollicular skin.

H & E histological staining of sectioned heel skin revealed that heel epidermis is much thicker than back skin, containing a thicker layer of cornified keratin to protect the feet from continuous friction (Figure 3. 4). Histological analysis showed plantar (heel) epidermis consisted primarily of keratinocytes, and typical epidermal rete ridges that help to hold the epidermis to the dermis were deepened to resist increased friction. No hair follicles were found in the heel skin that is devoid of hair.

Similar to back skin, immunostaining of heel sections revealed Cx26, Cx30 and Cx43 protein expressions at the expected locations of the heel epidermis. Interestingly, the gap junction plaques between the keratinocytes appeared larger in the heel than those in the back skin, possibly due to the thicker epidermal structures. Like the back skin, Cx43 was significantly downregulated in the heel epidermis of diabetic rats 8-weeks after induction (Table 3.4; Figure 3. 4, $P = 0.0446$). Intriguingly, Cx43 expression was also significantly downregulated in the diabetic heel dermis ($P = 0.0039$), as opposed to the upregulation observed in the back skin.

In the spinous and granular layers of heel skin, immunostaining revealed a high level of Cx26 and Cx30 expression in both control and diabetic epidermis (Figure 3.5). Different to the data found in the back skin, no significant change in Cx26 and Cx30 protein expression was identified in the epidermis 8-weeks after diabetes induction ($P > 0.05$; Table 3.4; Figure 3.5).

Table 3.4 Changes in connexin expression in Wistar 8-week diabetic heel skin.

	Cx		No. of plaques /100 μm	Total staining /10,000 μm^2
Epidermis	Cx43	Control	39.08 ± 8.38	65.91 ± 18.68
		Diabetes	22.81 ± 4.38	49.43 ± 13.06
	Cx26	Control	5.08 ± 1.46	7.00 ± 1.48
		Diabetes	3.93 ± 1.71	7.81 ± 3.83
	Cx30	Control	17.33 ± 1.15	86.18 ± 5.72
		Diabetes	13.53 ± 2.35	78.09 ± 11.30
			No. of plaques / 10,000 μm^2	Total staining /10,000 μm^2
Dermis	Cx43	Control	8.24 ± 1.01	5.62 ± 0.85
		Diabetes	3.16 ± 0.49	2.47 ± 0.48

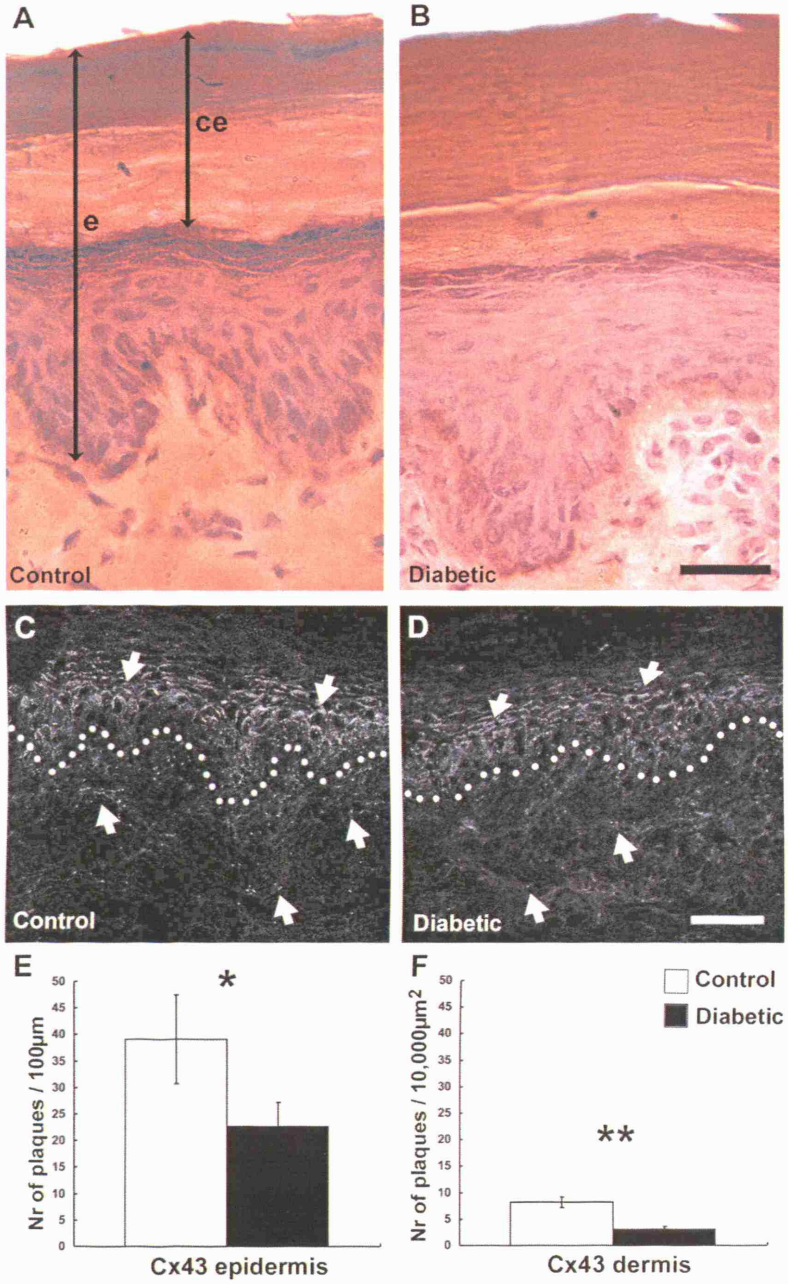

Figure 3. 4 Cx43 expression in control and 8-week diabetic heel skin. H & E histological staining showed the typical thick layer of cornified epidermis (ce) in the heel epidermis (e) in both control (A) and diabetic (B) animals. Cx43 was expressed in the basal and suprabasal layers of the epidermis and also in high abundance in the dermis (arrows). Cx43 expression was reduced in both the epidermis and dermis of diabetic (D) heel skin compared to control (C). Quantification of Cx43 expression in the heel skin epidermis (E) and dermis (F) showed the number of Cx43 plaques was significantly reduced in diabetic heel skin (*$P < 0.05$, **$P < 0.01$). Control is represented in white bars, diabetic black bars. Scale bar 50 µm.

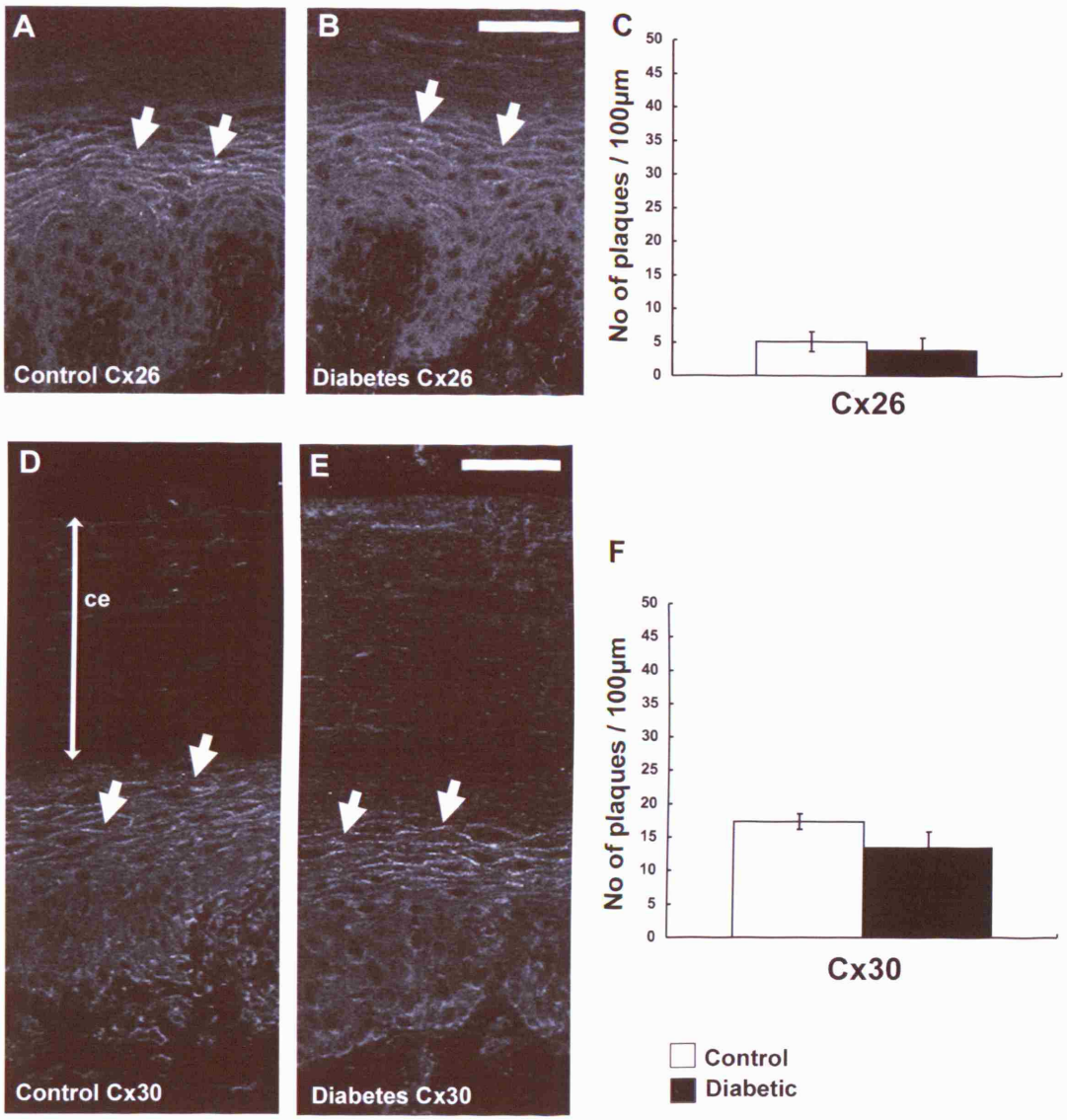

Figure 3. 5 Cx26 and Cx30 staining in control and 8-week diabetic heel skin. Cx26 (A, B) and Cx30 (D, E) are expressed in the epidermal spinous/granular layer keratinocytes beneath the cornified layer (ce) as expected in both groups (white puncta, arrows). There were no significant difference in the number of Cx26 and Cx30 plaques between control and diabetes (C, F respectively). Histogram white bar represents control, black bar diabetic. Scale bar 50 µm.

3.6 Gap junctional intercellular communication in diabetic back skin

To assess the gap junctional intercellular communication (GJIC) in diabetic epidermis and dermis, a scrape-loading dye transfer experiment was performed using Lucifer Yellow (LY). Lucifer Yellow passes through many gap junctions freely and is commonly used as an indicator for gap junctional communication. Here, gel-foam loaded with LY dye was placed in the freshly cut ("scraped") skin and served as a reservoir for dye to enter into damaged cells and transfer across the skin through gap junctions. The extent of transfer of the gap-junction-permeant dye LY through the tissue in 1, 2 and 5 minutes was recorded and examined. However the dye diffused in 1 and 2 min was not far enough for analysis hence 5 min was taken as the optimal time for dye transfer. At 5 minutes the extent of dye transfer was significantly different between control and diabetic skin (Figure 3.6). Lucifer Yellow diffused through basal and spinous layers of the epidermis in both groups but did not travel as far in the diabetic epidermis compared to control. Quantification of distance spread revealed significantly reduced coupling in the diabetic epidermis ($P = 0.0132$), with the dye travelling about 50% further to 712.78 ± 76.17 μm (mean ± SEM) in control epidermis versus 528.44 ± 57.56 μm in the diabetic epidermis ($N = 4$ for each group). In the diabetic dermis, dye transfer was significantly enhanced ($P < 0.05$; Figure 3.6). These results were consistent with the changes in connexin protein expression observed previously.

To confirm dye transfer was via gap junctions, additional experiments were carried out with combined administration of cascade blue and Dextran-FITC tracer dyes. Dextran

molecules (10kDa) are too big to pass through gap junctions, thus these molecules were limited to cells damaged at the edge of the excision and did not diffuse through the skin. Cascade blue on the other hand can pass through GJs freely similar to Lucifer Yellow. Application of the gap junction blocker octanol to the scrape for 5 minutes prior to application of LY also prevented dye transfer through the skin (Figure 3.6). Scrape loading experiment using an unfixable Lucifer Yellow methoxycarbonyl showed the same dye transfer properties as Lucifer Yellow CH (Figure 3.6). Unfixable LY can only be retained once inside a cell and extracellular dyes will be washed off during rehydration processes. Scrape loading using unfixable LY demonstrated similar result to fixable LY in the dermis (Figure 3.6). Taken together all of these experimental controls indicate that dye transfer indeed occurred through gap junctions rather than diffusion through the extracellular space.

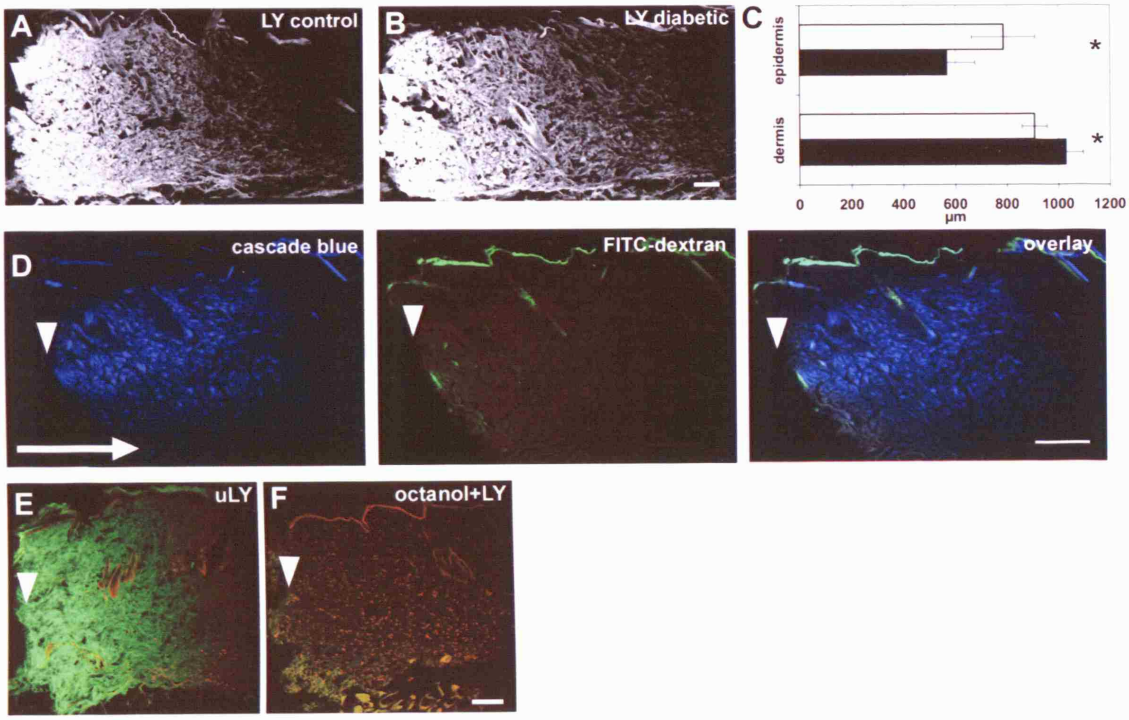

Figure 3.6 Scrape loading dye transfer to access cell coupling in back skin. Quantification of the distance that LY dye transferred in five minutes in the epidermis and dermis of normal (A) and diabetic (B) rat skin, eight weeks after induction of diabetes. (C) In the epidermis of diabetic skin dye transfer was significantly reduced compared to control skin, whereas in the dermis dye transfer was significantly increased (*$P < 0.05$). (D) Cascade blue diffused through skin via gap junction where as Dextran-FITC was too large to travel through gap junctions. White arrow indicates the direction of dye transfer. (E) Unfixable form of LY (uLY) showed intracellular cell communication. (F) Dye transfer was inhibited by gap junction blocker octanol. Scale bars (A, B) 200 µm, (D) 500 µm, (E, F) 200 µm.

3.7 Chapter discussion

The presence of connexins in the skin has been well documented in the past decade (Butterweck et al., 1994; Di et al., 2001; Richard, 2000; Risek et al., 1994). Several studies demonstrated important functions of gap junctions in the structural development and organisation of the skin (Fitzgerald et al., 1994; Risek et al., 1992), and this became more evident as mutations in connexins were shown to underlie various skin diseases such as palmoplantar keratoderma and erythrokeratoderma variabilis (Kelsell et al., 2000; Richard, 2000). The expression of Cx26, Cx30 and Cx43 in diabetic back and heel skin was studied in order to understand the effect of diabetes on connexins in skin. In this chapter I have demonstrated that in the uninjured skin of streptozotocin-induced diabetic rats, all three connexin proteins studied were significantly reduced in the back skin epidermis within 8-weeks of induction. However, Cx43 was increased in the dermal connective tissue. Interestingly in heel skin only Cx43 was reduced, and not Cx26 or Cx30, after diabetes induction. Cx43 was downregulated in both back and heel epidermis but the dermis showed a site specific change in Cx43 expression. In the back, the Cx43 protein expression increased and in the heel dermis it decreased. Functional cell coupling data examining LY dye transfer in freshly excised back skin corresponded to the connexin expression changes. Reduced extent of dye transfer was observed in the epidermis whereas in the dermis an increase in distance of dye travel was recorded.

Recent studies have shown that hyperglycaemia affects connexin expression and function in many tissue types such as endothelial cells, fibroblasts or gomerular vasculature (Abdullah et al., 1999; Fernandes et al., 2004; Inoguchi et al., 2001; Li et

al., 2003; Oku et al., 2001; Zhang and Hill, 2005). In high glucose culture conditions, aortic smooth muscle cells showed reduced gap junctional permeability due to increased protein kinase C (PKC) phosphorylation (Kuroki et al., 1998). Similar results were demonstrated in rat microvascular endothelial cells and human retinal pericytes (Li et al., 2003; Sato et al., 2002). In these *in vitro* models the inhibition of Cx43 protein expression was shown to be a result of high glucose activating the PKC pathway. Other *in vivo* studies have also shown a reduced Cx43 expression in the perineurium (Pitre et al., 2001), heart (Okruhlicova et al., 2002), oocyte (Chang et al., 2005) and glomerular vasculature (Zhang and Hill, 2005) in diabetic rodents. Although different systems were used, the reduced Cx expression in the epidermis of the back in the present study corresponded to the previous trends seen in Cx studies in diabetic models where Cx was reduced. A possible explanation for this phenomenon is the increased PKC phosphorylation under hyperglycaemic conditions (Xia et al., 1994). Both Cx30 and Cx43 have multiple phosphorylation sites on their C-termini that allow regulation in a post-translational manner. In conditions with increased PKC activity, excess phosphorylation can lead to Cx removal from the membrane for degradation (Laird, 2005); alternatively phosphorylation can also prevent the formation of gap junctions (Richards et al., 2004). Cx30 and Cx43 expression in back epidermis may, therefore, have reduced due to excess PKC phosphorylation. However, Cx26 does not have any phosphorylation or other post-translational regulatory sites on its C-terminus and therefore cannot be downregulated via the PKC pathway. Using RT-PCR Sato et al. (2002) noted a reduction in the Cx43 mRNA level in rat microvascular endothelial cells in high glucose culture conditions, and noted that no changes were seen in Cx37 and Cx40 mRNA levels in the same endothelial cells. Together, these observations would suggest that there is a more upstream effect of hyperglycaemia on connexin

expression that may be connexin or tissue specific. More than one mechanism probably exists to control connexin expression in diabetic conditions.

Although the number of Cx26, Cx30 and Cx43 gap junction plaques was significantly lower in the back epidermis of diabetic rats, the extent of reduction differed for each of the connexins. The degree of decrease was more pronounced for Cx26 and Cx30 protein expression than for Cx43. This distinction in the observations could be related to the differential expression and roles of each connexin in the epidermis. Cx26 is expressed in the spinous layer and is associated with keratinocyte differentiation (Kamibayashi et al., 1993; Lucke et al., 1999). Changes in epidermal proliferation, differentiation and thickness are some of the most commonly documented complications in diabetic skin (Sakai et al., 2003; Wertheimer et al., 2001). Keratinocytes change phenotypically due to the enhanced Ca^{2+}-induced differentiation in the presence of high glucose (Spravchikov et al., 2001). The reduction in Cx26 and Cx30 expression in diabetic epidermis can lead to the loss of the normal Ca^{2+} gradient which is required for proper epidermal differentiation (Brissette et al., 1994; Wiszniewski et al., 2000). Cx43 is expressed in the suprabasal keratinocytes which are actively undergoing cell proliferation (Gibson et al., 1997). Reduced cell proliferation in diabetic keratinocytes (Terashi et al., 2005) could lead to the decreased number of Cx43 gap junctions in the epidermis. Alternatively, given the close association of Cx43 and keratinocyte proliferation, downregulation of Cx43 due to regulatory controls mentioned in the previous paragraph may have caused a decrease in cell proliferation in keratinocytes.

Besides the direct action of hyperglycaemia, keratinocytes can also be affected by the lack of insulin in STZ-rats. The gene encoding Cx26 has binding domains for the transcription factors Sp1 and Sp3 in the promoter region of its gene (Tu and Kiang, 1998) but both of these transcription factors are diminished in the absence of insulin (Pan et al., 2001). This offers another explanation for the low presence of Cx26 in the diabetic back epidermis.

However, contrary to the findings in the epidermis, the number of Cx43 GJ plaques was shown to have increased in diabetic back dermis. This was also demonstrated previously in cultured primary human diabetic fibroblasts with increased dye coupling (Abdullah et al., 1999), which the authors suggested was associated with a slower cell growth rate. In my studies, the increase in the number of Cx43 gap junction plaques and the significantly increased total protein (staining area) per unit area was reflected by scrape loading dye transfer which showed significantly higher GJIC across the dermis. Increased Cx43 seen in the dermis may be associated with reduced cell proliferation in the fibroblasts as Abdullah et al. (1999) suggested. Another interesting observation was that the skin of STZ diabetic rats often became thinner as the animal became thinner with diabetes progression; this could be associated with increased matrix metalloproteinase (MMP) production by diabetic fibroblasts as has been reported in human diabetic patients (Wall et al., 2003). MMPs degrade extracellular matrix proteins as well as cell-to-cell adhesion by cleaving extracellular loops of tight junction proteins (Yang et al., 2007). Interestingly, increased Cx43 expression is linked with increased MMP production in synovial cells in osteoarthritis (Marino et al., 2004). The diabetic dermal increase in Cx43 protein expression reported in this chapter may contribute to excess MMP activity, causing the thinning of the rat diabetic skin.

Vice versa, the excess MMP production by diabetic fibroblast may also influence Cx43 expression indirectly via signalling pathways triggered by protease activity.

Both keratinocytes and fibroblasts have different properties in the interfollicular and plantar types of skin, so it is not perhaps surprising that their response to diabetes were different and should be considered separately. Intriguingly, Cx26 and Cx30 expression in the plantar skin of the heel did not decrease eight weeks after STZ diabetes induction as was seen in the interfollicular skin of the back. The difference in the observations can be explained by the histological differences between interfollicular and plantar skin, related to their separate functional specialisations. The thickness of epidermis varies considerably across the body. In humans, the thickness can vary from 0.5 mm at the eyelid to 1.5 mm or more in the sole or heel of the foot (Young, 2000). The palmoplantar skin (palm and sole) is much thicker than skin elsewhere because it is adapted to continuous friction by developing a very thick stratum corneum. No hair follicles or sebaceous glands are found in palmoplantar skin. Because of the friction and pressure, plantar skin keratinocytes have increased keratin filament content for anchorage compared to interfollicular skin (Swensson and Eady, 1996) and a higher number of desmosomes between the cells in the stratum spinosum (the 'prickle' cells can be seen in Figure 3.4). Many studies have shown that connexin expression is closely associated with desmosomes and adherens junctions at the plasma membrane (Brandner et al., 2003; Hentula et al., 2001; Risek et al., 1992; Wei et al., 2005). Connexins are expressed at the sites where adherens proteins are localised at plasma membranes (Brandner et al., 2003; Hentula et al., 2001) and are dependent on each other to establish gap or adherens junctions (Meyer et al., 1992; Wei et al., 2005). The additional desmosomes expressed between the differentiating keratinocytes in the

heel epidermis may help in stabilising Cx26 and Cx30 gap junction plaques in diabetic conditions and thus prevent the heel epidermis from undergoing the reduced expression observed in interfollicular epidermis.

The back dermis showed increased Cx43 expression but the heel dermis showed decreased expression. These contradictory results are puzzling. Direct comparison could not be made due to the vast difference in their innate histology (presence of skin appendages). Nevertheless, the lack of skin appendages and the consequent difference in the vasculature and the neuronal network in the heel skin may offer an explanation. In diabetic rats, neuropathic and angiopathic complications will have developed in the extremities by 8 weeks after diabetes induction. The effect of these complications could vary between the extremities and the trunk. However, it is interesting to note that perineurium subjected to diabetes and oxidative stress loses Cx43 expression (Pitre et al., 2001). Whether these neuropathies contribute to the downregulation of Cx43 in heel dermal fibroblasts cannot be confirmed here.

Results in this chapter have demonstrated that the onset of diabetes has a marked effect on the protein expression level of connexins in the skin. The mechanism whereby diabetes alters the expression of connexins, with a differential effect on different connexin proteins, is at present unknown. The mechanism of action remains to be determined. Understanding how and at what level (transcriptional, translational, or post-translational) hyperglycaemia affects Cx expression will be important, as this will help in understanding protein regulation and restoration of homeostasis in skin.

4 DYNAMICS OF CONNEXIN EXPRESSION IN DIABETIC WOUNDS

4.1 Chapter introduction

The prevalence of diabetes is increasing annually worldwide, causing heavy burdens in health services (National Diabetes Information Clearinghouse, NIH, USA). Chronic wounds are a major problem in diabetic patients where diabetic complications such as peripheral neuropathy and peripheral vascular diseases predispose patients to wound ulceration and increase morbidity (Dinh and Veves, 2005). Other factors have also been reported to contribute to delayed diabetic wound healing, including prolonged inflammation (Komesu et al., 2004; Loots et al., 1998; Wetzler et al., 2000), alterations in levels of growth factors and proteases in the wound microenviroment (Beer et al., 1997; Harris et al., 1995; Werner et al., 1994) and abnormal wound contraction (Franzen and Roberg, 1995).

The expression of connexin proteins is dynamically regulated during skin repair and the changes in expression have been associated with different phases of the wound healing process (Coutinho et al., 2003; Goliger and Paul, 1995). Connexins have been shown to have a regulatory role in the process of normal wound repair in repair initiation, synchronisation of cell migration and modulating ECM production (Cao et al., 2002; Coutinho et al., 2003; Kretz et al., 2003; Moyer and Ehrlich, 2003). Brandner et al. (2004) have shown that in *ex vivo* chronic leg ulcers, Cx43 protein expression remained high in the wound edge epidermis, suggesting abnormal regulation in Cx protein expression. However, the role of connexins in diabetic wound healing has not yet been fully investigated. In Chapter 3 I have demonstrated

that Cx protein expression in the back skin of STZ diabetic rats is abnormal. I have therefore investigated the dynamics of expression of Cx43 and Cx26 in the wound edge epidermis during the course of normal and diabetic wound repair, in order to further understand roles of gap junctions in diabetic wound healing.

4.2 Brief methodology

Streptozotocin-induced diabetic rats are an established model for diabetic wound healing studies (Bitar, 1998; Komesu et al., 2004). Sprague-Dawley rats were made diabetic with a single intraperitoneal injection of Streptozotocin (65 mg/kg) and diabetes was allowed to develop for two weeks after its induction (see Chapter 2.3). Diabetes was confirmed with urine test strips (Bayer) and blood glucose level measured on termination as mentioned in Chapter 3.2. Pairs of 5 x 5 mm full thickness excisional wounds were made on the shaved back of diabetic and weight-matched healthy rats using a number 15 scalpel (Figure 2.1). Wounds were allowed to heal naturally and tissue collected on days 1, 2, 5, 10 and 15 (N = 6 control, N = 6 diabetic for each time point). The collected wounds were freshly frozen in OCT and cryosectioned (10-12 μm) for immunostaining or H & E histological staining.

Tissue sections were immunostained for Cx26 (Monaghan et al., 1994) and Cx43 (Wright et al., 2001) and imaged using confocal microscopy. For quantifying Cx expression dynamics during days 1, 2, and 5 after wounding, three areas denoted 'leading edge (LE)', 'wound edge (WE)' and 'adjacent zone 500 μm away (AD)'

were imaged (see Figure 4.1). The leading edge (LE) zone was only imaged on day 5 when obvious leading keratinocyte migration was observed. For each zone (AD, WE and LE) six images were taken for each of the animals with an optimal setting that was kept constant for all images obtained. The images were thresholded to account for connexin protein, and areas of epidermis were demarcated using NIH ImageJ software to quantify protein expression in all the three zones. A two-way ANOVA followed by a Newman-Keuls post-hoc test was used to compare the connexin protein expression in zones on different days. For 10 and 15 day wounds, images of four zones of epidermis across the wound were acquired: (1) uninjured skin, (2) wound edge, (3) edge of nascent epidermis and (4) centre of nascent epidermis (Figure 4.1).

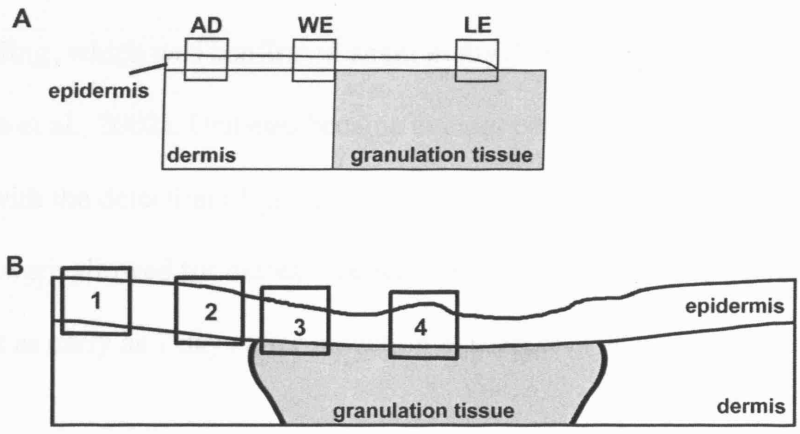

Figure 4.1 Diagrams of areas in the epidermis examined. (A) Diagram of re-epithelialising epidermis. Images of connexin protein expression were taken at the adjacent epidermis (AD), wound edge (WE) and leading edge (LE) zones for quantification on days 1, 2 and 5 after injury. (B) Diagram showing the regions of the epidermis imaged in day 10 and 15 wounds. Zones were indicated as follows: (**1**) uninjured skin, (**2**) wound edge, (**3**) edge of the nascent epidermis and (**4**) centre of nascent epidermis.

H & E stained slides were imaged using a light microscope and digital images acquired for re-epithelialisation measurements. The extent of re-epithelialisation was calculated by measuring the total length that the nascent epidermis had migrated from the two wound edges expressed as a percentage of the wound bed. The extent of re-epithelialisation was measured and calculated for wounds 1, 2 and 5 days after injury as by day 10 all the wounds have re-epithelialised completely.

4.3 Streptozotocin-induced delayed diabetic wounds in rats

The use of STZ to induce diabetes in rats is a recognised model for delayed diabetic wound healing, which was confirmed again in my thesis (Bitar, 1998; Seifter et al., 1981; Witte et al., 2002). Diabetes became evident between 2 and 4 days after induction with the detection of glucose in urine using urine test strips. In our model two weeks were allowed for diabetes progression but the delay in wound healing can be apparent as early as 7 days after induction of diabetes (Witte et al., 2002).

Reduced extent of re-epithelialisation is a sign of the wound healing poorly. The rate of re-epithelialisation was consistently slower in the diabetic rats compared to control rats in days 1, 2 and 5 after wounding ($P < 0.05$, $P < 0.001$ and $P < 0.01$ respectively). By day 10 the epidermis has re-epithelialised the wound completely in both groups and the skin was resealed (Figure 4.2).

A

day	Control (%)	Diabetic	
1	7.5	2.5	*
2	15.7	6.1	***
5	41.0	27.4	**

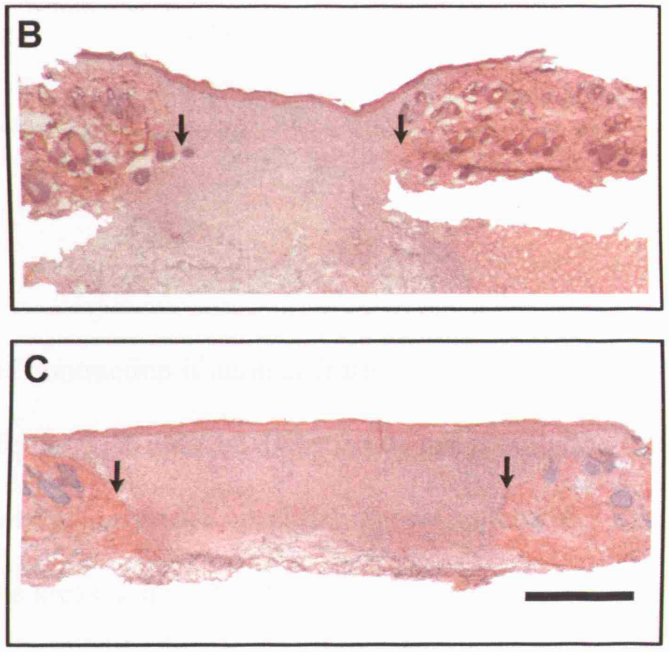

Figure 4.2 Wounds in streptozotocin induced diabetic animals show delayed healing. (A) The extent of re-epithelialisation (%) is retarded in the diabetic wound at all the time points: days 1, 2 and 5 after injury (*P < 0.05, ** P < 0.01, ***P < 0.001). H & E histology in 10-days wound showed poor granulation tissue contraction in the diabetic wound (C) compared to control animals (B). Arrows mark the wound edges; scale bar 1 mm.

Table 4.1 Granulation tissue area in control and diabetic wounds 5, 10 and 15 days after injury. Between days 5 and 10 the granulation tissue contracted; the measured area reduced in control wounds but this was not evident in diabetic wounds (data provided by MSc student Mr Kieran Power).

Days	Control wound (arbitrary unit)	Diabetic wound (arbitrary unit)
5	6.60 ± 1.18	5.29 ± 0.44
10	3.35 ± 0.07	4.49 ± 0.39
15	4.27 ± 0.10	3.79 ± 0.43

Abnormal wound contraction is another feature of diabetic wounds (Franzen and Roberg, 1995). In the STZ-induced diabetic rats the granulation tissue contraction at days 10 and 15 was also retarded, as clearly shown in the H&E image (Figure 4.2). Granulation tissue areas in days 5, 10 and 15 were measured from H & E images by Mr Kieran Power, an MSc student who worked in the lab under my supervision (Table 4.1). Granulation tissue area was demarcated from digital images of the wounds (N = 6) and quantified using ImageJ. A significant reduction in granulation tissue area was seen between days 5 and 10 of control wounds ($P < 0.01$). In diabetic rats the granulation tissue contracted but the level of contraction was lower compared to control rats. Interestingly, the granulation tissue area was smaller in diabetic wounds to begin with on day 5 compared to control wounds ($P < 0.05$). This was possibly due to reduced cell infiltration during tissue formation.

4.4 Connexin 43 expression in diabetic wound healing

4.4.1 Days 1, 2 and 5 after injury

In control wounds, there was reduced Cx43 expression in the epidermal WE region relative to the AD region 1 day after wounding (Figure 4.3; Table 4.2) as reported previously in the literature (Coutinho et al., 2003; Goliger and Paul 1995). This downregulation has been associated with the change in the keratinocytes to a migratory phenotype. In marked contrast, and surprising in view of the decreased expression of Cx43 in intact diabetic skin shown in Chapter 3, no reduction in Cx43 protein expression was observed and actually a greater protein expression was observed in the WE region than the AD region in the diabetic rats (Figure 4.3). Cx43 protein expression in the WE region of diabetic rats was more than double that of the WE region in controls ($P < 0.001$; Figure 4.4). The initial wound healing response of Cx43 in diabetic wounds was the opposite to that observed in the control wounds.

At 1 day after wounding, the diabetic keratinocytes formed a thickened bulb at the wound edge, whereas in controls they had thinned out prior to crawling forward to close the wound. The change to a migratory phenotype was observed at 2 days after wounding in the diabetic WE, by which time Cx43 expression had reduced to low levels, similar to those of controls (Figure 4.3, Figure 4.4).

On day 5, re-epithelialisation was well underway in both diabetic and control groups although the extent in diabetic wounds was significantly retarded (Figure 4.2). A

leading edge (LE) zone was included with AD and WE for Cx43 quantification. Cx43 expression increased dramatically in the WE region of control wounds but in diabetic wounds Cx43 protein expression remained low (Figure 4.3; Figure 4.4). The level of expression at WE was significantly higher in control WE ($P < 0.01$), a pattern similar to that observed in intact skin. Only low levels of Cx43 expression were observed in keratinocytes in the migrating tongue in the LE region of both control and diabetic wounds. Although the extent of re-epithelialisation was different, the Cx43 protein expression level was similar in the LE of both wounds (Table 4.2; Figure 4.4).

Table 4.2 Dynamic expression of Cx43 protein in the epidermis during wound healing of control and diabetic rats.

day		AD (No. of plaques /100μm)	WE (No. of plaques /100μm)	LE (No. of plaques /100μm)
1	Control	7.04 ± 0.70	4.27 ± 0.59	N/A
	Diabetic	5.52 ± 0.42	12.28 ± 2.37	
2	Control	5.47 ± 1.19	3.84 ± 0.62	
	Diabetic	7.52 ± 0.67	4.33 ± 0.48	
5	Control	12.31 ± 2.89	10.08 ± 1.93	3.20 ± 0.85
	Diabetic	8.08 ± 1.63	3.21 ± 1.02	2.25 ± 0.93

The Cx43 expression data were analyzed by a two-way ANOVA with diabetes and time after injury as factors. This revealed that there was a highly significant

interaction (P = 0.0001) between the effect of diabetes and that of time on Cx43 expression in the wound edge, indicating that diabetes was influencing the dynamic changes in Cx43 expression in the WE region associated with wound healing. No such interaction was demonstrated for Cx43 expression in the intact AD region adjacent to the wound; quantification showed no significant difference in the dynamic expression during the healing process (Figure 4.4).

Figure 4.3 Cx43 immunostaining at the epidermal edge of control and diabetic wounds on days 1, 2 and 5 after injury. Cx43 shown in green and nuclear counterstaining in red. (A) At 1 day, Cx43 protein expression is downregulated in the wound edge (WE) keratinocytes of control rats compared to adjacent (AD) epidermis but has been upregulated in the corresponding region in diabetic animals, which appears swollen (B, thick arrow). (C, D) At 2 days, Cx43 staining has reduced in the diabetic (D) wound-edge keratinocytes and is similar that of control wound (C). At 5 days after wounding some Cx43 can be observed at the leading-edge (LE) in control (E) but not in diabetic (F) keratinocytes. Thin arrows mark the edge of the wound; the white dotted line represents basement membrane; scale bar 100 μm.

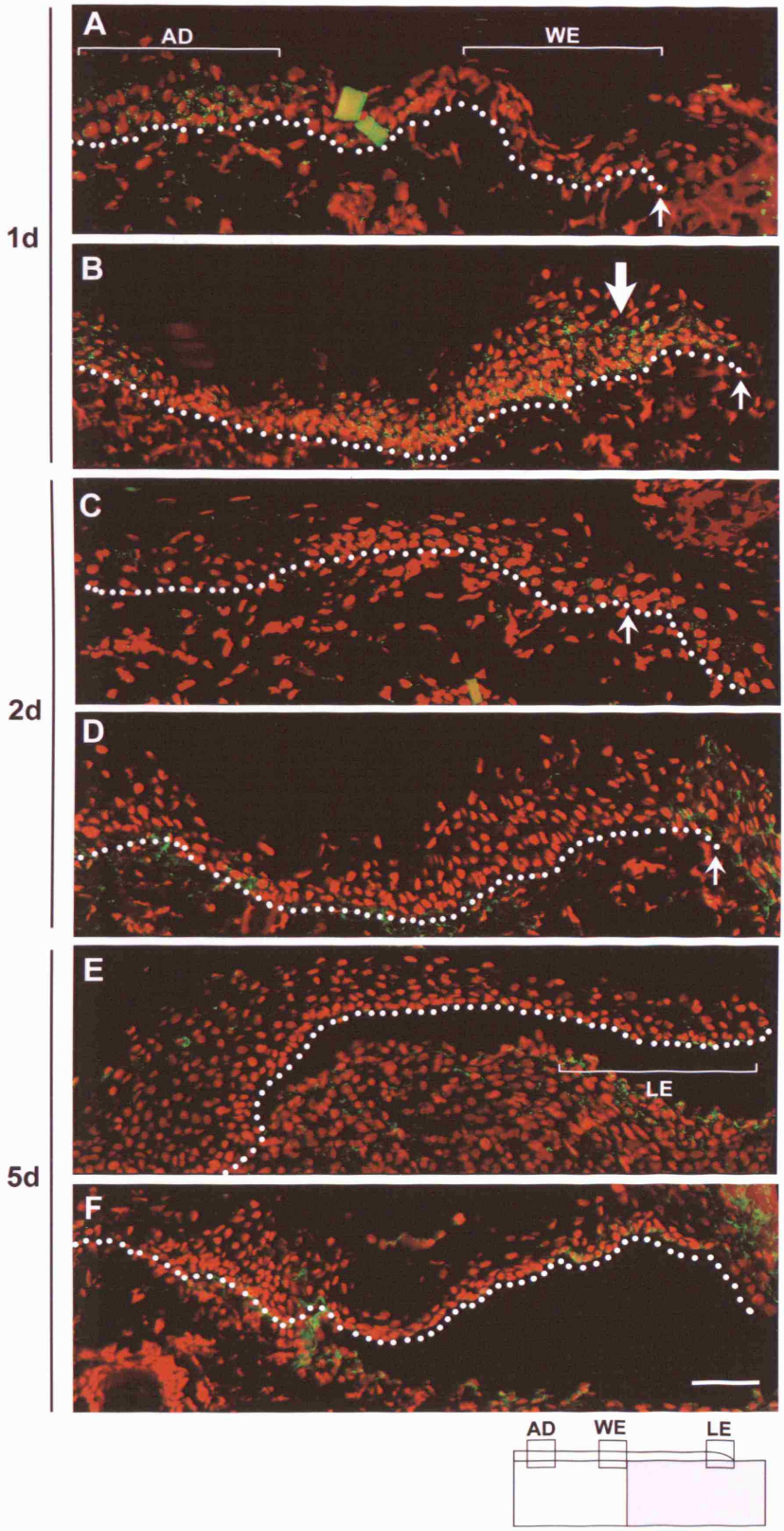
A
AD
WE
1d
B
C
2d
D
E
LE
5d
F
AD
WE
LE

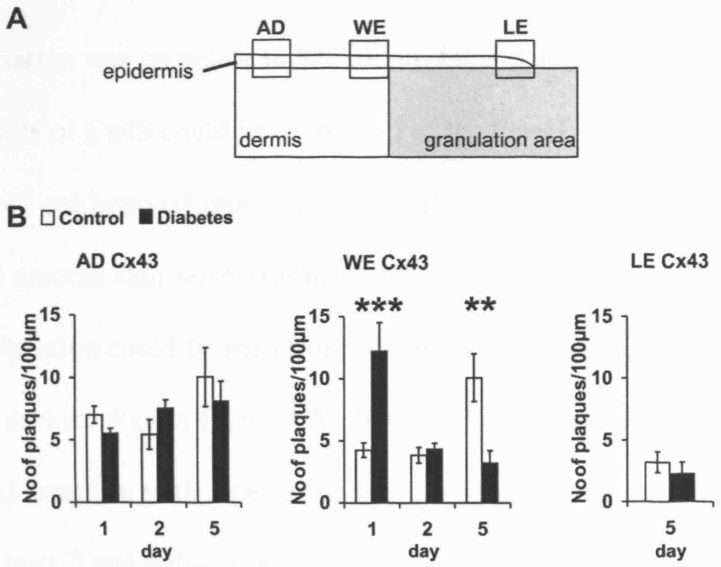

Figure 4.4 The dynamic responses of Cx43 protein levels following injury in control and diabetic epidermis. A: Diagram shows the zones in which connexin staining was quantified, by counting plaques at 1, 2 and 5 days after wounding. On days 1, 2 and 5, quantification was carried out at the wound edge (WE) and adjacent (AD) epidermis, 500 µm away; and on day 5 an additional zone was included at the leading edge (LE) of the nascent epidermis. B: The dynamic response of Cx43 protein expression to injury was found to be very different in diabetic skin (black bars) and normal skin (white bars). Cx43 staining in zone WE normally reduces in the first 24 hours after injury but in diabetic skin it increases significantly (***$P < 0.001$), returning to near control levels by 2 days; but Cx43 was found at significantly (**$P < 0.01$) reduced levels in zone WE at 5 days after wounding.

4.4.2 Days 10 and 15 after injury

Re-epithelialisation was complete in both control and diabetic animals by day 10, when high levels of Cx43 could be seen in all of the layers of the proliferative, hyper-thickened epidermis (Figure 4.5). Four different zones of epidermis across the uninjured and nascent skin were examined (Figure 4.1). In both groups, a gradient of epidermal maturation could be seen from the edge to the centre of the wound (from zones 2 towards 4 marked in Figure 4.5). In the uninjured epidermis in zone 1, the usual stratified structure with established stratum corneum can be observed. However in zones 3 and 4 this was still absent as the newly fused leading edge epidermis still needed to mature into the laminar maturation and nuclear rearrangement. In this newly formed epidermis Cx43 protein expression was not restricted to the basal layer as in the uninjured skin but was expressed throughout the whole thickness of the epidermis. At this stage the newly formed epidermis in both groups still has to achieve its mature stratification pattern. At day 10, newly formed diabetic epidermis has consistently higher levels of Cx43 expression compared to control (zones 2-3), although in the uninjured skin (zone 1) the expression is lower as reported in Chapter 3 (Figure 4.5).

At 15 days, the nascent epidermis began to mature into a stratified epithelium in all the zones studied. Clear laminar structures had formed in zone 2 in both control and diabetic epidermis. However, a marked gradient of maturation from the edge to the centre of the wound was still evident and this reflected the gradual restriction of Cx43 expression to the basal layers. The expression remained high at the site of

leading edge fusion (zone 4) but staining appeared more linearly expressed in the plasma membrane. Similar to the 10-day wounds, Cx43 expression was higher in the diabetic nascent epidermis at 15 days but not in the uninjured skin.

In summary, Cx43 in the wound edge epidermis down regulated as keratinocyte migration initiated in order to re-epithelialise and seal the open wound. However, the proliferating keratinocytes, behind the growing leading edge, expressed Cx43 as they continuously supplied keratinocytes for migration. When migration was over and the nascent epidermis started to mature and differentiate, Cx43 protein expression started to decrease to more normal levels and became restricted to the basal layers as in the uninjured skin.

Interestingly, the dynamic expression of Cx43 protein in response to injury in diabetic skin was initially abnormal, with high upregulation of Cx43 instead of the normal downregulation at the wound edge. The regulation of Cx43 protein expression at the wound edge suffered a lag initially but after 2 days the expression appeared to follow the normal pattern. Following the decrease in Cx43 expression, the re-epithelialisation began at 2 days but at a slower rate compared to control. In the migrating keratinocytes, Cx43 expression gradually increased behind the leading edge until wound closure occurred, as in control wounds. Thereafter, the Cx43 expression increased, correlating with epidermal proliferation, and only decreased to normal levels after the completion of differentiation.

Next page

Figure 4.5 Connexin 43 staining (green puncta) and nuclear staining (red) in control and diabetic skin at days 10 and 15 after injury showing the dynamic changes in expression during maturation of the nascent epidermis. The zones marked represent (1) uninjured epidermis away from the wound, (2) uninjured epidermis at the edge of the wound, (3) nascent epidermis at the edge of the wound and (4) nascent epidermis in the centre of the wound. The dotted white line shows the border between the epidermis and the dermis. Cx43 can be seen to be in all layers of the newly formed, hyper-thickened epidermis, returning to a more basal expression as the skin thins down during tissue remodelling. This change can be seen both in time and as a gradient of maturation from the edge to the centre of the wound. A green band of autofluorescent keratin can be seen over the intact skin (E, M) but this has not yet formed in the nascent epidermis. Scale bar 25 μm.

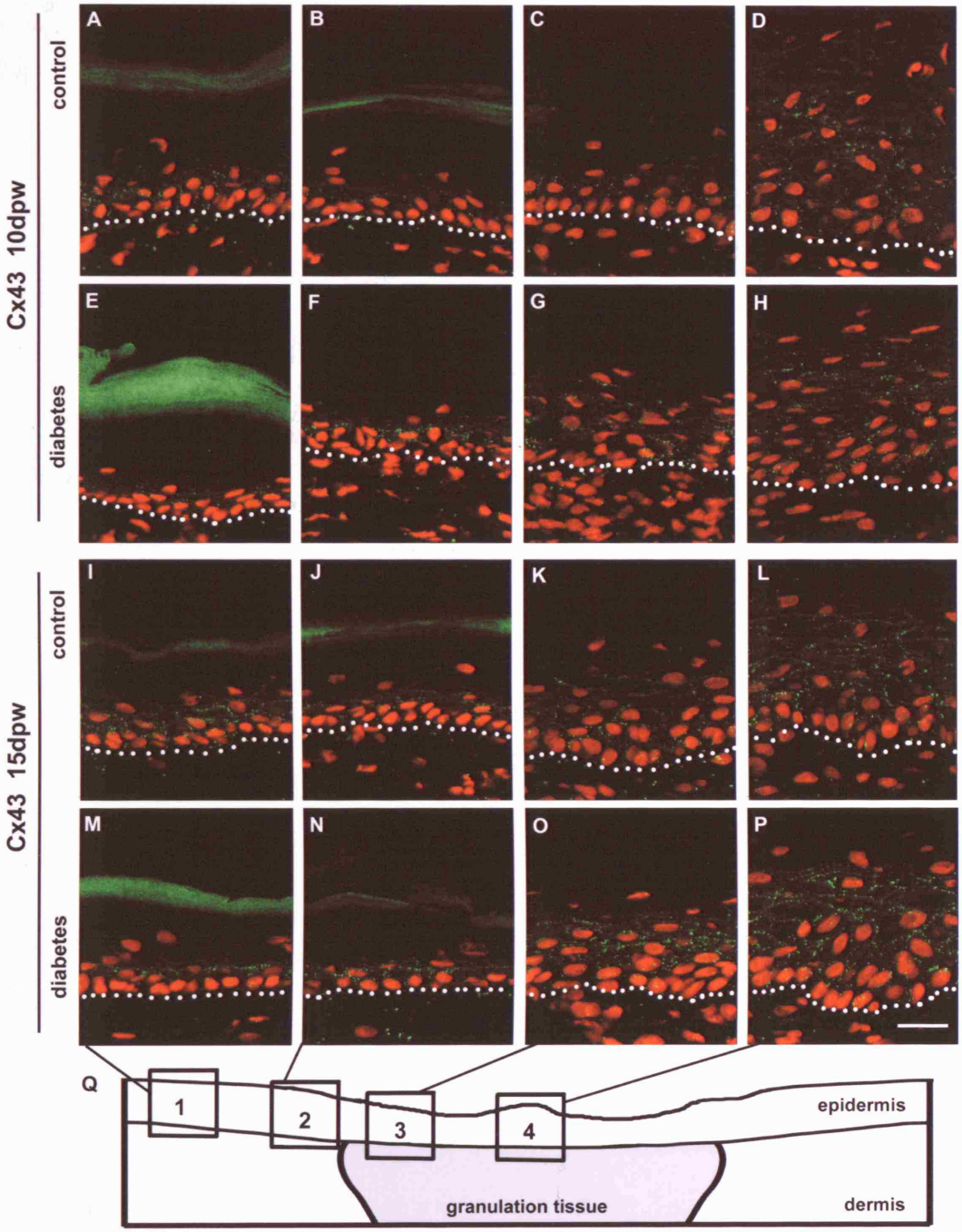
Cx43 10dpw
control
diabetes
Cx43 15dpw
control
diabetes
A
B
C
D
E
F
G
H
I
J
K
L
M
N
O
P
Q
1
2
3
4
epidermis
granulation tissue
dermis

4.5 Connexin 26 expression during diabetic wound healing

4.5.1 Connexin 26 and connexin 30 co-localisation?

The expression of Cx26 and Cx30 proteins increases at the epidermal wound edge after injury (Coutinho et al., 2003). At the wound edge where the normal epidermal laminar structure was lost, immunostaining revealed that increases in Cx26 and Cx30 expression were found in the whole wound edge epidermis (Figure 4.6). Further away from the wound edge, a transition zone can be seen where the previously restricted connexin expression switched from the spinous layer to the basal layer and then to all the keratinocytes in the wound edge (Figure 4.6). Double labelling of Cx26 and Cx30 proteins showed a similar trend of transition and increase in expression at the wound edge (Figure 4.6). Co-localisation analysis was performed with the help of Dr Kevin Webb on the confocal image, using Imaris software. Positive staining was selected using an optimal threshold to eliminate the background noise and then projected into individual particles. The particles (connexin plaques) from the two colour channels were then analysed for co-localisation. Although both connexins were upregulated similarly, very little or no co-localisation of the two connexins was found in any of the three AD, transition (TS) and WE zones analysed (

Figure **4.7**).

For the rest of the chapter only Cx26 is considered for expression quantification.

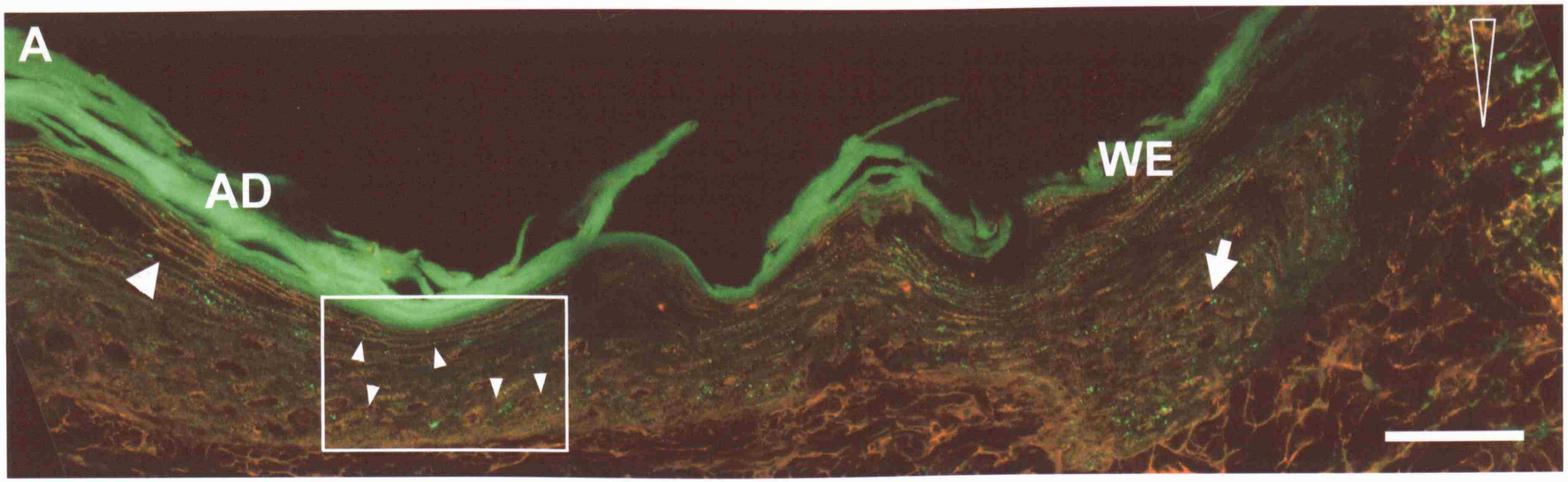

Figure 4.6 Cx26 (red) and Cx30 (green) staining in the control wound edge epidermis 1 day post wounding. Both connexins were expressed in the spinous layers of the epidermis in the adjacent (AD) unwounded epidermis (large arrowhead). At the wound edge (WE) the expression of both connexins was elevated and no obvious co-localisation was found (arrow). There appeared to be a transition zone (boxed where the location of Cx expression switched from the spinous layer to the basal layers (arrowheads in the box) towards the WE, where the usual epidermal structure was lost. The open arrowhead marks the wound; scale bar 50 μm.

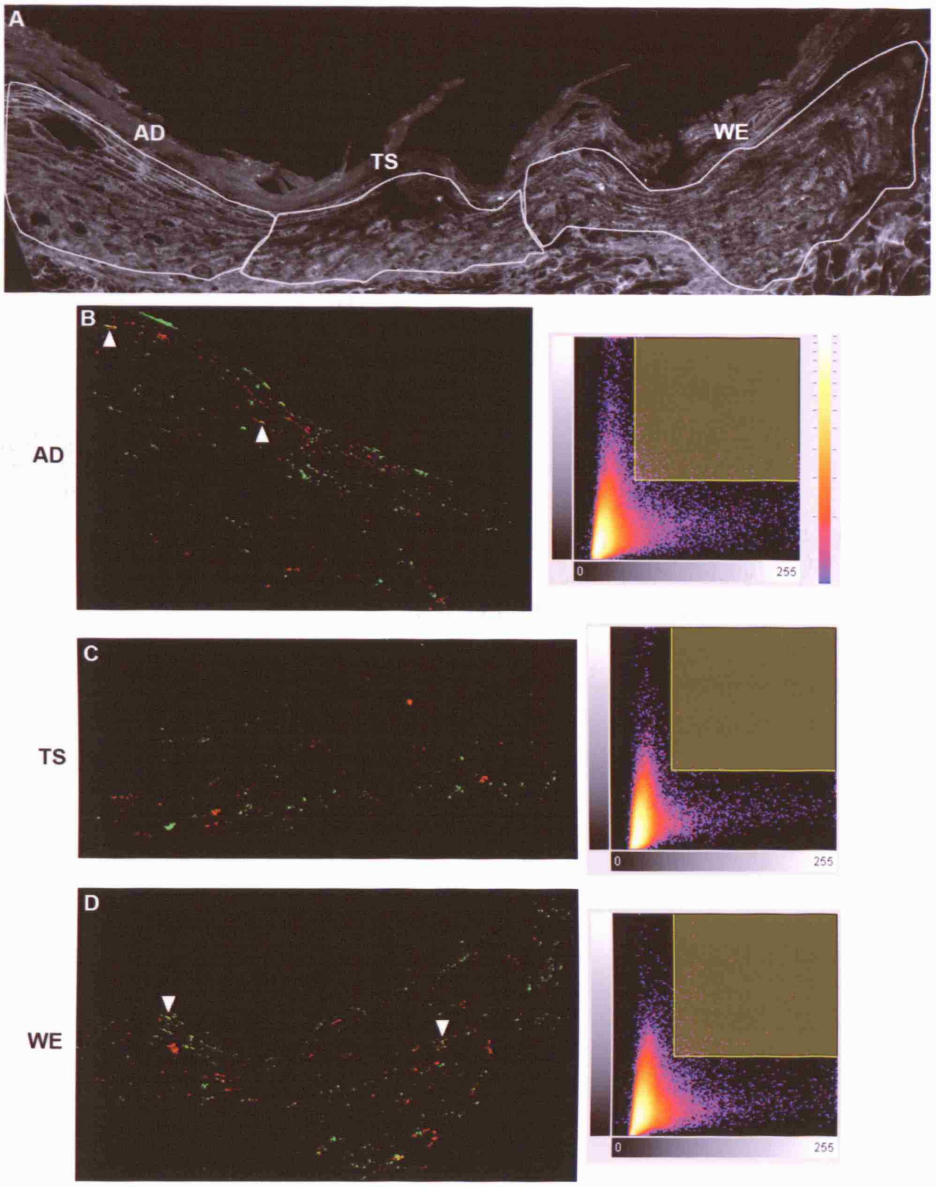

Figure 4.7 Analysis of Cx26 and Cx30 co-localisation in the epidermal wound edge. (A) Diagram indicating the three zones AD, transition section (TS) and WE analysed for connexin co-localisation. Each area is encircled within the white line. (B) A few co-localised Cx26 (green) and Cx30 (red) protein plaques were seen in zone AD (arrowhead). The right panel of B-D shows particle intensity scatter graph, the thresholds for the 2 colour channels were marked (shaded yellow box). The particles above the selected thresholds were used for analysis. The colour key shows the level of particle density. (C) No obvious co-localisation was observed in the TS zone. D: A few co-localisation plaques were observed (arrowhead) but there was largely no co-localisation of the two connexins.

4.5.2 Days 1, 2 and 5 after injury

Cx26 staining was quantified from immunofluorescent images in the same way as Cx43. The same three zones: adjacent epidermis (AD), wound edge (WE), and leading edge (LE) were used to compare Cx26 protein expression in the wound healing process. In contrast to Cx43, Cx26 was upregulated at day 1 in response to injury (Table 4.3, Figure 4.8). In both control and diabetic wounds, Cx26 was upregulated in the WE epidermis at day 1 after wounding, and the expression continued to increase at day 2 after wounding (Figure 4.8, Figure 4.9). By day 5 after wounding, Cx26 expression remained constant in the WE and AD zones of control wounds but in diabetic wounds the expression decreased from the high levels at day 2 in both regions.

Table 4.3 Epidermal Cx26 expression in control and diabetic wounds.

day		AD (No. of plaques / 100μm)	WE (No. of plaques / 100μm)	LE (No. of plaques / 100μm)
1	Control	6.35 ± 0.49	14.54 ± 1.35	N/A
	Diabetic	8.84 ± 1.45	13.03 ± 1.75	
2	Control	13.48 ± 3.39	21.41 ± 4.61	
	Diabetic	24.47 ± 3.06	31.85 ± 4.32	
5	Control	14.59 ± 3.75	21.44 ± 2.95	17.01 ± 4.16
	Diabetic	5.19 ± 0.93	13.99 ± 3.17	13.66 ± 2.02

Interestingly, the increase of Cx26 expression at day 2 was significantly more widespread and evident further into the adjacent intact skin in the diabetic wounds, where high Cx26 expression was seen in zone AD ($P < 0.05$, Figure 4.8, Figure 4.9).

Further statistical analysis revealed that diabetes did not significantly affect the dynamic changes in Cx26 expression in zone WE but there was a significant interaction between diabetes and Cx26 expression in the intact AD zone (two-way ANOVA, $P = 0.016$).

At day 5 after wounding, Cx26 expression in the leading edge was normally high (while Cx43 was very low) and the predominant staining was found in the suprabasal and differentiating layers of nascent epidermis (Figure 4.8). There were no significant differences in the expression of Cx26 in the zones AD, WE or LE in control or diabetic wounds 5 days after wounding.

Next page

Figure 4.8 Cx26 immunostaining at the epidermal edge of control and diabetic wounds on days 1, 2 and 5 after injury. Cx26 was stained green and nuclei were counterstained in red. Cx26 was upregulated similarly in both control (A) and diabetic (B) epidermis after injury. Cx26 expression continued to increase in all diabetic keratinocytes into the AD region (D), to significantly higher levels than in control wounds (C) at day 2. E and F: At 5 days, Cx26 is clearly observed in the differentiating keratinocytes. Thin arrows mark the edge of the wound; the line of white dots represents basement membrane; Scale bar 100 μm.

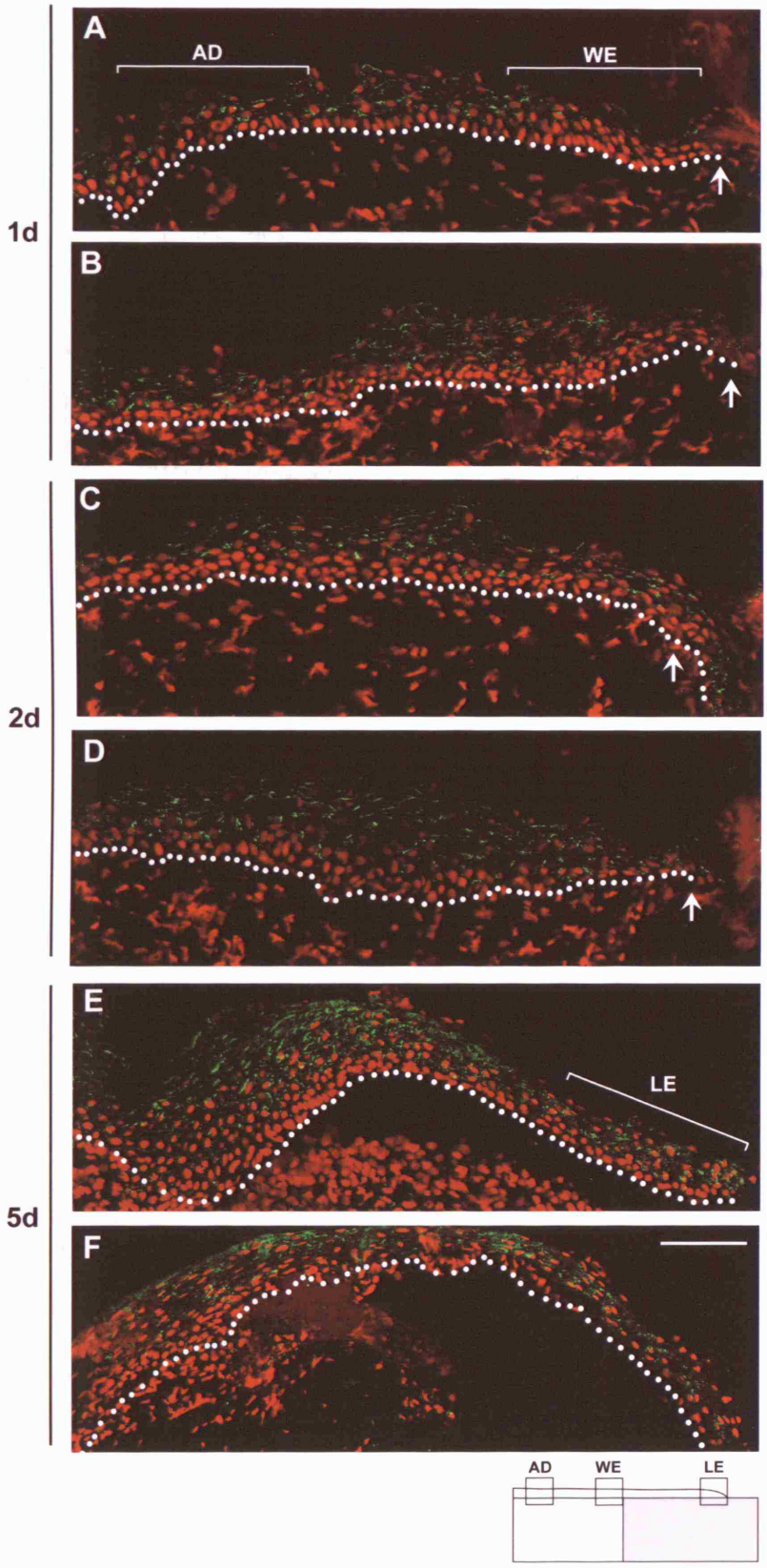
A
AD
WE
1d
B
C
2d
D
E
LE
5d
F
AD
WE
LE

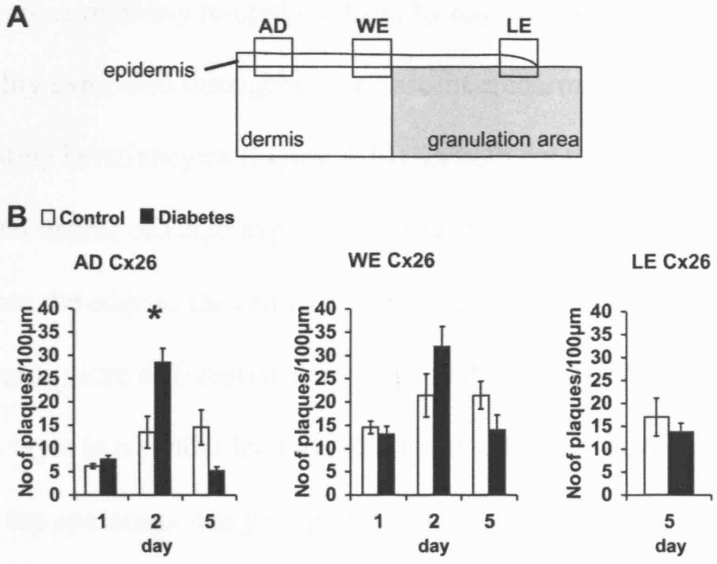

Figure 4.9 The dynamic responses of Cx26 protein levels following injury in control and diabetic epidermis. A: Diagram shows the zones in which connexin staining was quantified, by counting plaques at 1, 2 and 5 days after wounding. On days 1, 2 and 5, quantification was carried out at the wound edge (WE) and adjacent (AD) epidermis, 500 μm away; and on day 5 an additional zone was included at the leading edge (LE) of the nascent epidermis. B: The normal response of Cx26 to injury is an elevation of staining in WE and this occurred in both control and diabetic animals at 1 and 2 days after wounding; however, the elevation was greater in diabetic skin.

4.5.3 Days 10 and 15 after injury

All wounds were completely re-epithelialised by day 10 after wounding. Like Cx43, Cx26 was highly expressed throughout the nascent epidermis but more specifically in the differentiating keratinocytes (Figure 4.10). In both control and diabetic wounds, the location and degree of Cx26 expression were related to the gradient of epidermal maturation from the edge to the centre of the wound (Figure 4.10). When the epidermis became more differentiated as it matured (zone 2), Cx26 became restricted to the spinous layer in a similar location to normal uninjured skin. In the centre of the wound where the epidermis was youngest, Cx26 protein was expressed in multiple layers of the proliferating keratinocytes. In diabetic wounds, the Cx26 expression appeared lower in all the zones examined, and this associated with fewer cells in the diabetic epidermis due to its delayed healing.

At 15 days, the advancement of epidermal differentiation was obvious in both groups as the number of keratinocyte nuclei decreased and they became more aligned. In control wounds, Cx26 expression became further restricted to the anuclear spinous/granular layers of the stratifying epidermis. The nascent epidermis of the diabetic wounds was also maturing, although it was not as advanced as that of control wounds. Cx26 expression was also predominantly seen in the differentiating granular/spinous layers, where nuclei could still be observed. In both control and diabetic epidermis, Cx26 expression decreased with the maturation of newly formed epidermis (zones 2 to 4).

In summary, all keratinocytes at the wound edge where stratification was lost upregulated Cx26 expression in response to injury. The effect of injury was also evident in adjacent tissue (AD) 500μm away from the wound edge which also showed an increase in Cx26 expression in the spinous layer of epidermis. The expression continued to increase at both AD and WE sites and also in the leading edge of the nascent epidermis and remained constant as re-epithelialisation got underway. In the migrating leading edge (LE), Cx26 expression was primarily seen in the differentiating layers. After wound closure was completed, Cx26 protein expression gradually decreased towards the level prior to injury as the epidermal stratification was re-established.

Connexin 26 expression in the diabetic epidermal wound edge increased in response to injury. However, the extent of the increase was much higher in diabetic animals compared to controls, and the spread of increased expression was evident into the adjacent uninjured skin (AD) at 2 days. Cx26 expression in diabetic wounds decreased dramatically at day 5 from the high levels observed at AD at day 2 and a statistical difference was no longer found between the diabetic and control wounds. After complete re-epithelialisation the Cx26 expression pattern in diabetic wounds was similar to that of control but always at lower levels.

Next page

Figure 4.10 Connexin 26 staining (green puncta) and nuclear staining (red) in control and diabetic skin at days 10 and 15 after injury showing the dynamic changes in expression during maturation of the nascent epidermis. The zones marked represent (1) uninjured epidermis away from the wound, (2) uninjured epidermis at the edge of the wound, (3) nascent epidermis at the edge of the wound and (4) nascent epidermis in the centre of the wound, respectively, as diagrammed in (Q). The dotted white line shows the border between the epidermis and the dermis. Cx26 can be seen to be in all layers of the newly formed, hyper-thickened epidermis at day 10, returning to a more superficial expression in the upper spinous layers as the skin thins down during tissue remodelling. This change can be seen both in time and as a gradient of maturation from the edge to the centre of the wound. A green band of auto-fluorescent keratin can be seen over the intact skin. A little keratin can be seen to be forming at the edge of the wound in control rats at day 15 but not in diabetics. Scale bar 25 μm.

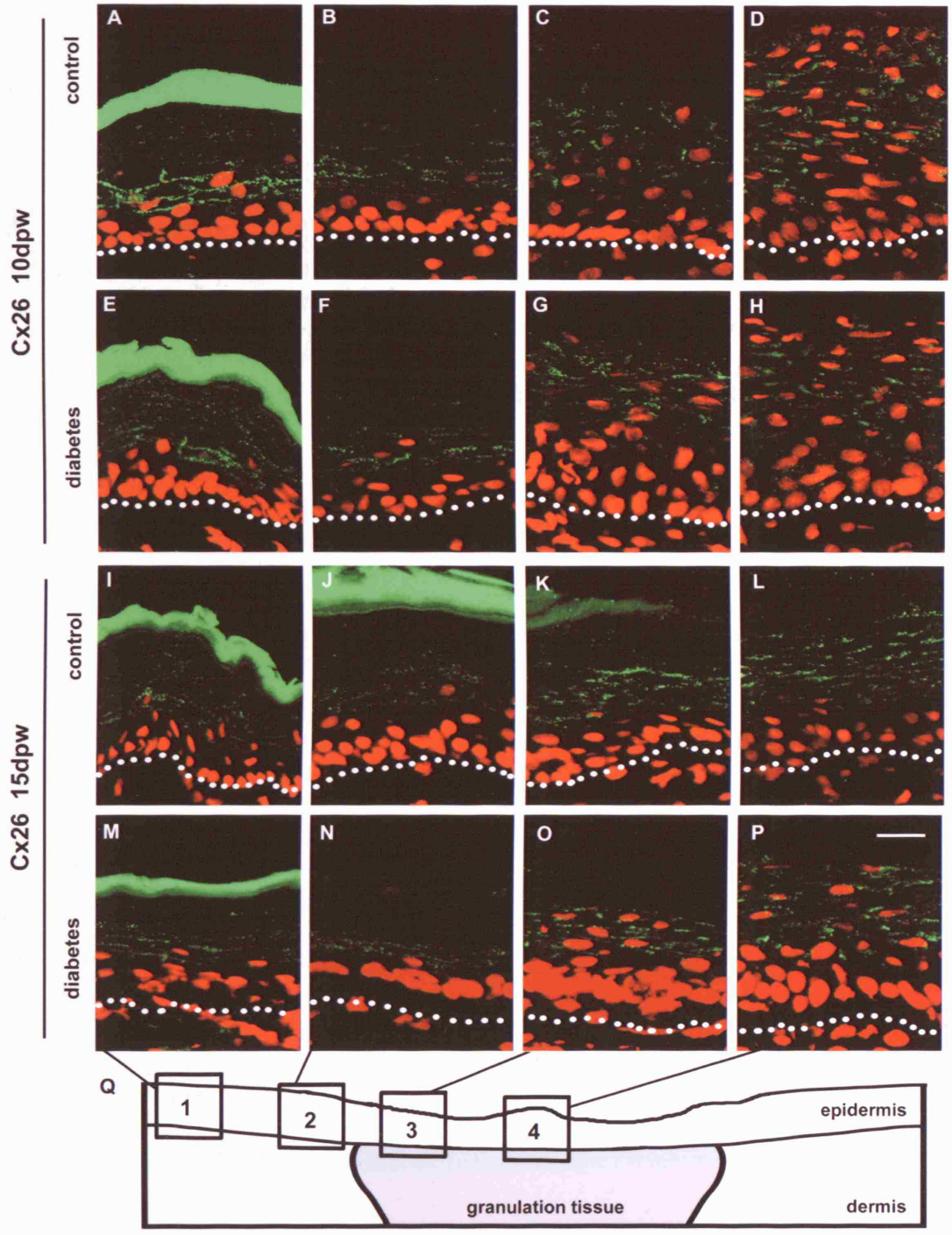
Cx26 10dpw
control
diabetes
Cx26 15dpw
control
diabetes
A
B
C
D
E
F
G
H
I
J
K
L
M
N
O
P
Q
1
2
3
4
epidermis
granulation tissue
dermis

4.6 Chapter discussion

Diabetic wounds are one of the major problems for diabetic patients where wounds do not heal or develop into ulcerations. Connexin expression is dynamically regulated and has been shown to have important roles in regulating wound healing events (Coutinho et al., 2003; Goliger and Paul, 1995). In Chapter 3 of my thesis I have demonstrated that diabetes has a significant influence on connexin protein expression in rat skin. In this chapter, using streptozotocin-induced diabetic rats I have examined the dynamic expression of Cx43 and Cx26 in the epidermal wound edge of diabetic wounds. The dynamic expression of both connexins after injury was abnormal in diabetic rats. Cx43 expression upregulated massively in diabetic wounds instead of downregulating as observed in control wounds after wounding (Wang et al., 2007). The elevation of Cx26 expression was more pronounced and widespread in diabetic wounds than controls. Evidently the regulatory mechanisms for connexin expression after injury are profoundly affected by diabetes.

Impaired wound healing has been reported to occur as early as one to two weeks after induction of Type I diabetes in rats using streptozotocin (Shi et al., 2003; Witte et al., 2002a). The diabetic wound healing model was set up using STZ-induced diabetic rats that develop Type I diabetes. Diabetes was evident as early as 2-4 days as confirmed using urine glucose test strips, and delayed healing was apparent two weeks after induction. The STZ-induced diabetic rats were used at two weeks after induction. Wounds in STZ-rats showed slower re-epithelialisation and reduced granulation tissue contraction compared to their weight-matched healthy controls. The pathological features associated with long-standing diabetes in humans were not

present in this acute model. However, the observation of a delay in wound repair after only two weeks indicates that wound healing can be impaired before diabetic complications such as neuropathy or microangiopathy, that are also known to affect healing, have developed (Goodson and Hunt, 1977; Shi et al., 2003). It is therefore likely that the delay in wound healing occurring in acute STZ-diabetes was a direct consequence of hyperglycaemia and/or lack of insulin.

In normal wound healing, Cx43 expression in the wound edge keratinocytes is dynamic, with an initial downregulation and a gradual increase during wound closure (Coutinho et al., 2003; Goliger and Paul, 1995). However, in diabetic wounds, instead of downregulation, Cx43 expression at the wound edge is elevated significantly (Wang et al., 2007). Very few papers presently exist on the topic of connexin expression in diabetic wound healing. Brandner et al (2004) reported a study of *ex vivo* diabetic chronic and venous ulcers in which Cx26 and Cx43 expression remained continuously high. The STZ-diabetic rat wound healing model was not chronic but only delayed as re-epithelialisation began 2 days after wounding. Interestingly the initiation of re-epithelialisation coincided with the downregulation of Cx43 protein at the wound edge. More recently, Brandner et al. (2007) also identified a difference in the dynamic expression of Cx43. Taking the data (Wang et al., 2007) from these two papers and data from this chapter together, it maybe speculated that high Cx43 expression in the epidermal wound edge is a marker of non-healing wounds. Only when Cx43 protein expression decreased could the re-epithelialisation process begin again to seal the wound.

The Cx43 expression downregulation after injury was in the wound edge keratinocytes that will migrate and regenerate the epidermis (Goliger and Paul, 1995). Activated keratinocytes at the wound edge undergo changes in order to prepare for the migration process. It is not understood how gap junctions play a role in initiating migration but it appears that the downregulation of Cx43 expression is required prior to migration. One of the changes for mobility is the change in anchorage to the substrates from hemidesmosome-based anchorage to a more dynamic adhesion. Close association of connexins and adherens junctions has been found in studies where blocking connexins prevented formation of adherens junctions (Meyer et al., 1992; Paul et al., 1995; Wei et al., 2005). Vice versa, the alteration in cell-cell and cell-matrix adhesion systems for migration can also prevent gap junction formation (Meyer et al., 1992; Wei et al., 2005). The elevated Cx43 expression in 1 day diabetic wounds could interfere with the process of adopting a migratory phenotype. The downregulation of Cx43-based GJIC in the epidermal wound edge has been attributed to the temporally (space and time) phosphorylation of the C-terminus and to the creation of a leading edge compartment to synchronise migration (Richards et al., 2004). Recently the transcription factor Activator Protein-1 (AP-1) has also been implicated in regulating Cx43 expression during wound healing (Neub et al., 2007) but how AP-1 is affected by diabetes is unknown. Understanding the complete mechanism of Cx43 regulation will provide answers to the regulatory role of Cx43 in wound healing but further research is required.

The abnormal upregulation of Cx43 in diabetic wounds at 1 day after wounding suggests an alteration in the regulatory mechanism in diabetic animals. Not only was no downregulation observed; an elevation was also found at the wound edge. Unlike

uninjured skin, where hyperglycaemia or absence of insulin can affect Cx expression, a wide range of cytokines and growth factors present in the wound could also influence the dynamic regulation of Cx expression in response to injury. The more normal pattern of Cx26 and Cx43 expressions at the later time points also suggests that changes in the early diabetic wound microenvironment may be particularly significant in causing changes in connexin expression. Immediately after wounding, the repair process starts with bleeding and clot formation. Platelets release high levels of cytokines such as PDGF and EGF that will in turn activate the subsequent wound healing cascade. In diabetes, the release of cytokines is reduced (Beer et al., 1997; Harris et al., 1995) and the inflammation process is prolonged (Komesu et al., 2004; Werner et al., 1994; Wetzler et al., 2000). The changes in these factors would be expected to have some effect on the initial response in keratinocytes and Cx43 expression. PDGF can mediate tyrosine kinase phosphorylation of Cx43 causing loss of GJIC between cells (Hossain et al., 1999), so reduced PDGF levels in diabetic wounds could mean a loss of triggering mechanisms for terminating GJIC or expression in the wound edge keratinocytes. Delayed diabetic wound healing can be rescued with various applications of the growth factor PDGF (Brown et al., 1994; Keswani et al., 2004). It may be interesting to examine Cx43 expression in these wound models where delayed healing is prevented by PDGF application. In contrast to a decrease in Cx43 expression after injury, diabetic wounds expressed increased level of Cx43 protein. Interestingly, folliculostellate and dendritic cells incubated with the pro-inflammatory cytokines TNF-α and IL-1 both showed transient increase in Cx43 expression (Corvalan et al., 2007; Fortin et al., 2006). Elevated pro-inflammatory signals in diabetic wounds could act as triggers for the increased Cx43 expression at the wound edge.

The upregulation of Cx26 expression after wounding at the epidermal wound edge is a normal response to injury. Similar upregulation was observed in inflamed hepatocytes stimulated by lipopolysaccharide or IL-1 (Temme et al., 2000; Temme et al., 1998). Upregulation was observed in both control and diabetic wound edges but the extent of upregulation was larger in diabetic wounds and this could be triggered by the difference in pro-inflammatory signals. Upregulation of Cx26 expression has been associated with keratinocyte proliferation in skin and some hyperproliferative disorders such as warts or psoriasis, where Cx26 was found in the basal and granular layers of the epidermis (Djalilian et al., 2006; Labarthe et al., 1998). This suggests an association of Cx26 expression with epidermal stratification and maturation in which Cx26 expression must gradually return to normal in order for normal stratification to develop (Wiszniewski et al., 2000; Wiszniewski et al., 2001).

Two-way ANOVA statistical testing identified a significant influence of diabetes on Cx43 expression after injury in zone WE but not in zone AD in days 1, 2 and 5 after wounding. However, diabetes showed a significant influence on expression in zone AD and not in zone WE at the same time points. In diabetic wounds, Cx43 expression was significantly elevated at the WE, and the elevation of Cx26 protein expression in the wound edge was observed in zone AD. Taken together these findings suggest a differential influence of diabetes on the dynamics of connexin expression during wound healing. These data also suggest that Cx26 and Cx43 have distinct roles in epidermal wound healing, depending on the zones where they are expressed (migration or proliferation) and that they are regulated separately. Further

aspects of the roles of Cx43 will be discussed in Chapter 5.9. In summary, the dynamics of connexin expression were abnormal in diabetic wounds. The correct dynamic expression of connexins in the keratinocytes appears to be crucial for the progress of normal skin wound repair.

5 PREVENTING THE ABNORMAL UPREGULATION OF Cx43 EXPRESSION IMPROVES THE QUALITY OF DIABETIC WOUND HEALING

5.1 Chapter introduction

Wound healing in diabetic tissues is markedly delayed or impaired resulting in prolonged open wounds that are prone to infection. Chronic wounds are one of the major problems in the management of diabetes, where patients often suffer from wound ulceration and increased morbidity (Dinh and Veves, 2005; Falanga, 2005). Many factors have been reported to contribute to delayed diabetic wound healing, including prolonged inflammation (Komesu et al., 2004; Loots et al., 1998; Wetzler et al., 2000), alterations in levels of growth factors and proteases in the wound microenvironment (Beer et al., 1997; Harris et al., 1995; Werner et al., 1994) and abnormal wound contraction (Franzen and Roberg, 1995).

Connexins have been shown to have a regulatory role in the process of normal wound repair, in the initiation and synchronisation of cell migration and later on in the modulation of ECM production in the granulation tissue (Cao et al., 2002; Coutinho et al., 2003; Kretz et al., 2003; Moyer and Ehrlich, 2003). Results in Chapter 4 and previous work from our lab have both shown that the dynamic regulation of Cx43 protein expression is important in the wound healing process (Coutinho et al., 2003). In uninjured diabetic epidermis, Cx43 protein expression is reduced compared to control; but in response to injury, instead of the downregulation observed in the normal wounds, the expression was initially highly elevated in the wound-edge epidermis (Chapters 3 and 4; Wang et al., 2007). This phenomenon was also observed in chronic

wounds where Cx43 expression remained high in the surrounding epidermis of *ex vivo* diabetic venous ulcers (Brandner et al., 2004).

The downregulation of Cx43 expression appeared to be essential for the initiation of re-epithelialisation, as observed in normal wounds and in the STZ-induced diabetic wound model used in this thesis. Interestingly, knocking down Cx43 expression at the wound edge using antisense ODN (asODN) accelerated the rate of wound repair in cutaneous incision, excision and thermal wound models (Coutinho et al., 2005; Mori et al., 2006, Qiu et al., 2003). In these studies we have shown that transient knockdown of Cx43 in the wound region immediately after injury has a profound effect on the subsequent wound healing process. During the early inflammatory response in the Cx43-asODN-treated wounds, the number of leukocytes was reduced concomitantly with lower levels of pro-inflammatory chemokines TNF-α and CCL-2 (Mori et al., 2006). The level of TGF-β1 in the wound keratinocytes and fibroblasts was significantly increased at day 2 after wounding, and a faster rate of re-epithelialisation and an increased number of proliferating cells was found in both the epidermis and the dermis. Increased type I collagen production and granulation tissue maturation were observed in the late wound healing processes (Mori et al., 2006). Faster skin wound closure was also observed in transgenic mice with an inducible Cx43 deletion (Kretz et al., 2003) and in organotypic skin wounds treated with connexin mimetic peptide blocker (Kandyba et al., 2007). In this chapter, I examine how preventing the abnormal upregulation of Cx43 expression in the diabetic delayed wound using antisense oligodeoxynucleotide may affect the rate and the quality of diabetic wound repair.

5.2 Brief methodology

Antisense oligodeoxynucleotide to Cx43 mRNA was designed previously in the lab (Becker et al., 1999). The antisense ODN knocks down gene expression by binding to the target mRNA, resulting in the degradation of the RNA duplex by RNase H, thereby preventing protein translation. Pairs of 5 x 5 mm full thickness excisional wounds were made on the back of the 2-week STZ-diabetic and weight-matched control rats. After excision, 50 μl of 10 μM antisense or control sense oligodeoxynucleotide (asODN and sODN) in 30% pluronic gel was applied immediately to the wounds after excision.

Wounds were collected at 1, 2, 5, 10 and 15 days after wounding (N = 6 each control or diabetic groups per time point) and cryosectioned to examine the progress of wound repair, in particular the re-epithelialisation, inflammatory response, cell proliferation and granulation tissue maturation processes. Wounds were immunostained for neutrophils, collagen types I and III, proliferating (Ki-67-positive) cells, and Cx43 to confirm the successful protein knockdown. HRP staining was used to identify neutrophils and proliferating cells, counterstained using methyl green, and imaged in the centre of the wound beds using light microscopy for cell counting. H & E staining was used to study the histology of the wounds and re-epithelialisation. A minimum of four images was acquired for each animal for each type of immunostain and analysed digitally using NIH ImageJ software. For the blood vessel leakiness, the wounded rats were injected via the tail vein with 300 μl of PBS solution containing 3% FITC-BSA 3 hours after wounding and tissue was collected 1 hour after FITC-BSA injection. The collected wound tissue was cryosectioned and imaged using confocal microscopy. Images were acquired in the dermis adjacent to the wound edge (site I) and 300 μm

away (site II). Images were made binary and quantified for the amount of FITC fluorescence.

One-way ANOVA statistics were used to test the data (number of cells, re-epithelialisation, permeability). Numbers are expressed as mean ± SEM.

5.3 Extent of re-epithelialisation

In Chapter 4 I showed that wound edge keratinocytes in diabetic wounds appear swollen and express abnormally high levels of Cx43 protein in 1-day wounds (Wang et al., 2007). In order to knockdown Cx43 expression at the wound sites, 50μl of 10 μM Cx43-asODN in pluronic gel was applied immediately after wounding. The knockdown of Cx43 protein expression was confirmed 1 day after wounding using immunofluorescent staining. The protein knockdown observed was similar to the normal wound healing model in mice used previously in the lab (Mori et al., 2006; Qiu et al., 2003). No upregulation of Cx43 expression was observed after Cx43-asODN knockdown and furthermore, Cx43 was mostly absent in the wound edge epidermis and dermis (Figure 5.1). Phenotypically, the diabetic WE keratinocytes became thin and flattened, adopting a migratory signature after Cx43-asODN application, similar to that of control wounds.

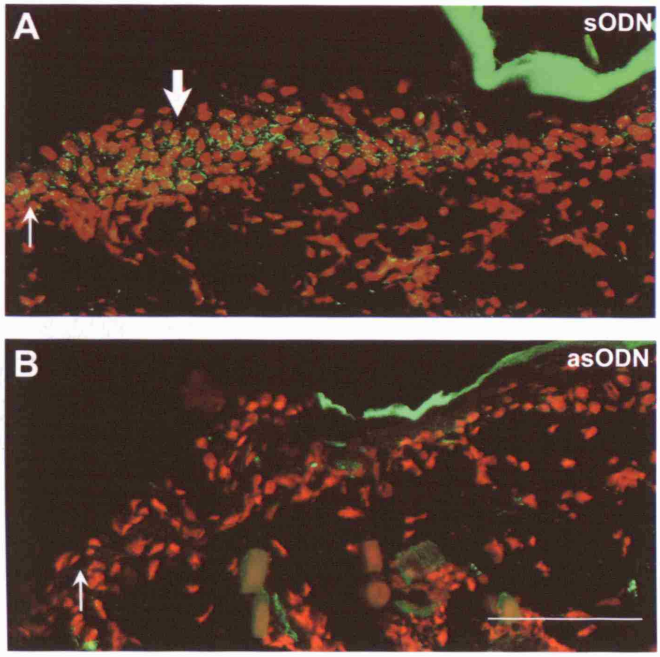

Figure 5.1 Effects of Cx43 sense and antisense ODN treatment on Cx43 expression one day after wounding. (A) An elevated level of Cx43 staining (green puncta – thick arrow) was observed in the swollen epidermal bulb (red nuclei) at the edge of a diabetic wound treated with Cx43 sODN, 1 day after wounding. However, this elevation in Cx43 protein was prevented by Cx43-asODN (B), which also resulted in a thinner layer of keratinocytes that appeared more like those of control animals rather than a bulb of cells (N = 6). Thin arrows mark the edge of the wound. Scale bar 50 μm.

The extent of re-epithelialisation was measured in wounds of healthy and diabetic rats treated with either sODN or Cx43-asODN. The distances re-epithelialised by the migrating keratinocytes from both wound edges were expressed as the percentage of the wound bed (refer to Chapter 2.3). The extent of re-epithelialisation was measured at 1, 2, and 5 days after wounding as by day 10 both control and diabetic wounds have re-epithelialised completely (Figure 5.2). Control wounds treated with Cx43-asODN showed accelerated re-epithelialisation compared to sODN wounds, as expected from previous publications (Mori et al., 2006; Qiu et al., 2003). In these Cx43-asODN-treated control wounds, the extent of re-epithelialisation was significantly greater on days 1, 2 and 5 ($P < 0.001$), and by day 5 the wounds had completely re-epithelialised.

Diabetic wounds treated with sODN showed significantly slower re-epithelialisation at all the time points examined, compared to control wounds treated with sODN (1 day $P < 0.05$; 2 and 5 day $P < 0.001$). However, diabetic wounds treated with Cx43-asODN showed significant acceleration in re-epithelialisation compared to diabetic sODN wounds on days 1 ($P < 0.05$), 2 ($P < 0.001$) and 5 ($P < 0.001$). In fact, the extent of re-epithelialisation doubled on days 1 and 2, matching those of control sODN treated wounds. At day 5, the extent of re-epithelialisation was even higher in the asODN treated wounds in control healthy animals than in sODN wounds in healthy animals.

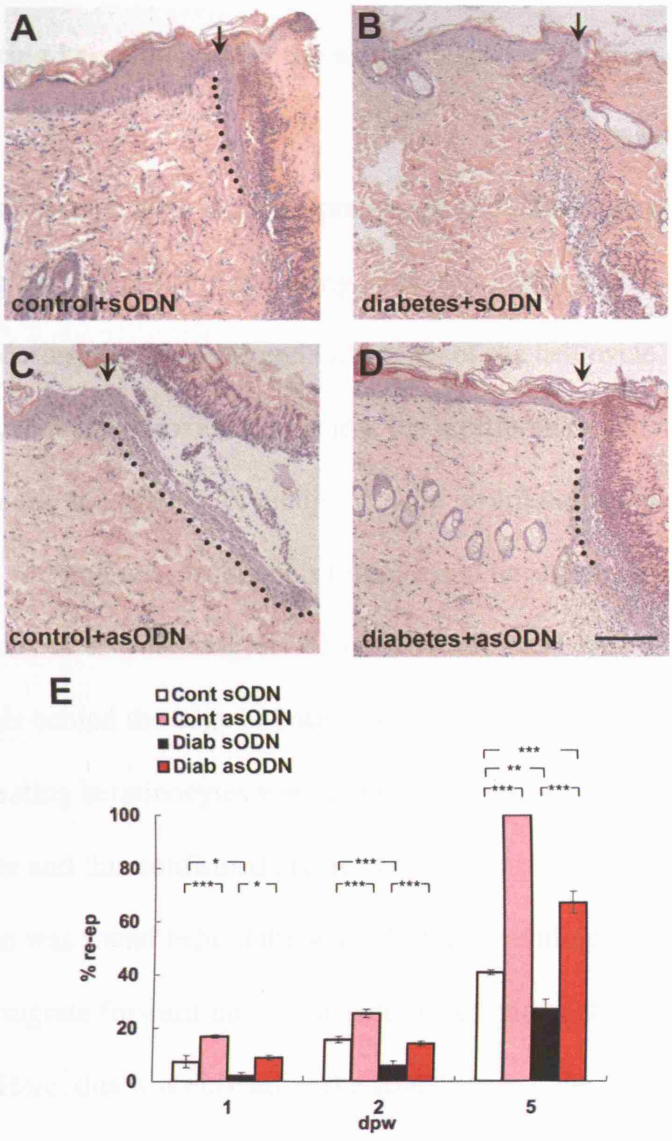

Figure 5.2 Extent of re-epithelialisation at one, two and five days. (A-D) H & E staining of skin sections at the edge of the wound at 1 day after wounding in diabetic (B, D) and control (A, C) rats, treated with Cx43 sense (A, B) or antisense (C, D) ODNs. The black dotted line show the distance migrated by the keratinocytes. Arrow marks the wound edge. (E) Antisense ODN treatment resulted in doubling the extent of re-epithelialisation for both control and diabetic rats. Importantly, it brought the rate of diabetic wound healing to that of sense-treated (or untreated) control levels. The significantly increased degree of re-epithelialisation, following antisense treatment of both control and diabetic skin, was maintained 1, 2 and 5 days after wounding. Scale bar 50 μm. * $P < 0.05$; ** $P < 0.01$. *** $P < 0.001$.

5.4 Proliferating keratinocytes at the wound edge

Keratinocytes are activated after injury to proliferate and migrate in order to reseal the skin. Proliferating cells were identified using antibody against Ki-67, a nuclear protein that is expressed during the G1, S, M and G2 phases of the cell cycle. Using the HRP staining protocol, after the peroxidase reaction, the proliferating cells were stained brown for easy image acquisition. In uninjured skin, proliferating cells were identified in the basal layer of epidermis, within hair follicles and occasionally in the dermal fibroblasts. At 1 day after wounding, Ki-67-positive keratinocytes were found in the adjacent epidermis behind the edge of both control and diabetic wounds (Figure 5.3). Very few proliferating keratinocytes were found in the epidermis immediately adjacent to the wound edge and this confirmed previous data (Coutinho et al., 2003). A zone of hyperproliferation was found behind the wound edge, providing a pool of keratinocytes to migrate forward into the wound (Coutinho et al., 2003; Martin, 1997; Wedlich, 2005). Here, this was defined as the zone between the wound edge and the location of the first consecutively Ki-67-expressing cells. In the control wounds, occasional proliferating keratinocytes were found within the migrating cell population. In the diabetic wounds the population of migrating keratinocytes appeared to be smaller than in control wounds (Figure 5.3). No proliferating keratinocytes were identified within the migrating front of diabetic wounds.

In both control and diabetic 1-day wounds treated with Cx43-asODN, the front migratory zone appeared to be longer than in their sODN-treated wound counterparts (Figure 5.3). Within the migratory front, more Ki-67 positive cells were identified in

both control and diabetic asODN-treated wounds towards the wound edge. The Cx43-asODN-treated diabetic wounds had a longer migrating front than diabetic sODN-treated wounds, and few proliferating keratinocytes were now identified within this zone.

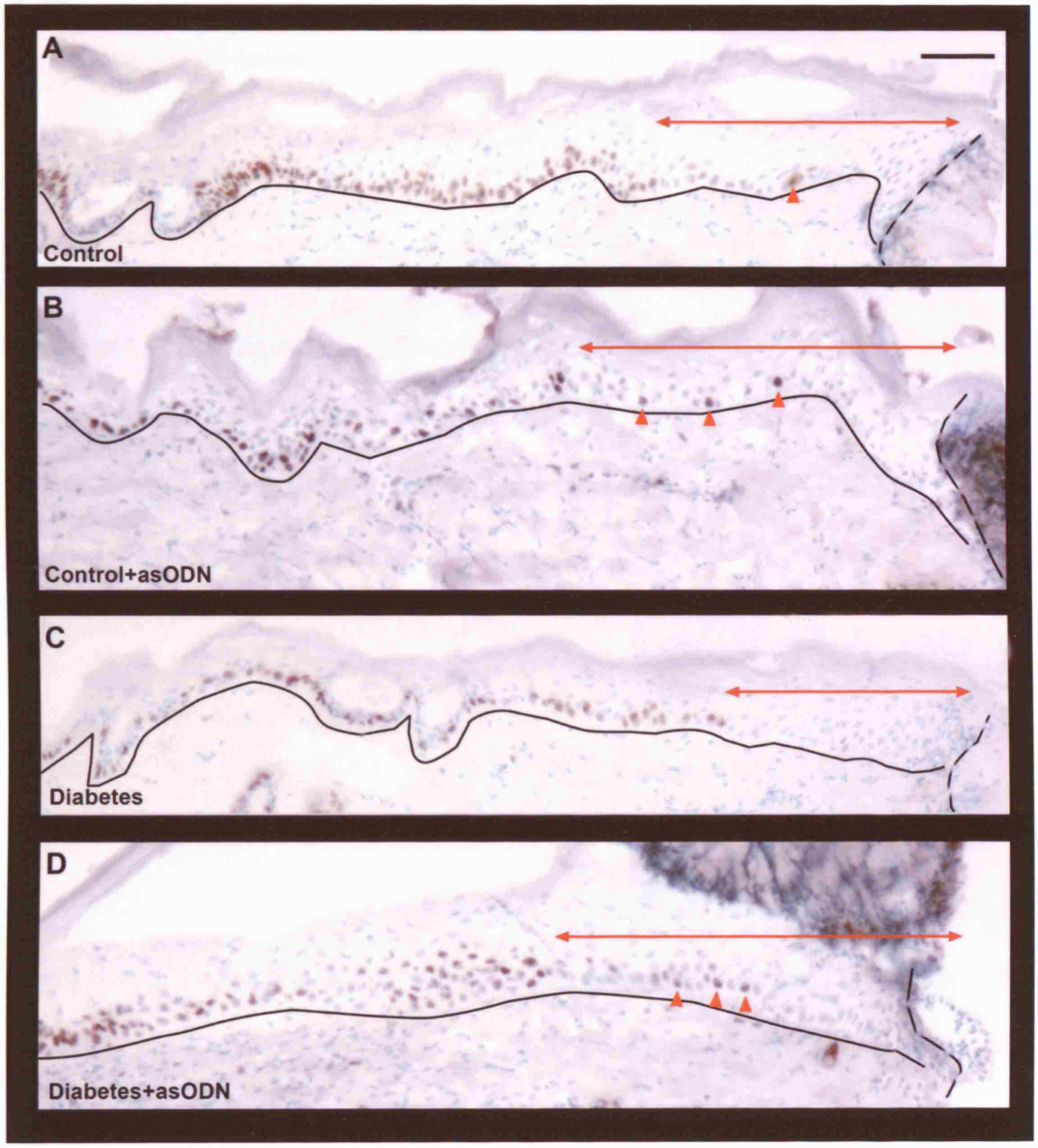

Figure 5.3 Proliferating keratinocytes and migratory zone behind the epidermal wound edge 1 day after wounding. Ki-67-positive (brown) cells were clearly visible behind the wound edge in all the wound groups. However, at the wound edge (dotted line) a zone with very few proliferating cells (zone marked by double arrowed red line), the migratory zone, was identified. Occasional proliferating cells were present in this zone (red arrowheads) in control (A) but not in diabetic (C) wounds. In both control and diabetic wounds treated with Cx43-asODN (B and D respectively), the front migratory zone appeared to be longer than in their sODN-treated counterparts. More proliferating keratinocytes were present within the front zones of these asODN-treated wounds. Black line represents the basement membrane. Scale bar 100 μm.

5.5 Blood vessel leakiness in the wound region

Immediately after injury, blood vessels near a wound vasoconstrict to limit the extent of blood loss. However, minutes after clot formation, vessels start to vasodilate under the influence of prostaglandins and nitric oxide to increase vessel permeability for leukocyte transmigration. Where blood vessels become more permeable, plasma fluid rich in protein such as albumin (exudate) enters the tissue, causing the wound area to swell (tumor). The leakiness of the blood vessels can be viewed as one of the earliest inflammatory responses after clot formation.

To assess the early inflammatory response of the blood vessels, wound tissue was collected 4 hours after injury. To examine the leakiness of the blood vessels around the wounds, FITC-labelled bovine serum albumin (FITC-BSA, 3% in PBS) was injected via the tail vein 1 hour prior to killing and tissue collection to allow complete blood circulation. Two area of dermis were examined: site I immediately by the wound edge and site II approximately 300 μm away from the wound (Figure 5.4). FITC-BSA was imaged using confocal microscopy with the same settings across the four different wound groups (C+sODN, D+sODN, C+asODN, D+asODN) at both sites of interest. Images were thresholded to a set level and made binary in order to quantify the amount of leakage (FITC-BSA) in the sites. For each animal, data obtained were normalised against the highest value (positive number of pixels) within the animal and expressed as a percentage for each site I and II. This was done because the level of leakage varied considerably between animals.

Four hours after wounding, vascular permeability increased dramatically and the exudation process was apparent as indicated by the presence of FITC-BSA in the dermal tissue. Diabetic wounds were consistently more leaky at both site I and site II than control wounds. Right next to the wound in site I, exudation was much more severe than at site II, an area 300 μm away from the wound. This is perhaps not surprising as the immediacy of the wound will have a larger impact on site I, causing vascular permeability. In site II the exudation is less pronounced but still clearly visible (Figure 5.4).

After Cx43-asODN application, the amount of FITC-BSA leakage at site I was significantly less (ANOVA $P < 0.05$). In particular, the level of FITC-BSA leakage is significantly reduced in the Cx43-asODN treated diabetic wounds 4 hours after injury to approximately 60% of diabetic sODN wounds ($P < 0.05$). Normal wounds with Cx43-asODN application reduced leakiness to 80% of control sODN wounds although this did not reach statistical significance.

The presence of exudation was evident at site II; it was clear that not only does injury have a strong impact on the wound edge tissue but the adjacent undamaged tissue can also be affected (Figure 5.4). At site II, the total level of exudation was lower than site I but the effect of Cx43 expression knockdown was still observed. The Cx43-asODN treated wounds showed significantly less FITC-BSA leakage at site II than the sODN wounds (control $P < 0.05$; diabetic $P < 0.001$).

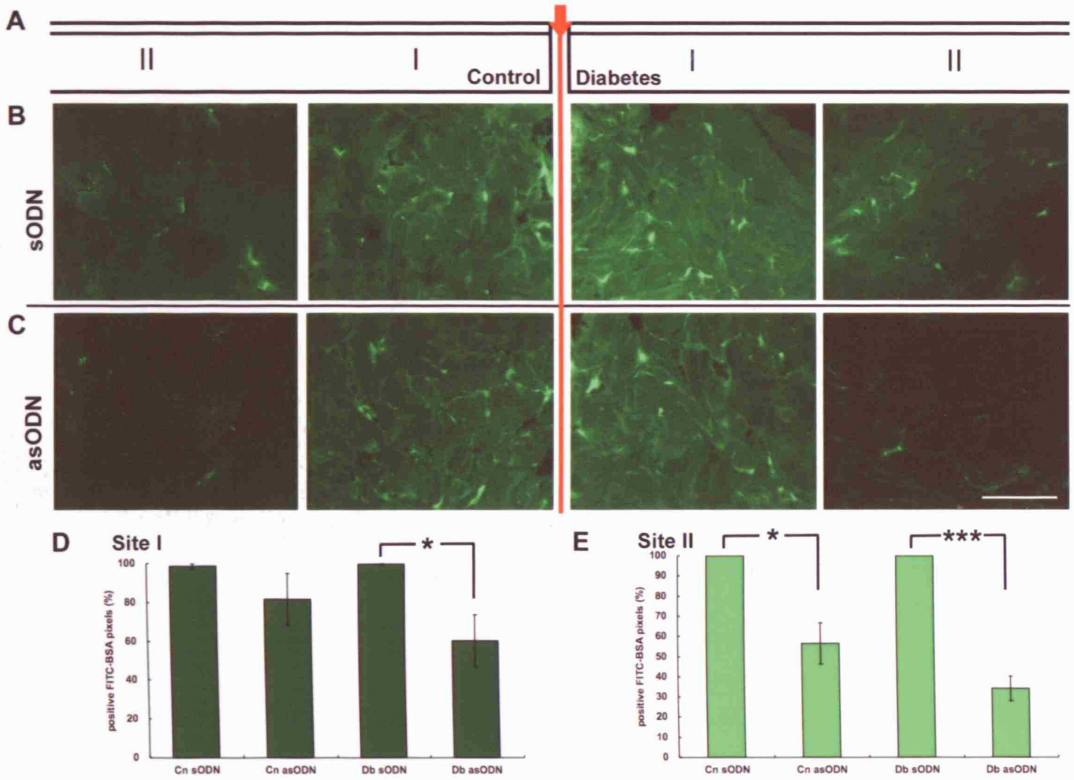

Figure 5.4 Reduced blood vessel leakiness near the wound edge 4 hours after Cx43-asODN treatment. FITC-BSA is shown in green. (A) Diagram of skin and the location of sites I and II imaged in relation to the wound edge (red arrow). Site I is immediately next to the wound edge and site II is approximately 300 μm away. Diagram not to scale. (B) Sense ODN treated wounds at sites I and II of control (normal) and diabetic wounds. The panel layout corresponds to the cartoon in A. At both sites I and II, the diabetic wound was more leaky compared to control. (C) Wounds treated with 10 μM Cx43-asODN were less leaky at both sites I and II of both normal and diabetic wounds compared to corresponding sODN treated wounds. (D) Quantification of FITC-BSA at site I. Antisense ODN treatment significantly reduces leakiness in diabetic wounds. (E) Quantification of FITC-BSA at site II. Knockdown of Cx43 expression significantly reduced leakiness in both control and diabetic wounds (*$P < 0.05$, ***$P < 0.001$). Scale bar 50 μm.

5.6 The morphology and the number of neutrophils

Neutrophils are the first inflammatory cells to arrive in the wound site as the primary line of defence against pathogens. Once activated, neutrophils transmigrate through the adherens and tight junctions between endothelial cells towards the wound, and in some tissues follow a transcellular pathway as well (Dejana, 2006). At the wound site, neutrophils begin the phagocytic debridement process and secrete further cytokines and chemokines to amplify the inflammatory response for the next steps of the healing process (Martin, 1997). It has been established that activated leukocytes express Cx43 protein and couple with endothelial cells during transmigration (Eugenin et al., 2006; Jara et al., 1995; Oviedo-Orta et al., 2002; Oviedo-Orta et al., 2001; Zahler et al., 2003). Immunofluorescent double-staining of Cx43 and the neutrophil marker myeloperoxidase identified numerous neutrophils in the wound edge tissue at 1 day after wounding but only a subpopulation of them expressed Cx43 protein (Figure 5.5).

Previously in the lab we found that applying Cx43-asODN immediately after wounding reduces the number of neutrophils in the wound bed and adjacent tissue in incisional and excisional wounds in mice (Mori et al., 2006; Qiu et al., 2003). Here I have examined whether the number of recruited neutrophils changes in diabetic wounds after Cx43-asODN application. Neutrophils were stained using marker myeloperoxidase with secondary antibody conjugated with horseradish peroxidase and developed using DAB.

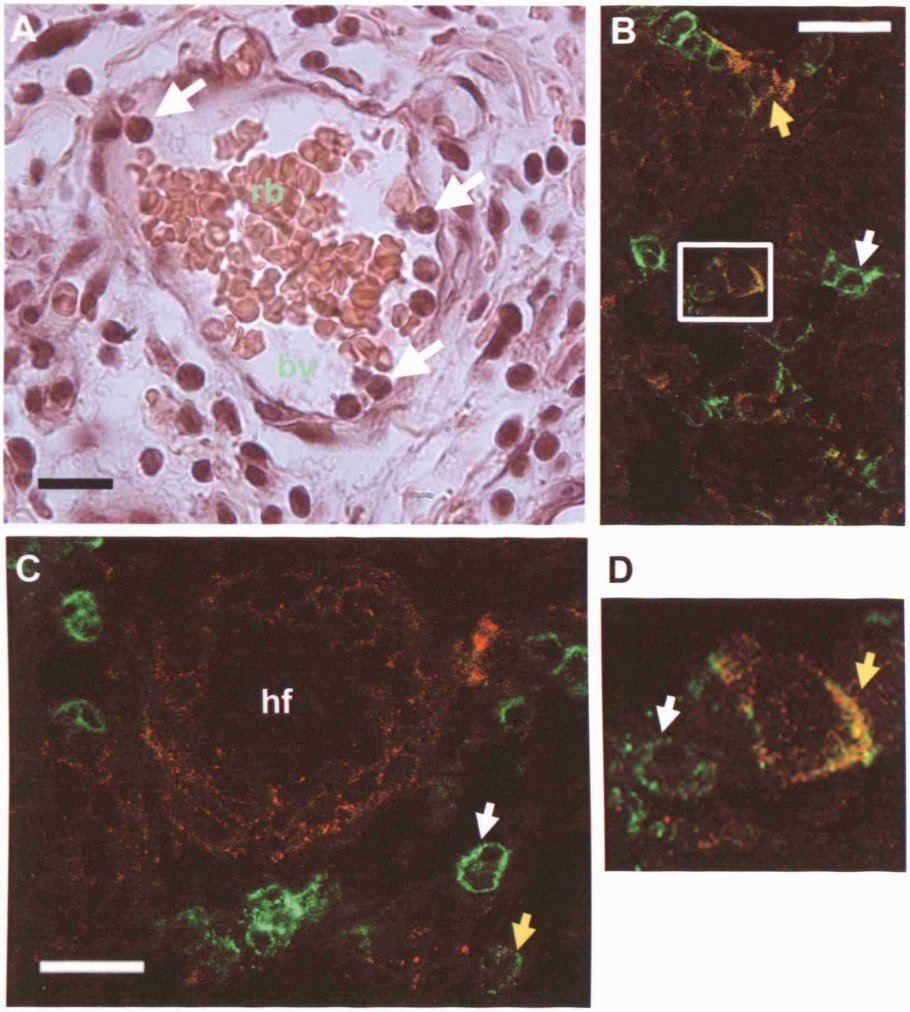

Figure 5.5 Neutrophils are the first inflammatory cells that arrive at the wound site to combat infection and to release cytokines. (A) H & E image of a blood vessel (bv) containing erythrocytes (rb) and numerous neutrophils (white arrows) in the process of transmigration. Many neutrophils can also been seen in the surrounding tissue. (B, C) Neutrophils (green) and Cx43 (red) double staining revealed neutrophils with very little or no Cx43 expression (white arrows) and co-localisation in only a subpopulation of neutrophils (yellow arrows). Hair follicles (hf) express high levels of Cx43. (D) Enlarged picture of neutrophils expressing high levels of Cx43 (yellow) or lower levels (white arrow) boxed white in B. Scale bars 25 μm.

Using HRP-DAB secondary staining, neutrophils stained brown and were clearly visible for counting. In both diabetic and normal wounds, neutrophils had transmigrated from the blood vessels into the dermal tissue and migrated towards the wound area. Immunostaining showed that neutrophils were the main cell population in the open wound bed at days 1 and 2, and by day 5 they were no longer detectable in the wound.

At day 1 after wounding, a high density of neutrophils was present in the centre of the wound bed. There was no difference in the number of neutrophils in the wound bed between control and diabetic wounds (Figure 5.6). Both control and diabetic wounds treated with Cx43-asODN showed the same number of neutrophils in the wound at 1 day after wounding compared to sODN treated wounds. However, interestingly, the neutrophils appeared smaller and the provisional wound matrix appeared drier in the asODN-treated wounds.

At day 2 after wounding, the number of neutrophils remained constant in control acute wounds, but in the diabetic wound bed the number increased to approximately 50% more than at day 1 ($P < 0.01$). In control wounds, the appearance of the neutrophils changes from a rounded appearance on day 1 to a more irregular appearance on the second day (Figure 5.7). In diabetic wounds, the neutrophils were still rounded on day 2, as previously on day 1 after wounding. The increased neutrophil recruitment and the rounded morphology, taken together, are an indication of prolonged inflammation, a feature commonly observed in diabetic wounds (Loots et al., 1998; Wetzler et al., 2000). After Cx43-asODN treatment, the number of neutrophils reduced significantly in both control and diabetic 2-day wounds ($P < 0.001$). The number of neutrophils did

not differ between control and diabetic wounds after Cx43-asODN treatment (Figure 5.7). The decrease in recruitment of neutrophils induced by antisense treatment was more pronounced in diabetic wounds as the initial number of neutrophils was significantly higher in the sODN treated wounds (Figure5.6; Figure 5.7).

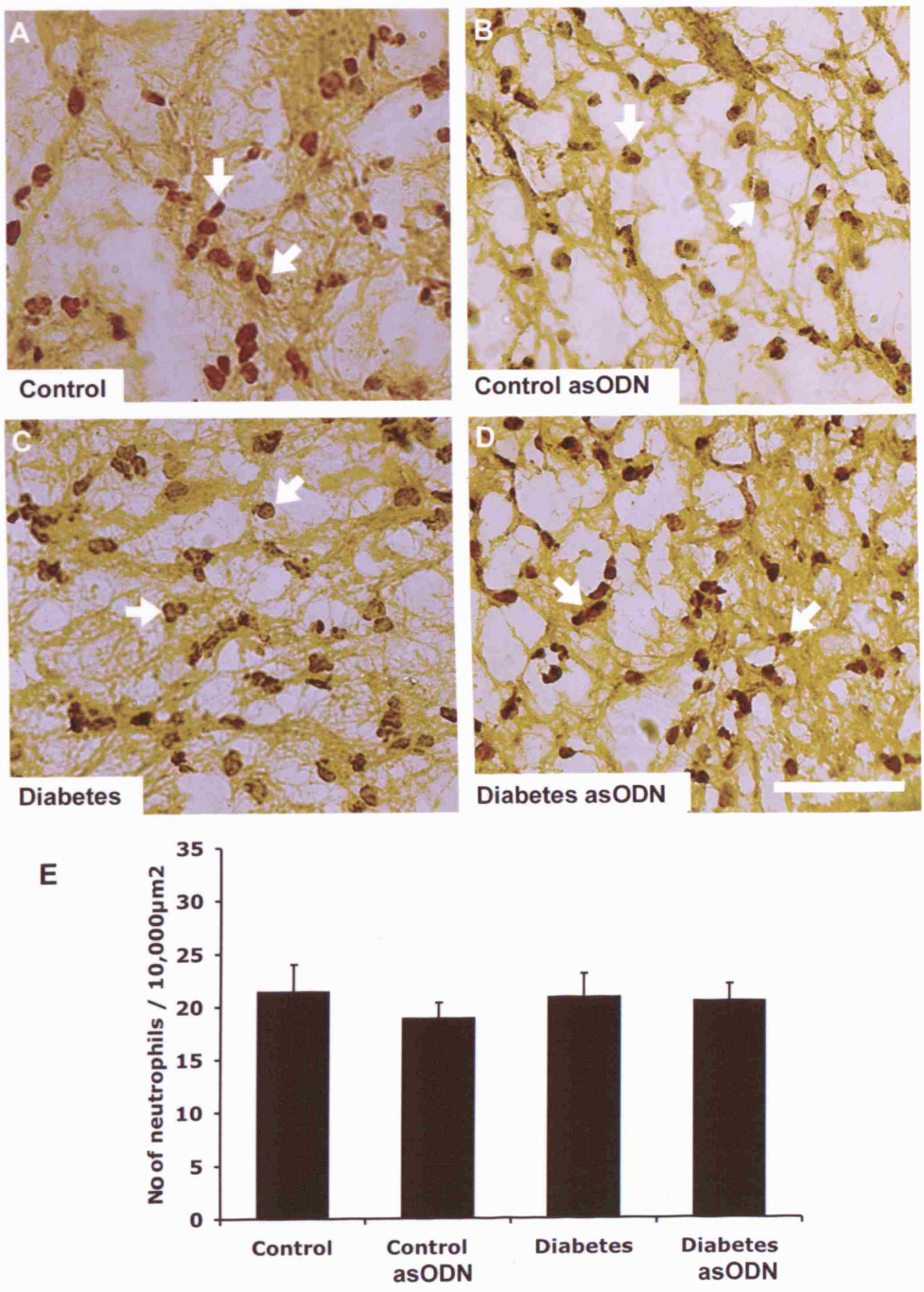

Figure 5.6 Similar number of neutrophils were found in control and diabetic wounds, 1 day after wounding. (A, B) Neutrophils (brown cells, white arrows) in the wound area of sense- (A) and Cx43-asODN-treated (B) control wounds. (C, D) Neutrophils in the wound area of diabetic wounds treated with sense (C) or Cx43-asODN (D). (E) The number of neutrophils was similar in both control and diabetic wounds treated with sense or antisense. Scale bar 100 µm.

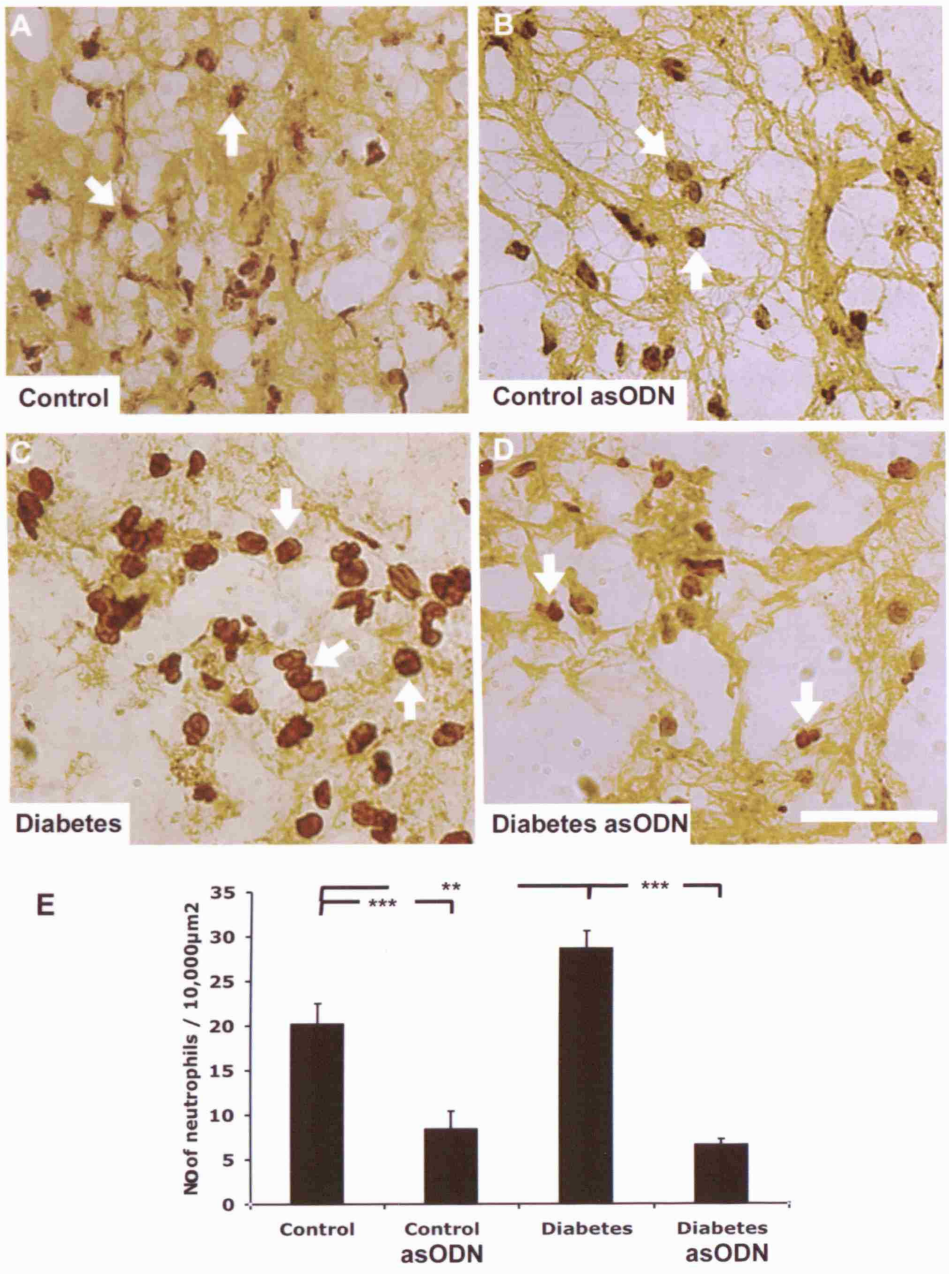

Figure 5.7 Reduced number of neutrophils in the wound area 2 days after injury after 10 µM Cx43-asODN application. (A, B) Neutrophils (brown cells, white arrows) in the wound area of Cx43 sense (A) and antisense (B) treated control wounds. (C, D) Neutrophils in the wound area of diabetic wounds treated with sense (C) or antisense (D). Scale bar 100 µm. (E) The number of neutrophils is decreased in both control and diabetic wounds treated with asODN (** $P < 0.01$, *** $P < 0.001$).

5.7 Cell proliferation in the granulation tissue

In the key proliferative phase after wounding, fibroblasts and endothelial cells begin to infiltrate the wound and proliferate, to form a densely populated granulation tissue. Granulation tissue formation is a key event in the wound healing processes that shapes the new dermis. Here, 5, 10 and 15-day wound sections were stained for Ki-67, a nuclear marker for proliferation (Figure 5.8). Images of proliferating cells were acquired in the centre of granulation tissues. The number of Ki-67 positive cells was counted using the cell counter plug-in in the ImageJ software.

At day 5, a high number of proliferating cells were present in both control and diabetic wounds (~ 110-130 cells /0.41 mm^2). The numbers of proliferating cells in the granulation tissue of both types of wounds were similar (Figure 5.9). By day 10, the number of proliferating cells had decreased dramatically in both control and diabetic wound as the granulation tissue began to mature into nascent dermis. However, there were far more proliferating cells present in the diabetic wounds compared to controls ($P < 0.01$, Figure 5.8, Figure 5.9). By 15 days, the numbers of proliferating cells in the granulation tissue of both control and diabetic wounds further decreased and there was no significant difference between the two groups.

In the control wounds treated with Cx43-asODN after injury, no significant change in the number of proliferating cells was found at any of the time points studied. Interestingly, at 5 and 10 days after wounding, the numbers of proliferating cells in the diabetic Cx43-asODN treated wounds had all reduced significantly ($P < 0.05$) to a level similar to controls (Figure 5.9).

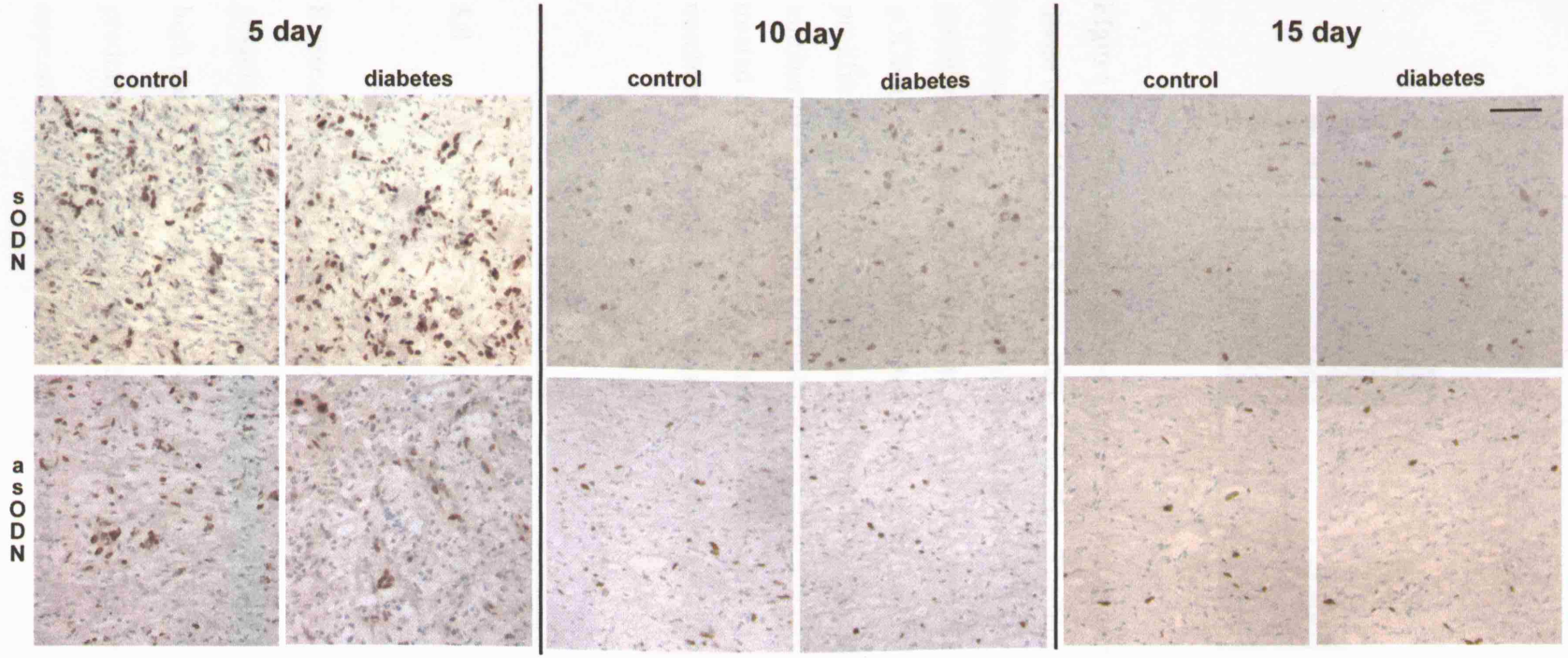

Figure 5.8 Proliferating cells in the centre of granulation tissue 5, 10 and 15 days after wounding. Ki-67 positive cells (brown cells) were clearly visible in the granulation tissue in all the time points examined. Non-proliferating cells were counterstained in blue. The number of proliferating cells decreased dramatically between day 5 and 10 in both control and diabetic wounds. By day 15 after wounding the number of proliferating cells reduced a little further. Interestingly, at all time points there appeared to be more proliferating cells in the diabetic wounds than control wounds. Bar 100 μm.

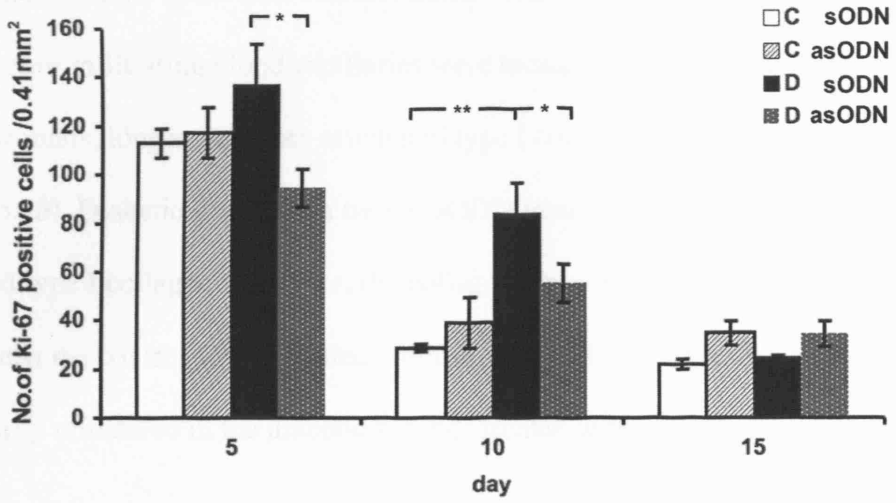

Figure 5.9 The number of Ki-67 positive cells in control and diabetic granulation tissue on 5, 10 and 15 days after wounding. The number of proliferating cells decreased dramatically in all the groups between days 5 and 10 after injury. No statistically significant difference was found between control wounds treated with sODN or asODN. In diabetic wounds, at both 5 and 10 day after injury, the number of proliferating cells in asODN treated wounds was significantly reduced. The lowered number of Ki-67 positive cells indicated more advanced wound repair in asODN-treated than in sODN-treated diabetic wounds. By 15 days all groups had similar numbers of proliferating cells in the granulation tissue. $^{**}P < 0.01$, $^{*}P < 0.05$

5.8 Collagen matrix in the granulation tissue

Extracellular matrix and collagen were secreted by the infiltrating fibroblasts in the granulation tissue to form the nascent dermis. Type I collagen bundles were present at high abundance in the uninjured dermis of both control and diabetic animals as the predominant protein of the ECM (Figure 5.10). The collagen fibres were thick and appeared tightly woven. In the 15-day control granulation tissue (sODN treated), thin type I collagen fibres were found between cells. These thin collagen fibres were short

and oriented parallel to the skin surface. Some vertical hollow gaps were visible in the matrix where infiltrating blood capillaries were located. In the Cx43-asODN treated control wounds, longer and more orientated type I collagen fibres were identified (Figure 5.10). Diabetic granulation tissue (sODN treated) at 15 days after injury also contained type I collagen. However, the collagen fibres were not orientated and much shorter than the control sODN treated wounds. The collagen fibres became longer and horizontally orientated in the diabetic wounds treated with asODN.

Type III collagen is another component of the ECM in uninjured dermis. Thin, wispy type III collagen fibres were found in both uninjured control and diabetic skins as expected. At 15 days after injury, type III collagen in the granulation tissues was not long and wispy but dispersed in small patches (Figure 5.11). In the control asODN treated wounds the density of the type III collagen increased compared to sODN treated wounds. Similarly, in diabetic asODN treated wounds, increases in type III collagen density and clearer formation of fibres were observed compared to diabetic sODN treated wounds. In both control and diabetic wounds, the orientation of thin type III collagen fibres in asODN treated wounds was parallel to the skin surface.

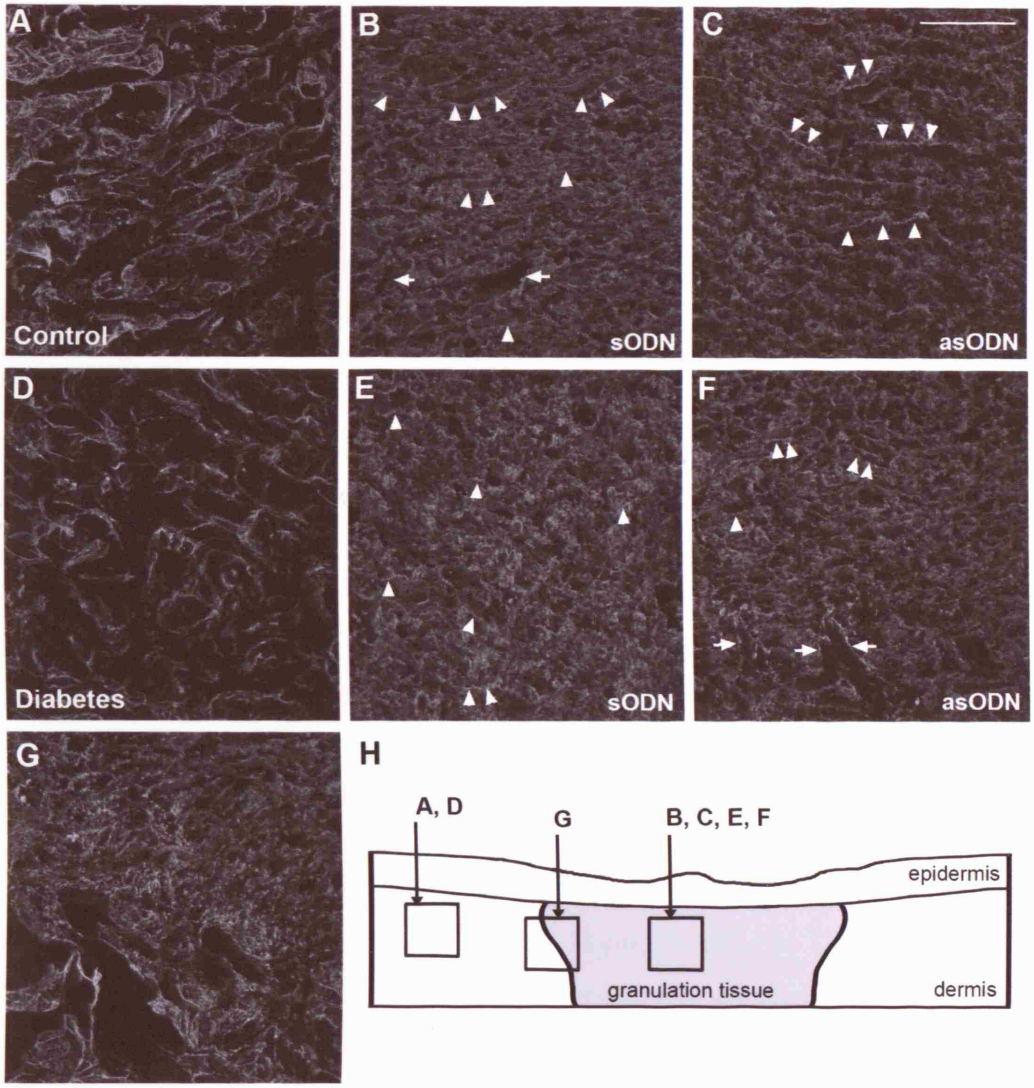

Figure 5.10 Type I collagen staining in 15-day control and diabetic wounds. (A) Thick type I collagen bundles in uninjured dermis of control animals. The collagen fibres appeared thick and tightly woven. (B) Thin, horizontally orientated collagen fibres were visible in the granulation tissue in control wounds (arrowheads). Vertical gaps where infiltrating blood vessels reside were also visible (arrows). (C) In the asODN treated control wounds, longer and more orientated collagen fibres were found. (D) Thickly woven type I collagen in uninjured diabetic dermis. (E) Short, unorientated type I collagen fibres were observed in the diabetic wound granulation tissue 10 days after injury. (F) Longer, more orientated collagen fibres were found in diabetic wounds treated with asODN than in diabetic wound treated with sODN. (G) Junction between uninjured dermis and granulation tissue in control wounds. Difference in collagen fibre size and orientation were clearly visible. (H) Schematic diagram of where each image in this figure was taken in the wounds. Scale bar 50 μm.

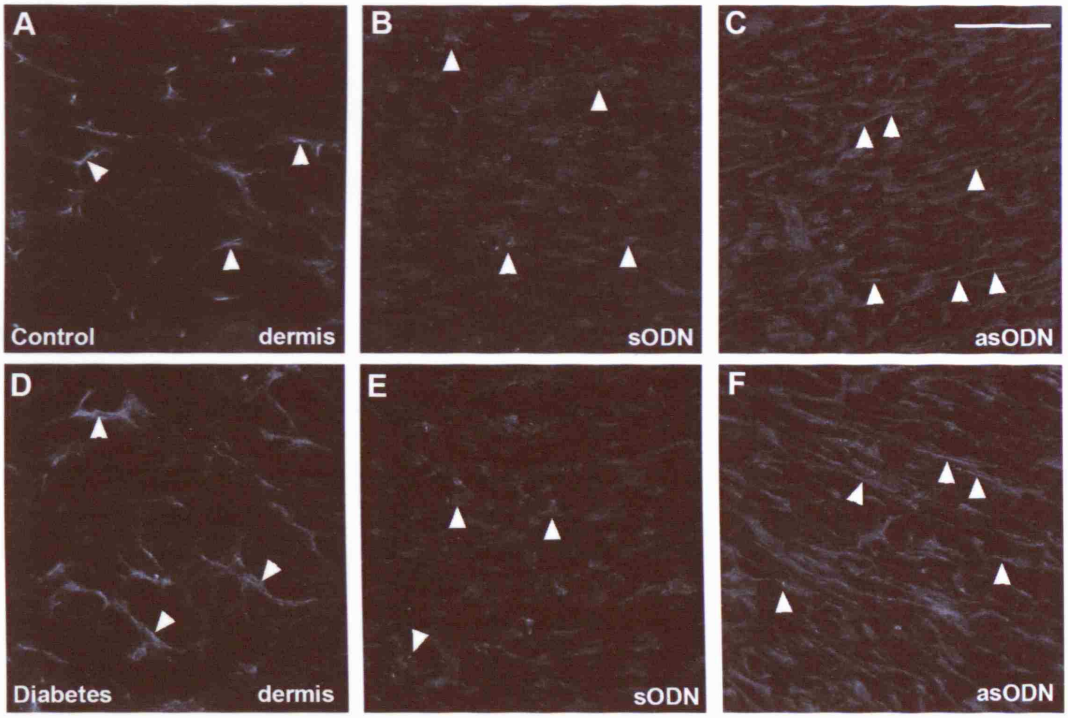

Figure 5.11 Type III collagen staining in 15-day control and diabetic wounds. For a schematic diagram of the image location see Figure 5.10H. (A) Thin, wispy type III collagen was observed in the uninjured control dermis (arrowheads). (B, C) More type III collagen was present in granulation tissue of wounds treated with Cx43-asODN (C), compared to sODN (B) treated wounds. (D) Type III collagen fibres were found in the uninjured diabetic dermis as expected. (E, F) More type III collagen fibres were found in the diabetic wounds treated with Cx43-asODN (F) compared to sODN-treated wounds (E). Scale bar 50 μm.

5.9 Aged wounds

Wounds in elderly people heal slowly. During the repair process, the level of inflammation and cytokine release is reduced and the wounds heal with a smaller scar (Ballas and Davison, 2001; Ashcroft et al., 2003). A pilot wound healing study was carried out on 28-30 months old SD rats to examine the Cx43 expression after wounding and the effect of Cx43-asODN in these wounds. The elderly SD rats were provided by Professor Tim Cowen, Dept of Anatomy and Developmental Biology, UCL. The same 5 x 5 mm full thickness wounds were made on the rats and the surgery was carried out in the animal unit of the Royal Free Campus, UCL.

Immunofluorescent staining of Cx43 protein at the 1-day wound edge in the elderly rats showed an abnormally high level of expression (Figure 5.12), similar to that reported in Chapter 4 of the diabetic delayed wounds. The epidermal wound edge appeared bulbous and the keratinocytes had not adopted the phenotype for migration.

Application of Cx43-asODN immediately after wounding successfully prevented the upregulation of Cx43 expression 1-day after injury. Wound re-epithelialisation initiated as early as day 1 after wounding (Figure 5.12). By day 3, the re-epithelialisation process was well underway in both elderly control sODN and Cx43-asODN treated wounds and the extent of keratinocyte migration did not appear to differ in either set of wounds. However, a small amount of granulation tissue began to form in the Cx43-asODN-treated and not in the sODN treated wounds.

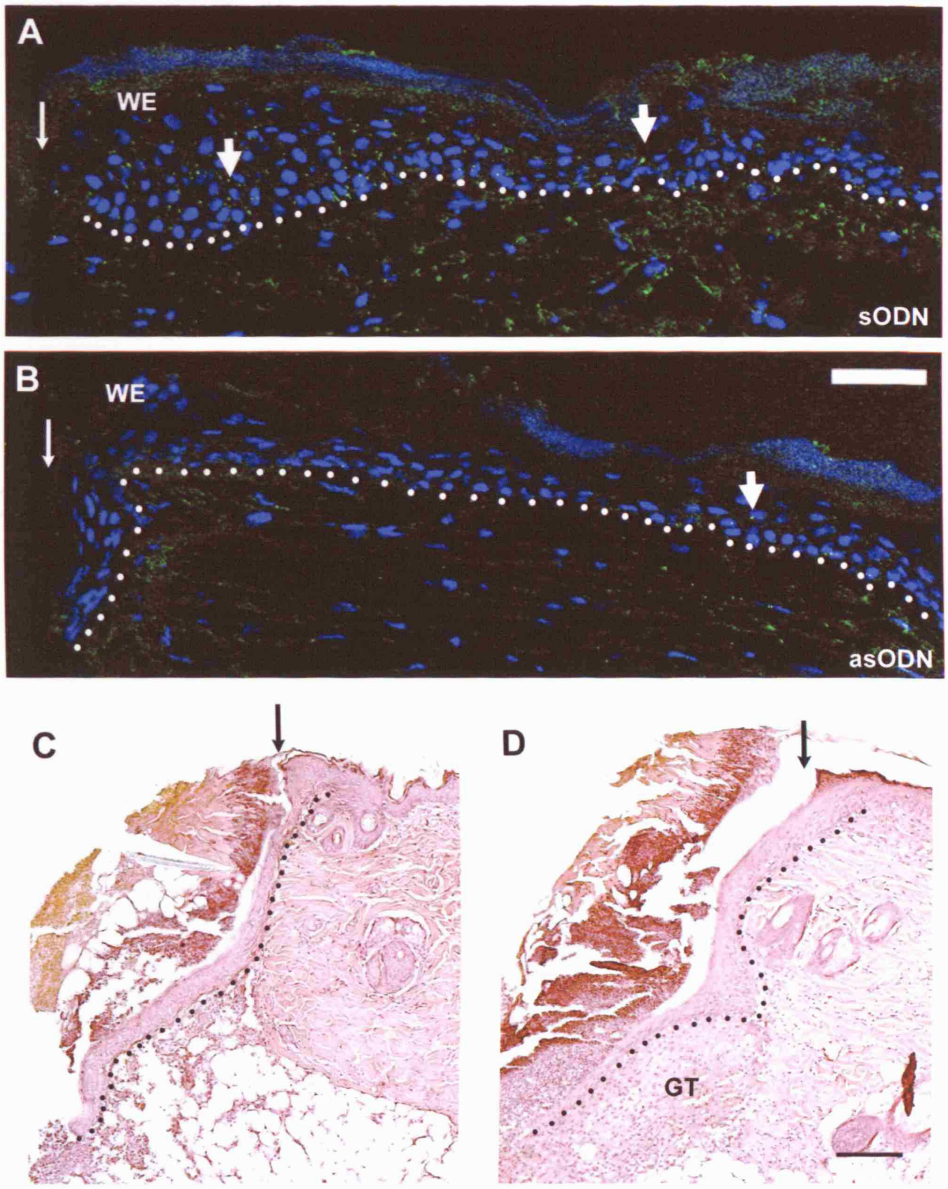

Figure 5.12 Cx43 expression in aged skin wounds, which are known to heal slowly. (A) Cx43 (green puncta, thick arrows) in the wound edge (WE) keratinocytes elevated at 1 day, similar to diabetic wound edge Cx43 elevation. (B) Cx43-asODN treated wounds began to re-epithelialise and little Cx43 was expressed in the wound edge epidermis or dermis, although some Cx43 was expressed further away from the edge (thick arrow). The white dotted line separates the epidermis and dermis. (C, D) H & E histology of 3-day wounds showed similar re-epithelialisation (dotted line) in control (C) or Cx43-asODN (D) treated wounds. Granulation tissue (GT) formation was more advanced in the asODN-treated wound. Thin arrows mark the wound edge., A and B: scale bar 50 μm, C and D: scale bar 200 μm.

5.10 Chapter discussion

The wound healing process in diabetic skin is delayed, where the open wounds are more prone to infection. A prolonged inflammatory response and alterations in the levels of cytokines in the wound microenvironment are the most recurrent observations reported in diabetic and chronic wounds (Harris et al., 1995; Loots et al., 1998; Maruyama et al., 2007; Wetzler et al., 2000). The dynamic expression of Cx43 at the wound edge is important in the process of wound healing (Coutinho et al., 2003; Goliger and Paul, 1995; Moyer et al., 2002) but in diabetic wounds this expression was shown to be abnormal (Chapter 4, Wang et al., 2007). Instead of the normal downregulation of Cx43 in the keratinocytes 6 – 24 hours after injury, the expression was significantly upregulated in diabetic delayed and chronic wounds (Brandner et al., 2004; Wang et al., 2007). Previous studies in the lab have demonstrated that transient knockdown of Cx43 using antisense ODN immediately after wounding can improve the rate and quality of wound repair (Coutinho et al., 2005; Mori et al., 2006; Qiu et al., 2003). In this chapter I have examined the effect of antisense Cx43 application in the wounds of streptozotocin-induced diabetic rats.

I have examined the wound progression of diabetic and normal healthy animals treated with either Cx43-asODN or control Cx43-sODN. Different stages of the wound-healing process from the initial inflammatory response until granulation tissue maturation were examined. Diabetic wounds treated with asODN showed improved wound healing with accelerated re-epithelialisation, reduced albumin exudation and

vascular permeability, decreased neutrophil recruitment and advanced granulation tissue maturation.

5.10.1 Inflammatory response

The assessment of vessel leakiness 4 hours after injury using FITC-BSA at the dermal wound edge (site I) and 300 μm away (site II) showed that Cx43 has a great impact on vessel permeability. Vessel leakiness was more dramatic at site I than site II in both control and diabetic wounds, either sODN or asODN treated. The proximity of the wound edge is likely to have greater influence on the immediate vasculature than those further away. Interestingly, the application of Cx43-asODN significantly reduced albumin leakiness in site II of both control and diabetic wounds. In site I only diabetic wounds showed significant reduction in leakiness after asODN application.

Initially after haemorrhage, blood vessels around the wound edge vasocontrict but soon after begin to vasodilate to facilitate leukocyte recruitment. The endothelial cells and vessels in site I and site II may be activated to different degrees in response to injury. The cause behind the different results between site I and site II is unclear but the proximity and the impact of the wounds on the blood vessels may be too great for asODN to have an obvious effect in the immediate wound edge. Nevertheless, the knockdown of Cx43 in the wound region appeared to affect the early inflammatory response of the blood vessels. The reduction in blood vessel leakiness or inflammatory response as early as 4 hours after injury can cause a dramatic change in the subsequent downstream wound healing processes. The potential role of Cx43 protein in endothelial permeability is further explored in Chapter 6 of this thesis.

The number of neutrophils recruited to the wound bed was similar on day 1 after injury in the four groups studied. In control wounds, the level of neutrophil recruitment was similar in day 1 and 2 in the sODN treated wounds. However, for the diabetic wounds, the number of neutrophils increased considerably on day 2. This was perhaps not surprising as elevated and prolonged presence of neutrophils and other leukocytes has previously been found in diabetic wounds (Loots et al., 1998; Wetzler et al., 2000). Interestingly, in both Cx43-asODN treated control and diabetic wounds, the number reduced significant on day 2 after injury. Previous results on mouse wounds from the lab showed a dramatic decrease in the number of neutrophils on days 1 and 2 after Cx43-asODN treatment (Coutinho et al., 2005; Mori et al., 2006; Qiu et al., 2003) but this was not seen in the rats. The different observations may be caused by differences in sampling site or species differences. In the thermal wounds studied by Coutinho et al. (2005), no differences in neutrophil numbers were found between control and Cx43-asODN-treated wounds at 6 hours, but only 24 hours after injury. This suggests that the reduction in neutrophil number in the Cx43-asODN wounds did not occur immediately after ODN application but probably as a cumulative effect over time. The decrease in number at day 2 in the Cx43-asODN-treated rat wounds may have resulted from reduction in recruitment over time as well as an earlier clearing or exclusion from the wound bed into the eschar/scab, where it would be excluded from the cell counts.

In vitro studies have shown that activated leukocytes express Cx43 and are coupled with endothelial cells during the transmigration process (Eugenin et al., 2006; Jara et al., 1995; Oviedo-Orta et al., 2002; Zahler et al., 2003). Mononcytes/macrophages express Cx43 upon TNF-α and IFN-γ stimulation (Eugenin et al., 2006). Similarly,

leukocytes activated by lipopolysaccharide begin to express leukocyte-leukocyte and leukocyte-endothelial cell gap junctions (Jara et al., 1995). The active cell coupling between leukocytes and endothelial cells was shown to modulate transendothelial migration processes (Oviedo-Orta et al., 2002; Zahler et al., 2003). In Cx43-asODN-treated wounds, the recruitment of neutrophils may have been reduced due to the loss of Cx43 expression in the inflammatory and endothelial cells. However, the effect of Cx43-asODN was still observed after the ODN itself would have been degraded (2 day wounds); this suggests that other mechanisms may exist to regulate neutrophil recruitment indirectly, downstream of Cx43 modulation.

5.10.2 Re-epithelialisation

The wound edge epidermis in diabetic wounds appeared to be bulbous (Chapter 4) and showed no signs of active migration at 1-day after wounding. Data presented in this chapter suggest that downregulation of Cx43 expression at the wound edge may be important to initiate keratinocyte migration to close the open wound. A decrease in Cx43 expression was observed concomitantly with the thinning of wound edge epidermis into a migrating tongue in control animals at day 1. However, for diabetic wounds this only happened at day 2, after the abnormal Cx43 protein upregulation at day 1. To achieve a swift re-epithelialisation, active keratinocyte proliferation and migration at the wound edge are required. Cell migration is a dynamically controlled process involving directional cell protrusion, cell body contraction and rear detachment in order to move forward. The spatial arrangement of the actin cytoskeleton and focal adhesion to the migration substrate are heavily involved in these processes (Vasioukhin et al., 2000). The Rho family of small GTPases (RhoA, Rac1 and Cdc42)

are the key regulators in these dynamic spatial rearrangements. Rho GTPase activation leads to the assembly of actin stress fibres that facilitate the contraction of the cell (Ridley and Hall, 1992). Rac and Cdc42 activation lead to cell protrusion via actin polymerisation that results in the formation of lamellipodia and filopodia (Nobes and Hall, 1995a; Nobes and Hall, 1995b).

In order to initiate keratinocyte migration, anchoring hemidesmosomes on the basement membrane are first removed and integrin expression is redistributed. Cadherins, a well-known family of transmembrane glycoproteins that mediate cell-cell adhesion, are regulated by the Rho GTPases during migration. The cytoplasmic domain of cadherins binds to β- and α- catenins and other F-actin binding proteins such as zonula occludens 1 (ZO-1), providing linkage between the cytoskeleton and the plasma membrane. The anchorage of E-cadherins to the actin cytoskeleton is particularly important for rigid adhesions in epithelia (Tsukita et al., 1992). Rho GTPases can act directly on components of the E-cadherin–catenin complex to recycle E-cadherin to the cell surface, promoting cleavage by MMPs and resulting in the loss of cell adhesion and the promotion of motility (Ito et al., 1999). Cx43 has been shown to be co-expressed with, and to interact with, many actin binding proteins, including ZO-1, E-cadherin and debrin (Butkevich et al., 2004; Fujimoto et al., 1997; Giepmans, 2004). The downregulation of Cx43 in the wound-edge keratinocytes may promote the destabilisation of cell-cell adhesion to promote re-epithelialisation.

The expression of connexins, nevertheless, can be important in mediating migration in some cell types. Recently Cx26 and Cx43 were shown to be required for neuronal stem cell migration to reach the cortical plate during development (Elias et al., 2007). Cx43

is also involved in neural crest cell migration, modulating armadillo protein p120 catenin with small GTPases (Lo et al., 1999; Noren et al., 2000; Xu et al., 2001). Reducing Cx43 expression in neural crest cells was associated with reduced cell migration (Sullivan et al., 1998). However, the knockdown of Cx43 expression in keratinocytes in the present study increased the extent of re-epithelialisation in control, diabetic, and similarly in the aged wounds, contradicting its apparent role in the neural crest cells. Long term blockage of connexin hemichannels (and thus prevention of GJ formation) has also been shown to improve wound closure of keratinocytes *in vitro* (Kandyba et al., 2007). How the absence of Cx43 or blockage of hemichannels promotes keratinocyte migration is unknown. An interesting view is that many tumour cells express little or no connexin (Wilgenbus et al., 1992) and show little functional GJIC (Holder et al., 1993; Rose et al., 1993). It has been suggested that extensive cell-cell contact was required for inhibition of cell growth. By the same argument, lack of cell-cell contact may be required to promote general cell growth.

Apart from destabilising keratinocyte cell adhesion, the removal of Cx43 and synergistic upregulation of Cx26 (Chapter 4) at the wound edge may be important for the creation of a specialised signalling compartment. In the cochlea, differential connexin expression creates selective compartments that are dedicated to different signalling functions (Jagger and Forge, 2006). In the asODN treated wounds this putative migration compartment was elongated at 1 day after injury, supporting the idea of the creation of a specialised migration cohort or sheet.

Keratinocyte migration and proliferation are closely associated during the re-epithelialisation process. Cytokines secreted in the wounds are mitogenic but can also

modulate the expression of integrins for lamellipodial migration . One such cytokine is TGF-β, released by fibroblasts and degranulating neutrophils, stimulating keratinocytes to migrate into the wound bed (Gailet et al., 1994; Mori et al., 2006). EGF, a mitogen and motogen of keratinocytes, is also known to activate Rac-mediated migration (Barrandon and Green, 1987; Nobes and Hall, 1995a; Ridley et al., 1995). We have previously found that the application of Cx43-asODN to a wound caused an elevation in TGF-β1 release by keratinocytes in mice excisional wounds (Mori et al., 2006). This increased TGF-β1 level may have stimulated keratinocyte migration as observed *in vitro* and *in vivo*.

5.10.3 Granulation tissue formation

Granulation tissue is formed by infiltration of fibroblasts and endothelial cells that continue to proliferate to create the tissue matrix for the new nascent dermis. High numbers of proliferating cells (Ki-67-positive cells) were seen on day 5, and between the day 5 and 10 time points, a dramatic decrease in proliferation was observed in all four of the wound groups studied. The decrease in the initial proliferation boom signals the progression of the wounds as, once the granulation tissue is formed, a long period of tissue maturation follows with a fine balance of proliferation and apoptosis. In the Cx43-asODN-treated diabetic wounds, the number of proliferating cells was significantly less at days 5 and 10 than in the sODN treated counterparts. No difference between treatments was found at day 15. The decrease in the number of Ki-67 positive cells may mean that the asODN treated wounds began tissue maturation earlier and that the peak of proliferation had been reached before the 5 day time point. No changes in the number of apoptotic cells in the asODN treated granulation tissue

were identified in the previous mouse study (Mori et al., 2006). This further suggests that asODN application could bring the early completion in proliferation during granulation tissue maturation but not the later scar reconstruction. No difference in the level of proliferation was found between the control sODN and asODN wounds.

It appeared that in many studies in this chapter the application of Cx43 specific asODN improved the diabetic delayed healing but did not make a significant effect on the healthy control wounds. It may be that 10 μM of asODN was optimal for diabetic wounds but not for healthy wounds. Preliminary data from the lab suggests that an excessively high concentration of asODN may not be beneficial to the wound healing process and may even have an adverse effect. While 1 μM ODN was used for the mouse studies, rat and mouse skin are very different therefore cannot be compared directly for optimal concentration. The optimal concentration of Cx43-asODN was not estimated for the studies in this chapter for control nor diabetic wounds. Nevertheless, the optimal Cx43-asODN concentration to improve control wound healing is probably between 1 and 10 μM. The knockdown of Cx43 expression using the optimal concentration of asODN immediately after injury can cause a profound improvement on the process of wound healing.

6 ENDOTHELIAL CELL PERMEABILITY AND CONNEXIN 43

6.1 Chapter introduction

Endothelial cells form the inner epithelium of the vascular wall. They are very thin and specifically designed to facilitate diffusion and exchange of oxygen, carbon dioxide and metabolites in the blood with adjacent tissues. After injury, endothelial cells become activated and partake in the initiation of the inflammatory phase. The process of acute inflammation involves a rapid series of responses by endothelial cells from within minutes to the first few hours after injury (Pober and Cotran, 1990). Endothelial cells are involved in controlling the blood flow to the site of injury, vessel permeability and the transmigration of inflammatory cells into the injured tissue. Initially after injury and bleeding, the vessels near the wound site begin to vasoconstrict to minimise the loss of blood, and this is soon followed by vasodilation to increase the blood flow into the region. The activated endothelial cells are generally responsible for the macroscopic appearance of wounds: the increased volume of blood at the wound region causes the wound to appear swollen (tumor), red (rubor), warm (calor) and is sometimes associated with pain (dolor).

In resting conditions, endothelial cells regulate the normal blood flow and vessel tone by releasing nitric oxide (NO) produced by nitric oxide synthase 3 (NOS3) within the cells (Moncada and Higgs, 2006a). NO is a potent vasorelaxant that regulates blood flow by modifying vascular smooth muscle tone (Moncada and Higgs, 2006b). Soon after injury, vasoactive mediators such as histamine are released from degranulating mast cells and platelets in the wounds. Histamine causes a local dilation of small vessels and increases vascular permeability by binding to histamine H1 receptors on

endothelial cells. The binding of extracellular ligands to histamine H1 receptors activates endothelial cells and in turn prompts the acute inflammatory response (Ehringer et al., 1996). Ligand binding triggers the release of IP_3 from the plasma membrane that induces an elevation in intracellular cytosolic free Ca^{2+}, achieved by releasing Ca^{2+} from endoplasmic reticulum (Birch et al., 1994; Ehringer et al., 1996; Rotrosen and Gallin, 1986). The elevation of cytosolic Ca^{2+} concentration activates cellular phospholipase A_2 to free arachidonic acid from the plasma membrane (Millanvoye-Van Brussel et al., 1999). Free arachidonic acids are converted by the enzymes cyclooxygenase –1 and –2 (COX-1, COX-2) into prostaglandin I_2 (PGI_2) and prostaglandin E_2 (PGE_2), major vasorelaxants of blood vessels (Egan and FitzGerald, 2006; Eligini et al., 2005; Mitchell et al., 1995; Wu, 1996). Cytosolic Ca^{2+} ions also form complexes with calmodulin that activate NOS3 to produce more NO (Groschner et al., 1994; Lantoine et al., 1998). Prostaglandins and NO together increase vessel leakiness during acute inflammation (Egan and FitzGerald, 2006; Teixeira et al., 1993). Therefore, the release of these two vasoactive factors by endothelial cells contribute to the increased blood flow and permeability associated with inflammation.

The lumen of blood vessels is usually sealed by the formation of tight junctions between endothelial cells. Tight junctions are important in controlling the permeability barrier and preventing the escape of blood from the lumen. During inflammation, tight junctions are removed locally (Muller, 2001; Shaw et al., 2001) and endothelial cells retract to increase permeability thus assisting fluid exudation and leukocyte transmigration (Andriopoulou et al., 1999; Kolodney and Wysolmerski, 1992; Rowland et al., 1984). Histamine and prostanoids (prostaglandins and thromboxane) mediate the retraction of cells forming gaps that permit larger molecules to escape the

circulation and thus allow inflammatory mediators to reach the sites of wound and inflammation (Wilgus et al., 2000). The activated endothelial cells at the same time begin to undergo morphological changes and express surface adhesion molecules to promote leukocyte adhesion and the transmigration process (Huang et al., 1993; Miki et al., 1996; Rotrosen and Gallin, 1986). In response to injury, endothelial cells also secrete mediators of acute inflammatory responses including IL-1, IL-6 and IL-8 to amplify the process and growth factors such as PDGF and FGF to assist wound repair (Gomaraschi et al., 2005; Li et al., 2001; Lin et al., 2006).

Alongside tight junctions and adherens junctions, endothelial cells also express gap junctions. Gap junctions are found between endothelial cells, between smooth muscle cells, and also between the two different cell types (Bruzzone et al., 1993; Haefliger et al., 1992; Larson et al., 1990; Little et al., 1995; Pepper et al., 1992; Reed et al., 1993; Van Rijen et al., 1997). Cx37, Cx40 and Cx43 have all been identified in endothelial cells and form functional gap junctions (Little et al., 1995; Pepper et al., 1992; Reed et al., 1993). Possible heterotypic gap junctions may be formed from these connexins in the vascular wall (Bruzzone et al., 1993; He et al., 1999; Valiunas et al., 2001; Yeh et al., 1998). Endothelial Cx37 and Cx40 appear to be uniformly expressed within the circulatory system whereas Cx43 expression is more heterogeneous and associated with sites of high shear stress (Gabriels and Paul, 1998). Gap junctions between endothelial cells and smooth muscle cells have been suggested to contribute to non-prostaglandin/NO dependent vascular relaxation by mediating electric signal conductions between the cells (Beny and Connat, 1992; Chaytor et al., 1998; Christ et al., 1996). Vasoconstriction and vasodilation signals travel rapidly longitudinally along the vessel network due to the transmission of endothelium-derived hyperpolarising

factor (EDHF) via the gap junctions, thus maintaining vessel tone (Beny and Connat, 1992; Chaytor et al., 1998).

There is evidence that gap junctions are involved in several aspects of the endothelial response to injury. When activated by histamine or the pro-inflammatory chemokine TNF-α, connexin protein expression and cell coupling change in a time-dependent fashion in endothelial cells (Figueroa et al., 2004; Van Rijen et al., 1997). Gap junctions have been directly implicated in leukocyte endothelial transmigration in several studies (Eugenin et al., 2003; Jara et al., 1995; Oviedo-Orta et al., 2002; Zahler et al., 2003). They are also thought to coordinate the migration of endothelial cells during wound repair (Larson and Haudenschild, 1988; Pepper et al., 1992; Pepper et al., 1989). Increases in Cx43 mRNA and protein were observed after mechanical injury in endothelial cells, suggesting a role for Cx43 in the injury response (Pepper et al., 1992). However, in these studies, analysis of Cx43 mRNA, protein and cell coupling showed that the response to mechanical wounding differed between small and large vessels. Enhanced coupling and increased Cx43 were seen in the microvasculature (Pepper et al., 1992) but this was not seen in large vessels (Larson and Haudenschild, 1988). Thus, the role of gap junctions in endothelial cells may vary according to vascular sites. More recently Kwak et al. (2001) demonstrated that endothelial cells expressing dominant negative Cx43 fusion inhibitor healed significantly slower *in vitro*, providing further evidence for roles of gap junction in endothelial wound repair.

In recent years, undocked connexons or hemichannels, have been implicated in several non-gap junctional functions (Goodenough and Paul, 2003). Hemichannels were shown to be involved in glutamate (Parpura et al., 2004; Ye et al., 2003), ATP and IP_3

release or uptake during inflammatory responses in different cell types (Boitano et al., 1992; Braet et al., 2003; Contreras et al., 2003; Gomes et al., 2005; Leybaert et al., 2003). Of particular interest, hemichannels formed by Cx43 were also involved in the release of PGE_2 from osteocytes under flow stress (Cherian et al., 2005). In Chapter 5 I demonstrated that knocking down Cx43 expression in the wound region with Cx43-asODN significantly reduced the extent of albumin extravasation from blood vessels 4 hours after wounding. It is possible to hypothesise that the removal of Cx43 expression and hence hemichannels by Cx43-asODN may have caused a reduction in PGE_2 release and the subsequent decrease in vessel permeability during inflammation *in vivo*. The early inflammatory response of endothelial cells is particularly important during wound healing, as the successive processes including leukocyte transmigration and pro-inflammatory signals would be initiated based on the early events. Understanding the role of Cx43 in endothelium permeability would also help to explain the reduced leukocyte recruitment and cytokine levels observed in Cx43-asODN treated wounds (Mori et al., 2006; Qiu et al., 2003).

The binding of mimetic peptides to the extracellular loop of connexin can inhibit hemichannel opening and, depending on the length of incubation, can also prevent gap junction formation (Boitano and Evans, 2000; Chaytor et al., 1997; Dahl et al., 1994). Incubation of cells with connexin mimetic peptides *in vitro* can block release of ATP or the penetration of propidium iodide within 20 minutes (Boitano and Evans, 2000; Braet et al., 2003; Chaytor et al., 1997). The inhibition in gap junction formation can be observed after 1 hour of incubation (Boitano and Evans, 2000). To test my hypothesis I set up an *in vitro* model where increased endothelial cell permeability was induced by histamine. This model was used to examine the expression and function of

Cx43 based communication via gap junctions and to investigate the role of hemichannels in the release of PGE_2 using mimetic peptide GAP27.

The majority of the experiments and pilot data in this chapter were performed in Dept of Pharmacological Sciences, University of Milan, Italy under the supervision of Dr Susanna Colli and Dr Sonia Eligini while on a 5-month EU Marie Curie Early Stage Training fellowship.

6.2 Brief methodology

Primary human umbilical vein endothelial cells (HUVECs) were isolated from individual umbilical cords or purchased from TCS CellWorks for the experiments. Cells were grown directly on culture plates or on plastic coverslips coated with gelatin. Cells were incubated at 37°C in incubators with 5% CO_2. M199 culture medium containing L-glutamine (BioWhittaker), human or fetal calf serum, endothelial cell growth factor (crude extract), heparin (Sigma), and antibiotics (Sigma) was used to maintain the cells. In experiments involving the use of antisense ODN to knockdown Cx43 expression, serum was omitted from the medium to minimise ODN degradation. Antisense ODN (custom ordered from Sigma Genosys, 10 mM stocks dissolved in DEPC water) was added directly to the culture medium without pluronic gel or other transfection agents to achieve the appropriate concentrations.

Histamine (Sigma, 100 nM and 1 μM) was used to stimulate an injury response in the HUVECs. Whole cell lysates were used for Western Blot analysis of Cx43 (Sigma Anti-Cx43 rabbit polyclonal antibody, 1:5000) and COX-2 (Cayman rabbit polyclonal antibody, 1:500) protein expression after 3, 6 and 24 hours of incubation with histamine (N = 4 for 100 nM histamine and N = 7 for 1 μM histamine). Protein bands from Western blots were quantified using ImageJ software. In addition, immunofluorescent staining was used to study Cx43 (Sigma rabbit polyclonal antibody, 1:4000) and hemichannel expression (GAP7M or HC rabbit polyclonal antibodies, 1:200) in intact cells. Gap junctional intercellular communication was examined at the same time points using Lucifer Yellow dye (4%) microinjection. Cells were injected with LY and dye allowed to transfer to neighbouring cells for 1 min (N = 4, a minimum of 10 cells were injected for each coverslip). Digital images were taken of each microinjection and thresholded using ImageJ software. The number of cells with visible LY dye was counted.

Enzyme-Linked Immunosorbent Assay (ELISA) kits were purchased from Cayman Chemicals to measure the production and release of PGE_2 by the HUVECs upon histamine stimuli (N = 6). Culture media and cell lysates were collected following incubation with histamine for 3 and 6 hours for analysis by ELISA to estimate the PGE_2 concentration released into the media and intracellular PGE_2 content. ELISA was also performed on HUVECs stimulated with histamine in the presence of the gap junction mimetic peptide GAP27 (600 μM) and COX-2 inhibitor NS398 (10 μM). Gap junction mimetic peptide GAP27 binds to the extracellular loop of Cx43 and, once bound, blocks hemichannel opening and prevents gap junction formation. NS398

inhibits the enzymatic activity of COX-2, preventing the synthesis of prostanoids including PGE_2.

To assess the possibility of hemichannel opening, propidium iodide (2 μg/ml) was added to the culture medium alongside histamine (1 μM, N = 3). Propidium iodide is normally impermeable to cells but in the event of hemichannel opening can enter cells and stain their nuclei. HUVECs were incubated with histamine and propidium iodide up to 6 hours. Each hour a coverslip was removed and the cells thoroughly washed with PBS and fixed before fluorescent imaging.

An in vitro endothelial cell permeability assay using culture inserts (Figure 2.3) was set up to examine the role of Cx43 during the inflammatory response. HUVECs were grown to confluency on the inserts (3 μm pores) in 24-well plates. The permeability of the HUVEC monolayer was measured by the amount of BSA conjugated with the fluorescent label FITC (100 ng/ml) that diffused from the upper culture chamber through the cells into the lower chamber. FITC-BSA collected in the lower chamber medium was read at 3, 6 and 24 hours with histamine (1 μM) incubation using a fluorescent microplate reader alongside a known FITC-BSA standard curve (N = 6). Endothelial cell permeability was measured in resting HUVECs, cells stimulated by histamine, and cells stimulated by histamine in the presence of either human Cx43-asODN (2 doses of 25 μM 40 min apart) or COX-2 inhibitor NS398 (10 μM).

To compare multiple groups or time points in the experiments One-way ANOVA statistics was used throughout this chapter. A post-hoc Newman-Keuls Test was used

to identify the statistical differences between the sample groups when a significant difference was found in the ANOVA. Data is expressed as mean ± SEM.

6.3 HUVECs express Cx43 and functional gap junctions

The expression Cx43 protein was confirmed in the cultured HUVECs in both cytoplasm and at the plasma membrane at cell junctions. The injection of Lucifer Yellow dye for 1 min showed a high abundance of dye coupling between the cells with clearly visible secondary and tertiary degree of cell coupling (Figure 6.1). Cx43 gap junction plaques were observed in the plasma membranes between neighbouring contacting cells in a confluent cell culture, however, Cx43 plaques were also expressed in the membrane where no cellular contact was present (Figure 6.1). Hemichannels/Connexons were found at low levels within the cytoplasm and at the plasma membrane in HUVECs (Figure 6.1). Other connexins, Cx37 and Cx40 are known to be expressed in HUVECS (van Rijen et al., 1997) but these were not studied in this pilot project. The focus of this set of experiments was placed on Cx43 because in vivo experiments in rats showed that the knockdown of Cx43 protein immediately after injury had a significant effect on skin wound healing and in particular reduced BSA extravasation within 4 hours of injury (Chapter 5.4).

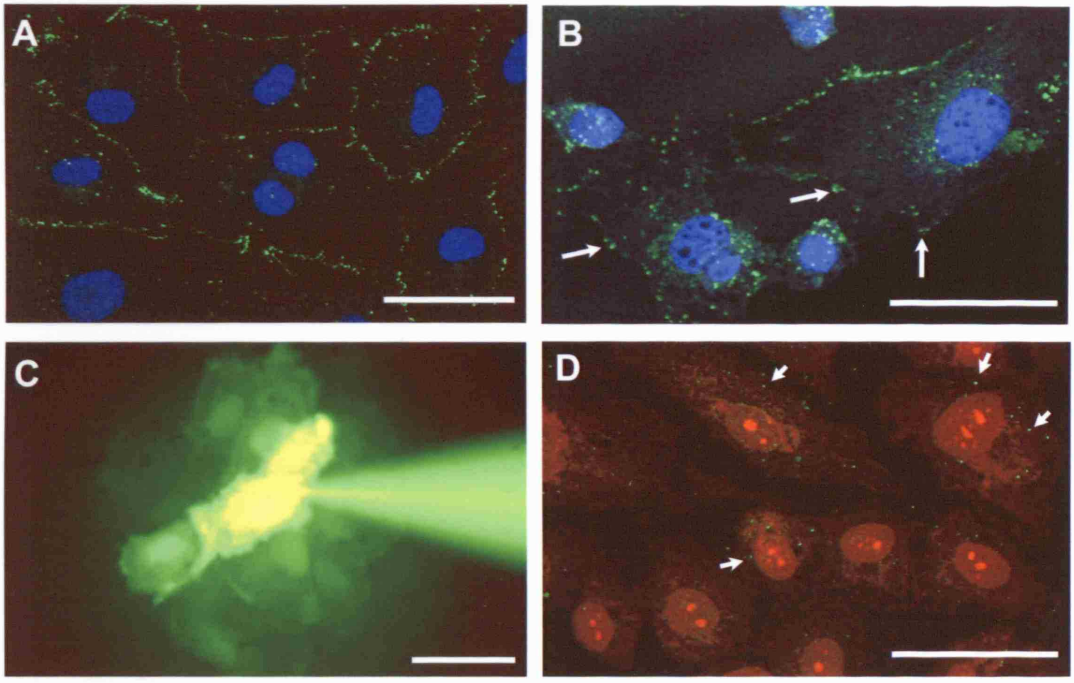

Figure 6.1 HUVECs express high levels of Cx43 with active GJIC channels. (A) Cx43 protein (green) was expressed in the cytosol and plasma membranes between neighbouring cells (nuclei in blue). (B) Cx43 plaques were also found in plasma membranes where there was no neighbouring cell contact (long arrows). (C) LY microinjection demonstrated strong cell coupling between HUVECs. (D) Low levels of hemichannel clusters (green, short arrows) were observed in the cytosol and plasma membrane (nuclei in red). All scale bars 25 μm.

6.4 Histamine induced changes in Cx43 and COX-2 protein expression

To investigate the hypothesis that PGE_2 can be released via Cx43 hemichannels in endothelial cells, expression of Cx43 and COX-2 proteins in HUVECs were examined during the inflammatory response after incubation with 100 nM or 1 μM of histamine. Histamine is usually released by degranulating mast cells after injury or an inflammatory response, and it exerts its action on endothelial cells by binding to H_1 histamine receptors to trigger pathways for vasodilation and down stream inflammatory response (Hill, 1992; Li et al., 2001). Immunofluorescent staining of Cx43 showed increased protein expression in the cytosol upon stimulation with1 μM histamine. This occurred particularly in the perinuclear region, and also in the plasma membrane between 3 and 6 hours after incubation (Figure 6.2). Actin filaments also became denser at the same time and morphological changes were observed as spaces began to appear between cells that were previously confluent. Cx43 protein was expressed in the plasma membrane of cells, both at points of cellular contact and places without contact (Figure 6.2). However, hemichannel staining did not reveal any changes in the level of expression throughout the time points.

A difference in level of cellular response was observed adding 100 nM or 1 μM of histamine in the culture medium. Incubation of histamine at 100 nM did not alter the level of Cx43 protein and elevated slightly the COX-2 expression in the HUVECS. The higher histamine concentration (1μM), however, increased the expression of Cx43 and COX-2 proteins in a time dependent manner (Figure 6.3). Western blot analysis and quantification revealed up to 30% increase in total Cx43 protein expression, with

1 μM histamine concentration, after 3 and 6 hours of incubation. The increase was observed in all the phosphorylated and non-phosphorylated forms (Figure 6.3). However, the increase of Cx43 protein expression at 3 and 6 hours of 1 μM histamine incubation did not reach statistical significance. By 24 hours the Cx43 protein expression had returned to normal levels in the cells incubated in either concentrations of histamine.

COX-2 protein (72kDa) expression is very low and nearly non detectable in HUVECs in a resting state. After 100 nM or 1 μM histamine incubation, the COX-2 protein expression increased dramatically 2-3 fold. The increase in COX-2 protein was most dramatic after of 3 hours of incubation and the expression increased further, although less dramatically, to reach a peak expression at 6 hours in both concentrations (Figure 6.3). COX-2 expression was significantly increased in HUVECS stimulated by 1 μM histamine at both 3 and 6 hours in ($P < 0.05$; Figure 6.3). By 24 hours the COX-2 expression had returned back to normal levels. The rise and fall of Cx43 and COX-2 protein expression after histamine incubation appeared to be concomitant, although COX-2 elevation was more dramatic than Cx43. The difference in the magnitude of elevation was observed because COX-2 protein expression is barely expressed at resting state and is only induced in inflammatory responses. In HUVECs, high level of Cx43 protein is usually present in non-stimulated cells (Figure 6.1).

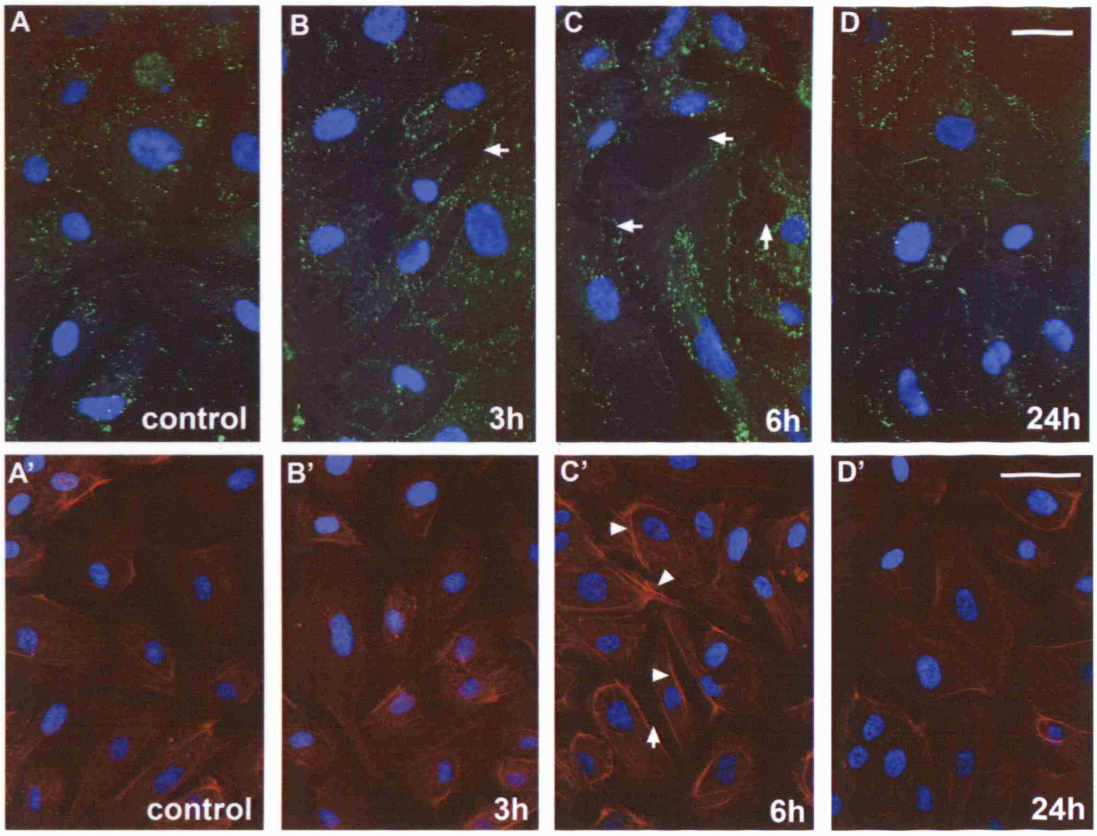

Figure 6.2 Histamine causes an elevation in Cx43 protein expression in HUVECs in time dependent manner. (A and A') HUVECs in resting conditions express Cx43 (green) in the cytosol and plasma membranes. (B, C) By 3 and 6 hours after 1 μM histamine incubation the Cx43 increases and by 24 hours (D) the expression returns to normal levels. Some gaps between cells are observed as cells responded to histamine incubation (arrows). The density of F-actin (red, arrowhead) also appeared to increase between 3 and 6 hours. Nuclei counterstain in blue, scale bars 25 μm.

The observation of increasing membrane Cx43 protein expression in HUVECs incubated in 1 μM histamine suggested a possible change in gap junctional intercellular communication. HUVECs were microinjected with Lucifer Yellow for 1 min and the extent of dye transfer (number of cells to which dye transferred) was assessed. The level of LY gap junctional transfer did not alter significantly at all the time points examined with histamine incubation. At resting conditions, HUVECs transfer Lucifer Yellow to 8-9 cells with secondary or tertiary cells positive for the dye (Figure 6.4). After 3 hours of histamine incubation, the extent of dye coupling decreased slightly but by 6 hours coupling was comparable to control levels (Figure 6.4). The histamine-induced change in cell coupling did not match entirely with the Western blot Cx43 protein analysis. A trend of increase in Cx43 protein expression was observed at 3 and 6-hour time points but no change in cell coupling was observed. Interestingly, intracellular gaps induced by histamine were apparent at 3 and 6 hours of histamine incubation but the loss of cell-to-cell contact did not alter cell dye coupling at the these time points.

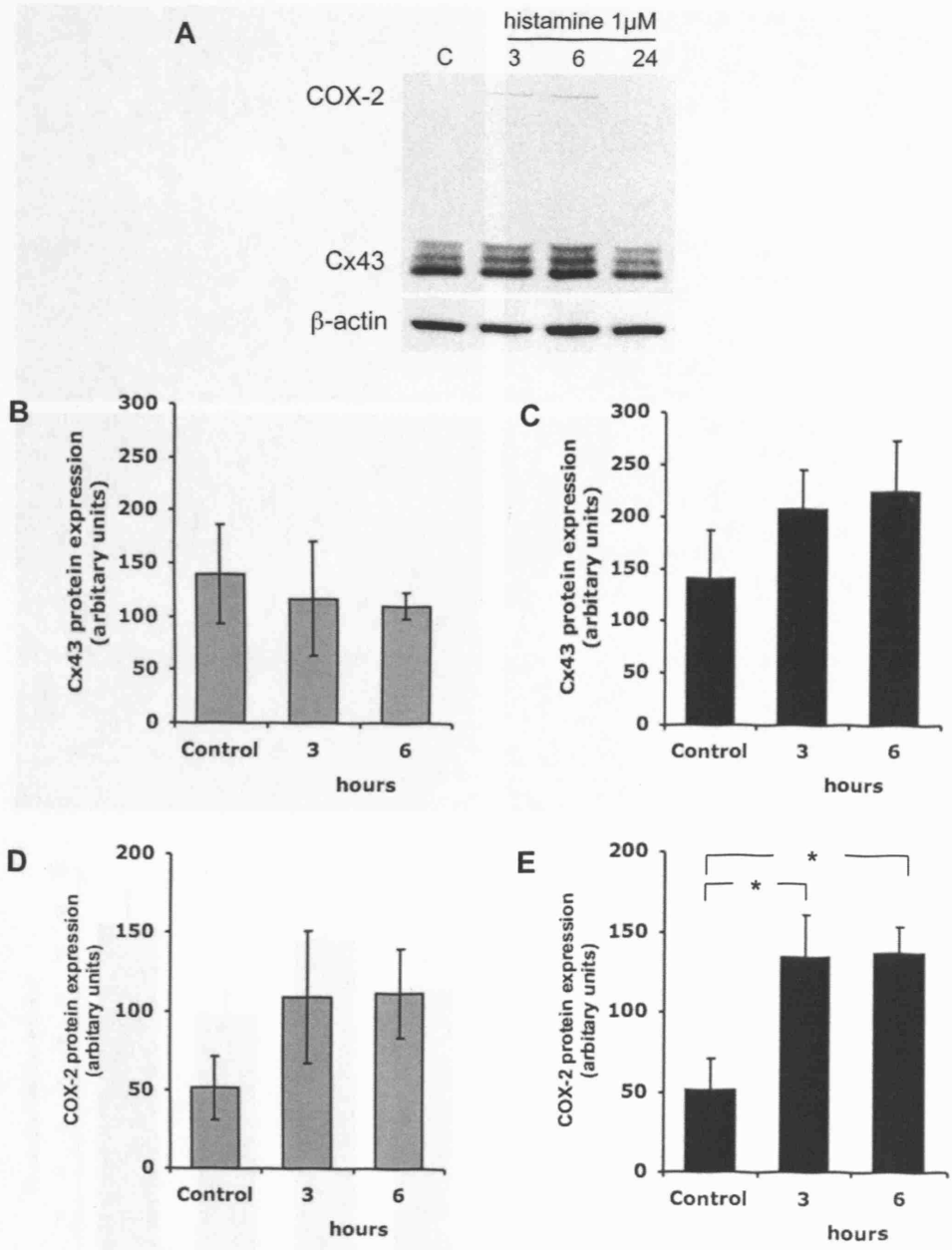

Figure 6.3 Western blot revealed increased of Cx43 and COX-2 in HUVECs incubated in histamine. (A) Both COX-2 and Cx43 increase between 3 and 6 hours after 1μM histamine incubation. (B, C) Quantification of total Cx43 protein bands from Western blots after histamine incubation, 100 nM (B, N = 4) and 1 μM (C, N = 7) concentrations respectively. No change in Cx43 total protein was observed in 100 nM (B) but protein expression appeared to increase in 1 μM (C) histamine. Quantification of COX-2 bands from Western blots with 100nM (D, N = 4) or 1 μM (E, N = 7) histamine incubation respectively. In the higher histamine concentration COX-2 increased 2-3 fold in expression, peaking at 6 hours. (*$P < 0.05$).

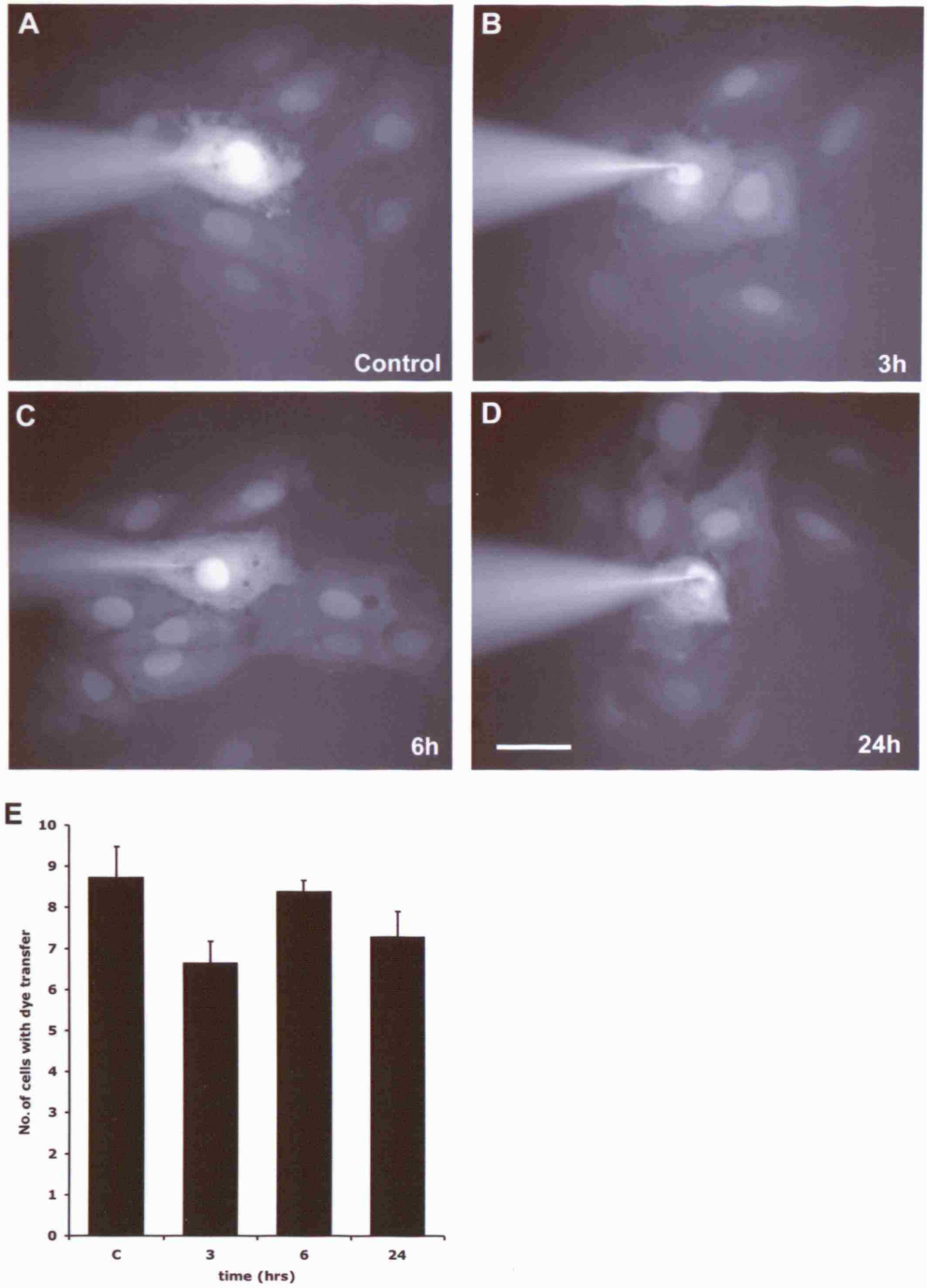

Figure 6.4 Lucifer Yellow dye coupling between HUVECs changed with histamine incubation. (A-D) Dye coupling between the HUVECs at time points 0, 3, 6 and 24 hours with histamine incubation respectively. No significant alternation in LY transfer was identified in the HUVECs stimulated with 1 μM histamine. Scale bar 25 μm. (E) Extent of dye coupling was quantified at each time point. An initial decrease in coupling at 3 hours was observed but increased again by 6 hours. At 24 hours the level of cell coupling returned to control levels (N = 4).

6.5 Knockdown of Cx43 protein expression in HUVECs

In the rat *in vivo* wound healing model a Cx43 antisense sequence designed specifically for rodents was used (Qiu et al., 2003; Mori et al, 2006). Therefore, to manipulate Cx43 protein expression in HUVECs before establishing *in vitro* models for endothelial permeability assay and PGE_2 release, both rodent and human Cx43 specific antisense ODNs were first tested for efficacy and suitable dosage.

Both human and rodent antisense ODN sequences were designed by Dr David Becker and custom ordered from Sigma Genosys. Both ODNs were designed to bind to a conserved sequence of the Cx43 mRNA on the C-tail (Figure 6.5; Figure 6.6). The protein sequence alignment showed 100% conservation between the rat, mouse and human but there are two base mismatches at the ODN binding site between the rodents and human mRNA sequences (Figure 6.6). Application of rodent or human antisense ODNs to HUVECs (80% confluency) showed different efficacy in Cx43 protein knockdown. For rodent or human antisense, two applications of 20 μM ODN successfully reduced the number of Cx43 protein plaques and total amount of positive staining (Figure 6.7). The knockdown was more effective using human antisense ODN to Cx43 on HUVECs, reducing expression to approximately 15% of control versus 33% of control expression using rodent specific antisense ODN ($P < 0.01$ in both). The complete match of antisense ODN sequence and human Cx43 mRNA clearly was important to achieve maximal knockdown. For the subsequent experiments antisense ODN to human Cx43 mRNA was used.

```
Rat             MGDWSALGKLLDKVQAYSTAGGKVWLSVLFIFRILLLGTAVESAWGDEQSAFRCNTQQPG 60
Mouse           MGDWSALGKLLDKVQAYSTAGGKVWLSVLFIFRILLLGTAVESAWGDEQSAFRCNTQQPG 60
Human           MGDWSALGKLLDKVQAYSTAGGKVWLSVLFIFRILLLGTAVESAWGDEQSAFRCNTQQPG 60
                ************************************************************

Rat             CENVCYDKSFPISHVRFWVLQIIFVSVPTLLYLAHVFYVMRKEEKLNKKEEELKVAQTDG 120
Mouse           CENVCYDKSFPISHVRFWVLQIIFVSVPTLLYLAHVFYVMRKEEKLNKKEEELKVAQTDG 120
Human           CENVCYDKSFPISHVRFWVLQIIFVSVPTLLYLAHVFYVMRKEEKLNKKEEELKVAQTDG 120
                ************************************************************

Rat             VNVEMHLKQIEIKKFKYGIEEHGKVKMRGGLLRTYIISILFKSVFEVAFLLIQWYIYGFS 180
Mouse           VNVEMHLKQIEIKKFKYGIEEHGKVKMRGGLLRTYIISILFKSVFEVAFLLIQWYIYGFS 180
Human           VNVDMHLKQIEIKKFKYGIEEHGKVKMRGGLLRTYIISILFKSIFEVAFLLIQWYIYGFS 180
                ***:*****************************************:****************

Rat             LSAVYTCKRDPCPHQVDCFLSRPTEKTIFIIFMLVVSLVSLALNIIELFYVFFKGVKDRV 240
Mouse           LSAVYTCKRDPCPHQVDCFLSRPTEKTIFIIFMLVVSLVSLALNIIELFYVFFKGVKDRV 240
Human           LSAVYTCKRDPCPHQVDCFLSRPTEKTIFIIFMLVVSLVSLALNIIELFYVFFKGVKDRV 240
                ************************************************************

Rat             KGRSDPYHATTGPLSPSKDCGSPKYAYFNGCSSPTAPLSPMSPPGYKLVTGDRNNSSCRN 300
Mouse           KGRSDPYHATTGPLSPSKDCGSPKYAYFNGCSSPTAPLSPMSPPGYKLVTGDRNNSSCRN 300
Human           KGKSDPYHATSGALSPAKDCGSQKYAYFNGCSSPTAPLSPMSPPGYKLVTGDRNNSSCRN 300
                **:*******:*.***:***** ************************************

Rat             YNKQASEQNWANYSAEQNRMGQAGSTISNSHAQPFDFPDDNQNAKKVAAGHELQPLAIVD 360
Mouse           YNKQASEQNWANYSAEQNRMGQAGSTISNSHAQPFDFPDDSQNAKKVAAGHELQPLAIVD 360
Human           YNKQASEQNWANYSAEQNRMGQAGSTISNSHAQPFDFPDDNQNSKKLAAGHELQPLAIVD 360
                ************************************.**:**:**************

Rat             QRPSSRASSRASSRPRPDDLEI 382
Mouse           QRPSSRASSRASSRPRPDDLEI 382
Human           QRPSSRASSRASSRPRPDDLEI 382
                **********************
```

Figure 6.5 Rat, mouse and human Cx43 protein sequence alignment. There is a high conservation of sequences between the species. Red box marks the location of antisense ODN binding site in protein sequences.

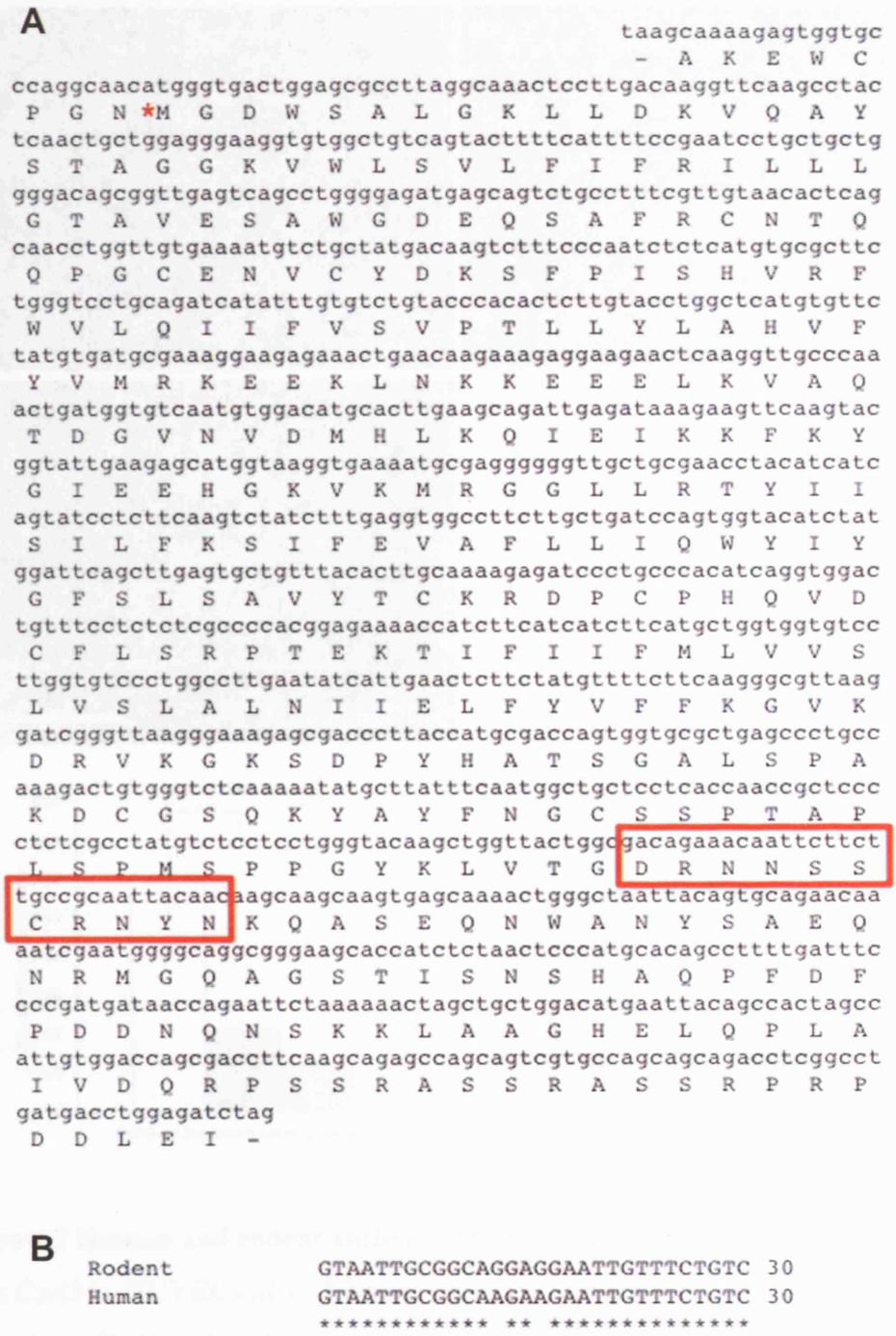

Figure 6.6 Cx43 mRNA sequence and Cx43 - asODN sequences. (A) Cx43 mRNA 5' to 3' sequence and the corresponding amino acid sequence in the correct reading frame. The red asterisk marks the start of protein, red box marks the antisense ODN binding site. (B) Human and rodent antisense ODN sequences (5' to 3') and alignment, there are two base mismatches.

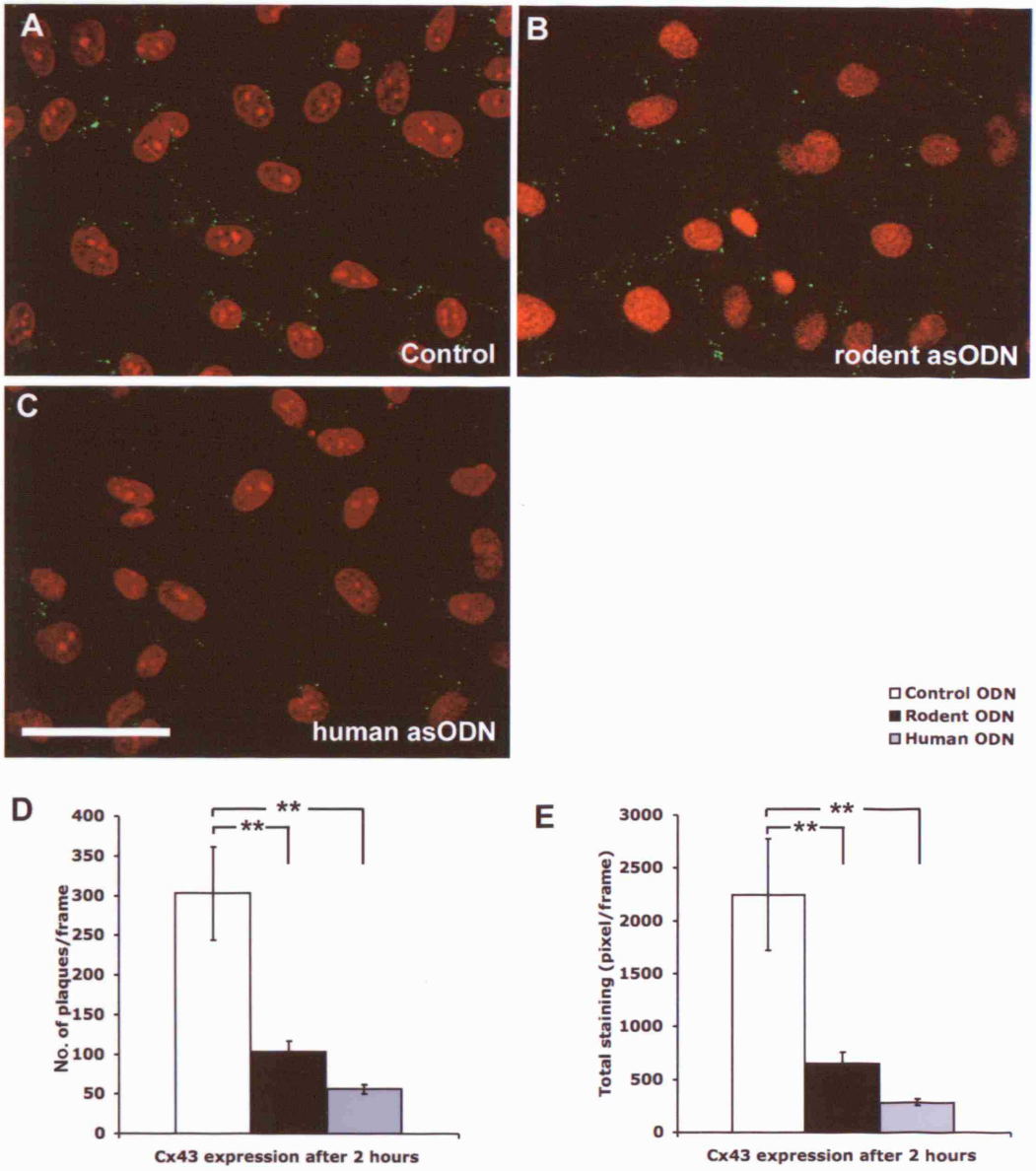

Figure 6.7 Human and rodent antisense ODNs have different efficacy in knocking down Cx43 in HUVECs after 2 hours. (A) HUVECs control Cx43 with sense ODN application. (B) Cx43 knockdown in HUVECs using two applications of 20 μM rodent asODN. (C) Cx43 knockdown in HUVECs using two applications of 20 μM human asODN. (D, E) Human asODN is more effective in the knock down of Cx43 protein expression in HUVECS than rodent asODN after 2 hours of incubation. Scale bar 50 μm; **P < 0.01.

After establishing antisense ODN for human Cx43 was more efficient for Cx43 protein knockdown, a suitable concentration was estimated for the HUVECs. These HUVECs were primary cells and thus protein expression knockdown using antisense without any method of transfection was not easy to achieve. A series of different concentrations of Cx43–asODN at 15, 30 and 50 μM was tested using either single or two doses on confluent HUVECs (Figure 6.8). Multiple applications of asODN were tried because asODN are not recyclable after mRNA binding and RNase H cleavage. To maintain a supply of Cx43–asODN in the culture medium for protein knockdown a second dose of asODNs was added 40 min after the first application.

After 2 hours of asODN incubation, with single dose concentrations 15 and 30 μM of asODN did not appear to have significant effect on Cx43 protein expression as revealed by immunofluorescent staining (Figure 6.8). Cells that received two doses of 15 μM asODN over 40 min showed moderate Cx43 protein knockdown after 2 hours but the level was not satisfactory (Figure 6.8). The most successful protein knockdown was using a single application of 50 μM asODN, which reduced Cx43 protein expression to a third of control level. However, at this concentration the cells did not look well and some cell detachment was observed. The optimal concentration to knockdown Cx43 protein expression using asODN in confluent HUVECs was using two applications of 25 μM asODN. Using this application Cx43 protein knockdown was achieved satisfactorily, reducing expression to approximately 65% of control level without a toxic effect. This method of application and concentration was used in the later endothelial permeability assay.

The knockdown of Cx43 protein was reflected in the loss of LY dye coupling between the HUVECs over the 2-hour asODN incubation period (Figure 6.9). High levels of Lucifer Yellow dye coupling were normally observed between the resting confluent HUVECs. A decrease in dye coupling became evident after 60 min of incubation with two applications of 25 μM Cx43-asODN. Thereafter Lucifer Yellow dye coupling continued to decrease and by 120 min coupling was barely observable in the treated HUVECs (Figure 6.9).

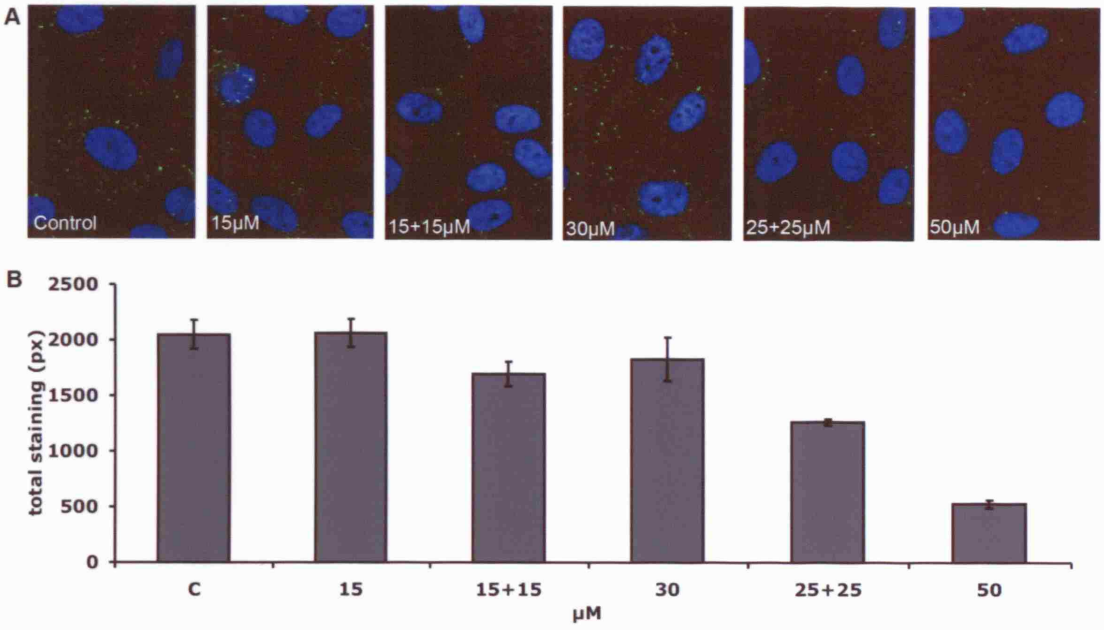

Figure 6.8 Various concentrations of Cx43 antisense ODN were tested to identify the best working protocol. (A) Cx43 protein (green) knockdown was effective after 2 hours using two applications of 15 μM or 25 μM at 40 min apart, or 1 application of 50 μM. (B) Corresponding Cx43 staining quantification. The most effective concentration was one dose of 50 μM but there was a toxic effect on the cells. The 25+25 μM concentration was used for subsequent experiments.

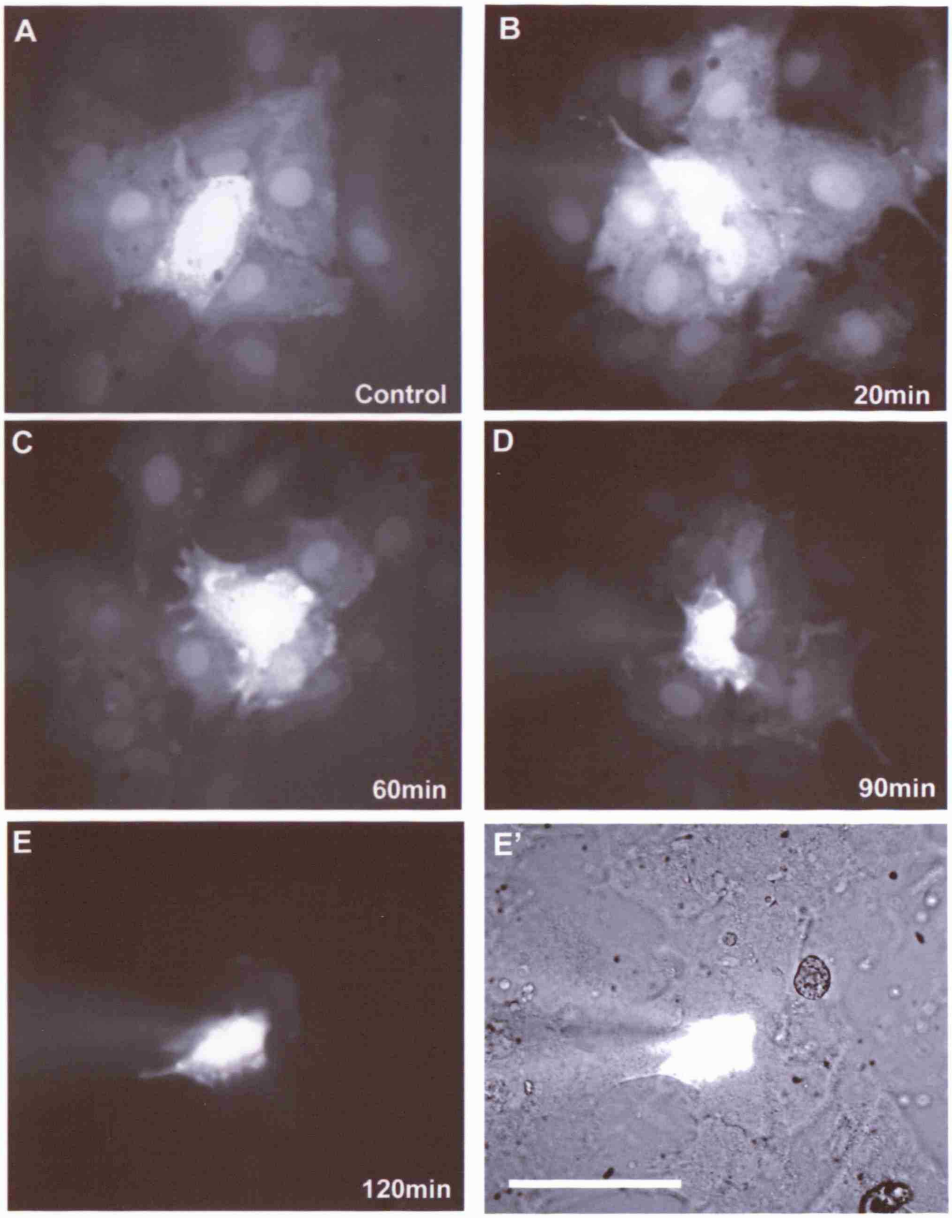

Figure 6.9 Antisense-Cx43 successfully reduces LY cell coupling by 2 hours after asODN incubation. (A-E) The level of LY transfer between the HUVECs decreased over time with the targeted knockdown of Cx43 protein. The decrease in LY transfer only became evident 60 min after asODN incubation and by 120 min majority of LY transfer was lost. (E') Brightfield view of the cells in panel E. Little coupling was observed between neighbouring cells after 120 min. Scale bar 50μm.

6.6 Knock down of Cx43 reduces HUVEC permeability in vitro

In order to assess the role of Cx43 in endothelial cell permeability, an in vitro model using culture inserts was set up. FITC-BSA (100 ng/ml) was added to the upper well chamber and allowed to diffuse across the HUVEC monolayer. This was carried out in wells treated with histamine alone, or with either Cx43-asODN (H+asODN) or NS398 (H+NS398). NS398 was added 30 min before FITC-BSA, Cx43-ODN and histamine were added at time 0. The remaining FITC-BSA in the upper chamber and FITC-BSA collected in the lower chamber was read at 3, 6 and 24 hours of incubation (Figure 6.10).

In the control well where no stimulus was added, a passive loss of FITC-BSA from the upper to the lower chamber was observed over 24 hours. At 3 hours in the histamine treated wells, a significantly higher amount of FITC-BSA was lost from the upper well compared to control ($P < 0.001$) indicating high permeability of endothelial cells. The H+asODN and H+NS398 wells showed a minor loss in FITC-BSA that was similar to control. Data from lower wells was complimentary to the upper well, and the amount of FITC-BSA increased over the 24 hours. At 3 hours of incubation, high level of FITC-BSA was detected in the wells treated with histamine alone. Endothelial cells in H+NS398 showed similar level of permeability to histamine alone at this time point.

At 6 hours of incubation, histamine stimulated endothelial cells remained highly permeable to FITC-BSA ($P < 0.05$). The endothelial cells in control, H+asODN and H+NS398 wells showed steady passive diffusion of FITC-BSA (Figure 6.10). At this

point, endothelial cell permeability appeared to be even lower than controls but this was not significant.

In all the wells, most of the FITC-BSA diffused from the upper to the lower chamber in the first 6 hours of the experiment. This was perhaps due to the response in initial concentration differences in the upper and lower wells. Between 6 to 24 hours FITC-BSA continued to diffuse through in all the wells but at a lower stable rate (little endothelial permeability). The interesting observation was the effect of Cx43-asODN on endothelial cell permeability. Similar to the *in vivo* observation 4 hours after injury (Chapter 5), the endothelial cells were less permeable when Cx43 expression was knocked down. In the culture system the cells appeared even less permeable than control cells. These data indicate an important role of Cx43 protein in regulating endothelial cell permeability.

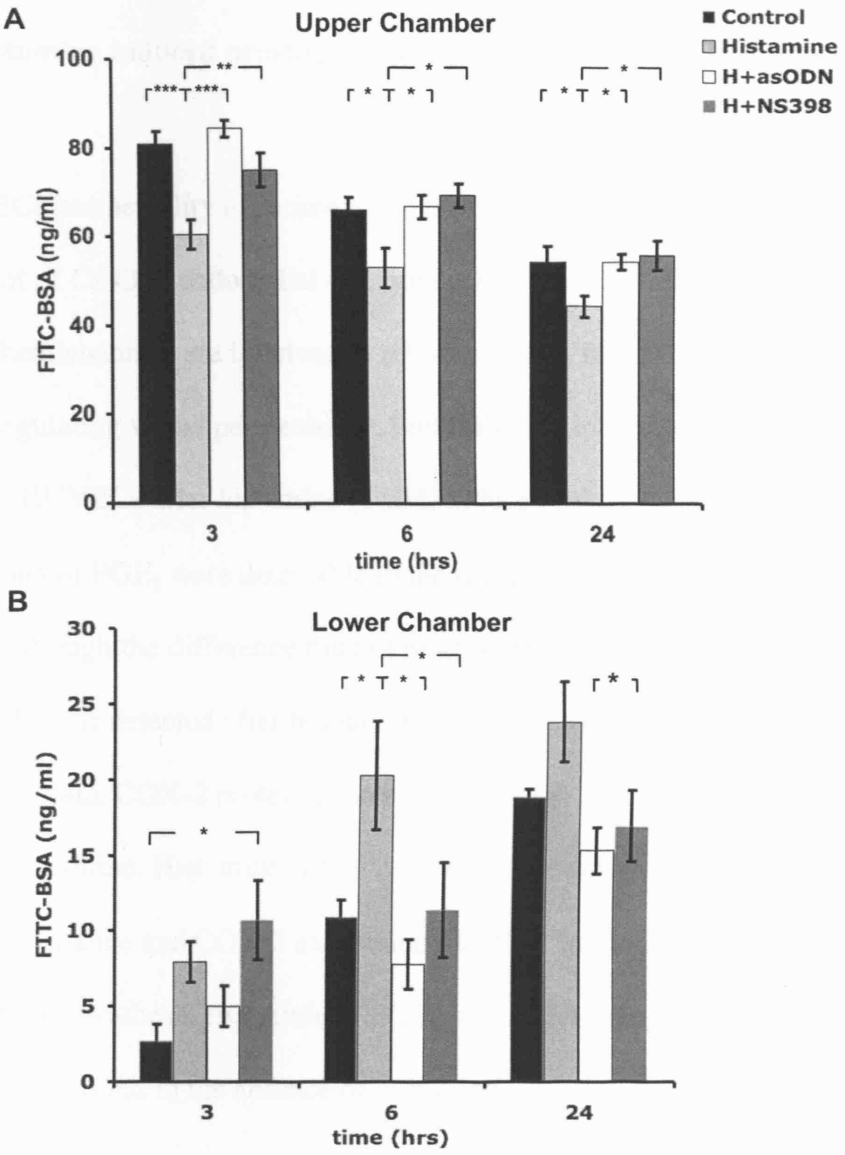

Figure 6.10 In vitro endothelial cell permeability assay using FITC-BSA. (A) A loss of FITC-BSA was observed in the upper chamber of all the wells over time. The most dramatic loss of FITC-BSA was found in wells incubated with histamine alone. Control, histamine with Cx43-asODN (H+asODN) and histamine with COX-2 inhibitor NS398 (H+NS398) wells showed a similar passive loss of BSA to the lower wells. (B) The amount of FITC-BSA in the lower wells increased over time. Histamine induced increase in permeability in the HUVECs. Knockdown of Cx43 with antisense significantly reduced HUVECs permeability (***$P < 0.001$, **$P < 0.01$, *$P < 0.05$).

6.7 Histamine induced prostaglandin E_2 release in HUVECs

The HUVECs permeability experiment using FITC-BSA clearly showed an involvement of Cx43 in endothelial cell permeability *in vitro*. To test my hypothesis that Cx43 hemichannels are involved in releasing PGE_2 from HUVECs after injury and therefore regulating vessel permeability, I used ELISA to measure the level of PGE_2 released by HUVECs after histamine (1 μM) induced injury response (Figure 6.11). High amounts of PGE_2 were detectable in the media after 3 hours of incubation with histamine although the difference did not reach statistical significance (N=6). A similar level of PGE_2 was detected after 6 hours of incubation (Figure 6.11). Corresponding to Western Blot data, COX-2 protein expression was high 3 and 6 hours after incubation with 1 μM histamine. Histamine stimulated an injury response in the HUVECs (morphology change and COX-2 expression). COX-2 inhibitor NS398 successfully prevented PGE_2 synthesis and minimal PGE_2 was detected in the media, levels being similar to those found in the absence of histamine.

The addition of mimetic peptide GAP27 (600 μM) to the medium did not affect the release of PGE_2 by the HUVECs (Figure 6.11). The binding of the mimetic peptide to the extracellular loops of hemichannels would have blocked channel opening and the release of PGE_2 through the hemichannels but this was not the case at the 3 and 6 hour time points. The amount of PGE_2 released was nearly identical to the amount released by cells incubated with histamine (1 μM) alone (Figure 6.11). Thus there was no evidence for the release of through PGE_2 hemichannels.

Intracellular PGE_2 ELISA did not reveal any difference in cellular PGE_2 contents in control cells, cells stimulated with histamine (1 μM) or those also treated with histamine and GAP27 for 3 and 6 hours (Figure 6.11). Cells treated with GAP27 did not retain more PGE_2 in the cells.

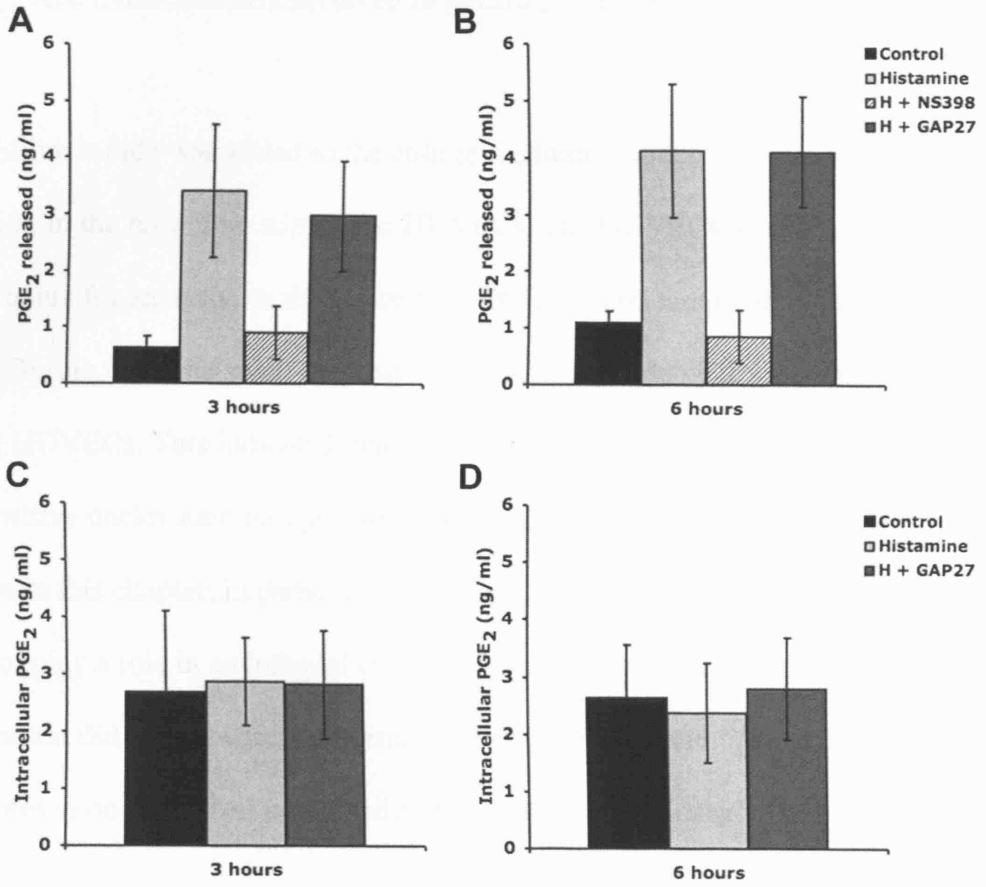

Figure 6.11 Prostaglandin E_2 is released by the HUVECs upon histamine stimulation. (A) PGE_2 released into the culture medium was measured by ELISA (ng/ml). Histamine (1 μM, light grey bar) caused an increase of PGE_2 released by the HUVECs after 3 hours of incubation compared to control (black bar). COX-2 inhibitor NS398 prevented PGE_2 production and hence only baseline level of PGE_2 was detected over time (striped bar). Similar levels of PGE_2 were released by cells incubated with histamine alone, and with mimetic peptide GAP27 (dark grey bar). (B) At 6 hours, further PGE_2 was released compared to 3 hour in all the groups except cells treated with NS398. (C, D) Intracellular PGE_2 measured by ELISA. Initially, intracellular levels of PGE_2 were higher in HUVECs stimulated with histamine but decreased with time as PGE_2 was released into the medium.

6.8 Are hemichannels involved in prostaglandin E_2 release from HUVECs?

Propidium iodide was added to the culture medium in order to detect hemichannel opening in the histamine stimulated HUVECs. The HUVECs were fixed at every hour for 6 hours for analysis, as the majority of PGE_2 was released within this period of time. During this time span, no positive propidium iodide nuclei staining was detected in the HUVECs. This indicated that hemichannels did not open or open long enough for positive nuclei staining upon stimulation with histamine. Taken together with the results in this chapter, in particular the ELISA study, connexin hemichannels probably did not play a role in endothelial cell PGE_2 release. However, the knockdown of Cx43 expression did reduce vascular permeability both *in vivo* and *in vitro*; how Cx43 regulates endothelial cell permeability remains to be elucidated.

6.9 Chapter discussion

Endothelial cell activation is one of the earliest events during acute inflammation and is important for the progression of wound healing. Gap junctions and hemichannels have been shown to be involved in the normal homeostasis of vessel tone and endothelia (Beny and Connat, 1992; Chaytor et al., 1998). In wounds, connexins contribute to endothelial wound repair and leukocyte transmigration (Eugenin et al., 2003; Jara et al., 1995; Oviedo-Orta et al., 2002). Interestingly, full thickness excisional wounds treated with Cx43-asODN showed a significant reduction in albumin exudation in the wound region (Chapter 5). Activated endothelial cells release vasorelaxants including prostanoids and nitric oxide that increase vascular permeability during inflammation (Egan and FitzGerald, 2006; Groschner et al., 1994; Teixeira et al., 1993).

The aim of this chapter was to investigate whether PGE_2 is released via Cx43 hemichannels in endothelial cells during an acute inflammatory response initiated by histamine. Both Cx43 and COX-2 protein expression in HUVECs increased similarly in a time dependent manner after histamine stimulation. However, the level of GJIC did not change significantly during histamine incubation. The application of Cx43-asODN in the *in vitro* model reduced the monolayer permeability of HUVECs, further highlighting a role of Cx43 during histamine-induced permeability in endothelial cells. However, the data in this chapter did not suggest that PGE_2 was released from

endothelial cells via connexin hemichannels. The function of Cx43 during endothelial cell permeability remains to be elucidated.

The increase in COX-2 expression in HUVECs after 1 μM histamine incubation was expected and was in accordance to the literature (Egan and FitzGerald, 2006; Mitchell et al., 1995). By 24 hours of histamine incubation, the histamine H1 receptors would have become desensitised and as Western blot analysis showed, COX-2 expression had returned to normal. Tan et al. (2007) demonstrated a similar histamine-induced COX-2 expression response in human coronary artery endothelial cells (HCAECs). Interestingly, Western blot analysis showed that Cx43 protein expression increased in the same time dependent manner as COX-2 protein in 1 μM histamine. A lower concentration of histamine (100 nM) did not stimulate an increase in Cx43 expression response as 1 μM histamine. The trend of histamine-induced increase in Cx43 protein expression in the HUVECs indicates a possible role or function in the inflammatory response. It is not known where there is a direct interaction between COX-2 and Cx43, although this seems unlikely. The concomitant increase and decrease in both protein expressions at the 3 and 6 time points was likely to be the response to histamine and H1 receptor binding. Immunostaining images showed an increase in Cx43 protein at 3 hour and 6 hour which was mostly found in the cytoplasm with some increase at the membrane. Similarly, HUVECs treated with TNF-α, a potent pro-inflammatory chemokine, also showed increased Cx43 perinuclear or cytoplasmic staining (Van Rijen et al., 1997). These changes in Cx43 expression after inflammatory stimuli suggest a function during endothelial cell activation.

Histamine did not induce a change in LY transfer between HUVECs despite the increasing trend in Cx43 protein expression. This was perhaps not surprising as most of the increased expression of Cx43 was cytoplasmic. Coupling dropped slightly at 3 hours of histamine incubation when intercellular gaps began to appear in the culture monolayer. The formation of intercellular gaps between endothelial cells is a well-known event in inflammation, increasing vascular permeability (Baluk et al., 1997). The decline in cellular contacts can reduce the level of GJIC. However, despite the continuing presence of intercellular gaps, no significant change in LY transfer was observed by 6 hours of histamine incubation. At the 6-hour point, Cx43 protein expression had elevated to the maximum observed during the time course. The cytoplasmic Cx43 may have reached the cell membrane to maintain the level of dye transfer, but the significance of this is unknown. A decrease in GJIC has been reported in human tonsil endothelial cells for 3 hours with 1 μM histamine incubation (Figueroa et al., 2004). No data was provided for between 3 and 24 hours in the same study, but GJIC had returned to normal levels at 24 hours. Despite a decrease in cellular contact, more gap junction plaques could be formed as a part of Ca^{2+} signal transduction during inflammation and therefore maintain cell coupling. The secretion of NO during inflammation has been shown to result in *de novo* Cx40 plaque formation, which may contribute to the maintenance of GJIC in HUVECs (Hoffmann et al., 2003).

Application of human sequence-specific Cx43-asODN knocked down Cx43 protein expression in HUVECs more efficiently than rodent Cx43-asODN. This was expected as there were two base mismatches between the human and rodent Cx43 mRNA sequences at the ODN binding site. Nevertheless, the use of antisense as a means to knockdown Cx43 protein expression was difficult in primary cultures of HUVECs. In

HUVECs, protein expression knockdown was more successful in subconfluent cell cultures than those at 100% confluency. Primary cells do not have a high protein turnover in general compared to cell lines, especially when cells are 100% confluent. Following the asODN dosage experiment it was concluded that two applications of 25 μM asODN at 40 min intervals were more effective in Cx43 knockdown than one application. After each binding of asODN to the target mRNA, the RNA duplex is cleaved by resident RNase H to prevent translation. Since asODNs were not renewed after each mRNA binding, the second application of asODN would replenish the supply of ODNs and prolong the expression knockdown. However, Cx43-asODN dramatically reduced LY transfer within 2 hours of ODN application even though Cx37 and Cx40 were unlikely to be affected. A decline in dye coupling between endothelial cells was observed because LY permeability is selective between Cx37, Cx40 and Cx43 gap junctions. LY passes through Cx43 gap junctions more readily than Cx40 gap junctions (Valiunas et al., 2002), and Cx37 gap junctions preferentially transfer even smaller dyes (Weber et al., 2004). Another likely explanation is the presence of heterotypic gap junctions between the endothelial cells (Bruzzone et al., 1993; Valiunas et al., 2001; Yeh et al., 1998). More tracer dyes should be included in future experiment to fully assess the level of GJIC in HUVECs.

The results of Western analysis and ELISA measurements showed increased COX-2 expression and a trend for increased release of PGE_2 into the culture medium during histamine induced endothelial cell activation cascade. The majority of PGE_2 was released within the first 6 hours of histamine incubation. After 6 hours, the level of PGE_2 in the medium remained constant and no more PGE_2 was released due to the feedback from the high concentration in the medium (Akarasereenont et al., 2001;

Akarasereenont et al., 1999). Interestingly the intracellular PGE_2 content was similar to control levels throughout the time points when the extracellular level increased dramatically. A possible explanation is that PGE_2 was not stored but was secreted very quickly once produced and therefore intracellular concentration remained stable between the time points. The release of PGE_2 within 6 hours of histamine incubation coincided with increased COX-2 and Cx43 protein expression. Similar histamine-induced COX-2 expression increase and PGE_2 release were reported by Tan et al. (2007) in HCAECs. However, application of the connexin mimetic peptide GAP27 on the HUVECs in my experiments did not alter the intracellular level of PGE_2 or that released into the culture medium. The binding of GAP27 would have blocked Cx37 and Cx43 hemichannels but neither these nor probably any other types of connexin hemichannel would seem to be involved in PGE_2 release in HUVECs because no open hemichannels were detected with PI within 6 hours of histamine incubation. The uptake or release of other secondary messengers such as IP_3 and ATP were thus also unlikely to be mediated via hemichannels during inflammation in HUVECs.

A significant increase in albumin (FITC-BSA) permeability was observed in the histamine treated HUVECs using the *in vitro* assay model. The COX-2 enzymatic inhibitor NS398 successfully reduced histamine-induced permeability by preventing prostaglandin production. However, knockdown of Cx43 expression using Cx43-asODN also prevented the histamine-induced elevation in endothelial albumin permeability. A similar observation was seen in *in vivo* wounds treated with Cx43-asODN, where blood vessels were less leaky to FITC-BSA. Clearly Cx43 gap junctions or closed connexin hemichannels contributed to the mediation of permeability but this was not attributable to hemichannel release of secondary

messengers or prostaglandins. Further work is required to understand how Cx43 partakes in endothelial cell activation and induction of permeability.

A possible locus of involvement of Cx43 in endothelial permeability is the transcytosis process via caveolae. In the paracellular pathway, transportation of molecules is between adjacent cells and is closely regulated by tight junctions. Transcytosis is the transportation of macromolecules from one side of a cell to the other, involving invagination of plasma membrane, vesicle movement and fusion with the plasma membrane (Tuma and Hubbard, 2003). Caveolae are lipid-enriched vesicular, or 'flask-shaped', structures in the plasma membrane formed and maintained by cholesterol-binding caveolin-1 and caveolin-2 proteins (Rothberg et al., 1992). Caveolae and lipid rafts in the plasma membranes have been shown to be involved in many signal transduction processes including PDGF and MAPK signalling (Anderson, 1998; Li et al., 2005; Liu et al., 1997). Endothelial cells are rich in caveolae, which may occupy up to 50% of their luminal plasma membrane (Gratton et al., 2004). Transport of albumin has been demonstrated through capillary endothelium via the transcellular caveolar pathway (Ghitescu et al., 1986; Milici et al., 1987). Interestingly, lipid rafts contain connexins and hemichannels (Locke et al., 2005; Tillman and Cascio, 2003) and Cx43 co-localises and interacts directly with caveolin-1 within a raft (Schubert et al., 2002). The exact function of connexins in caveolae is unclear but the knockdown of Cx43 protein expression in the HUVECs may have led to a change in the albumin transcytosis pathway, limiting the histamine-induced increase in the overall FITC-BSA permeability.

Another possible role for Cx43 is mediating vascular permeability via the spread of Ca^{2+} during endothelial cell activation. Histamine can trigger a release of IP_3 from the plasma membrane, inducing an elevation in intracellular cytosolic free Ca^{2+} and activating endothelial cells to signal relaxation (Birch et al., 1994; Ehringer et al., 1996; Rotrosen and Gallin, 1986). Cx43 has been shown to mediate the spread of Ca^{2+} dependent pro-inflammatory responses in lung capillaries (Parthasarathi et al., 2006). The increase in cytosolic free Ca^{2+} concentration causes a rearrangement of the actin cytoskeleton and an increase in transendothelial albumin flux (Rotrosen and Gallin, 1986). Constraining the spread of Ca^{2+} via gap junctions during inflammation may limit the cytoskeleton-dependent albumin leakage through the endothelial cell monolayer. The increase in cytosolic free Ca^{2+} and the formation of a calmodulin complex can mediate vessel relaxation, but they can also induce P-selectin expression which is involved in the leukocyte transmigration process (Birch et al., 1992; Huang et al., 1993). Initial knockdown of Cx43 using asODN can limit the spread of Ca^{2+} between endothelial cells, leading to the reduced albumin permeability and decreased leukocyte recruitment observed at the later time points *in vivo* (Mori et al., 2006, Qiu et al., 2003).

The data from this pilot study strongly suggest a role of Cx43 in endothelial cell activation and vascular permeability. The time-dependent manner in which histamine elevates Cx43 expression, and the potential functions of Cx43 in Ca^{2+} mediation and transcytosis during inflammation, will be interesting areas to explore. Understanding these processes will allow us to further appreciate the involvement of connexins in the wound healing process.

7 GENERAL DISCUSSION

7.1 The relationship between connexins, wound healing and diabetes

Wound healing is a cascade of overlapping processes involving many cell types working together in order to repair the damaged tissue as swiftly as possible. Unfortunately, wound healing is often delayed in diabetes. This delay is caused by disease pathology and unbalanced chemokines in the wound microenvironment (Falanga, 2005; Franzen and Roberg, 1995; Goren et al.; Loots et al., 1998; Werner et al., 1994). Co-ordination between the different cell types is important to orchestrate the wound healing response. Using streptozotocin-induced diabetic rats, I have demonstrated in this thesis that the expression of gap junction proteins Cx26, Cx30 and Cx43 was abnormal in uninjured interfollicular skin. Cx43 protein expression was also atypical in the plantar skin in the diabetic rats. In diabetic wounds, the dynamic expression of Cx26 and Cx43 was also abnormal in the epidermis at the wound edge (Figure 7.1). In particular, instead of being downregulated as in normal wounds, Cx43 expression was significantly elevated in the 1-day diabetic wound. When the abnormal Cx43 upregulation was prevented by the application of pluronic gel containing Cx43-asODN, the quality of diabetic wound healing was greatly improved to control levels or better. In these treated wounds, blood vessels were less leaky, the number of neutrophils recruited was decreased and re-epithelialisation was accelerated. More collagen matrix was laid down in the granulation tissue and the maturation was improved as indicated by the reduction in the number of proliferating cells between days 5 and 10 after wounding. The role of Cx43 in the early inflammatory responses of endothelial cells was explored and although its function remains unknown, a role is definitely indicated in the vasculature during the inflammatory response.

The onset of diabetes had a marked effect on the level of connexin protein expression in the skin. Abnormal connexin protein expression in uninjured skin may have consequences for tissue homeostasis and trigger the abnormal expression in response to injury. The mechanism whereby diabetes alters the differential expression of connexin proteins in uninjured skin is at present unknown. Understanding how and at what level (transcription/translation/post-translation) hyperglycaemia affects Cx expression will help in understanding protein regulation and the restoration of homeostasis in skin. Recent studies have shown that hyperglycaemia affects connexin expression and gap junction function via different pathways both *in vivo* and *in vitro* (Kuroki et al., 1998; Li et al., 2003; Oku et al., 2001; Pitre et al., 2001; Sato et al., 2002). Aortic smooth muscle cells, cultured in hyperglycaemic conditions, showed a reduction in GJIC and a corresponding increase in the PKC phosphorylated form of Cx43 (Kuroki et al., 1998). However, Cx26 does not contain PKC post-translational modification sites and therefore could not be regulated this way. Alternatively, a protease dependent pathway has also been suggested to decrease GJIC in hyperglycaemic bovine retinal endothelial cells (Fernandes et al., 2004). Using RT-PCR, Sato et al (2002) noted a reduction in the Cx43 mRNA level in rat microvascular endothelial cells, and that no changes in expression were seen in Cx37 and Cx40. This would suggest that a more upstream control exists to regulate connexin expression in hyperglycaemia. Multiple mechanisms are likely to exist to regulate connexin expression and function in hyperglycaemic conditions. RT-PCR and Western blot analysis techniques would be useful to detect changes in the level of connexin mRNA and the phosphorylation status affected by hyperglycaemia. Such techniques could also be used to identify possible changes in connexin transcription factors such as SP-1 and SP-3.

The establishment of 3-dimensional epidermal cultures, such as those created by Kandyba et al. (2007) using murine keratinocytes, would allow more versatile experiments and closer studies of connexins in the epidermis under conditions such as hyperglycaemia, which causes an abnormal regulation of connexins and gap junctions. The use of cell culture will allow a closer examination of translational and post-translation regulatory mechanisms affecting connexins in hyperglycaemic conditions. Certainly, accurate measures of cell coupling in hyperglycaemia using dye microinjection or fluorescence recovery after photobleaching (FRAP) could be carried out. It may also be interesting to see whether it is possible to prevent the reduced expression of connexins in uninjured diabetic skin by bringing glucose concentration in culture back to normal levels.

7.2 The relationship of connexins to epidermal cell behaviour in wounds

Connexin expression in response to injury is dynamically regulated in the epidermis (Coutinho et al., 2003; Goliger and Paul, 1995; Wang et al., 2007). Cx43 in the wound edge keratinocytes is downregulated within 24 hours of injury and gradually increased with the advancement of wound closure (Coutinho et al., 2003; Goliger and Paul, 1995). The downregulation of Cx43 expression in the epidermal wound edge has been attributed to the temporal phosphorylation of the C-terminus for the creation of a leading edge compartment to synchronise migration (Richards et al., 2004). Recently the transcription factor Activator Protein-1 (AP-1) has also been implicated in regulating Cx43 expression during wound healing in human *ex vivo* skins (Neub et al.,

2007). AP-1 transcription factor subunits (Fos and Jun) were absent from the keratinocytes in the wound edge as early as 2-7 hours after wounding and gradually increased from 24 hours on. The biphasic (down- and upregulation) expression of AP-1 coincided with the normal dynamic expression of Cx43 expression after injury (Neub et al., 2007). However, *ex vivo* skin from leg ulcers (venous or diabetic) expressed AP-1 more intensely in the wound edge than the adjacent keratinocytes away from the wounds. The dynamic expression of Cx43 in normal wounds in the rats followed the same biphasic regulation of AP-1 in the human *ex vivo* wounds. The upregulation of Cx43 expression in diabetic wounds observed in this thesis corresponds to, and further complements, the data presented by Neub and colleagues (2007). Both post-translational (PKC) and transcriptional (AP-1) regulatory mechanisms can cause downregulation of Cx43 expression at the wound edge, but the implications of this will require further studies.

Downregulation of Cx43 expression at the wound edge, however, appears to be essential prior to the initiation of keratinocyte migration. In controls, diabetic wounds and diabetic wounds treated with Cx43-asODN have all begun, and have only begun, re-epithelialisation when Cx43 expression was absent in the wound edge. Contrary to the data in this thesis, Elias et al. (2007) demonstrated that Cx26 and Cx43 are required for neuronal stem cell migration to reach the cortical plate. In their study, Cx26 and Cx43 were shown to be involved in the stabilisation of the actin cytoskeleton during cell migration and Cx26 also mediated cell-cell adhesion. Interestingly, classical intercellular communication of gap junctions or Ca^{2+} mediation via porous hemichannels were not involved in the migration process (Elias et al., 2007). The interaction between connexins and cytoskeleton and actin binding proteins

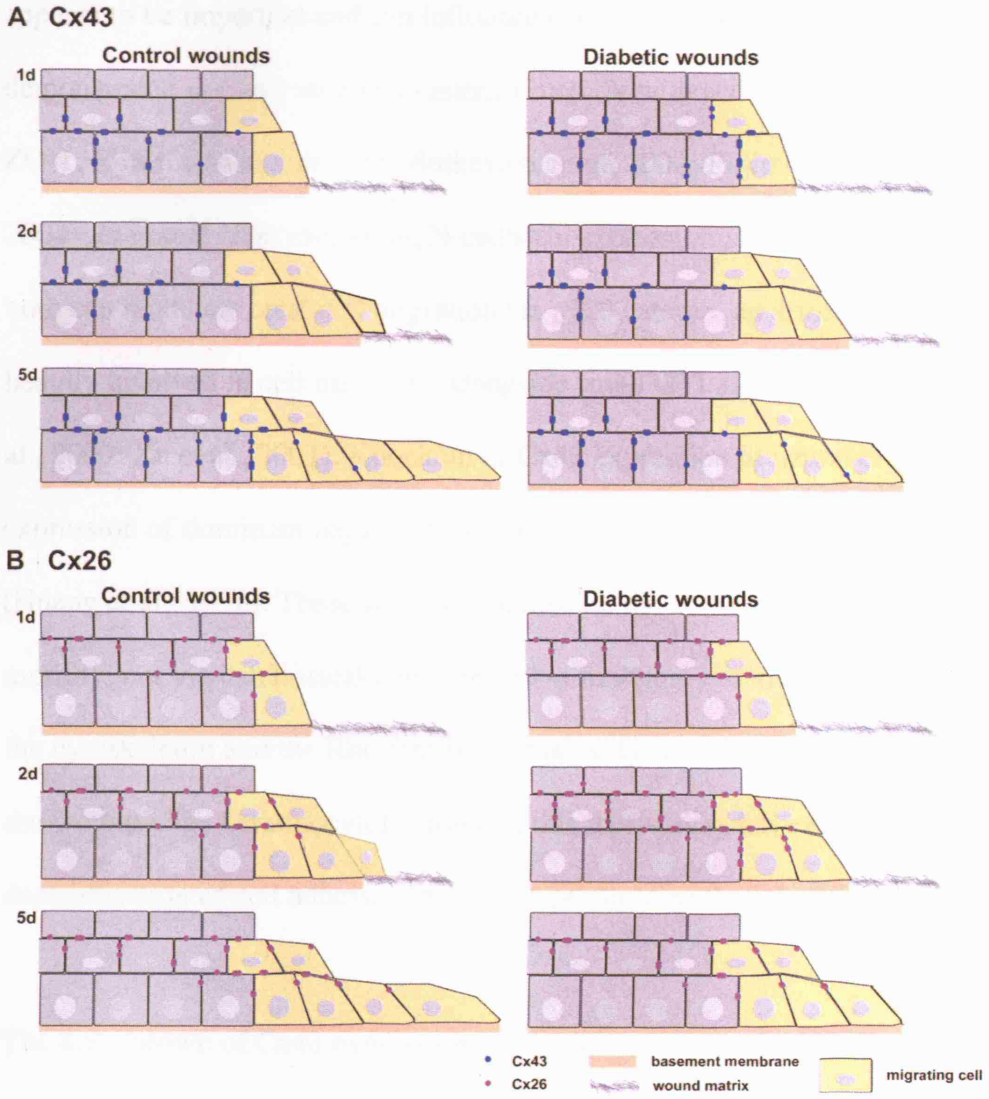

Figure 7.1 Dynamic Cx43 and Cx26 protein expression in the epidermis during control and diabetic wound healing. (A) Cx43 expression initially downregulates in the control 1-day wound edge keratinocytes. However, in diabetic wounds Cx43 expression is abnormally elevated. Cx43 expression gradually increases behind the migrating keratinocytes as re-epithelialisation progresses. (B) Cx26 protein expression is elevated at the epidermal edge in both control and diabetic wounds. In uninjured skin Cx26 expression is restricted to the spinous layer of epidermis but at the wound edge it is expressed in all layers of epidermis. However, Cx26 is significantly increased in the adjacent epidermis behind the edge of diabetic wounds.

appears to be important and can influence cell migration. Connexin43 has been demonstrated in many studies to interact directly with actin binding proteins such as ZO-1, E-cadherin and drebrin (Butkevich et al., 2004; Fujimoto et al., 1997; Giepmans, 2004). In neural crest migration, N-cadherin expression is co-localised with Cx43 and both can modulate crest cell migration via p120 catenin, an armadillo protein that is heavily involved in cell migration alongside small GTPases (Lo et al., 1999; Noren et al., 2000; Xu et al., 2001). Knockout of Cx43 expression in neural crest cells or expression of dominant negative Cx43 was associated with reduced cell migration (Huang et al., 1998). These studies demonstrate the active role of connexins in cell motility, not via its classical communicative function, but via its close association with the cytoskeleton and the Rho family of small GTPases. The downregulation of Cx43 in the wound-edge keratinocytes, shown in this thesis, may have encouraged the destabilisation of cell adhesion in order to promote epithelial migration.

The knockdown of Cx43 expression in keratinocytes in wounds increased cell migration, arguing against the promotional role of Cx43 seen during neural crest cell migration. The absence of Cx43 or functional connexin hemichannels has also been shown to improve wound closure of keratinocytes *in vitro* (Kandyba et al., 2007). Nevertheless, the exact mechanism of how Cx43 is involved in keratinocyte migration remains unclear. Keratinocytes at the wound edge undergoing migration need to change from hemidesmosome-based anchorage to a more dynamic adhesion. A possibility is that the decrease in the number of Cx43 plaques causes an alteration in the cell-cell and cell-matrix adhesion systems to promote migration (Meyer et al., 1992; Wei et al., 2005). Alternatively, the absence of Cx43 GJ plaques could form a specialised keratinocyte compartment at the wound edge that communicated

differently to the adjacent epidermis (Lampe et al., 2000; Martin, 1997). The formation of the front migratory compartment could be important to allow selective signalling to dedicate different properties to the compartments or zones (i. e. migration, proliferation) as observed in cochlea (Jagger and Forge, 2006; Sun et al., 2005). The selective gating of heteromeric Cx26/Cx30 gap junctions was shown using tracer dyes, where neurobiotin diffused through freely but not LY (Forge et al., 2003). The elevation of Cx26 and Cx30 expression in the epidermal wound edge can form a compartment that conducted differential signalling. Once again, the incorporation of *in vitro* 3-D models provides an advantage of the possibility of time-lapse recording to examine the motility of cells after injury and the details of connexin assembly and degradation alongside associated proteins. Understanding the purpose of dynamic Cx43 regulation after injury will provide answers to the role of Cx43 in keratinocytes in wound healing.

7.3 Interactions between connexins and other signalling systems in the skin

Keratinocytes in diabetic wounds respond to injury by increasing Cx43 protein expression at the wound edge. Lack of downregulation as in control wounds could be the result of a delay in Cx43 plaque removal/degradation and an increase in protein translation/transcription. Numerous cytokines found in the wound region are known to influence connexin expression. Degranulating platelets release high levels of growth factors such as PDGF and EGF that will in turn activate the subsequent multiple processes of wound healing. In diabetes, the release of cytokines and growth factors, including PDGF and EGF, is decreased, causing an abnormal wound

microenvironment (Beer et al., 1997; Bitar and Labbad, 1996; Shukla et al., 1998; Werner et al., 1994). In particular, a reduced level of PDGF could decrease the mediation of tyrosine kinase phosphorylation of Cx43 protein (Hossain et al., 1999). EGF can also induce Cx43 phosphorylation and plaque internalisation (Lau et al., 1992; Leithe and Rivedal, 2004; Ueki et al., 2001). A decrease in cytokine level in the diabetic wound microenvironment may perturb the initial downregulation of Cx43 expression. Diabetic-delayed wound healing was rescued to different degrees with various applications of growth factors (Bitar, 1997; Brown et al., 1994; Keswani et al., 2004; Obara et al., 2005). Studying the effect of growth factor application in wounds on Cx dynamic expression may shed more light on the interaction between growth factors and connexin. Further investigation in the connexin dynamic response in diabetic wounds of insulin treated animals would also provide clues to regulatory mechanisms in diabetic wound-healing, particularly compartmentalisation at the wound edge during migration.

7.4 The relationship of connexins to cytokine signalling

Application of Cx43-specific antisense oligodeoxynucleotides immediately after wounding had a profound effect on many aspects of the downstream wound healing events. The early inflammatory response, both in terms of leukocyte recruitment and cytokine content, was significantly reduced (Qiu et al., 2003; Mori et al., 2006). One of the most dramatic changes identified in the 2-day mouse wounds treated with Cx43-asODN was a 5-fold increase of TGF-β1 (Mori et al., 2006). Endogenous Cx43 has been shown to mediate TGF-β signalling via the release of Smad2/3 from microtubules

by competitive binding (Dai et al., 2007). The knockdown of endogenous Cx43 using shRNA was shown to abrogate TGF-β-induced Smad-mediated gene transcription (Dai et al., 2007). However, binding of Cx43 to β-tubulin induced an accumulation of Smad2/3 that activates targeted gene transcription. While this report does not explain the increase of TGF-β1 in Cx43-asODN treated wounds that we observed, it does demonstrate a close association of Cx43 with the TGF-β signalling pathway. During an immunological response, Cx43-expressing leukocytes and lymphocytes were shown to mediate immunoglobulin and cytokine secretion (Oviedo-Orta et al., 2001; Oviedo-Orta and Evans, 2004). Data exist to demonstrate the direct mediation of connexins in cytokine signalling in immunological cells and my data suggests that Cx43 can exert control over cytokine release in wounds after injury which in turn will shape the later wound-healing events (Mori et al., 2006; Figure 7.2).

An early alteration in the wound cytokine content will have a strong influence on the quality and speed of the subsequent wound repair processes. I, along with my colleagues and our collaborators have reported a decrease in chemokines CCL-2 and TNF-α and an increase in TGF-β1 in mouse wounds treated with Cx43-asODN (Mori et al., 2006). In the diabetic wounds, re-epithelialisation, granulation tissue maturation and collagen matrix laid down at the later time points were greatly improved even after the effect of asODNs had worn off. An interesting future direction would be inclusion of microarray analysis on Cx43-asODN treated wounds. Microarray analysis will not only identify the changes in gene expression responsible for the improvement in the wound healing process that we observed, but will also identify genes that are key for a successful and swift wound repair.

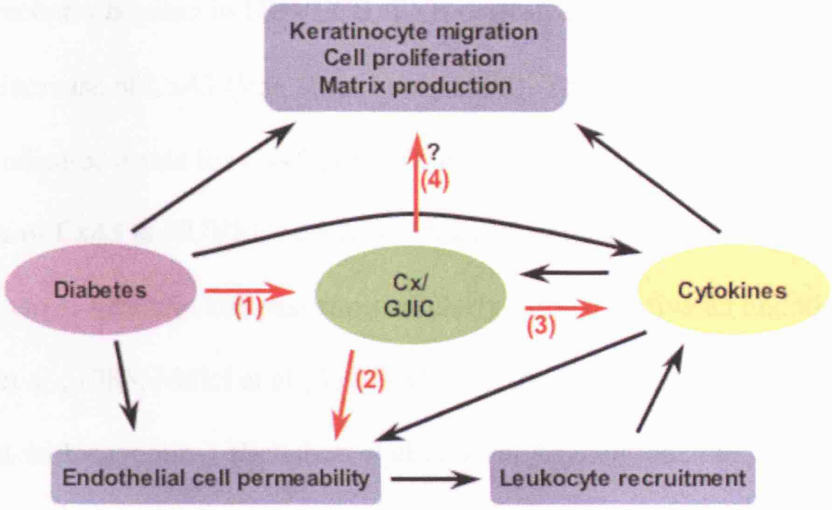

Figure 7.2 The relationships between diabetes, connexins and cytokines in the cutaneous wound healing process. Connexin and GJIC play a central part in the wound healing process. The black arrows indicate a direct effect of one element on another. The red arrows indicate the effects reported in this thesis. (1) Diabetes has a profound effect on connexin expression. (2) Connexin43 plays a role in endothelial permeability which subsequently affects leukocyte recruitment and release of cytokines in the wound. Cytokines have mitogenic and motogenic effect on wound healing processes such as keratinocyte migration, cell proliferation and matrix production. Diabetes is known to alter the level of cytokines in wounds and the wound healing processes. The effects of applying Cx43-specific asODN in wounds suggest (3) a direct regulatory role on wound cytokine release, and further regulatory roles in later wound repair processes, either (4) directly or (3) indirectly via cytokines.

7.5 The relationship of connexins to vascular permeability

The precise involvement of Cx43 in endothelial cell permeability remains an open question. The trend of increase in total Cx43 protein, although not significant, coincided with the increase of COX-2, an enzyme involved in inflammation, after

histamine receptor binding in HUVECS. TNF-α-treated HUVECs also showed time-dependent increase of Cx43 (Van Rijen et al., 1997). The *in vitro* leakiness assay using HUVECs indicated a role for Cx43 during histamine-induced permeability. The knockdown of Cx43 in HUVECs decreased histamine-induced permeability to albumin *in vitro*. Albumin can pass transcellularly through activated endothelial cells (Ghitescu et al., 1986; Milici et al., 1987). Cx43 protein has been shown to co-localise and interact with caveolin-1 (Schubert et al., 2002). As mentioned in the previous chapter discussion, Cx43 may be involved in albumin transcytosis via caveolin-containing lipid rafts. Alternatively, the spread of cytosolic free calcium via gap junctions could mediate the pro-inflammatory signal upon histamine binding. Binding of histamine triggers the release of IP_3 from the plasma membrane which in turn induces an elevation in intracellular cytosolic free Ca^{2+} to signal vessel relaxation (Birch et al., 1994; Ehringer et al., 1996; Rotrosen and Gallin, 1986). Cx43 gap junctions can mediate the spread of pro-inflammatory Ca^{2+} signals in lung capillaries (Parthasarathi et al., 2006). Limiting the spread of Ca^{2+} via Cx43 gap junctions using asODN may reduce histamine induced vessel relaxation. Investigation into the role of Cx43 in endothelial cell permeability in the future would help to explain the reduced vessel leakiness and the reduction in leukocyte recruitment observed in the *in vivo* wounds treated with Cx43-asODN.

7.6 Conclusion

Wound healing is a series of overlapping events involving many cell types working together in a coordinated manner. The diabetes-induced upregulation of Cx43 expression in the epidermis after injury may contribute to the delayed wound healing and is a potential target for therapeutic intervention. The data in this thesis has provided further evidence to add to our understanding of connexins in diabetic skin and the co-ordination of the wound healing process (Figure 7.2). Most importantly, the early participation of connexins during the wound inflammatory response can have a substantial impact on the quality and the speed of wound repair. The recognition that connexin participation in many biological processes can be multifaceted is particularly important. Classic gap-junctional intercellular communication, hemichannels and connexin interactions with the cytoskeleton can all mediate different responses after injury. The continuous development and creation of new experimental tools and models in the research field will promote further investigations to help us to better elucidate the fascinating properties and functions of connexins and gap junctions in complex biological processes.

BIBLIOGRAPHY

Abdullah, K. M., Luthra, G., Bilski, J. J., Abdullah, S. A., Reynolds, L. P., Redmer, D. A. and Grazul-Bilska, A. T. (1999). Cell-to-cell communication and expression of gap junctional proteins in human diabetic and nondiabetic skin fibroblasts: effects of basic fibroblast growth factor. *Endocrine* **10**, 35-41.

Ackert, C. L., Gittens, J. E., O'Brien, M. J., Eppig, J. J. and Kidder, G. M. (2001). Intercellular communication via connexin43 gap junctions is required for ovarian folliculogenesis in the mouse. *Dev Biol* **233**, 258-70.

Akarasereenont, P., Chotewuttakorn, S., Techatraisak, K. and Thaworn, A. (2001). The effects of COX-metabolites on cyclooxygenase-2 induction in LPS-treated endothelial cells. *J Med Assoc Thai* **84 Suppl 3**, S696-709.

Akarasereenont, P., Techatrisak, K., Chotewuttakorn, S. and Thaworn, A. (1999). The induction of cyclooxygenase-2 in IL-1beta-treated endothelial cells is inhibited by prostaglandin E2 through cAMP. *Mediators Inflamm* **8**, 287-94.

Anderson, R. G. (1998). The caveolae membrane system. *Annu Rev Biochem* **67**, 199-225.

Andriopoulou, P., Navarro, P., Zanetti, A., Lampugnani, M. G. and Dejana, E. (1999). Histamine induces tyrosine phosphorylation of endothelial cell-to-cell adherens junctions. *Arterioscler Thromb Vasc Biol* **19**, 2286-97.

Ashcroft, G. S., Yang, X., Glick, A. B., Weinstein, M., Letterio, J. L., Mizel, D. E., Anzano, M., Greenwell-Wild, T., Wahl, S. M., Deng, C. et al. (1999). Mice lacking Smad3 show accelerated wound healing and an impaired local inflammatory response. *Nat Cell Biol* **1**, 260-6.

Assoian, R. K., Komoriya, A., Meyers, C. A., Miller, D. M. and Sporn, M. B. (1983). Transforming growth factor-beta in human platelets. Identification of a major storage site, purification, and characterization. *J Biol Chem* **258**, 7155-60.

Aurrand-Lions, M., Johnson-Leger, C. and Imhof, B. A. (2002). The last molecular fortress in leukocyte trans-endothelial migration. *Nat Immunol* **3**, 116-8.

Barrandon, Y. and Green, H. (1987). Cell migration is essential for sustained growth of keratinocyte colonies: the roles of transforming growth factor-alpha and epidermal growth factor. *Cell* **50**, 1131-7.

Barrio, L. C., Suchyna, T., Bargiello, T., Xu, L. X., Roginski, R. S., Bennett, M. V. and Nicholson, B. J. (1991). Gap junctions formed by connexins 26 and 32 alone and in combination are differently affected by applied voltage. *Proc Natl Acad Sci U S A* **88**, 8410-4.

Beardslee, M. A., Laing, J. G., Beyer, E. C. and Saffitz, J. E. (1998). Rapid turnover of connexin43 in the adult rat heart. *Circ Res* **83**, 629-35.

Becker, D. L. and Mobbs, P. (1999). Connexin alpha1 and cell proliferation in the developing chick retina. *Exp Neurol* **156**, 326-32.

Becker, D. L., McGonnell, I., Makarenkova, H. P., Patel, K., Tickle, C., Lorimer, J. and Green, C. R. (1999). Roles for alpha 1 connexin in morphogenesis of chick embryos revealed using a novel antisense approach. *Dev Genet* **24**, 33-42.

Becker, D., Bonness, V. and Mobbs, P. (1998). Cell coupling in the retina: patterns and purpose. *Cell Biol Int* **22**, 781-92.

Beer, H. D., Longaker, M. T. and Werner, S. (1997). Reduced expression of PDGF and PDGF receptors during impaired wound healing. *J Invest Dermatol* **109**, 132-8.

Bennett, M. V., Barrio, L. C., Bargiello, T. A., Spray, D. C., Hertzberg, E. and Saez, J. C. (1991). Gap junctions: new tools, new answers, new questions. *Neuron* **6**, 305-20.

Bennett, M. V., Spira, M. E. and Spray, D. C. (1978). Permeability of gap junctions between embryonic cells of Fundulus: a reevaluation. *Dev Biol* **65**, 114-25.

Beny, J. L. and Connat, J. L. (1992). An electron-microscopic study of smooth muscle cell dye coupling in the pig coronary arteries. Role of gap junctions. *Circ Res* **70**, 49-55.

Bergoffen, J., Scherer, S. S., Wang, S., Scott, M. O., Bone, L. J., Paul, D. L., Chen, K., Lensch, M. W., Chance, P. F. and Fischbeck, K. H. (1993). Connexin mutations in X-linked Charcot-Marie-Tooth disease. *Science* **262**, 2039-42.

Betz, P., Nerlich, A., Wilske, J., Tubel, J., Penning, R. and Eisenmenger, W. (1993). Immunohistochemical localization of collagen types I and VI in human skin wounds. *Int J Legal Med* **106**, 31-4.

Beyer, E. C., Paul, D. L. and Goodenough, D. A. (1987). Connexin43: a protein from rat heart homologous to a gap junction protein from liver. *J Cell Biol* **105**, 2621-9.

Bhora, F. Y., Dunkin, B. J., Batzri, S., Aly, H. M., Bass, B. L., Sidawy, A. N. and Harmon, J. W. (1995). Effect of growth factors on cell proliferation and epithelialization in human skin. *J Surg Res* **59**, 236-44.

Birch, K. A., Ewenstein, B. M., Golan, D. E. and Pober, J. S. (1994). Prolonged peak elevations in cytoplasmic free calcium ions, derived from intracellular stores, correlate with the extent of thrombin-stimulated exocytosis in single human umbilical vein endothelial cells. *J Cell Physiol* **160**, 545-54.

Birch, K. A., Pober, J. S., Zavoico, G. B., Means, A. R. and Ewenstein, B. M. (1992). Calcium/calmodulin transduces thrombin-stimulated secretion: studies in intact

and minimally permeabilized human umbilical vein endothelial cells. *J Cell Biol* **118**, 1501-10.

Birkedal-Hansen, H. (1995). Proteolytic remodeling of extracellular matrix. *Curr Opin Cell Biol* **7**, 728-35.

Bitar, M. S. (1997). Insulin-like growth factor-1 reverses diabetes-induced wound healing impairment in rats. *Horm Metab Res* **29**, 383-6.

Bitar, M. S. (1998). Glucocorticoid dynamics and impaired wound healing in diabetes mellitus. *Am J Pathol* **152**, 547-54.

Bitar, M. S. and Labbad, Z. N. (1996). Transforming growth factor-beta and insulin-like growth factor-I in relation to diabetes-induced impairment of wound healing. *J Surg Res* **61**, 113-9.

Boitano, S. and Evans, W. H. (2000). Connexin mimetic peptides reversibly inhibit Ca(2+) signaling through gap junctions in airway cells. *Am J Physiol Lung Cell Mol Physiol* **279**, L623-30.

Boitano, S., Dirksen, E. R. and Sanderson, M. J. (1992). Intercellular propagation of calcium waves mediated by inositol trisphosphate. *Science* **258**, 292-5.

Braet, K., Vandamme, W., Martin, P. E., Evans, W. H. and Leybaert, L. (2003). Photoliberating inositol-1,4,5-trisphosphate triggers ATP release that is blocked by the connexin mimetic peptide gap 26. *Cell Calcium* **33**, 37-48.

Brandner, J. M., Houdek, P., Husing, B., Kaiser, C. and Moll, I. (2004). Connexins 26, 30, and 43: differences among spontaneous, chronic, and accelerated human wound healing. *J Invest Dermatol* **122**, 1310-20.

Brandner, J. M., McIntyre, M., Kief, S., Wladykowski, E. and Moll, I. (2003). Expression and localization of tight junction-associated proteins in human hair follicles. *Arch Dermatol Res* **295**, 211-21.

Brandner, J. M., Zacheja, S., Houdek, P., Moll, I. and Lobmann, R. (2007). Expression of matrix metalloproteinases, cytokines and connexins in diabetic and non-diabetic human keratinocytes before and after transplantation into an ex-vivo wound healing model. *Diabetes Care*.

Brissette, J. L., Kumar, N. M., Gilula, N. B., Hall, J. E. and Dotto, G. P. (1994). Switch in gap junction protein expression is associated with selective changes in junctional permeability during keratinocyte differentiation. *Proc Natl Acad Sci U S A* **91**, 6453-7.

Britz-Cunningham, S. H., Shah, M. M., Zuppan, C. W. and Fletcher, W. H. (1995). Mutations of the Connexin43 gap-junction gene in patients with heart malformations and defects of laterality. *N Engl J Med* **332**, 1323-9.

Brown, L. F., Yeo, K. T., Berse, B., Yeo, T. K., Senger, D. R., Dvorak, H. F. and van de Water, L. (1992). Expression of vascular permeability factor (vascular endothelial growth factor) by epidermal keratinocytes during wound healing. *J Exp Med* **176**, 1375-9.

Brown, R. L., Breeden, M. P. and Greenhalgh, D. G. (1994). PDGF and TGF-alpha act synergistically to improve wound healing in the genetically diabetic mouse. *J Surg Res* **56**, 562-70.

Bruzzone, R., Haefliger, J. A., Gimlich, R. L. and Paul, D. L. (1993). Connexin40, a component of gap junctions in vascular endothelium, is restricted in its ability to interact with other connexins. *Mol Biol Cell* **4**, 7-20.

Bruzzone, R., White, T. W. and Paul, D. L. (1994). Expression of chimeric connexins reveals new properties of the formation and gating behavior of gap junction channels. *J Cell Sci* **107 (Pt 4)**, 955-67.

Bruzzone, R., White, T. W. and Paul, D. L. (1996). Connections with connexins: the molecular basis of direct intercellular signaling. *Eur J Biochem* **238**, 1-27.

Buetow, B. S., Crosby, J. R., Kaminski, W. E., Ramachandran, R. K., Lindahl, P., Martin, P., Betsholtz, C., Seifert, R. A., Raines, E. W. and Bowen-Pope, D. F. (2001). Platelet-derived growth factor B-chain of hematopoietic origin is not necessary for granulation tissue formation and its absence enhances vascularization. *Am J Pathol* **159**, 1869-76.

Butkevich, E., Hulsmann, S., Wenzel, D., Shirao, T., Duden, R. and Majoul, I. (2004). Drebrin is a novel connexin-43 binding partner that links gap junctions to the submembrane cytoskeleton. *Curr Biol* **14**, 650-8.

Butterweck, A., Elfgang, C., Willecke, K. and Traub, O. (1994). Differential expression of the gap junction proteins connexin45, -43, -40, -31, and -26 in mouse skin. *Eur J Cell Biol* **65**, 152-63.

Cao, F., Eckert, R., Elfgang, C., Nitsche, J. M., Snyder, S. A., DF, H. u., Willecke, K. and Nicholson, B. J. (1998). A quantitative analysis of connexin-specific permeability differences of gap junctions expressed in HeLa transfectants and Xenopus oocytes. *J Cell Sci* **111 (Pt 1)**, 31-43.

Cao, Z., Wu, H. K., Bruce, A., Wollenberg, K. and Panjwani, N. (2002). Detection of differentially expressed genes in healing mouse corneas, using cDNA microarrays. *Invest Ophthalmol Vis Sci* **43**, 2897-904.

Carter, T. D., Chen, X. Y., Carlile, G., Kalapothakis, E., Ogden, D. and Evans, W. H. (1996). Porcine aortic endothelial gap junctions: identification and permeation by caged InsP3. *J Cell Sci* **109 (Pt 7)**, 1765-73.

Caspar, D. L., Goodenough, D. A., Makowski, L. and Phillips, W. C. (1977). Gap junction structures. I. Correlated electron microscopy and x-ray diffraction. *J Cell Biol* **74**, 605-28.

Chang, A. S., Dale, A. N. and Moley, K. H. (2005). Maternal diabetes adversely affects preovulatory oocyte maturation, development, and granulosa cell apoptosis. *Endocrinology* **146**, 2445-53.

Chanson, M., Roy, C. and Spray, D. C. (1994). Voltage-dependent gap junctional conductance in hepatopancreatic cells of Procambarus clarkii. *Am J Physiol* **266**, C569-77.

Chaytor, A. T., Evans, W. H. and Griffith, T. M. (1997). Peptides homologous to extracellular loop motifs of connexin 43 reversibly abolish rhythmic contractile activity in rabbit arteries. *J Physiol* **503 (Pt 1)**, 99-110.

Chaytor, A. T., Evans, W. H. and Griffith, T. M. (1998). Central role of heterocellular gap junctional communication in endothelium-dependent relaxations of rabbit arteries. *J Physiol* **508 (Pt 2)**, 561-73.

Cherian, P. P., Siller-Jackson, A. J., Gu, S., Wang, X., Bonewald, L. F., Sprague, E. and Jiang, J. X. (2005). Mechanical strain opens connexin 43 hemichannels in osteocytes: a novel mechanism for the release of prostaglandin. *Mol Biol Cell* **16**, 3100-6.

Christ, G. J., Spray, D. C., el-Sabban, M., Moore, L. K. and Brink, P. R. (1996). Gap junctions in vascular tissues. Evaluating the role of intercellular communication in the modulation of vasomotor tone. *Circ Res* **79**, 631-46.

Clore, J. N., Cohen, I. K. and Diegelmann, R. F. (1979). Quantitation of collagen types I and III during wound healing in rat skin. *Proc Soc Exp Biol Med* **161**, 337-40.

Contreras, J. E., Saez, J. C., Bukauskas, F. F. and Bennett, M. V. (2003). Functioning of cx43 hemichannels demonstrated by single channel properties. *Cell Commun Adhes* **10**, 245-9.

Corvalan, L. A., Araya, R., Branes, M. C., Saez, P. J., Kalergis, A. M., Tobar, J. A., Theis, M., Willecke, K. and Saez, J. C. (2007). Injury of skeletal muscle and specific cytokines induce the expression of gap junction channels in mouse dendritic cells. *J Cell Physiol* **211**, 649-60.

Coutinho, P., Qiu, C., Frank, S., Tamber, K. and Becker, D. (2003). Dynamic changes in connexin expression correlate with key events in the wound healing process. *Cell Biol Int* **27**, 525-41.

Coutinho, P., Qiu, C., Frank, S., Wang, C. M., Brown, T., Green, C. R. and Becker, D. L. (2005). Limiting burn extension by transient inhibition of Connexin43 expression at the site of injury. *Br J Plast Surg* **58**, 658-67.

Cronin, M., Anderson, P. N., Green, C. R. and Becker, D. L. (2006). Antisense delivery and protein knockdown within the intact central nervous system. *Front Biosci* **11**, 2967-75.

Dahl, G. (1996). Where are the gates in gap junction channels? *Clin Exp Pharmacol Physiol* **23**, 1047-52.

Dahl, G. and Isenberg, G. (1980). Decoupling of heart muscle cells: correlation with increased cytoplasmic calcium activity and with changes of nexus ultrastructure. *J Membr Biol* **53**, 63-75.

Dahl, G., Nonner, W. and Werner, R. (1994). Attempts to define functional domains of gap junction proteins with synthetic peptides. *Biophys J* **67**, 1816-22.

Dahl, G., Werner, R., Levine, E. and Rabadan-Diehl, C. (1992). Mutational analysis of gap junction formation. *Biophys J* **62**, 172-80; discussion 180-2.

Dai, P., Nakagami, T., Tanaka, H., Hitomi, T. and Takamatsu, T. (2007). Cx43 mediates TGF-beta signaling through competitive Smads binding to microtubules. *Mol Biol Cell* **18**, 2264-73.

Darrow, B. J., Laing, J. G., Lampe, P. D., Saffitz, J. E. and Beyer, E. C. (1995). Expression of multiple connexins in cultured neonatal rat ventricular myocytes. *Circ Res* **76**, 381-7.

De Maio, A., Vega, V. L. and Contreras, J. E. (2002). Gap junctions, homeostasis, and injury. *J Cell Physiol* **191**, 269-82.

De Vuyst, E., Decrock, E., Cabooter, L., Dubyak, G. R., Naus, C. C., Evans, W. H. and Leybaert, L. (2006). Intracellular calcium changes trigger connexin 32 hemichannel opening. *Embo J* **25**, 34-44.

Dejana, E. (2006). The transcellular railway: insights into leukocyte diapedesis. *Nat Cell Biol* **8**, 105-7.

Dermietzel, R., Meier, C., Bukauskas, F. and Spray, D. C. (2003). Following tracks of hemichannels. *Cell Commun Adhes* **10**, 335-40.

Desmouliere, A., Redard, M., Darby, I. and Gabbiani, G. (1995). Apoptosis mediates the decrease in cellularity during the transition between granulation tissue and scar. *Am J Pathol* **146**, 56-66.

Devalaraja, R. M., Nanney, L. B., Du, J., Qian, Q., Yu, Y., Devalaraja, M. N. and Richmond, A. (2000). Delayed wound healing in CXCR2 knockout mice. *J Invest Dermatol* **115**, 234-44.

Dewey, M. M. and Barr, L. (1962). Intercellular Connection between Smooth Muscle Cells: the Nexus. *Science* **137**, 670-672.

Dewey, M. M. and Barr, L. (1964). A Study Of The Structure And Distribution Of The Nexus. *J Cell Biol* **23**, 553-85.

Di, W. L., Rugg, E. L., Leigh, I. M. and Kelsell, D. P. (2001). Multiple epidermal connexins are expressed in different keratinocyte subpopulations including connexin 31. *J Invest Dermatol* **117**, 958-64.

Diegelmann, R. F., Cohen, I. K. and McCoy, B. J. (1979). Growth kinetics and collagen synthesis of normal skin, normal scar and keloid fibroblasts in vitro. *J Cell Physiol* **98**, 341-6.

Dinh, T. L. and Veves, A. (2005). A review of the mechanisms implicated in the pathogenesis of the diabetic foot. *Int J Low Extrem Wounds* **4**, 154-9.

Dipietro, L. A., Reintjes, M. G., Low, Q. E., Levi, B. and Gamelli, R. L. (2001). Modulation of macrophage recruitment into wounds by monocyte chemoattractant protein-1. *Wound Repair Regen* **9**, 28-33.

Djalilian, A. R., McGaughey, D., Patel, S., Seo, E. Y., Yang, C., Cheng, J., Tomic, M., Sinha, S., Ishida-Yamamoto, A. and Segre, J. A. (2006). Connexin 26 regulates epidermal barrier and wound remodeling and promotes psoriasiform response. *J Clin Invest* **116**, 1243-53.

Dovi, J. V., He, L. K. and DiPietro, L. A. (2003). Accelerated wound closure in neutrophil-depleted mice. *J Leukoc Biol* **73**, 448-55.

Dovi, J. V., Szpaderska, A. M. and DiPietro, L. A. (2004). Neutrophil function in the healing wound: adding insult to injury? *Thromb Haemost* **92**, 275-80.

Dupont, E., el Aoumari, A., Briand, J. P., Fromaget, C. and Gros, D. (1989). Cross-linking of cardiac gap junction connexons by thiol/disulfide exchanges. *J Membr Biol* **108**, 247-52.

Efron, J. E., Frankel, H. L., Lazarou, S. A., Wasserkrug, H. L. and Barbul, A. (1990). Wound healing and T-lymphocytes. *J Surg Res* **48**, 460-3.

Egan, K. and FitzGerald, G. A. (2006). Eicosanoids and the vascular endothelium. *Handb Exp Pharmacol*, 189-211.

Ehringer, W. D., Edwards, M. J. and Miller, F. N. (1996). Mechanisms of alpha-thrombin, histamine, and bradykinin induced endothelial permeability. *J Cell Physiol* **167**, 562-9.

Ehrlich, H. P. and Diez, T. (2003). Role for gap junctional intercellular communications in wound repair. *Wound Repair Regen* **11**, 481-9.

Ek, J. F., Delmar, M., Perzova, R. and Taffet, S. M. (1994). Role of histidine 95 on pH gating of the cardiac gap junction protein connexin43. *Circ Res* **74**, 1058-64.

Elfgang, C., Eckert, R., Lichtenberg-Frate, H., Butterweck, A., Traub, O., Klein, R. A., Hulser, D. F. and Willecke, K. (1995). Specific permeability and selective formation of gap junction channels in connexin-transfected HeLa cells. *J Cell Biol* **129**, 805-17.

Elias, L. A., Wang, D. D. and Kriegstein, A. R. (2007). Gap junction adhesion is necessary for radial migration in the neocortex. *Nature* **448**, 901-7.

Elias, P. M., Nau, P., Hanley, K., Cullander, C., Crumrine, D., Bench, G., Sideras-Haddad, E., Mauro, T., Williams, M. L. and Feingold, K. R. (1998). Formation of the epidermal calcium gradient coincides with key milestones of barrier ontogenesis in the rodent. *J Invest Dermatol* **110**, 399-404.

Eligini, S., Stella Barbieri, S., Cavalca, V., Camera, M., Brambilla, M., De Franceschi, M., Tremoli, E. and Colli, S. (2005). Diversity and similarity in signaling events leading to rapid Cox-2 induction by tumor necrosis factor-alpha and phorbol ester in human endothelial cells. *Cardiovasc Res* **65**, 683-93.

Eugenin, E. A., Branes, M. C., Berman, J. W. and Saez, J. C. (2003). TNF-alpha plus IFN-gamma induce connexin43 expression and formation of gap junctions between human monocytes/macrophages that enhance physiological responses. *J Immunol* **170**, 1320-8.

Eugenin, E. A., Osiecki, K., Lopez, L., Goldstein, H., Calderon, T. M. and Berman, J. W. (2006). CCL2/monocyte chemoattractant protein-1 mediates enhanced transmigration of human immunodeficiency virus (HIV)-infected leukocytes across the blood-brain barrier: a potential mechanism of HIV-CNS invasion and NeuroAIDS. *J Neurosci* **26**, 1098-106.

Evans, W. H. (1994). Assembly of gap junction intercellular communication channels. *Biochem Soc Trans* **22**, 788-92.

Evans, W. H., Ahmad, S., Diez, J., George, C. H., Kendall, J. M. and Martin, P. E. (1999). Trafficking pathways leading to the formation of gap junctions. *Novartis Found Symp* **219**, 44-54; discussion 54-9.

Falanga, V. (2000). Growth factors, The food in diabetes. 3rd Edition, UK: John Wiley & Sons.

Falanga, V. (2005). Wound healing and its impairment in the diabetic foot. *Lancet* **366**, 1736-43.

Falk, M. M., Buehler, L. K., Kumar, N. M. and Gilula, N. B. (1997). Cell-free synthesis and assembly of connexins into functional gap junction membrane channels. *Embo J* **16**, 2703-16.

Fernandes, R., Girao, H. and Pereira, P. (2004). High glucose down-regulates intercellular communication in retinal endothelial cells by enhancing degradation of connexin 43 by a proteasome-dependent mechanism. *J Biol Chem* **279**, 27219-24.

Figueroa, X. F., Isakson, B. E. and Duling, B. R. (2004). Connexins: gaps in our knowledge of vascular function. *Physiology (Bethesda)* **19**, 277-84.

Filson, A. J., Azarnia, R., Beyer, E. C., Loewenstein, W. R. and Brugge, J. S. (1990). Tyrosine phosphorylation of a gap junction protein correlates with inhibition of cell-to-cell communication. *Cell Growth Differ* **1**, 661-8.

Fishel, R. S., Barbul, A., Beschorner, W. E., Wasserkrug, H. L. and Efron, G. (1987). Lymphocyte participation in wound healing. Morphologic assessment using monoclonal antibodies. *Ann Surg* **206**, 25-9.

Fitzgerald, D. J., Fusenig, N. E., Boukamp, P., Piccoli, C., Mesnil, M. and Yamasaki, H. (1994). Expression and function of connexin in normal and transformed human keratinocytes in culture. *Carcinogenesis* **15**, 1859-65.

Flagg-Newton, J., Simpson, I. and Loewenstein, W. R. (1979). Permeability of the cell-to-cell membrane channels in mammalian cell juncton. *Science* **205**, 404-7.

Forge, A., Marziano, N. K., Casalotti, S. O., Becker, D. L., Jagger, D. (2003). The inner ear contains heteromeric channels composed of Cx26 and Cx30 and deafness-related mutations in Cx26 have a dominant negative effect on Cx30. *Cell Commun Adhes.* **10**, 341-6

Fortin, M. E., Pelletier, R. M., Meilleur, M. A. and Vitale, M. L. (2006). Modulation of GJA1 turnover and intercellular communication by proinflammatory cytokines in the anterior pituitary folliculostellate cell line TtT/GF. *Biol Reprod* **74**, 2-12.

Frank, S., Hubner, G., Breier, G., Longaker, M. T., Greenhalgh, D. G. and Werner, S. (1995). Regulation of vascular endothelial growth factor expression in cultured keratinocytes. Implications for normal and impaired wound healing. *J Biol Chem* **270**, 12607-13.

Franzen, L. E. and Roberg, K. (1995). Impaired connective tissue repair in streptozotocin-induced diabetes shows ultrastructural signs of impaired contraction. *J Surg Res* **58**, 407-14.

Fujimoto, K., Nagafuchi, A., Tsukita, S., Kuraoka, A., Ohokuma, A. and Shibata, Y. (1997). Dynamics of connexins, E-cadherin and alpha-catenin on cell membranes during gap junction formation. *J Cell Sci* **110 (Pt 3)**, 311-22.

Furshpan, E. J. (1964). "Electrical Transmission" At An Excitatory Synapse In A Vertebrate Brain. *Science* **144**, 878-80.

Furshpan, E. J. and Potter, D. D. (1959). Transmission at the giant motor synapses of the crayfish. *J Physiol* **145**, 289-325.

Gabriels, J. E. and Paul, D. L. (1998). Connexin43 is highly localized to sites of disturbed flow in rat aortic endothelium but connexin37 and connexin40 are more uniformly distributed. *Circ Res* **83**, 636-43.

Gaietta, G., Deerinck, T. J., Adams, S. R., Bouwer, J., Tour, O., Laird, D. W., Sosinsky, G. E., Tsien, R. Y. and Ellisman, M. H. (2002). Multicolor and electron microscopic imaging of connexin trafficking. *Science* **296**, 503-7.

Gallucci, R. M., Simeonova, P. P., Matheson, J. M., Kommineni, C., Guriel, J. L., Sugawara, T. and Luster, M. I. (2000). Impaired cutaneous wound healing in interleukin-6-deficient and immunosuppressed mice. *Faseb J* **14**, 2525-31.

Garlick, J. A. and Taichman, L. B. (1994). Fate of human keratinocytes during reepithelialization in an organotypic culture model. *Lab Invest* **70**, 916-24.

George, C. H., Kendall, J. M. and Evans, W. H. (1999). Intracellular trafficking pathways in the assembly of connexins into gap junctions. *J Biol Chem* **274**, 8678-85.

Ghazizadeh, M., Tosa, M., Shimizu, H., Hyakusoku, H. and Kawanami, O. (2007). Functional implications of the IL-6 signaling pathway in keloid pathogenesis. *J Invest Dermatol* **127**, 98-105.

Ghitescu, L., Fixman, A., Simionescu, M. and Simionescu, N. (1986). Specific binding sites for albumin restricted to plasmalemmal vesicles of continuous capillary endothelium: receptor-mediated transcytosis. *J Cell Biol* **102**, 1304-11.

Gibson, D. F., Bikle, D. D., Harris, J. and Goldberg, G. S. (1997). The expression of the gap junctional protein Cx43 is restricted to proliferating and non differentiated normal and transformed keratinocytes. *Exp Dermatol* **6**, 167-74.

Giepmans, B. N. (2004). Gap junctions and connexin-interacting proteins. *Cardiovasc Res* **62**, 233-45.

Goldberg, G. S., Valiunas, V. and Brink, P. R. (2004). Selective permeability of gap junction channels. *Biochim Biophys Acta* **1662**, 96-101.

Goliger, J. A. and Paul, D. L. (1995). Wounding alters epidermal connexin expression and gap junction-mediated intercellular communication. *Mol Biol Cell* **6**, 1491-501.

Gomaraschi, M., Basilico, N., Sisto, F., Taramelli, D., Eligini, S., Colli, S., Sirtori, C. R., Franceschini, G. and Calabresi, L. (2005). High-density lipoproteins attenuate interleukin-6 production in endothelial cells exposed to pro-inflammatory stimuli. *Biochim Biophys Acta* **1736**, 136-43.

Gomes, P., Srinivas, S. P., Van Driessche, W., Vereecke, J. and Himpens, B. (2005). ATP release through connexin hemichannels in corneal endothelial cells. *Invest Ophthalmol Vis Sci* **46**, 1208-18.

Goodenough, D. A. and Paul, D. L. (2003). Beyond the gap: functions of unpaired connexon channels. *Nat Rev Mol Cell Biol* **4**, 285-94.

Goodenough, D. A. and Revel, J. P. (1970). A fine structural analysis of intercellular junctions in the mouse liver. *J Cell Biol* **45**, 272-90.

Goodson, W. H., 3rd and Hunt, T. K. (1977). Studies of wound healing in experimental diabetes mellitus. *J Surg Res* **22**, 221-7.

Goren, I., Muller, E., Pfeilschifter, J. and Frank, S. (2006). Severely impaired insulin signaling in chronic wounds of diabetic ob/ob mice: a potential role of tumor necrosis factor-alpha. *Am J Pathol* **168**, 765-77.

Grainger, D. J., Mosedale, D. E., Metcalfe, J. C., Weissberg, P. L. and Kemp, P. R. (1995). Active and acid-activatable TGF-beta in human sera, platelets and plasma. *Clin Chim Acta* **235**, 11-31.

Gratton, J. P., Bernatchez, P. and Sessa, W. C. (2004). Caveolae and caveolins in the cardiovascular system. *Circ Res* **94**, 1408-17.

Greenhalgh, D. G., Sprugel, K. H., Murray, M. J. and Ross, R. (1990). PDGF and FGF stimulate wound healing in the genetically diabetic mouse. *Am J Pathol* **136**, 1235-46.

Greiling, D. and Clark, R. A. (1997). Fibronectin provides a conduit for fibroblast transmigration from collagenous stroma into fibrin clot provisional matrix. *J Cell Sci* **110 (Pt 7)**, 861-70.

Grellner, W., Georg, T. and Wilske, J. (2000). Quantitative analysis of proinflammatory cytokines (IL-1beta, IL-6, TNF-alpha) in human skin wounds. *Forensic Sci Int* **113**, 251-64.

Grinnell, F. (1994). Fibroblasts, myofibroblasts, and wound contraction. *J Cell Biol* **124**, 401-4.

Groschner, K., Graier, W. F. and Kukovetz, W. R. (1994). Histamine induces K+, Ca2+, and Cl- currents in human vascular endothelial cells. Role of ionic currents in stimulation of nitric oxide biosynthesis. *Circ Res* **75**, 304-14.

Grose, R. and Werner, S. (2003). Wound healing studies in transgenic and knockout mice. A review. *Methods Mol Med* **78**, 191-216.

Guan, X. and Ruch, R. J. (1996). Gap junction endocytosis and lysosomal degradation of connexin43-P2 in WB-F344 rat liver epithelial cells treated with DDT and lindane. *Carcinogenesis* **17**, 1791-8.

Guan, X., Wilson, S., Schlender, K. K. and Ruch, R. J. (1996). Gap-junction disassembly and connexin 43 dephosphorylation induced by 18 beta-glycyrrhetinic acid. *Mol Carcinog* **16**, 157-64.

Guerrero, P. A., Schuessler, R. B., Davis, L. M., Beyer, E. C., Johnson, C. M., Yamada, K. A. and Saffitz, J. E. (1997). Slow ventricular conduction in mice heterozygous for a connexin43 null mutation. *J Clin Invest* **99**, 1991-8.

Guo, L., Degenstein, L. and Fuchs, E. (1996). Keratinocyte growth factor is required for hair development but not for wound healing. *Genes Dev* **10**, 165-75.

Haefliger, J. A., Bruzzone, R., Jenkins, N. A., Gilbert, D. J., Copeland, N. G. and Paul, D. L. (1992). Four novel members of the connexin family of gap junction proteins. Molecular cloning, expression, and chromosome mapping. *J Biol Chem* **267**, 2057-64.

Han, Y. P., Tuan, T. L., Hughes, M., Wu, H. and Garner, W. L. (2001). Transforming growth factor-beta - and tumor necrosis factor-alpha -mediated induction and proteolytic activation of MMP-9 in human skin. *J Biol Chem* **276**, 22341-50.

Harks, E. G., de Roos, A. D., Peters, P. H., de Haan, L. H., Brouwer, A., Ypey, D. L., van Zoelen, E. J. and Theuvenet, A. P. (2001). Fenamates: a novel class of reversible gap junction blockers. *J Pharmacol Exp Ther* **298**, 1033-41.

Harris, A. L. (2001). Emerging issues of connexin channels: biophysics fills the gap. *Q Rev Biophys* **34**, 325-472.

Harris, I. R., Yee, K. C., Walters, C. E., Cunliffe, W. J., Kearney, J. N., Wood, E. J. and Ingham, E. (1995). Cytokine and protease levels in healing and non-healing chronic venous leg ulcers. *Exp Dermatol* **4**, 342-9.

He, D. S., Jiang, J. X., Taffet, S. M. and Burt, J. M. (1999). Formation of heteromeric gap junction channels by connexins 40 and 43 in vascular smooth muscle cells. *Proc Natl Acad Sci U S A* **96**, 6495-500.

Heldin, C. H. and Westermark, B. (1999). Mechanism of action and in vivo role of platelet-derived growth factor. *Physiol Rev* **79**, 1283-316.

Hentula, M., Peltonen, J. and Peltonen, S. (2001). Expression profiles of cell-cell and cell-matrix junction proteins in developing human epidermis. *Arch Dermatol Res* **293**, 259-67.

Heynkes, R., Kozjek, G., Traub, O. and Willecke, K. (1986). Identification of a rat liver cDNA and mRNA coding for the 28 kDa gap junction protein. *FEBS Lett* **205**, 56-60.

Hill, S. J. (1992). Multiple histamine receptors: properties and functional characteristics. *Biochem Soc Trans* **20**, 122-5.

Hills, C. E., Bland, R., Wheelans, D. C., Bennett, J., Ronco, P. M. and Squires, P. E. (2006). Glucose-evoked alterations in connexin43-mediated cell-to-cell communication in human collecting duct: a possible role in diabetic nephropathy. *Am J Physiol Renal Physiol* **291**, F1045-51.

Holder, J. W., Elmore, E. and Barrett, J. C. (1993). Gap junction function and cancer. *Cancer Res* **53**, 3475-85.

Hossain, M. Z. and Boynton, A. L. (2000). Regulation of Cx43 gap junctions: the gatekeeper and the password. *Sci STKE* **2000**, PE1.

Hossain, M. Z., Ao, P. and Boynton, A. L. (1998). Platelet-derived growth factor-induced disruption of gap junctional communication and phosphorylation of connexin43 involves protein kinase C and mitogen-activated protein kinase. *J Cell Physiol* **176**, 332-41.

Hossain, M. Z., Jagdale, A. B., Ao, P., Kazlauskas, A. and Boynton, A. L. (1999). Disruption of gap junctional communication by the platelet-derived growth factor is mediated via multiple signaling pathways. *J Biol Chem* **274**, 10489-96.

Howarth, F. C., Nowotny, N., Zilahi, E., El Haj, M. A. and Lei, M. (2007). Altered expression of gap junction connexin proteins may partly underlie heart rhythm disturbances in the streptozotocin-induced diabetic rat heart. *Mol Cell Biochem* **305**, 145-51.

Huang, A. J., Manning, J. E., Bandak, T. M., Ratau, M. C., Hanser, K. R. and Silverstein, S. C. (1993). Endothelial cell cytosolic free calcium regulates neutrophil migration across monolayers of endothelial cells. *J Cell Biol* **120**, 1371-80.

Huang, G. Y., Cooper, E. S., Waldo, K., Kirby, M. L., Gilula, N. B., Lo, C. W. (1998). Gap junction-mediated cell-cell communication modulates mouse neural crest migration. *J Cell Biol* **143**, 1725-34.

Inoguchi, T., Yu, H. Y., Imamura, M., Kakimoto, M., Kuroki, T., Maruyama, T. and Nawata, H. (2001). Altered gap junction activity in cardiovascular tissues of diabetes. *Med Electron Microsc* **34**, 86-91.

Iocono, J. A., Colleran, K. R., Remick, D. G., Gillespie, B. W., Ehrlich, H. P. and Garner, W. L. (2000). Interleukin-8 levels and activity in delayed-healing human thermal wounds. *Wound Repair Regen* **8**, 216-25.

Issekutz, A. C., Chuluyan, H. E. and Lopes, N. (1995). CD11/CD18-independent transendothelial migration of human polymorphonuclear leukocytes and monocytes: involvement of distinct and unique mechanisms. *J Leukoc Biol* **57**, 553-61.

Ito, K., Okamoto, I., Araki, N., Kawano, Y., Nakao, M., Fujiyama, S., Tomita, K., Mimori, T. and Saya, H. (1999). Calcium influx triggers the sequential proteolysis of extracellular and cytoplasmic domains of E-cadherin, leading to loss of beta-catenin from cell-cell contacts. *Oncogene* **18**, 7080-90.

Jackman, S. H., Yoak, M. B., Keerthy, S. and Beaver, B. L. (2000). Differential expression of chemokines in a mouse model of wound healing. *Ann Clin Lab Sci* **30**, 201-7.

Jaffe, E. A., Nachman, R. L., Becker, C. G. and Minick, C. R. (1973). Culture of human endothelial cells derived from umbilical veins. Identification by morphologic and immunologic criteria. *J Clin Invest* **52**, 2745-56.

Jagger, D. J. and Forge, A. (2006). Compartmentalized and signal-selective gap junctional coupling in the hearing cochlea. *J Neurosci* **26**, 1260-8.

Jara, P. I., Boric, M. P. and Saez, J. C. (1995). Leukocytes express connexin 43 after activation with lipopolysaccharide and appear to form gap junctions with endothelial cells after ischemia-reperfusion. *Proc Natl Acad Sci U S A* **92**, 7011-5.

John, S. A. and Revel, J. P. (1991). Connexon integrity is maintained by non-covalent bonds: intramolecular disulfide bonds link the extracellular domains in rat connexin-43. *Biochem Biophys Res Commun* **178**, 1312-8.

John, S. A., Kondo, R., Wang, S. Y., Goldhaber, J. I. and Weiss, J. N. (1999). Connexin-43 hemichannels opened by metabolic inhibition. *J Biol Chem* **274**, 236-40.

Jongen, W. M., Fitzgerald, D. J., Asamoto, M., Piccoli, C., Slaga, T. J., Gros, D., Takeichi, M. and Yamasaki, H. (1991). Regulation of connexin 43-mediated gap junctional intercellular communication by Ca2+ in mouse epidermal cells is controlled by E-cadherin. *J Cell Biol* **114**, 545-55.

Jordan, K., Chodock, R., Hand, A. R. and Laird, D. W. (2001). The origin of annular junctions: a mechanism of gap junction internalization. *J Cell Sci* **114**, 763-73.

Kadle, R., Zhang, J. T. and Nicholson, B. J. (1991). Tissue-specific distribution of differentially phosphorylated forms of Cx43. *Mol Cell Biol* **11**, 363-9.

Kamibayashi, Y., Oyamada, M., Oyamada, Y. and Mori, M. (1993). Expression of gap junction proteins connexin 26 and 43 is modulated during differentiation of keratinocytes in newborn mouse epidermis. *J Invest Dermatol* **101**, 773-8.

Kanczuga-Koda, L., Sulkowski, S., Koda, M. and Sulkowska, M. (2005). Alterations in connexin26 expression during colorectal carcinogenesis. *Oncology* **68**, 217-22.

Kandyba, E. E., Hodgins, M. B. and Martin, P. E. (2007). A Murine Living Skin Equivalent Amenable to Live-Cell Imaging: Analysis of the Roles of Connexins in the Epidermis. *J Invest Dermatol.*

Kanno, Y. and Loewenstein, W. R. (1966). Cell-to-cell passage of large molecules. *Nature* **212**, 629-30.

Karrer, H. E. (1960). Cell interconnections in normal human cervical epithelium. *J Biophys Biochem Cytol* **7**, 181-4.

Kelsell, D. P., Di, W. L. and Houseman, M. J. (2001). Connexin mutations in skin disease and hearing loss. *Am J Hum Genet* **68**, 559-68.

Kelsell, D. P., Dunlop, J., Stevens, H. P., Lench, N. J., Liang, J. N., Parry, G., Mueller, R. F. and Leigh, I. M. (1997). Connexin 26 mutations in hereditary non-syndromic sensorineural deafness. *Nature* **387**, 80-3.

Kelsell, D. P., Wilgoss, A. L., Richard, G., Stevens, H. P., Munro, C. S. and Leigh, I. M. (2000). Connexin mutations associated with palmoplantar keratoderma and profound deafness in a single family. *Eur J Hum Genet* **8**, 141-4.

Keswani, S. G., Katz, A. B., Lim, F. Y., Zoltick, P., Radu, A., Alaee, D., Herlyn, M. and Crombleholme, T. M. (2004). Adenoviral mediated gene transfer of PDGF-B enhances wound healing in type I and type II diabetic wounds. *Wound Repair Regen* **12**, 497-504.

King, T. J. and Bertram, J. S. (2005). Connexins as targets for cancer chemoprevention and chemotherapy. *Biochim Biophys Acta* **1719**, 146-60.

Koch, R. M., Roche, N. S., Parks, W. T., Ashcroft, G. S., Letterio, J. J. and Roberts, A. B. (2000). Incisional wound healing in transforming growth factor-beta1 null mice. *Wound Repair Regen* **8**, 179-91.

Kolodney, M. S. and Wysolmerski, R. B. (1992). Isometric contraction by fibroblasts and endothelial cells in tissue culture: a quantitative study. *J Cell Biol* **117**, 73-82.

Komesu, M. C., Tanga, M. B., Buttros, K. R. and Nakao, C. (2004). Effects of acute diabetes on rat cutaneous wound healing. *Pathophysiology* **11**, 63-67.

Kretz, M., Euwens, C., Hombach, S., Eckardt, D., Teubner, B., Traub, O., Willecke, K. and Ott, T. (2003). Altered connexin expression and wound healing in the epidermis of connexin-deficient mice. *J Cell Sci* **116**, 3443-52.

Kretz, M., Maass, K. and Willecke, K. (2004). Expression and function of connexins in the epidermis, analyzed with transgenic mouse mutants. *Eur J Cell Biol* **83**, 647-54.

Kreutziger, G. O. (1976). Lateral membrane morphology and gap junction structure in rabbit corneal endothelium. *Exp Eye Res* **23**, 285-93.

Kumar, N. M. and Gilula, N. B. (1996). The gap junction communication channel. *Cell* **84**, 381-8.

Kuroki, T., Inoguchi, T., Umeda, F., Ueda, F. and Nawata, H. (1998). High glucose induces alteration of gap junction permeability and phosphorylation of connexin-43 in cultured aortic smooth muscle cells. *Diabetes* **47**, 931-6.

Kwak, B. R. and Jongsma, H. J. (1996). Regulation of cardiac gap junction channel permeability and conductance by several phosphorylating conditions. *Mol Cell Biochem* **157**, 93-9.

Kwak, B. R., Pepper, M. S., Gros, D. B. and Meda, P. (2001). Inhibition of endothelial wound repair by dominant negative connexin inhibitors. *Mol Biol Cell* **12**, 831-45.

Labarthe, M. P., Bosco, D., Saurat, J. H., Meda, P. and Salomon, D. (1998). Upregulation of connexin 26 between keratinocytes of psoriatic lesions. *J Invest Dermatol* **111**, 72-6.

Laing, J. G. and Beyer, E. C. (1995). The gap junction protein connexin43 is degraded via the ubiquitin proteasome pathway. *J Biol Chem* **270**, 26399-403.

Laing, J. G., Tadros, P. N., Westphale, E. M. and Beyer, E. C. (1997). Degradation of connexin43 gap junctions involves both the proteasome and the lysosome. *Exp Cell Res* **236**, 482-92.

Laird, D. W. (1996). The life cycle of a connexin: gap junction formation, removal, and degradation. *J Bioenerg Biomembr* **28**, 311-8.

Laird, D. W. (2005). Connexin phosphorylation as a regulatory event linked to gap junction internalization and degradation. *Biochim Biophys Acta* **1711**, 172-82.

Laird, D. W., Yancey, S. B., Bugga, L. and Revel, J. P. (1992). Connexin expression and gap junction communication compartments in the developing mouse limb. *Dev Dyn* **195**, 153-61.

Lampe, P. D., TenBroek, E. M., Burt, J. M., Kurata, W. E., Johnson, R. G. and Lau, A. F. (2000). Phosphorylation of connexin43 on serine368 by protein kinase C regulates gap junctional communication. *J Cell Biol* **149**, 1503-12.

Lanning, D. A., Nwomeh, B. C., Montante, S. J., Yager, D. R., Diegelmann, R. F. and Haynes, J. H. (1999). TGF-beta1 alters the healing of cutaneous fetal excisional wounds. *J Pediatr Surg* **34**, 695-700.

Lantoine, F., Iouzalen, L., Devynck, M. A., Millanvoye-Van Brussel, E. and David-Dufilho, M. (1998). Nitric oxide production in human endothelial cells stimulated by histamine requires Ca2+ influx. *Biochem J* **330 (Pt 2)**, 695-9.

Larsen, W. J., Tung, H. N., Murray, S. A. and Swenson, C. A. (1979). Evidence for the participation of actin microfilaments and bristle coats in the internalization of gap junction membrane. *J Cell Biol* **83**, 576-87.

Larson, D. M. and Haudenschild, C. C. (1988). Junctional transfer in wounded cultures of bovine aortic endothelial cells. *Lab Invest* **59**, 373-9.

Larson, D. M., Haudenschild, C. C. and Beyer, E. C. (1990). Gap junction messenger RNA expression by vascular wall cells. *Circ Res* **66**, 1074-80.

Lau, A. F., Kanemitsu, M. Y., Kurata, W. E., Danesh, S. and Boynton, A. L. (1992). Epidermal growth factor disrupts gap-junctional communication and induces phosphorylation of connexin43 on serine. *Mol Biol Cell* **3**, 865-74.

Lau, A. F., Kurata, W. E., Kanemitsu, M. Y., Loo, L. W., Warn-Cramer, B. J., Eckhart, W. and Lampe, P. D. (1996). Regulation of connexin43 function by activated tyrosine protein kinases. *J Bioenerg Biomembr* **28**, 359-68.

Law, L. Y., Zhang, W. V., Stott, N. S., Becker, D. L. and Green, C. R. (2006). In vitro optimization of antisense oligodeoxynucleotide design: an example using the connexin gene family. *J Biomol Tech* **17**, 270-82.

Lazrak, A. and Peracchia, C. (1993). Gap junction gating sensitivity to physiological internal calcium regardless of pH in Novikoff hepatoma cells. *Biophys J* **65**, 2002-12.

Leibovich, S. J. and Ross, R. (1975). The role of the macrophage in wound repair. A study with hydrocortisone and antimacrophage serum. *Am J Pathol* **78**, 71-100.

Leithe, E. and Rivedal, E. (2004). Epidermal growth factor regulates ubiquitination, internalization and proteasome-dependent degradation of connexin43. *J Cell Sci* **117**, 1211-20.

Levenson, S. M., Geever, E. F., Crowley, L. V., Oates, J. F., 3rd, Berard, C. W. and Rosen, H. (1965). The Healing Of Rat Skin Wounds. *Ann Surg* **161**, 293-308.

Leybaert, L., Braet, K., Vandamme, W., Cabooter, L., Martin, P. E. and Evans, W. H. (2003). Connexin channels, connexin mimetic peptides and ATP release. *Cell Commun Adhes* **10**, 251-7.

Li, A. F., Sato, T., Haimovici, R., Okamoto, T. and Roy, S. (2003). High glucose alters connexin 43 expression and gap junction intercellular communication activity in retinal pericytes. *Invest Ophthalmol Vis Sci* **44**, 5376-82.

Li, X. A., Everson, W. V. and Smart, E. J. (2005). Caveolae, lipid rafts, and vascular disease. *Trends Cardiovasc Med* **15**, 92-6.

Li, Y., Chi, L., Stechschulte, D. J. and Dileepan, K. N. (2001). Histamine-induced production of interleukin-6 and interleukin-8 by human coronary artery endothelial cells is enhanced by endotoxin and tumor necrosis factor-alpha. *Microvasc Res* **61**, 253-62.

Liechty, K. W., Crombleholme, T. M., Cass, D. L., Martin, B. and Adzick, N. S. (1998). Diminished interleukin-8 (IL-8) production in the fetal wound healing response. *J Surg Res* **77**, 80-4.

Lin, C. I., Chen, C. N., Chen, J. H. and Lee, H. (2006). Lysophospholipids increase IL-8 and MCP-1 expressions in human umbilical cord vein endothelial cells through an IL-1-dependent mechanism. *J Cell Biochem* **99**, 1216-32.

Lin, Z. Q., Kondo, T., Ishida, Y., Takayasu, T. and Mukaida, N. (2003). Essential involvement of IL-6 in the skin wound-healing process as evidenced by delayed wound healing in IL-6-deficient mice. *J Leukoc Biol* **73**, 713-21.

Little, T. L., Beyer, E. C. and Duling, B. R. (1995). Connexin 43 and connexin 40 gap junctional proteins are present in arteriolar smooth muscle and endothelium in vivo. *Am J Physiol* **268**, H729-39.

Liu, P., Ying, Y. and Anderson, R. G. (1997). Platelet-derived growth factor activates mitogen-activated protein kinase in isolated caveolae. *Proc Natl Acad Sci U S A* **94**, 13666-70.

Liu, S., Taffet, S., Stoner, L., Delmar, M., Vallano, M. L. and Jalife, J. (1993). A structural basis for the unequal sensitivity of the major cardiac and liver gap junctions to intracellular acidification: the carboxyl tail length. *Biophys J* **64**, 1422-33.

Lo, C. W., Waldo, K. L. and Kirby, M. L. (1999). Gap junction communication and the modulation of cardiac neural crest cells. *Trends Cardiovasc Med* **9**, 63-9.

Locke, D., Liu, J. and Harris, A. L. (2005). Lipid rafts prepared by different methods contain different connexin channels, but gap junctions are not lipid rafts. *Biochemistry* **44**, 13027-42.

Loewenstein, W. R. and Kanno, Y. (1964). Studies On An Epithelial (Gland) Cell Junction. I. Modifications Of Surface Membrane Permeability. *J Cell Biol* **22**, 565-86.

Loots, M. A., Lamme, E. N., Zeegelaar, J., Mekkes, J. R., Bos, J. D. and Middelkoop, E. (1998). Differences in cellular infiltrate and extracellular matrix of chronic diabetic and venous ulcers versus acute wounds. *J Invest Dermatol* **111**, 850-7.

Low, Q. E., Drugea, I. A., Duffner, L. A., Quinn, D. G., Cook, D. N., Rollins, B. J., Kovacs, E. J. and DiPietro, L. A. (2001). Wound healing in MIP-1alpha(-/-) and MCP-1(-/-) mice. *Am J Pathol* **159**, 457-63.

Lucke, T., Choudhry, R., Thom, R., Selmer, I. S., Burden, A. D. and Hodgins, M. B. (1999). Upregulation of connexin 26 is a feature of keratinocyte differentiation in hyperproliferative epidermis, vaginal epithelium, and buccal epithelium. *J Invest Dermatol* **112**, 354-61.

Maass, K., Ghanem, A., Kim, J. S., Saathoff, M., Urschel, S., Kirfel, G., Grummer, R., Kretz, M., Lewalter, T., Tiemann, K. et al. (2004). Defective epidermal barrier in neonatal mice lacking the C-terminal region of connexin43. *Mol Biol Cell* **15**, 4597-608.

Macari, F., Landau, M., Cousin, P., Mevorah, B., Brenner, S., Panizzon, R., Schorderet, D. F., Hohl, D. and Huber, M. (2000). Mutation in the gene for connexin 30.3 in a family with erythrokeratodermia variabilis. *Am J Hum Genet* **67**, 1296-301.

Mackay, D., Ionides, A., Kibar, Z., Rouleau, G., Berry, V., Moore, A., Shiels, A. and Bhattacharya, S. (1999). Connexin46 mutations in autosomal dominant congenital cataract. *Am J Hum Genet* **64**, 1357-64.

Maestrini, E., Korge, B. P., Ocana-Sierra, J., Calzolari, E., Cambiaghi, S., Scudder, P. M., Hovnanian, A., Monaco, A. P. and Munro, C. S. (1999). A missense mutation in connexin26, D66H, causes mutilating keratoderma with sensorineural deafness (Vohwinkel's syndrome) in three unrelated families. *Hum Mol Genet* **8**, 1237-43.

Makowski, L., Caspar, D. L., Phillips, W. C. and Goodenough, D. A. (1977). Gap junction structures. II. Analysis of the x-ray diffraction data. *J Cell Biol* **74**, 629-45.

Mandracchia, V. J., Sanders, S. M. and Frerichs, J. A. (2001). The use of becaplermin (rhPDGF-BB) gel for chronic nonhealing ulcers. A retrospective analysis. *Clin Podiatr Med Surg* **18**, 189-209, viii.

Manthey, D., Banach, K., Desplantez, T., Lee, C. G., Kozak, C. A., Traub, O., Weingart, R. and Willecke, K. (2001). Intracellular domains of mouse connexin26 and -30 affect diffusional and electrical properties of gap junction channels. *J Membr Biol* **181**, 137-48.

Mantz, J., Cordier, J. and Giaume, C. (1993). Effects of general anesthetics on intercellular communications mediated by gap junctions between astrocytes in primary culture. *Anesthesiology* **78**, 892-901.

Marchese, C., Chedid, M., Dirsch, O. R., Csaky, K. G., Santanelli, F., Latini, C., LaRochelle, W. J., Torrisi, M. R. and Aaronson, S. A. (1995). Modulation of keratinocyte growth factor and its receptor in reepithelializing human skin. *J Exp Med* **182**, 1369-76.

Marino, A. A., Waddell, D. D., Kolomytkin, O. V., Meek, W. D., Wolf, R., Sadasivan, K. K. and Albright, J. A. (2004). Increased intercellular communication through gap junctions may contribute to progression of osteoarthritis. *Clin Orthop Relat Res*, 224-32.

Martin, P. (1997). Wound healing--aiming for perfect skin regeneration. *Science* **276**, 75-81.

Martin, P. E., Errington, R. J. and Evans, W. H. (2001). Gap junction assembly: multiple connexin fluorophores identify complex trafficking pathways. *Cell Commun Adhes* **8**, 243-8.

Martin, P., D'Souza, D., Martin, J., Grose, R., Cooper, L., Maki, R. and McKercher, S. R. (2003). Wound healing in the PU.1 null mouse--tissue repair is not dependent on inflammatory cells. *Curr Biol* **13**, 1122-8.

Maruyama, K., Asai, J., Ii, M., Thorne, T., Losordo, D. W. and D'Amore, P. A. (2007). Decreased macrophage number and activation lead to reduced lymphatic vessel formation and contribute to impaired diabetic wound healing. *Am J Pathol* **170**, 1178-91.

Massague, J., Andres, J., Attisano, L., Cheifetz, S., Lopez-Casillas, F., Ohtsuki, M. and Wrana, J. L. (1992). TGF-beta receptors. *Mol Reprod Dev* **32**, 99-104.

McNutt, N. S. and Weinstein, R. S. (1973). Membrane ultrastructure at mammalian intercellular junctions. *Prog Biophys Mol Biol* **26**, 45-101.

Meyer, R. A., Laird, D. W., Revel, J. P. and Johnson, R. G. (1992). Inhibition of gap junction and adherens junction assembly by connexin and A-CAM antibodies. *J Cell Biol* **119**, 179-89.

Miki, I., Kusano, A., Ohta, S., Hanai, N., Otoshi, M., Masaki, S., Sato, S. and Ohmori, K. (1996). Histamine enhanced the TNF-alpha-induced expression of E-selectin and ICAM-1 on vascular endothelial cells. *Cell Immunol* **171**, 285-8.

Milici, A. J., Watrous, N. E., Stukenbrok, H. and Palade, G. E. (1987). Transcytosis of albumin in capillary endothelium. *J Cell Biol* **105**, 2603-12.

Milks, L. C., Kumar, N. M., Houghten, R., Unwin, N. and Gilula, N. B. (1988). Topology of the 32-kd liver gap junction protein determined by site-directed antibody localizations. *Embo J* **7**, 2967-75.

Millanvoye-Van Brussel, E., David-Dufilho, M., Pham, T. D., Iouzalen, L. and Aude Devynck, M. (1999). Regulation of arachidonic acid release by calcium influx in human endothelial cells. *J Vasc Res* **36**, 235-44.

Mitchell, J. A., Larkin, S. and Williams, T. J. (1995). Cyclooxygenase-2: regulation and relevance in inflammation. *Biochem Pharmacol* **50**, 1535-42.

Moll, R., Franke, W. W., Volc-Platzer, B. and Krepler, R. (1982). Different keratin polypeptides in epidermis and other epithelia of human skin: a specific cytokeratin of molecular weight 46,000 in epithelia of the pilosebaceous tract and basal cell epitheliomas. *J Cell Biol* **95**, 285-95.

Monaghan, P., Perusinghe, N., Carlile, G. and Evans, W. H. (1994). Rapid modulation of gap junction expression in mouse mammary gland during pregnancy, lactation, and involution. *J Histochem Cytochem* **42**, 931-8.

Moncada, S. and Higgs, E. A. (2006a). The discovery of nitric oxide and its role in vascular biology. *Br J Pharmacol* **147 Suppl 1**, S193-201.

Moncada, S. and Higgs, E. A. (2006b). Nitric oxide and the vascular endothelium. *Handb Exp Pharmacol*, 213-54.

Montagna, W. and Parakkal, P. F. (1974). The Structure and Function of Skin. New York: Academic Press, Inc.

Montesano, R. and Orci, L. (1988). Transforming growth factor beta stimulates collagen-matrix contraction by fibroblasts: implications for wound healing. *Proc Natl Acad Sci U S A* **85**, 4894-7.

Moore, K., Ruge, F. and Harding, K. G. (1997). T lymphocytes and the lack of activated macrophages in wound margin biopsies from chronic leg ulcers. *Br J Dermatol* **137**, 188-94.

Moreno, A. P., Chanson, M., Elenes, S., Anumonwo, J., Scerri, I., Gu, H., Taffet, S. M. and Delmar, M. (2002). Role of the carboxyl terminal of connexin43 in transjunctional fast voltage gating. *Circ Res* **90**, 450-7.

Mori, R., Kondo, T., Ohshima, T., Ishida, Y. and Mukaida, N. (2002). Accelerated wound healing in tumor necrosis factor receptor p55-deficient mice with reduced leukocyte infiltration. *Faseb J* **16**, 963-74.

Mori, R., Power, K. T., Wang, C. M., Martin, P. and Becker, D. L. (2006). Acute downregulation of connexin43 at wound sites leads to a reduced inflammatory response, enhanced keratinocyte proliferation and wound fibroblast migration. *J Cell Sci* **119**, 5193-203.

Morley, G. E., Taffet, S. M. and Delmar, M. (1996). Intramolecular interactions mediate pH regulation of connexin43 channels. *Biophys J* **70**, 1294-302.

Moyer, K. E. and Ehrlich, H. P. (2003). Modulation of human fibroblast gap junction intercellular communication by hyaluronan. *J Cell Physiol* **196**, 165-70.

Moyer, K. E., Davis, A., Saggers, G. C., Mackay, D. R. and Ehrlich, H. P. (2002). Wound healing: the role of gap junctional communication in rat granulation tissue maturation. *Exp Mol Pathol* **72**, 10-6.

Muller, W. A. (2001). Migration of leukocytes across endothelial junctions: some concepts and controversies. *Microcirculation* **8**, 181-93.

Musil, L. S. and Goodenough, D. A. (1991). Biochemical analysis of connexin43 intracellular transport, phosphorylation, and assembly into gap junctional plaques. *J Cell Biol* **115**, 1357-74.

Musil, L. S. and Goodenough, D. A. (1993). Multisubunit assembly of an integral plasma membrane channel protein, gap junction connexin43, occurs after exit from the ER. *Cell* **74**, 1065-77.

Musil, L. S., Beyer, E. C. and Goodenough, D. A. (1990). Expression of the gap junction protein connexin43 in embryonic chick lens: molecular cloning, ultrastructural localization, and post-translational phosphorylation. *J Membr Biol* **116**, 163-75.

Nagai, M. K. and Embil, J. M. (2002). Becaplermin: recombinant platelet derived growth factor, a new treatment for healing diabetic foot ulcers. *Expert Opin Biol Ther* **2**, 211-8.

Nedergaard, M. (1994). Direct signaling from astrocytes to neurons in cultures of mammalian brain cells. *Science* **263**, 1768-71.

Nelles, E., Butzler, C., Jung, D., Temme, A., Gabriel, H. D., Dahl, U., Traub, O., Stumpel, F., Jungermann, K., Zielasek, J. et al. (1996). Defective propagation of signals generated by sympathetic nerve stimulation in the liver of connexin32-deficient mice. *Proc Natl Acad Sci U S A* **93**, 9565-70.

Neub, A., Houdek, P., Ohnemus, U., Moll, I. and Brandner, J. M. (2007). Biphasic regulation of AP-1 subunits during human epidermal wound healing. *J Invest Dermatol* **127**, 2453-62.

Niessen, F. B., Andriessen, M. P., Schalkwijk, J., Visser, L. and Timens, W. (2001). Keratinocyte-derived growth factors play a role in the formation of hypertrophic scars. *J Pathol* **194**, 207-16.

Nissen, N. N., Polverini, P. J., Koch, A. E., Volin, M. V., Gamelli, R. L. and DiPietro, L. A. (1998). Vascular endothelial growth factor mediates angiogenic activity during the proliferative phase of wound healing. *Am J Pathol* **152**, 1445-52.

Nobes, C. D. and Hall, A. (1995a). Rho, rac and cdc42 GTPases: regulators of actin structures, cell adhesion and motility. *Biochem Soc Trans* **23**, 456-9.

Nobes, C. D. and Hall, A. (1995b). Rho, rac, and cdc42 GTPases regulate the assembly of multimolecular focal complexes associated with actin stress fibers, lamellipodia, and filopodia. *Cell* **81**, 53-62.

Nodder, S. and Martin, P. (1997). Wound healing in embryos: a review. *Anat Embryol (Berl)* **195**, 215-28.

Noren, N. K., Liu, B. P., Burridge, K. and Kreft, B. (2000). p120 catenin regulates the actin cytoskeleton via Rho family GTPases. *J Cell Biol* **150**, 567-80.

Norgauer, J., Hildenbrand, T., Idzko, M., Panther, E., Bandemir, E., Hartmann, M., Vanscheidt, W. and Herouy, Y. (2002). Elevated expression of extracellular matrix metalloproteinase inducer (CD147) and membrane-type matrix metalloproteinases in venous leg ulcers. *Br J Dermatol* **147**, 1180-6.

Obara, K., Ishihara, M., Fujita, M., Kanatani, Y., Hattori, H., Matsui, T., Takase, B., Ozeki, Y., Nakamura, S., Ishizuka, T. et al. (2005). Acceleration of wound healing in healing-impaired db/db mice with a photocrosslinkable chitosan hydrogel containing fibroblast growth factor-2. *Wound Repair Regen* **13**, 390-7.

O'Kane, S. and Ferguson, M. W. (1997). Transforming growth factor beta s and wound healing. *Int J Biochem Cell Biol* **29**, 63-78.

Okruhlicova, L., Tribulova, N., Misejkova, M., Kucka, M., Stetka, R., Slezak, J. and Manoach, M. (2002). Gap junction remodelling is involved in the susceptibility of diabetic rats to hypokalemia-induced ventricular fibrillation. *Acta Histochem* **104**, 387-91.

Oku, H., Kodama, T., Sakagami, K. and Puro, D. G. (2001). Diabetes-induced disruption of gap junction pathways within the retinal microvasculature. *Invest Ophthalmol Vis Sci* **42**, 1915-20.

Ornitz, D. M. and Itoh, N. (2001). Fibroblast growth factors. *Genome Biol* **2**, 3005.

Oviedo-Orta, E. and Evans, H. W. (2004). Gap junctions and connexin-mediated communication in the immune system. *Biochim Biophys Acta* **1662**, 102-12.

Oviedo-Orta, E., Errington, R. J. and Evans, W. H. (2002). Gap junction intercellular communication during lymphocyte transendothelial migration. *Cell Biol Int* **26**, 253-63.

Oviedo-Orta, E., Gasque, P. and Evans, W. H. (2001). Immunoglobulin and cytokine expression in mixed lymphocyte cultures is reduced by disruption of gap junction intercellular communication. *Faseb J* **15**, 768-74.

Pan, X., Solomon, S. S., Borromeo, D. M., Martinez-Hernandez, A. and Raghow, R. (2001). Insulin deprivation leads to deficiency of Sp1 transcription factor in H-411E hepatoma cells and in streptozotocin-induced diabetic ketoacidosis in the rat. *Endocrinology* **142**, 1635-42.

Parpura, V., Scemes, E. and Spray, D. C. (2004). Mechanisms of glutamate release from astrocytes: gap junction "hemichannels", purinergic receptors and exocytotic release. *Neurochem Int* **45**, 259-64.

Parthasarathi, K., Ichimura, H., Monma, E., Lindert, J., Quadri, S., Issekutz, A. and Bhattacharya, J. (2006). Connexin 43 mediates spread of Ca2+-dependent proinflammatory responses in lung capillaries. *J Clin Invest* **116**, 2193-200.

Paul, D. L. (1986). Molecular cloning of cDNA for rat liver gap junction protein. *J Cell Biol* **103**, 123-34.

Paul, D. L., Yu, K., Bruzzone, R., Gimlich, R. L. and Goodenough, D. A. (1995). Expression of a dominant negative inhibitor of intercellular communication in the early Xenopus embryo causes delamination and extrusion of cells. *Development* **121**, 371-81.

Paul, R. G., Tarlton, J. F., Purslow, P. P., Sims, T. J., Watkins, P., Marshall, F., Ferguson, M. J. and Bailey, A. J. (1997). Biomechanical and biochemical study of a standardized wound healing model. *Int J Biochem Cell Biol* **29**, 211-20.

Payton, B. W., Bennett, M. V. and Pappas, G. D. (1969). Permeability and structure of junctional membranes at an electrotonic synapse. *Science* **166**, 1641-3.

Paznekas, W. A., Boyadjiev, S. A., Shapiro, R. E., Daniels, O., Wollnik, B., Keegan, C. E., Innis, J. W., Dinulos, M. B., Christian, C., Hannibal, M. C. et al. (2003). Connexin 43 (GJA1) mutations cause the pleiotropic phenotype of oculodentodigital dysplasia. *Am J Hum Genet* **72**, 408-18.

Pepper, M. S., Montesano, R., el Aoumari, A., Gros, D., Orci, L. and Meda, P. (1992). Coupling and connexin 43 expression in microvascular and large vessel endothelial cells. *Am J Physiol* **262**, C1246-57.

Pepper, M. S., Spray, D. C., Chanson, M., Montesano, R., Orci, L. and Meda, P. (1989). Junctional communication is induced in migrating capillary endothelial cells. *J Cell Biol* **109**, 3027-38.

Peracchia, C. and Bernardini, G. (1984). Gap junction structure and cell-to-cell coupling regulation: is there a calmodulin involvement? *Fed Proc* **43**, 2681-91.

Peters, K. G., De Vries, C. and Williams, L. T. (1993). Vascular endothelial growth factor receptor expression during embryogenesis and tissue repair suggests a role in endothelial differentiation and blood vessel growth. *Proc Natl Acad Sci U S A* **90**, 8915-9.

Peterson, J. M., Barbul, A., Breslin, R. J., Wasserkrug, H. L. and Efron, G. (1987). Significance of T-lymphocytes in wound healing. *Surgery* **102**, 300-5.

Phelan, P., Nakagawa, M., Wilkin, M. B., Moffat, K. G., O'Kane, C. J., Davies, J. A. and Bacon, J. P. (1996). Mutations in shaking-B prevent electrical synapse formation in the Drosophila giant fiber system. *J Neurosci* **16**, 1101-13.

Phelan, P., Stebbings, L. A., Baines, R. A., Bacon, J. P., Davies, J. A. and Ford, C. (1998). Drosophila Shaking-B protein forms gap junctions in paired Xenopus oocytes. *Nature* **391**, 181-4.

Pierce, G. F. and Mustoe, T. A. (1995). Pharmacologic enhancement of wound healing. *Annu Rev Med* **46**, 467-81.

Pitre, D. A., Seifert, J. L. and Bauer, J. A. (2001). Perineurium inflammation and altered connexin isoform expression in a rat model of diabetes related peripheral neuropathy. *Neurosci Lett* **303**, 67-71.

Pober, J. S. and Cotran, R. S. (1990). The role of endothelial cells in inflammation. *Transplantation* **50**, 537-44.

Qiu, C., Coutinho, P., Frank, S., Franke, S., Law, L. Y., Martin, P., Green, C. R. and Becker, D. L. (2003). Targeting connexin43 expression accelerates the rate of wound repair. *Curr Biol* **13**, 1697-703.

Rahman, S. and Evans, W. H. (1991). Topography of connexin32 in rat liver gap junctions. Evidence for an intramolecular disulphide linkage connecting the two extracellular peptide loops. *J Cell Sci* **100 (Pt 3)**, 567-78.

Rahman, S., Carlile, G. and Evans, W. H. (1993). Assembly of hepatic gap junctions. Topography and distribution of connexin 32 in intracellular and plasma membranes determined using sequence-specific antibodies. *J Biol Chem* **268**, 1260-5.

Reaume, A. G., de Sousa, P. A., Kulkarni, S., Langille, B. L., Zhu, D., Davies, T. C., Juneja, S. C., Kidder, G. M. and Rossant, J. (1995). Cardiac malformation in neonatal mice lacking connexin43. *Science* **267**, 1831-4.

Redd, M. J., Cooper, L., Wood, W., Stramer, B. and Martin, P. (2004). Wound healing and inflammation: embryos reveal the way to perfect repair. *Philos Trans R Soc Lond B Biol Sci* **359**, 777-84.

Redd, M. J., Kelly, G., Dunn, G., Way, M. and Martin, P. (2006). Imaging macrophage chemotaxis in vivo: studies of microtubule function in zebrafish wound inflammation. *Cell Motil Cytoskeleton* **63**, 415-22.

Reed, K. E., Westphale, E. M., Larson, D. M., Wang, H. Z., Veenstra, R. D. and Beyer, E. C. (1993). Molecular cloning and functional expression of human connexin37, an endothelial cell gap junction protein. *J Clin Invest* **91**, 997-1004.

Revel, J. P. and Karnovsky, M. J. (1967). Hexagonal array of subunits in intercellular junctions of the mouse heart and liver. *J Cell Biol* **33**, C7-C12.

Richard, G. (2000). Connexins: a connection with the skin. *Exp Dermatol* **9**, 77-96.

Richard, G., Brown, N., Rouan, F., Van der Schroeff, J. G., Bijlsma, E., Eichenfield, L. F., Sybert, V. P., Greer, K. E., Hogan, P., Campanelli, C. et al. (2003). Genetic heterogeneity in erythrokeratodermia variabilis: novel mutations in the connexin gene GJB4 (Cx30.3) and genotype-phenotype correlations. *J Invest Dermatol* **120**, 601-9.

Richard, G., Smith, L. E., Bailey, R. A., Itin, P., Hohl, D., Epstein, E. H., Jr., DiGiovanna, J. J., Compton, J. G. and Bale, S. J. (1998a). Mutations in the human connexin gene GJB3 cause erythrokeratodermia variabilis. *Nat Genet* **20**, 366-9.

Richard, G., White, T. W., Smith, L. E., Bailey, R. A., Compton, J. G., Paul, D. L. and Bale, S. J. (1998b). Functional defects of Cx26 resulting from a heterozygous missense mutation in a family with dominant deaf-mutism and palmoplantar keratoderma. *Hum Genet* **103**, 393-9.

Richard, J. L., Parer-Richard, C., Daures, J. P., Clouet, S., Vannereau, D., Bringer, J., Rodier, M., Jacob, C. and Comte-Bardonnet, M. (1995). Effect of topical basic fibroblast growth factor on the healing of chronic diabetic neuropathic ulcer of the foot. A pilot, randomized, double-blind, placebo-controlled study. *Diabetes Care* **18**, 64-9.

Richards, T. S., Dunn, C. A., Carter, W. G., Usui, M. L., Olerud, J. E. and Lampe, P. D. (2004). Protein kinase C spatially and temporally regulates gap junctional communication during human wound repair via phosphorylation of connexin43 on serine368. *J Cell Biol* **167**, 555-62.

Ridley, A. J. and Hall, A. (1992). The small GTP-binding protein rho regulates the assembly of focal adhesions and actin stress fibers in response to growth factors. *Cell* **70**, 389-99.

Ridley, A. J., Comoglio, P. M. and Hall, A. (1995). Regulation of scatter factor/hepatocyte growth factor responses by Ras, Rac, and Rho in MDCK cells. *Mol Cell Biol* **15**, 1110-22.

Risau, W. (1997). Mechanisms of angiogenesis. *Nature* **386**, 671-4.

Risek, B., Klier, F. G. and Gilula, N. B. (1992). Multiple gap junction genes are utilized during rat skin and hair development. *Development* **116**, 639-51.

Roberts, A. B. and Sporn, M. B. (1993). Physiological actions and clinical applications of transforming growth factor-beta (TGF-beta). *Growth Factors* **8**, 1-9.

Robson, M. C., Phillips, L. G., Lawrence, W. T., Bishop, J. B., Youngerman, J. S., Hayward, P. G., Broemeling, L. D. and Heggers, J. P. (1992a). The safety and effect of topically applied recombinant basic fibroblast growth factor on the healing of chronic pressure sores. *Ann Surg* **216**, 401-6; discussion 406-8.

Robson, M. C., Phillips, L. G., Thomason, A., Robson, L. E. and Pierce, G. F. (1992b). Platelet-derived growth factor BB for the treatment of chronic pressure ulcers. *Lancet* **339**, 23-5.

Romanello, M., Veronesi, V. and D'Andrea, P. (2003). Mechanosensitivity and intercellular communication in HOBIT osteoblastic cells: a possible role for gap junction hemichannels. *Biorheology* **40**, 119-21.

Rose, B. and Loewenstein, W. R. (1975). Permeability of cell junction depends on local cytoplasmic calcium activity. *Nature* **254**, 250-2.

Rose, B., Mehta, P. P. and Loewenstein, W. R. (1993). Gap-junction protein gene suppresses tumorigenicity. *Carcinogenesis* **14**, 1073-5.

Rossiter, H., Barresi, C., Pammer, J., Rendl, M., Haigh, J., Wagner, E. F. and Tschachler, E. (2004). Loss of vascular endothelial growth factor a activity in murine epidermal keratinocytes delays wound healing and inhibits tumor formation. *Cancer Res* **64**, 3508-16.

Rothberg, K. G., Heuser, J. E., Donzell, W. C., Ying, Y. S., Glenney, J. R. and Anderson, R. G. (1992). Caveolin, a protein component of caveolae membrane coats. *Cell* **68**, 673-82.

Rotrosen, D. and Gallin, J. I. (1986). Histamine type I receptor occupancy increases endothelial cytosolic calcium, reduces F-actin, and promotes albumin diffusion across cultured endothelial monolayers. *J Cell Biol* **103**, 2379-87.

Rowland, F. N., Donovan, M. J., Picciano, P. T. and Kreutzer, D. L. (1984). Fibrin-mediated vascular injury: demonstration of vascular endothelial cell retraction in response to soluble fibrin-associated factors. *J Exp Pathol* **1**, 217-40.

Saarialho-Kere, U. K. (1998). Patterns of matrix metalloproteinase and TIMP expression in chronic ulcers. *Arch Dermatol Res* **290 Suppl**, S47-54.

Saarialho-Kere, U. K., Chang, E. S., Welgus, H. G. and Parks, W. C. (1992). Distinct localization of collagenase and tissue inhibitor of metalloproteinases expression in wound healing associated with ulcerative pyogenic granuloma. *J Clin Invest* **90**, 1952-7.

Saez, J. C., Contreras, J. E., Bukauskas, F. F., Retamal, M. A. and Bennett, M. V. (2003). Gap junction hemichannels in astrocytes of the CNS. *Acta Physiol Scand* **179**, 9-22.

Saez, J. C., Gregory, W. A., Watanabe, T., Dermietzel, R., Hertzberg, E. L., Reid, L., Bennett, M. V. and Spray, D. C. (1989). cAMP delays disappearance of gap junctions between pairs of rat hepatocytes in primary culture. *Am J Physiol* **257**, C1-11.

Saez, J. C., Nairn, A. C., Czernik, A. J., Fishman, G. I., Spray, D. C. and Hertzberg, E. L. (1997). Phosphorylation of connexin43 and the regulation of neonatal rat cardiac myocyte gap junctions. *J Mol Cell Cardiol* **29**, 2131-45.

Saez, J. C., Nairn, A. C., Czernik, A. J., Spray, D. C., Hertzberg, E. L., Greengard, P. and Bennett, M. V. (1990). Phosphorylation of connexin 32, a hepatocyte gap-junction protein, by cAMP-dependent protein kinase, protein kinase C and Ca2+/calmodulin-dependent protein kinase II. *Eur J Biochem* **192**, 263-73.

Sakai, S., Endo, Y., Ozawa, N., Sugawara, T., Kusaka, A., Sayo, T., Tagami, H. and Inoue, S. (2003). Characteristics of the epidermis and stratum corneum of hairless mice with experimentally induced diabetes mellitus. *J Invest Dermatol* **120**, 79-85.

Salomon, D., Masgrau, E., Vischer, S., Ullrich, S., Dupont, E., Sappino, P., Saurat, J. H. and Meda, P. (1994). Topography of mammalian connexins in human skin. *J Invest Dermatol* **103**, 240-7.

Sato, T., Haimovici, R., Kao, R., Li, A. F. and Roy, S. (2002). Downregulation of connexin 43 expression by high glucose reduces gap junction activity in microvascular endothelial cells. *Diabetes* **51**, 1565-71.

Schubert, A. L., Schubert, W., Spray, D. C. and Lisanti, M. P. (2002). Connexin family members target to lipid raft domains and interact with caveolin-1. *Biochemistry* **41**, 5754-64.

Seifter, E., Rettura, G., Padawer, J., Stratford, F., Kambosos, D. and Levenson, S. M. (1981). Impaired wound healing in streptozotocin diabetes. Prevention by supplemental vitamin A. *Ann Surg* **194**, 42-50.

Severs, N. J. (1995). Microscopy of the gap junction: a historical perspective. *Microsc Res Tech* **31**, 338-46.

Shaw, S. K., Bamba, P. S., Perkins, B. N. and Luscinskas, F. W. (2001). Real-time imaging of vascular endothelial-cadherin during leukocyte transmigration across endothelium. *J Immunol* **167**, 2323-30.

Shotton, H. R., Clarke, S. and Lincoln, J. (2003). The effectiveness of treatments of diabetic autonomic neuropathy is not the same in autonomic nerves supplying different organs. *Diabetes* **52**, 157-64.

Shukla, A., Dubey, M. P., Srivastava, R. and Srivastava, B. S. (1998). Differential expression of proteins during healing of cutaneous wounds in experimental normal and chronic models. *Biochem Biophys Res Commun* **244**, 434-9.

Simon, A. M., Goodenough, D. A. and Paul, D. L. (1998). Mice lacking connexin40 have cardiac conduction abnormalities characteristic of atrioventricular block and bundle branch block. *Curr Biol* **8**, 295-8.

Simpson, D. M. and Ross, R. (1972). The neutrophilic leukocyte in wound repair a study with antineutrophil serum. *J Clin Invest* **51**, 2009-23.

Singer, A. J. and Clark, R. A. (1999). Cutaneous wound healing. *N Engl J Med* **341**, 738-46.

Sjostrand, F. S. and Andersson, E. (1954). Electron microscopy of the intercalated discs of cardiac muscle tissue. *Experientia* **10**, 369-70.

Sohl, G. and Willecke, K. (2003). An update on connexin genes and their nomenclature in mouse and man. *Cell Commun Adhes* **10**, 173-80.

Sosinsky, G. E. (1996). Molecular organization of gap junction membrane channels. *J Bioenerg Biomembr* **28**, 297-309.

Spravchikov, N., Sizyakov, G., Gartsbein, M., Accili, D., Tennenbaum, T. and Wertheimer, E. (2001). Glucose effects on skin keratinocytes: implications for diabetes skin complications. *Diabetes* **50**, 1627-35.

Spray, D. C., White, R. L., Mazet, F. and Bennett, M. V. (1985). Regulation of gap junctional conductance. *Am J Physiol* **248**, H753-64.

Spyrou, G. E., Watt, D. A. and Naylor, I. L. a. (1998). The origin and mode of fibroblast migration and proliferation in granulation tissue. *Br J Plast Surg* **51**, 455-61.

Starich, T. A., Lee, R. Y., Panzarella, C., Avery, L. and Shaw, J. E. (1996). eat-5 and unc-7 represent a multigene family in Caenorhabditis elegans involved in cell-cell coupling. *J Cell Biol* **134**, 537-48.

Stout, C. E., Costantin, J. L., Naus, C. C. and Charles, A. C. (2002). Intercellular calcium signaling in astrocytes via ATP release through connexin hemichannels. *J Biol Chem* **277**, 10482-8.

Sullivan, R., Huang, G. Y., Meyer, R. A., Wessels, A., Linask, K. K. and Lo, C. W. (1998). Heart malformations in transgenic mice exhibiting dominant negative inhibition of gap junctional communication in neural crest cells. *Dev Biol* **204**, 224-34.

Sullivan, S. R., Underwood, R. A., Gibran, N. S., Sigle, R. O., Usui, M. L., Carter, W. G. and Olerud, J. E. (2004). Validation of a model for the study of multiple wounds in the diabetic mouse (db/db). *Plast Reconstr Surg* **113**, 953-60.

Sun, J., Ahmad, S., Chen, S., Tang, W., Zhang, Y., Chen, P. and Lin, X. (2005). Cochlear gap junctions coassembled from Cx26 and 30 show faster intercellular Ca2+ signaling than homomeric counterparts. *Am J Physiol Cell Physiol* **288**, C613-23.

Swensson, O. and Eady, R. A. (1996). Morphology of the keratin filament network in palm and sole skin: evidence for site-dependent features based on stereological analysis. *Arch Dermatol Res* **288**, 55-62.

Szkudelski, T. (2001). The mechanism of alloxan and streptozotocin action in B cells of the rat pancreas. *Physiol Res* **50**, 537-46.

Tada, J. and Hashimoto, K. (1997). Ultrastructural localization of gap junction protein connexin 43 in normal human skin, basal cell carcinoma, and squamous cell carcinoma. *J Cutan Pathol* **24**, 628-35.

Tan, X., Essengue, S., Talreja, J., Reese, J., Stechschulte, D. J. and Dileepan, K. N. (2007). Histamine directly and synergistically with lipopolysaccharide stimulates cyclooxygenase-2 expression and prostaglandin I(2) and E(2) production in human coronary artery endothelial cells. *J Immunol* **179**, 7899-906.

Teixeira, M. M., Williams, T. J. and Hellewell, P. G. (1993). Role of prostaglandins and nitric oxide in acute inflammatory reactions in guinea-pig skin. *Br J Pharmacol* **110**, 1515-21.

Temme, A., Ott, T., Haberberger, T., Traub, O. and Willecke, K. (2000). Acute-phase response and circadian expression of connexin26 are not altered in connexin32-deficient mouse liver. *Cell Tissue Res* **300**, 111-7.

Temme, A., Traub, O. and Willecke, K. (1998). Downregulation of connexin32 protein and gap-junctional intercellular communication by cytokine-mediated acute-phase response in immortalized mouse hepatocytes. *Cell Tissue Res* **294**, 345-50.

Terashi, H., Izumi, K., Deveci, M., Rhodes, L. M. and Marcelo, C. L. (2005). High glucose inhibits human epidermal keratinocyte proliferation for cellular studies on diabetes mellitus. *Int Wound J* **2**, 298-304.

Tillman, T. S. and Cascio, M. (2003). Effects of membrane lipids on ion channel structure and function. *Cell Biochem Biophys* **38**, 161-90.

Tomasek, J. J., Gabbiani, G., Hinz, B., Chaponnier, C. and Brown, R. A. (2002). Myofibroblasts and mechano-regulation of connective tissue remodelling. *Nat Rev Mol Cell Biol* **3**, 349-63.

Tonnesen, M. G., Feng, X. and Clark, R. A. (2000). Angiogenesis in wound healing. *J Investig Dermatol Symp Proc* **5**, 40-6.

Traub, O., Look, J., Paul, D. and Willecke, K. (1987). Cyclic adenosine monophosphate stimulates biosynthesis and phosphorylation of the 26 kDa gap junction protein in cultured mouse hepatocytes. *Eur J Cell Biol* **43**, 48-54.

Tremoli, E., Camera, M., Maderna, P., Sironi, L., Prati, L., Colli, S., Piovella, F., Bernini, F., Corsini, A. and Mussoni, L. (1993). Increased synthesis of plasminogen activator inhibitor-1 by cultured human endothelial cells exposed to native and modified LDLs. An LDL receptor-independent phenomenon. *Arterioscler Thromb* **13**, 338-46.

Tsang, M. W., Wong, W. K., Hung, C. S., Lai, K. M., Tang, W., Cheung, E. Y., Kam, G., Leung, L., Chan, C. W., Chu, C. M. et al. (2003). Human epidermal growth factor enhances healing of diabetic foot ulcers. *Diabetes Care* **26**, 1856-61.

Tsukita, S., Tsukita, S., Nagafuchi, A. and Yonemura, S. (1992). Molecular linkage between cadherins and actin filaments in cell-cell adherens junctions. *Curr Opin Cell Biol* **4**, 834-9.

Tu, Z. J. and Kiang, D. T. (1998). Mapping and characterization of the basal promoter of the human connexin26 gene. *Biochim Biophys Acta* **1443**, 169-81.

Tuma, P. L. and Hubbard, A. L. (2003). Transcytosis: crossing cellular barriers. *Physiol Rev* **83**, 871-932.

Turin, L. and Warner, A. (1977). Carbon dioxide reversibly abolishes ionic communication between cells of early amphibian embryo. *Nature* **270**, 56-7.

Ueki, T., Fujita, M., Sato, K., Asai, K., Yamada, K. and Kato, T. (2001). Epidermal growth factor down-regulates connexin-43 expression in cultured rat cortical astrocytes. *Neurosci Lett* **313**, 53-6.

Unwin, P. N. and Ennis, P. D. (1983). Calcium-mediated changes in gap junction structure: evidence from the low angle X-ray pattern. *J Cell Biol* **97**, 1459-66.

Valiunas, V., Beyer, E. C. and Brink, P. R. (2002). Cardiac gap junction channels show quantitative differences in selectivity. *Circ Res* **91**, 104-11.

Valiunas, V., Gemel, J., Brink, P. R. and Beyer, E. C. (2001). Gap junction channels formed by coexpressed connexin40 and connexin43. *Am J Physiol Heart Circ Physiol* **281**, H1675-89.

Van Rijen, H., van Kempen, M. J., Analbers, L. J., Rook, M. B., van Ginneken, A. C., Gros, D. and Jongsma, H. J. (1997). Gap junctions in human umbilical cord endothelial cells contain multiple connexins. *Am J Physiol* **272**, C117-30.

Vasioukhin, V., Bauer, C., Yin, M. and Fuchs, E. (2000). Directed actin polymerization is the driving force for epithelial cell-cell adhesion. *Cell* **100**, 209-19.

Verselis, V. K., Ginter, C. S. and Bargiello, T. A. (1994). Opposite voltage gating polarities of two closely related connexins. *Nature* **368**, 348-51.

Wagner, L. M., Saleh, S. M., Boyle, D. J. and Takemoto, D. J. (2002). Effect of protein kinase Cgamma on gap junction disassembly in lens epithelial cells and retinal cells in culture. *Mol Vis* **8**, 59-66.

Wall, S. J., Sampson, M. J., Levell, N. and Murphy, G. (2003). Elevated matrix metalloproteinase-2 and -3 production from human diabetic dermal fibroblasts. *Br J Dermatol* **149**, 13-6.

Wang, C. M., Lincoln, J., Cook, J. E. and Becker, D. L. (2007). Abnormal connexin expression underlies delayed wound healing in diabetic skin. *Diabetes* **56**, 2809-17.

Wang, Y. and Rose, B. (1995). Clustering of Cx43 cell-to-cell channels into gap junction plaques: regulation by cAMP and microfilaments. *J Cell Sci* **108 (Pt 11)**, 3501-8.

Warn-Cramer, B. J., Cottrell, G. T., Burt, J. M. and Lau, A. F. (1998). Regulation of connexin-43 gap junctional intercellular communication by mitogen-activated protein kinase. *J Biol Chem* **273**, 9188-96.

Warner, A., Clements, D. K., Parikh, S., Evans, W. H. and DeHaan, R. L. (1995). Specific motifs in the external loops of connexin proteins can determine gap junction formation between chick heart myocytes. *J Physiol* **488 (Pt 3)**, 721-8.

Watanabe, A. and Grundfest, H. (1961). Impulse propagation at the septal and commissural junctions of crayfish lateral giant axons. *J Gen Physiol* **45**, 267-308.

Weber, C., Fraemohs, L. and Dejana, E. (2007). The role of junctional adhesion molecules in vascular inflammation. *Nat Rev Immunol* **7**, 467-77.

Weber, P. A., Chang, H. C., Spaeth, K. E., Nitsche, J. M. and Nicholson, B. J. (2004). The permeability of gap junction channels to probes of different size is dependent on connexin composition and permeant-pore affinities. *Biophys J* **87**, 958-73.

Wedlich, D. e. (2005). Cell Migration in Development and Disease. Weiheim: Wiley-VCH.

Wei, C. J., Francis, R., Xu, X. and Lo, C. W. (2005). Connexin43 associated with an N-cadherin-containing multiprotein complex is required for gap junction formation in NIH3T3 cells. *J Biol Chem* **280**, 19925-36.

Weissman, T. A., Riquelme, P. A., Ivic, L., Flint, A. C. and Kriegstein, A. R. (2004). Calcium waves propagate through radial glial cells and modulate proliferation in the developing neocortex. *Neuron* **43**, 647-61.

Weller, K., Foitzik, K., Paus, R., Syska, W. and Maurer, M. (2006). Mast cells are required for normal healing of skin wounds in mice. *Faseb J* **20**, 2366-8.

Werner, S. and Grose, R. (2003). Regulation of wound healing by growth factors and cytokines. *Physiol Rev* **83**, 835-70.

Werner, S., Breeden, M., Hubner, G., Greenhalgh, D. G. and Longaker, M. T. (1994). Induction of keratinocyte growth factor expression is reduced and delayed during wound healing in the genetically diabetic mouse. *J Invest Dermatol* **103**, 469-73.

Werner, S., Peters, K. G., Longaker, M. T., Fuller-Pace, F., Banda, M. J. and Williams, L. T. (1992). Large induction of keratinocyte growth factor expression in the dermis during wound healing. *Proc Natl Acad Sci U S A* **89**, 6896-900.

Werner, S., Weinberg, W., Liao, X., Peters, K. G., Blessing, M., Yuspa, S. H., Weiner, R. L. and Williams, L. T. (1993). Targeted expression of a dominant-negative FGF receptor mutant in the epidermis of transgenic mice reveals a role of FGF in keratinocyte organization and differentiation. *Embo J* **12**, 2635-43.

Wertheimer, E., Spravchikov, N., Trebicz, M., Gartsbein, M., Accili, D., Avinoah, I., Nofeh-Moses, S., Sizyakov, G. and Tennenbaum, T. (2001). The regulation of skin proliferation and differentiation in the IR null mouse: implications for skin complications of diabetes. *Endocrinology* **142**, 1234-41.

Wertheimer, E., Trebicz, M., Eldar, T., Gartsbein, M., Nofeh-Moses, S. and Tennenbaum, T. (2000). Differential roles of insulin receptor and insulin-like growth factor-1 receptor in differentiation of murine skin keratinocytes. *J Invest Dermatol* **115**, 24-9.

West, E., Simon, O. R. and Morrison, E. Y. (1996). Streptozotocin alters pancreatic beta-cell responsiveness to glucose within six hours of injection into rats. *West Indian Med J* **45**, 60-2.

Wetzler, C., Kampfer, H., Stallmeyer, B., Pfeilschifter, J. and Frank, S. (2000). Large and sustained induction of chemokines during impaired wound healing in the genetically diabetic mouse: prolonged persistence of neutrophils and macrophages during the late phase of repair. *J Invest Dermatol* **115**, 245-53.

White, T. W. and Bruzzone, R. (1996). Multiple connexin proteins in single intercellular channels: connexin compatibility and functional consequences. *J Bioenerg Biomembr* **28**, 339-50.

White, T. W., Bruzzone, R., Goodenough, D. A. and Paul, D. L. (1994a). Voltage gating of connexins. *Nature* **371**, 208-9.

White, T. W., Bruzzone, R., Wolfram, S., Paul, D. L. and Goodenough, D. A. (1994b). Selective interactions among the multiple connexin proteins expressed in the vertebrate lens: the second extracellular domain is a determinant of compatibility between connexins. *J Cell Biol* **125**, 879-92.

White, T. W., Paul, D. L., Goodenough, D. A. and Bruzzone, R. (1995). Functional analysis of selective interactions among rodent connexins. *Mol Biol Cell* **6**, 459-70.

Wieman, T. J., Smiell, J. M. and Su, Y. (1998). Efficacy and safety of a topical gel formulation of recombinant human platelet-derived growth factor-BB (becaplermin) in patients with chronic neuropathic diabetic ulcers. A phase III randomized placebo-controlled double-blind study. *Diabetes Care* **21**, 822-7.

Wilgenbus, K. K., Kirkpatrick, C. J., Knuechel, R., Willecke, K. and Traub, O. (1992). Expression of Cx26, Cx32 and Cx43 gap junction proteins in normal and neoplastic human tissues. *Int J Cancer* **51**, 522-9.

Wilgus, T. A., Ross, M. S., Parrett, M. L. and Oberyszyn, T. M. (2000). Topical application of a selective cyclooxygenase inhibitor suppresses UVB mediated cutaneous inflammation. *Prostaglandins Other Lipid Mediat* **62**, 367-84.

Willecke, K., Eiberger, J., Degen, J., Eckardt, D., Romualdi, A., Guldenagel, M., Deutsch, U. and Sohl, G. (2002). Structural and functional diversity of connexin genes in the mouse and human genome. *Biol Chem* **383**, 725-37.

Willecke, K., Hennemann, H., Dahl, E., Jungbluth, S. and Heynkes, R. (1991). The diversity of connexin genes encoding gap junctional proteins. *Eur J Cell Biol* **56**, 1-7.

Wiszniewski, L., Limat, A., Saurat, J. H., Meda, P. and Salomon, D. (2000). Differential expression of connexins during stratification of human keratinocytes. *J Invest Dermatol* **115**, 278-85.

Wiszniewski, L., Salomon, D. and Meda, P. (2001). Cx26 affects the in vitro reconstruction of human epidermis. *Cell Commun Adhes* **8**, 409-13.

Witte, M. B. and Barbul, A. (1997). General principles of wound healing. *Surg Clin North Am* **77**, 509-28.

Witte, M. B., Thornton, F. J., Tantry, U. and Barbul, A. (2002). L-Arginine supplementation enhances diabetic wound healing: involvement of the nitric oxide synthase and arginase pathways. *Metabolism* **51**, 1269-73.

Wolburg, H. and Rohlmann, A. (1995). Structure--function relationships in gap junctions. *Int Rev Cytol* **157**, 315-73.

Wood, E. J. and Bladon, P. (1985). The Human Skin. London: Edwawrd Arnold Publisher.

Wright, C. S., Becker, D. L., Lin, J. S., Warner, A. E. and Hardy, K. (2001). Stage-specific and differential expression of gap junctions in the mouse ovary: connexin-specific roles in follicular regulation. *Reproduction* **121**, 77-88.

Wrigley, N. G., Brown, E. and Chillingworth, R. K. (1984). Reversible structure transition in gap junction under Ca++ control seen by high-resolution electron microscopy. *Biophys J* **45**, 201-7.

Wu, J. C., Tsai, R. Y. and Chung, T. H. (2003). Role of catenins in the development of gap junctions in rat cardiomyocytes. *J Cell Biochem* **88**, 823-35.

Wu, K. K. (1996). Endothelial prostaglandin and nitric oxide synthesis in atherogenesis and thrombosis. *J Formos Med Assoc* **95**, 661-6.

Xia, P., Inoguchi, T., Kern, T. S., Engerman, R. L., Oates, P. J. and King, G. L. (1994). Characterization of the mechanism for the chronic activation of diacylglycerol-protein kinase C pathway in diabetes and hypergalactosemia. *Diabetes* **43**, 1122-9.

Xu, X., Li, W. E., Huang, G. Y., Meyer, R., Chen, T., Luo, Y., Thomas, M. P., Radice, G. L. and Lo, C. W. (2001). Modulation of mouse neural crest cell motility by N-cadherin and connexin 43 gap junctions. *J Cell Biol* **154**, 217-30.

Yamaki, K., Takano-Ishikawa, Y., Goto, M., Kobori, M. and Tsushida, T. (2002). An improved method for measuring vascular permeability in rat and mouse skin. *J Pharmacol Toxicol Methods* **48**, 81-6.

Ye, Z. C., Wyeth, M. S., Baltan-Tekkok, S. and Ransom, B. R. (2003). Functional hemichannels in astrocytes: a novel mechanism of glutamate release. *J Neurosci* **23**, 3588-96.

Yeager, M., Unger, V. M. and Falk, M. M. (1998). Synthesis, assembly and structure of gap junction intercellular channels. *Curr Opin Struct Biol* **8**, 517-24.

Yeh, H. I., Rothery, S., Dupont, E., Coppen, S. R. and Severs, N. J. (1998). Individual gap junction plaques contain multiple connexins in arterial endothelium. *Circ Res* **83**, 1248-63.

Young, B. H., JW. (2000). Wheather's Functional Histology: Churchill Livinstone.

Yue, T. L., Wang, X., Sung, C. P., Olson, B., McKenna, P. J., Gu, J. L. and Feuerstein, G. Z. (1994). Interleukin-8. A mitogen and chemoattractant for vascular smooth muscle cells. *Circ Res* **75**, 1-7.

Zahler, S., Hoffmann, A., Gloe, T. and Pohl, U. (2003). Gap-junctional coupling between neutrophils and endothelial cells: a novel modulator of transendothelial migration. *J Leukoc Biol* **73**, 118-26.

Zhang, J. and Hill, C. E. (2005). Differential connexin expression in preglomerular and postglomerular vasculature: accentuation during diabetes. *Kidney Int* **68**, 1171-85.

Zhang, Y., Tang, W., Ahmad, S., Sipp, J. A., Chen, P. and Lin, X. (2005). Gap junction-mediated intercellular biochemical coupling in cochlear supporting cells is required for normal cochlear functions. *Proc Natl Acad Sci U S A* **102**, 15201-6.

Zimmer, D. B., Green, C. R., Evans, W. H. and Gilula, N. B. (1987). Topological analysis of the major protein in isolated intact rat liver gap junctions and gap junction-derived single membrane structures. *J Biol Chem* **262**, 7751-63.

APPENDICES

APPENDIX I

Key cytokines in the wound healing process

CYTOKINE	SOURCE, CHARACTERISTICS AND ACTIONS	KO MICE	ADDITIONAL REFERENCES
	CHEMOKINES		
CCL-2/MCP-1	Main source: Mast cells, keratinocytes, endothelial cells, macrophages - Major monocyte/macrophage chemoattractants - Expression prolonged in diabetes (Wetzler et al., 2000).	Significantly delayed re-epithelialisation, angiogenesis and collagen synthesis (Low et al., 2001)	Jackman et al., 2000
IL-8/CXCL-8	Main source: neutrophils, macrophages, keratinocytes - Major chemoattractant for neutrophils - Expressed for shorter time in embryonic wound (Liechty et al., 1998) - If induced to express longer, inhibit keratinocyte proliferation and collagen contraction (Iocono et al., 2000) - Promote angiogenesis	Receptor CXCR-2 KO showed delayed re-epithelialisation and neovascularisation (Devalaraja et al., 2000)	Yue et al., 1994
	PROINFLAMMATORY CYTOKINES		
IL-1α, β	Main source: neutrophils, macrophages - Amplify inflammatory response - Fibroblast and keratinocyte motogen		Grellner et al., 2000

IL-6	Main source: platelets, macrophages - Amplify inflammatory response - Promote angiogenesis - Promote collagen synthesis	Delayed re-epithelialisation and reduced leukocyte infiltration, and angiogenesis. (Gallucci et al., 2000; Lin et al., 2003)	Grellner et al., 2000
TNFα	Main source: neutrophils, mast cells - Amplify inflammatory response - Promote diapedesis - Stimulate MMP production in fibroblast	P55 receptor deficient mice showed accelerated wound healing (Mori et al., 2002)	Han et al., 2001
	GROWTH FACTORS		
TGF-β	Main source: platelets, macrophages, fibroblasts, keratinocytes - 5 known isoforms, 3 of which expressed in mammalian cells - Three types of receptors: I and II are transmembrane serine/threonin kinases - chemoattractant to neutrophils, macrophages and fibroblasts - Promote angiogenesis and fibroplasia - Promote fibroblast collagen and fibronectin synthesis - Inhibit keratinocyte proliferation	Reduced granulation tissue with increased re-epithelialisation (Koch et al., 2000)	Massague et al., 1992; O'Kane and Ferguson, 1997; Roberts and Sporn, 1993
FGF	Main source: keratinocytes, macrophages, endothelial cells - 22 members in the FGF family. - Signal transduction via 4 transmembrane tyrosine kinase receptors. - Keratinocyte proliferation and migration - Fibroblast proliferation and migration	FGF7 KO showed no change in healing (Guo et al., 1996)	Ornitz and Itoh, 2001
VEGF	Main source: keratinocytes, macrophages - Family of 5 isoforms and Placenta growth factor (PLGF)	VEGF-A KO showed delayed healing and angiogenesis	Peters et al., 1993

	- Signal transduction via 3 transmembrane tyrosine kinase receptors - Vasculogenesis and angiogenesis		
PDGF	Main source: platelets, macrophages, keratinocytes - Family of homo- and hetero- dimers - Signal transduction via 3 tyrosine kinase receptors in epidermis, dermis and granulation tissue - Chemotactic to neutrophils and macrophages - Stimulate fibroplasia and angiogenesis - Promote ECM production - Promote myofibroblast contraction	PDGF-B KO show no differences in granulation tissue formation and increased vascularisation (Buetow et al., 2001)	Reviewed (Heldin and Westermark, 1999)

APPENDIX II

List of publications

Wang CM, Mendoza-Naranjo A, Trasivoulou C, Becker DL (manuscript in preparation) Preventing the abnormal upregulation of connexin43 improves the quality of diabetic wound healing.

Wang CM, Lincoln J, Cook JE, Becker DL (2007) Abnormal connexin expression underlies delayed wound healing in diabetic skin. *Diabetes* Nov;56(11):2809-17.

Wang CM, Green CR, Duft B, Becker DL (2007) Targeting connexin43 expression accelerates the rate of skin and diabetic wound repair. *J Biotechnol* Sept:131(2):Supplement:S64

Mori R, Power KT*, Wang CM*, Martin P, Becker DL (2006) Acute downregulation of connexin43 at wound sites leads to a reduced inflammatory response, enhanced keratinocyte proliferation and wound fibroblast migration. *J Cell Sci*. Dec 15;119(Pt 24):5193-203 [*equal contribution]

APPENDIX III

List of abstracts

Wang CM, Green CR, Duft B, Becker DL (2007) Targeting connexin43 expression accelerates the rate of skin and diabetic wound repair. *13th European Congress on Biotechnology, Barcelona, Spain*

Wang CM, Lincoln J, Becker DL (2006) Abnormal Connexin expression underlies delayed wound healing in diabetic skin. *46th American Society of Cell Biology, San Diego, USA*

Wang CM, Lincoln J, Becker DL (2005) Connexins in diabetic skin – response to wounding. *Gordon Research Conference - Tissue Repair and Regeneration, New Hampshire, USA*